Synthesis and Characterization of Hyperbranched Polyradicals

Thesis by

Chih-hsiu Lin

In Partial fulfillment of the Requirements

for the Degree Of

Doctor Of Philosophy

California Institute of Technology

Pasadena, California

1999

(Submitted May 17, 1999)

詩篇二十三篇

耶和華是我的牧者，我必不至缺乏。
他使我躺臥在青草地上，領我在可安歇的水邊。
他使我的靈魂甦醒，爲自己的名引導我走義路。
我雖然行過死蔭幽的谷，也不怕遭害，因爲你與我同在，
你的杖、你的竿、都安慰我。
在我敵人面前，你爲我擺設筵席；
你用油膏了我的頭，使我的福杯滿溢。
我一生一世必有恩惠慈愛隨著我，
我且要住在耶和華的殿中，直到永遠

Psalm 23

The Lord is my shepherd; I shall not want.
He maketh me to lie down in green pastures: he leadeth me beside the still waters.
He resotreth my soul: he leadeth me in the paths of righteousness for his name's sake.
Yea, though I walk through the valley of the shadow of death, I will fear no evil: for thou art with me; thy rod and thy staff they comfort me.
Thou preparest a table before me in the presence of mine enemies: thou anointest my head with oil; my cup runneth over.
Surely goodness and mercy shall follow me all the days of my life: and I will dwell in the house of the Lord for ever.

Acknowledgments

Before I sit down in front of the computer, about to write the acknowledgments, I never really expected that saying thanks would be a difficult task. How ignorant I was. First, it would take a photographic memory to put together all the seemingly trivial help given to me in great love during my years in Caltech. These acts of kindness usually came from an acquaintance, yet were sometimes anonymous. They often added ecstasy to joyous occasions but were more importantly the only hope to hold on to in utter frustration and despair. Compared to chemistry, friendship might not have much survival value, it gives real value to survival. Unfortunately, because of my forgetfulness and ignorance, only a few could be mentioned. May God Himself reward those unnoticed and unappreciated acts of love. Second, I find that to give heartfelt thanks demands true humility, a character I always thought I have but have only hitherto understood how infinitesimally little.

I would first of all like to thank my adviser Dennis Dougherty. He has the enthusiasm, excitement and financial generosity of a liberal and the cautious yet uncompromising commitment to truth as a conservative, really the best of both worlds. In order to inspire the individual creativity yet to be seen, he was willing to take the risk of letting me pursue my own project, often with dubious results. In addition, he also intervened when I went astray, showed great patience when I got stuck, and was ready to forgive when mistakes were made. Sometimes I could not help wondering "what good could I have done to deserve an adviser like him?"

I was also most fortunate to work with the brilliant and fun-loving chemists in Dougherty's group. The varieties of topics at our group meeting and informal discussions (although I hardly have the knowledge and language skill to join in) sometimes made me forget I was at Caltech. I

am grateful to Piotr Kaszynski, Josh Jacobs and Michael Murray for helping me to start the polytrityl project. Both Seth Miller and Josh Mauer have provided invaluable technical assistance. A dialogue with Kraig Anderson or Jeff Clites is always good to start (or kill) a new idea. Scott Silverman's ability to bring up intriguing possibilities and sharp questions never cease to amaze. On the other side of our group (where people make cyclophanes and kill frog eggs), Alison McCurdy, Sandro Mecozzi, Jonathan Forman, Wenge Zhong, Jennifer Ma, Sarah Ngola, Justin Gallivan and Gabriel Brandt, to name just a few, have all made my Caltech experience all the more enjoyable. Thank you all for the good time. Also forgive me for those occasions when I was obnoxious, inattentive or just plainly rude.

With angelic charity and patience, Pastor Shan-Yan Tan and Mimi Yeh counseled me through my darkest days. Even when we were mere acquaintances, John and Lucy Tsai, Philip and Mei-mei Chen showed unbelievable hospitality and opened their homes when I was in need. The prayers from the brothers and sisters in the Young Adult Fellowship at First Evangelical Church were my constant support. Thanks to all of you.

Finally, I have to thank my family, my parents and my sister, for all your love. You not only gave me my life and my faith, with your lives, you also has demonstrated to me that they are worth living for.

Abstract

The design, synthesis and magnetic characterization of hyperbranched polyradicals based on triphenylmethyl are described. The precursor polymers are synthesized via unimolecular polymerization with a A_2B type monomer employing palladium catalyzed Suzuki coupling reaction. The required dibromo-boronic acid monomers are synthesized by a newly developed selective lithium-iodo exchange reaction. The polytrityl methyl ethers are first converted to polytrityl trifluoroacetates. They are then transformed into corresponding polyradicals with various reductants. Cobaltocene proves to be the best choice. Magnetic characterization of the polyradicals, using SQUID magnetometry, indicates the samples contain small ferromagnetic-coupled radical clusters with spin concentration near 20 percent. In a futile attempt to minimize the defects in these systems, similar polyradicals with various substitutions are made. However, high-spin coupling is observed in a control system with neighboring antiferromagnetic interactions. This unexpected result is rationalized with a new mode of ferromagnetic interaction unique to hyperbranched or dentrimer systems. The new model provides new insights and implications to the designing of magnetic materials that is not hitherto appreciated.

A polyradical based on phenoxyl radical is also synthesized and characterized. In order to make the system defect-insensitive, the magnetic interaction is transmitted through a conducting polymer backbone. Although this polyradical has a pretty high spin concentration, the S value is only mediocre. Neither does the defect-insensitive property appear.

Table of Contents

List of Figures:

List of Tables

Chapter 1. Introduction

Historical Background

Magnetism has intrigued the human mind and also challenged our reasoning power almost since the beginning of civilization. The Greeks are possibly the first to record the remarkable property of lodestone and magnetite, the magnetic iron ore - Fe_2O_3[1]. The earliest documented magnetic technology is probably in the Chinese legend where a compass-like device led to a historical victory of the Hans over the invading barbarians on a foggy night[2]. During the twelfth century A.D., the compass was introduced to western Europe where it revolutionized navigation. Today, magnetic technology is still present in many aspects of our daily life, from a refrigerator magnet to medical magnetic resonance imaging[3].

The theory of bulk magnetism has eluded all the great scientific minds of the classical world. Even the blossoming of Newtonian mechanics and electromagnetism in the eighteenth and nineteenth centuries could not answer the mystery. The firm mathematical foundation of magnetism was finally established as a result of the advent of quantum mechanics and Pauli exclusion principle early in the twentieth century. Since then, a more refined understanding has been achieved, thanks to the interplay of theoretical and experimental solid state physics. Today, novel magnetic behaviors observed in new materials continue to challenge and excite theorists.

Traditionally, common commercial magnets are mostly atom-based, employing transition and lanthanide metals as spin sources. These spin are connected by heteroatoms to form networks in at least two dimensions. The syntheses of these materials normally employ high-temperature metallurgical processes. These low-cost materials are very effective and not likely to be replaced by molecular or polymer-based materials any time soon[4].

As chemists, our major intellectual pursuit is to put every physical phenomenon we observe into the context of molecular structures. Unfortunately, the trial-and-error approach described above renders almost no control over the composition and structure of the produced magnetic material. Although such procedure is very important in technology, it is not refined enough to produce the kind of subtle structural variations that allow chemists to study the relationship between magnetic behavior and molecular structure.

On the contrary, organic synthesis has the sophistication to systematically generate related compounds with slight variations in structures[5]. If magnetic materials can be produced by organic synthesis, magnetism can then be studied in a totally new context. In the long run, the information gathered can be a key to establishing better understanding of structure-property relationships in magnetic materials. Beyond pure scientific endeavor, organic solids or polymers can also possess such technologically important properties as optical transparency, solubility and true magneto-optical switching[6]. However, in the current project, the primary goals remain to extend present understanding of magnetism theory while challenging our ability to design and make novel materials. At this stage, those potential applications are given far less concern.

From Electron Spin to Magnetic Behavior

Magnetism is a purely quantum mechanical phenomenon that involves the electron spin. The simplest magnetic interaction is the parallel coupling of two electron spins. The classical dipole-dipole interaction model can not account for the phenomenon. Such coupling can only be explained by Pauli exclusion principle. The exclusion principle states that any two fermions, that is particles with half integral spin quantum numbers including

electron, can not have the same set of four quantum numbers. As a consequence, electrons that are spin parallel must occupy different regions in space. For example, in a two-electron triplet system, the exclusion principle forces the two electrons to stay apart spatially. This special coupling term between spatial and spin wave functions is called exchange coupling which has no classical counterpart. Since the spin-parallel electrons are kept separated spatially, the Coulombic repulsion between electrons in such a state is usually smaller than that between spin-antiparallel electrons. This stabilization leads to the triplet ground state. However, in the real world, electrons are usually in some potential wells that restrict their spatial distribution. If the energetic preference for such confinement overwhelms the exchange coupling, electrons can be forced to stay together and pair up, which results in a low-spin ground state. The interaction that leads to high-spin ground state is known as ferromagnetic interaction. Contrariwise, the low-spin ground state is the result of antiferromagnetic interactions.

This simple picture can also be extended to bulk magnetism. At least fourteen different types of magnetism have been reported so far[7], but the majority of materials exhibit one of the five classes of magnetic behavior. These five common classes are diamagnetism, paramagnetism, ferromagnetism, antiferromagnetism, and ferrimagnetism.

Diamagnetism arises when all electrons in the material are paired up into molecular or atomic orbitals. There is no net moment under any condition. Most materials fall into this category.

The other four classes all have unpaired electrons but are distinct from each other by the way electrons interact with each other in the absence of external magnetic field. A paramagnetic material contains unpaired spins that orient randomly throughout the material. The result is the cancellation

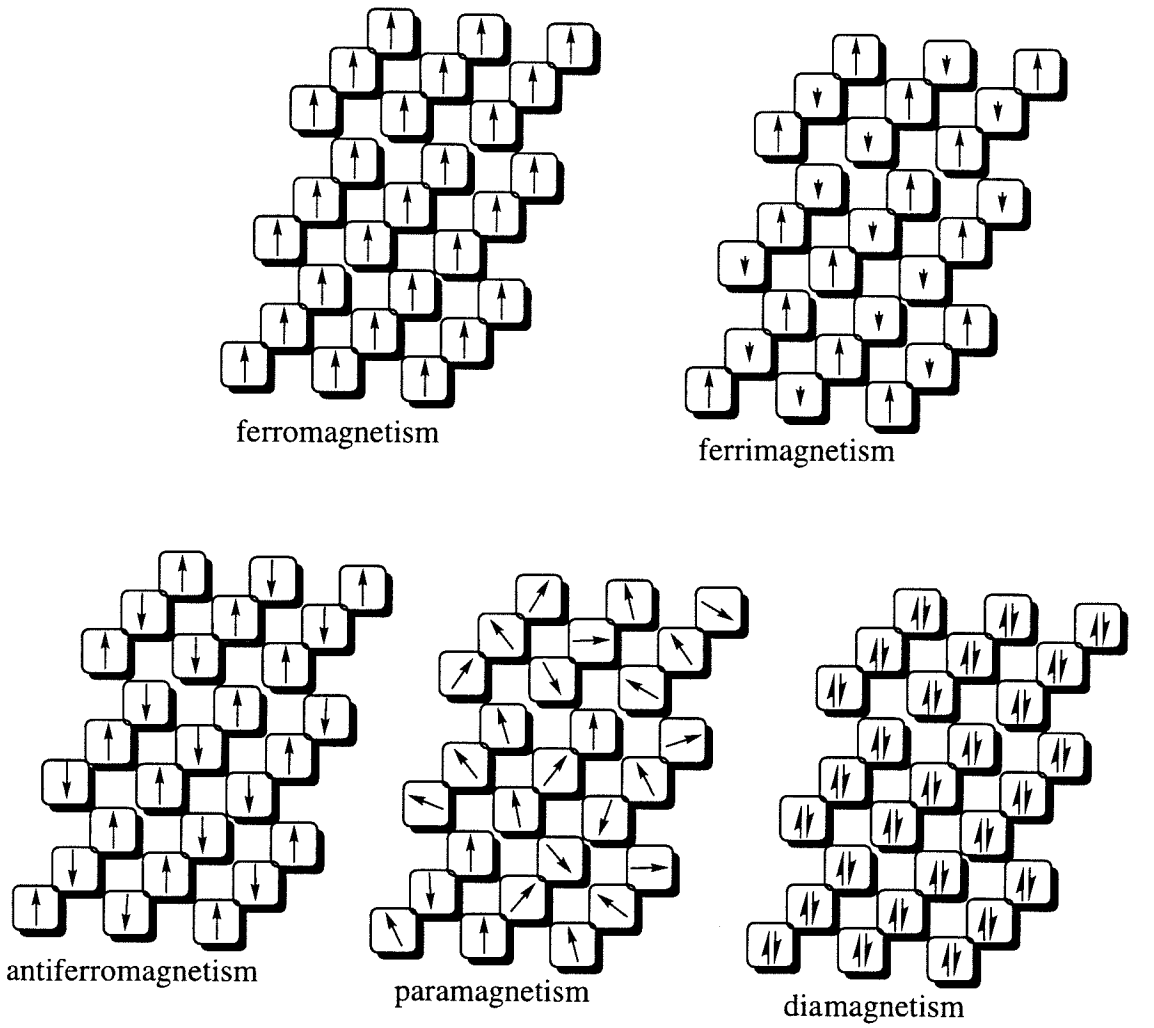

Figure 1-1 Five principal classes of magnetic behavior

of all spin angular momenta. A paramagnet has no bulk moment in the absence of an external field. The spin angular momenta in such system can usually be aligned parallel to an applied field. Such coerced ordering, however, can be overcome by moderate thermal energy.

Bulk ferromagnetism is observed only when all the unpaired spins in the material align in a particular direction spontaneously. This results in a measurable macroscopic net magnetic moment even in the absence of an external field. All ferromagnets become paramagnetic when heated to some

sufficiently high temperature. This occurs because the intrinsic preference for high-spin state is overcome by the thermal energy. The temperature where this transition to paramagnetic behavior occurs is called the Curie temperature. Iron, for example, has a high Curie temperature (T_c) of 770°C. On the other hand, a charge transfer salt, decamethyl chromocenium tetracyanoethylenide, has much lower T_c at 3.6 K[8].

In an antiferromagnetic material, the unpaired spins are locked into antiparallel arrangement by antiferromagnetic interactions. Most of the paramagnetic materials become antiferromagnets when the temperature is low and thermal energy is no longer sufficient to randomize the spin angular momenta.

When a material contains two types of spin sites carrying different spin angular momenta, these two sites can interact either ferromagnetically or antiferromagnetically. In the first case, the magnetic behavior will be indistinguishable from ferromagnetism. Interestingly, even if the two sites interact antiferromagnetically, there remains a bulk magnetic moment because the momenta can not completely cancel each other as in antiferromagnetism. The phenomenon is called ferrimagnetism. The most familiar magnet, Fe_3O_4, is in fact a ferrimagnet composed of Fe^{+2} and Fe^{+3}. Like ferromagnets, ferrimagnets also show spontaneous magnetization only below the Curie temperature.

Magnetism in Organic Compounds

As mentioned earlier, electrons in real materials can be forced to paired up into the same orbitals because of the potential imposed by the nuclear configuration. This inevitably leads to diamagnetism. It is thus crucial to introduce orbital degeneracy into the material intended to have high-spin ground state. In those conventional transition and lanthanide

metal-based magnets, the highly degenerate atomic d and f orbitals can be utilized as an intrinsic advantage. As for organic compounds, such convenience does not exist and the degeneracy has to be imposed by molecular symmetry. This principle has been used by Breslow and Miller to design ferromagnetic charge transfer salts[9]. However, mere orbital degeneracy is not adequate to guarantee a high-spin ground state. The degenerate orbitals must also overlap considerably so that the Coulombic repulsion is large enough to make the high-spin state stable. If the half filled molecular orbitals do not share common space, then the system is disjoint. A disjoint system either has a low-spin ground state or nearly degenerate low-spin and high-spin states. For example, the two half-filled molecular orbitals of cyclobutadiene do not span common atoms. Therefore cyclobutadiene has a singlet ground state. In contrast, the two half-filled molecular orbital of trimethylene methane overlap extensively at the peripheral atoms, which results in the experimentally confirmed triplet ground state[10].

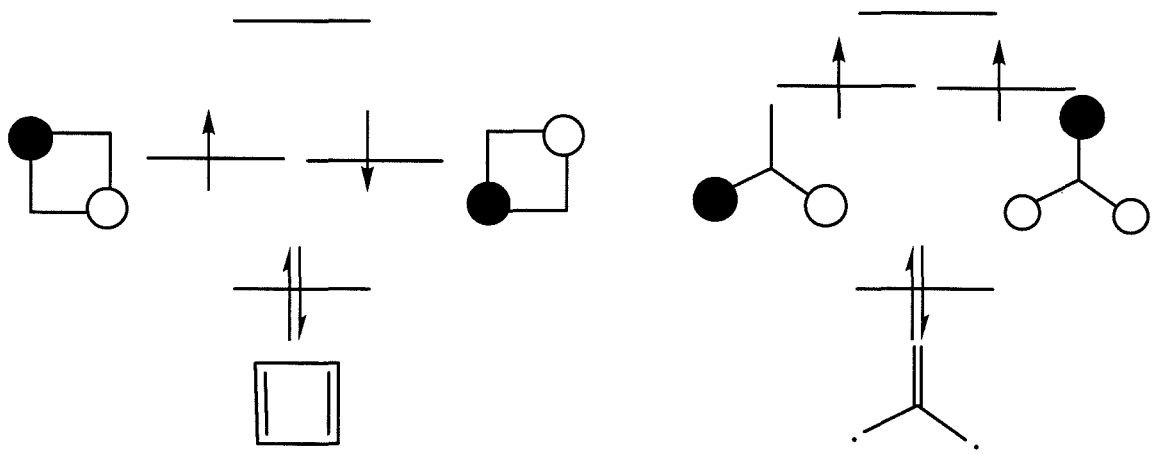

Figure 1-2 NBMOs and electronic ground states of square cyclobutadiene and trimethylene methyl

In larger conjugated organic compounds, the spatial distributions of molecular orbitals are not always intuitive and thus this principle might not be immediately applicable. A simpler topological rule has been developed by Ovchinnikov[11] and Borden[12] to predict the ground state of alternating hydrocarbons. In the first step, the atoms in the conjugated system are divided into two sets, starred and non-starred, so that no atom is connected to any atoms from the same set. (For some hydrocarbons, this division can not be achieved. In such cases, the hydrocarbons are said to be non-alternating and the theory is not applicable.)

The ground state spin multiplicity S is $|N^*-N^\circ| / 2$ where N^* is the number of the starred atoms and N° is the number of non-starred atoms.

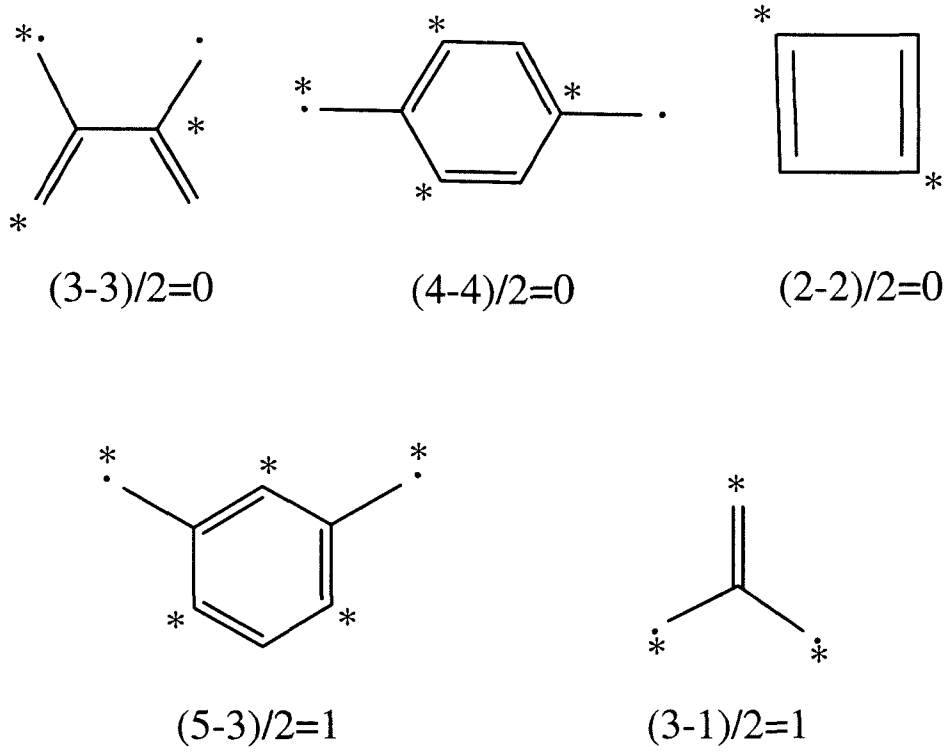

Figure 1-3 Ovchinnikov-Borden theory applied to various biradicals

Accordingly, in Figure 1-3, para-quinodimethane, tetramethylene ethane and cyclobutadiene are all ground state singlets, whereas meta-quinodimethane and trimethylene methane are ground state triplets. This theory can also be applied to polymeric systems. For example, the hypothetical system shown below should have spin multiplicity n+1.

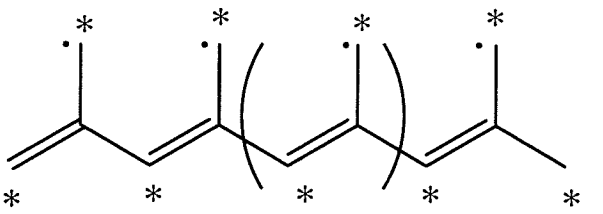

Although this theory is developed at simple Huckle level where the whole system is assumed to be planar, recent experiments have shown that it is still valid for some highly twisted compounds[13]. Its predictive power remains satisfactory even when charges and heteroatoms are introduced into the complex[14]. Because of such generality, Ovchinnikov-Borden rule has become the primary theoretical ground for designing high-spin organic compounds and polymers. This topic will be discussed in further details in the second chapter.

Magnetic Characterization

The following sections present a brief discussion of the basic physical and mathematical concepts used in this study to characterize the magnetic properties of the synthetic materials[15]. The more practical aspects of these formalisms will be discussed in the next chapter.

Fundamentally, magnetic dipole and electric dipole are similar in many ways. An applied magnetic field can induce a magnetic moment. This

analogue of electric polarization is called magnetization. When a sample is put in a external magnetic field, H, the net magnetic induction, B, inside the sample is the sum of the external field and the magnetization induced field.

$$B = H + 4\pi M \tag{1}$$

The magnetization term, M, is proportional to the strength of the applied field.

$$M = \chi H \tag{2}$$

The empirical constant χ is termed magnetic susceptibility which is analogous to the polarizability of electric dipoles. It is the sum of diamagnetic susceptibility, χ_{dia}, and paramagnetic susceptibility, χ_{para} .

$$\chi = \chi_{para} + \chi_{dia} \tag{3}$$

The diamagnetic susceptibility is present in all materials. It arises because of the paired-up electrons in the filled orbitals. This temperature independent term is always negative and usually quite small (approximately $-1 * 10^{-6}$ emu/G•mol). Paramagnetic susceptibility only exists in materials with unpaired electrons. It is always a positive number and is temperature dependent. Its magnitude also depends on how the electrons interact with each other.

Curie Analysis

The similarity between electric and magnetic moment leads to Curie law which is a magnetic analogue of Debye equation. In a weak applied field and high temperature, the paramagnetic susceptibility is inversely proportional to the absolute temperature.

$$\chi_{para} = \frac{C}{T}$$

$$\chi = \frac{C}{T} + \chi_{dia} \qquad (1\text{-}4)$$

According to Equation 1-4, the plot of an experimentally determined susceptibility versus the inverse of the absolute temperature should give a straight line. The slope C, the Curie constant, is proportional to the square of the molar magnetic moment and the intercept χ_{dia} is the residual diamagnetic susceptibility at infinite temperature.

When weak communication between spins is present in a paramagnetic sample, the Curie is modified to account for such interaction to yield to Curie-Weiss Law

$$\chi_{para} = \frac{C}{T - \theta} \qquad (5)$$

This is usually written as :

$$\frac{1}{\chi_{para}} = \frac{T}{C} - \frac{\theta}{C} \qquad (6)$$

The correction term θ is commonly known as the Weiss temperature. In a perfect paramagnet, the θ value is zero. It is positive for ferromagnetic interactions and negative for antiferromagnetic interactions. We should note that although Curie plot usually use high temperature susceptibility, χ_{para} , where T>10θ, it is possible extrapolate to very weak interaction that only manifest itself in very low temperature. Typical Curie-Weiss plots are shown in Figure 1-4.

The Weiss temperature is small in most cases and provides only a limited insight into the nature of the interaction. A more informative way is to plot the effective moment versus temperature to map out the onset of ferromagnetic or antiferromagnetic interactions. The effective moment μ_{eff} is related to the molar paramagnetic susceptibility, χ_m , by Langenvin function.

$$\chi_m H = \mu_{eff} \left(\frac{e^x + e^{-x}}{e^x - e^{-x}} - \frac{1}{x} \right) \tag{7}$$

where $x = \mu_{eff} H/kT$

In a weak applied field and high temperature, x<<1. Equation 1-7 is simplified to

$$\chi_m = \frac{N\mu^2_{eff}}{3kT} \tag{8}$$

or

$$\mu_{eff} = 2.824\sqrt{\chi_m T} \tag{9}$$

and

$$\mu_{eff} = g\sqrt{s\ (s+1)}\mu_B \tag{10}$$

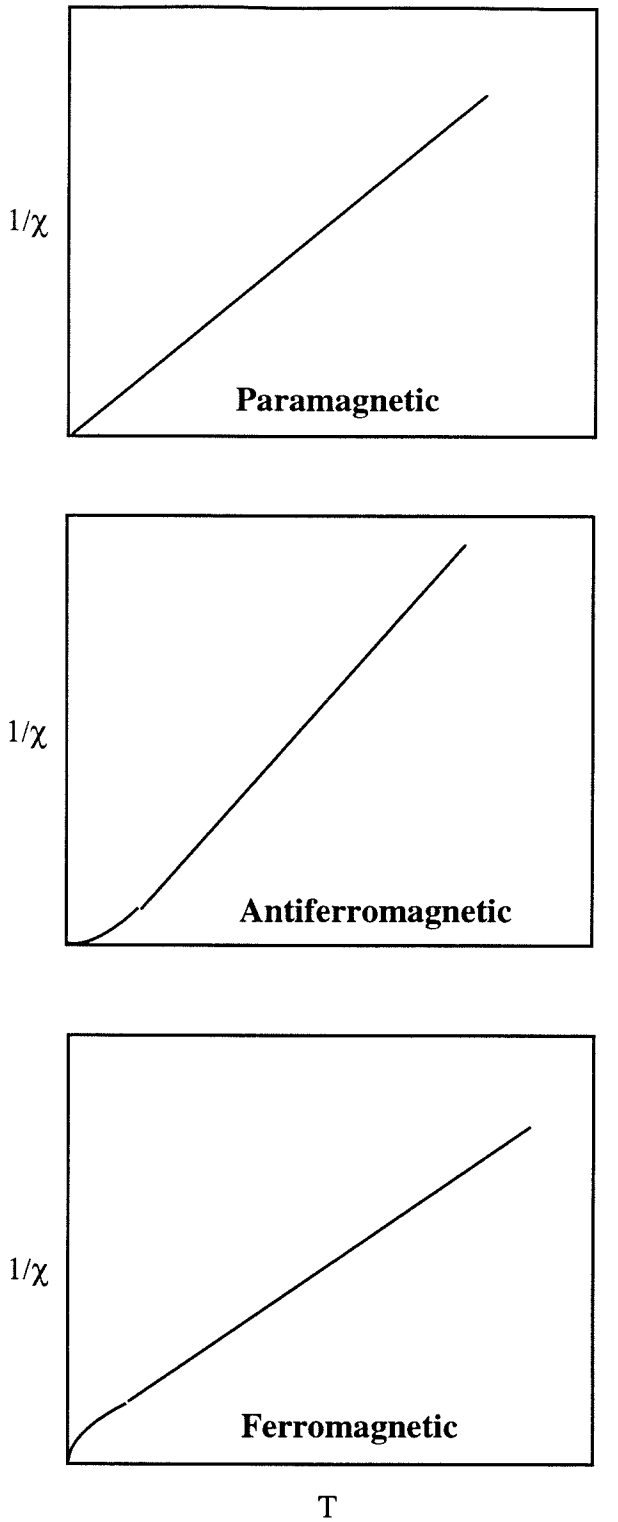

Figure 1-4 Idealized Curie-Weiss plots for paramagnetic, antiferromagnetic and ferromagnetic materials

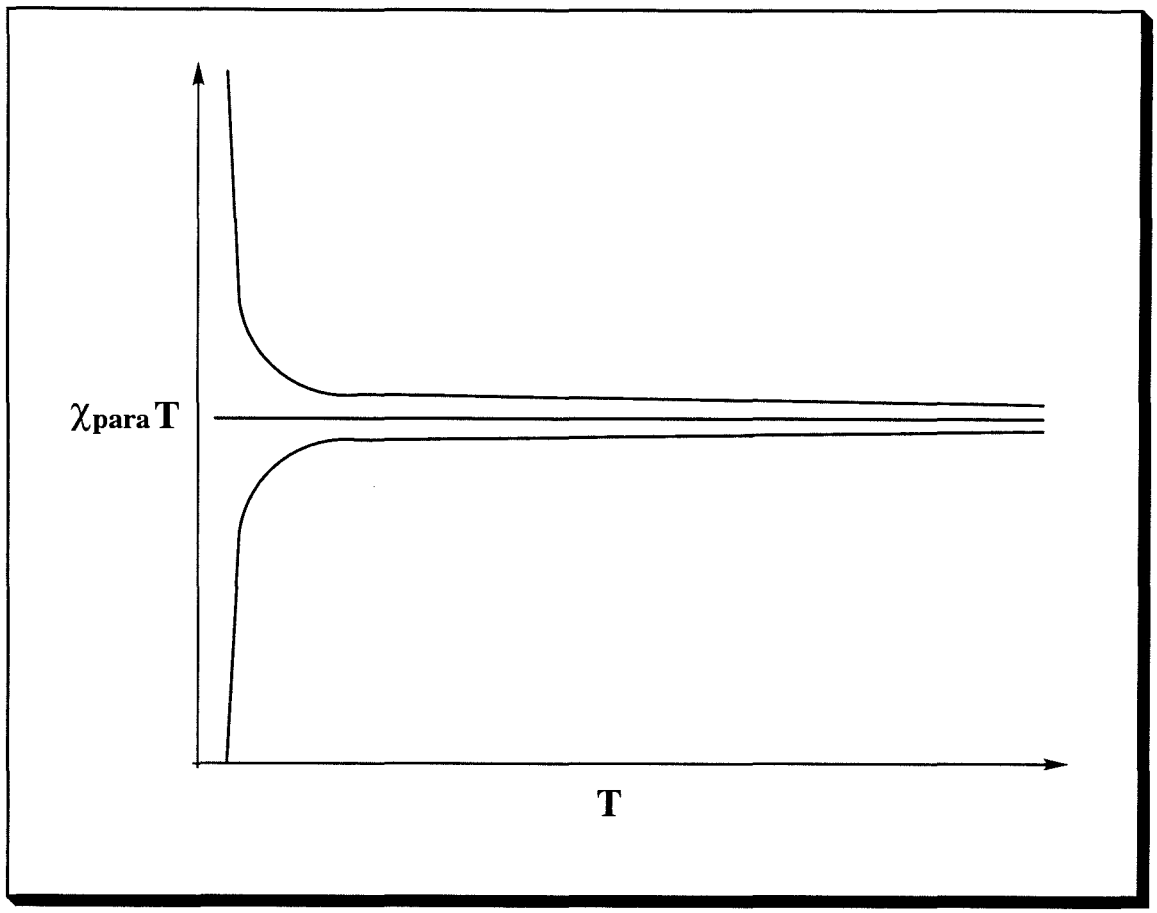

Figure 1-5 Idealized relative effective moment plots. The top line, increasing upward, indicates ferromagnetic behavior. The flat line is characteristic of a perfect paraferromagnet. The downward curving line describe a net antiferromagnetic coupling.

where s is the spin quantum number, μ_B is the Bohr magneton and g is the Lande constant. The effective moment is then expressed in the units of Bohr magneton.

For every sample of known weight and composition, the χ_m can be measured at every temperature. Thus the effective moment, μ_{eff}, and S can both be calculated using equation (9) and (10).

The μ_{eff} versus temperature plot presents tendency of electrons to align to external field as a function of temperature. If there is no interaction between the spins in a sample, its effective moment remains constant throughout the temperature range. Ferromagnetic interaction between spins causes an up turn in the effective moment plot. The temperature where this up turn occurs is indicative of the strength of the interaction. On the other hand, a down turn in the effective moment plot means the net interaction between the spins becomes antiferromagnetic.

Brillouin Plot

Curie law is used extensively in determining spin state of a well defined sample. However, the exact molecular composition of a magnetic sample is not always known. The Brillouin function plot, on the other hand, is applicable to any material and is used in many cases where the exact spin carrying species is hard to characterize. This section presents a simple derivation of the Brillouin function and how it is used in this study.

When a magnetic material is put in a field, all the projections of the spins in the sample along the axis of the applied field, usually defined as the z axis, are quantized.

$$E = -\vec{\mu} \bullet H = g\mu_b H_z m_s \tag{11}$$

The population in each of the m_s state is controlled by Boltzman distribution. The probability in each state m_s, $P(m_s)$, is

$$P(m_s) = \frac{e^{-g\mu b_B H_z m_s / kT}}{\sum_{m_s=-s}^{s} e^{-g\mu b_B H_z m_s / kT}} \tag{12}$$

The average magnetic moment of this sample is then given by

$$\langle \mu_z \rangle = \frac{\sum_{m_s=-s}^{s} g\mu_b m_s e^{-g\mu b_B H_z m_s / kT}}{\sum_{m_s=-s}^{s} e^{-g\mu b_B H_z m_s / kT}} \tag{13}$$

Notice that the denominator is exactly the magnetic partition function, W, of this system and the numerator is this W's partial derivative to H_z. The average moment can in turn be expressed as

$$\langle \mu_z \rangle = \frac{kT}{W}\frac{\partial W}{\partial H_z}$$
$$where\, W = \sum_{m_s=-s}^{s} e^{-g\mu_b H_z m_s / kT} \tag{14}$$

W can be easily calculated as the sum of an infinite series. To simplify the equation, we can define $\eta = g\,\mu_B h_z$.

$$W = \sum_{m_s=-s}^{s} e^{-\eta m_s} = \frac{e^{-\eta w} - e^{\eta(s-1)}}{1 - e^{-\eta m_s}} = \frac{e^{-\eta(s-1/2)} - e^{\eta(s+1/2)}}{e^{-\eta/2} - e^{\eta/2}} = \frac{\sinh(s+1/2)\eta}{\sinh(\eta/2)} \tag{15}$$

from equation (14)

$$\langle \mu_z \rangle = \frac{kT}{W}\frac{\partial W}{\partial H_z} = kT\frac{\partial W}{\partial \eta}\frac{\partial \eta}{\partial H_z} = g\mu_b \frac{\partial W}{\partial \eta}$$
$$= \frac{g\mu_b \sinh(\eta/2)}{\sinh \eta(s+1/2)}\left[\frac{(s+1/2)\cosh(s+1/2)\eta}{\sinh(\eta/2)} - \frac{\sinh \eta(s+1/2)\cosh(\eta/2)}{2\sinh^2(\eta/2)}\right] \quad (16)$$
$$= g\mu_b\left[(s+1/2)\coth(s+1/2)\eta - \frac{\coth(\eta/2)}{2}\right]$$

if the Brillouin function is defined as

$$B_S(\eta) = \frac{1}{S}\left[(s+1/2)\coth(s+1/2)\eta - \frac{\coth(\eta/2)}{2}\right]$$

then the magnetization term M can be expressed as

$$M = N\langle \mu_z \rangle = Ng\mu_B S B_S(\eta) \quad (17)$$

The purpose of introducing a 1/S factor into $B_S(\eta)$ is to make M the product of the saturation magnetization and $B_S(\eta)$. When in a high applied magnetic field and at low temperature, $\eta >> 1$ and the Brillouin function approaches unity. In such a condition, all the unpaired spins in the sample are already aligned with the field and the macroscopic magnetization does not respond to further rise in field strength. This phenomenon is called saturation. When interaction present between the electrons is ferromagnetic, the spins are already aligned to some extent. In this condition, the saturation can be reached with lower field strength at higher temperature. This is shown in the theoretical saturation plot for various S values in Figure 1-6. Conversely, an antiferromagnetically coupled system requires a stronger field to achieve saturation.

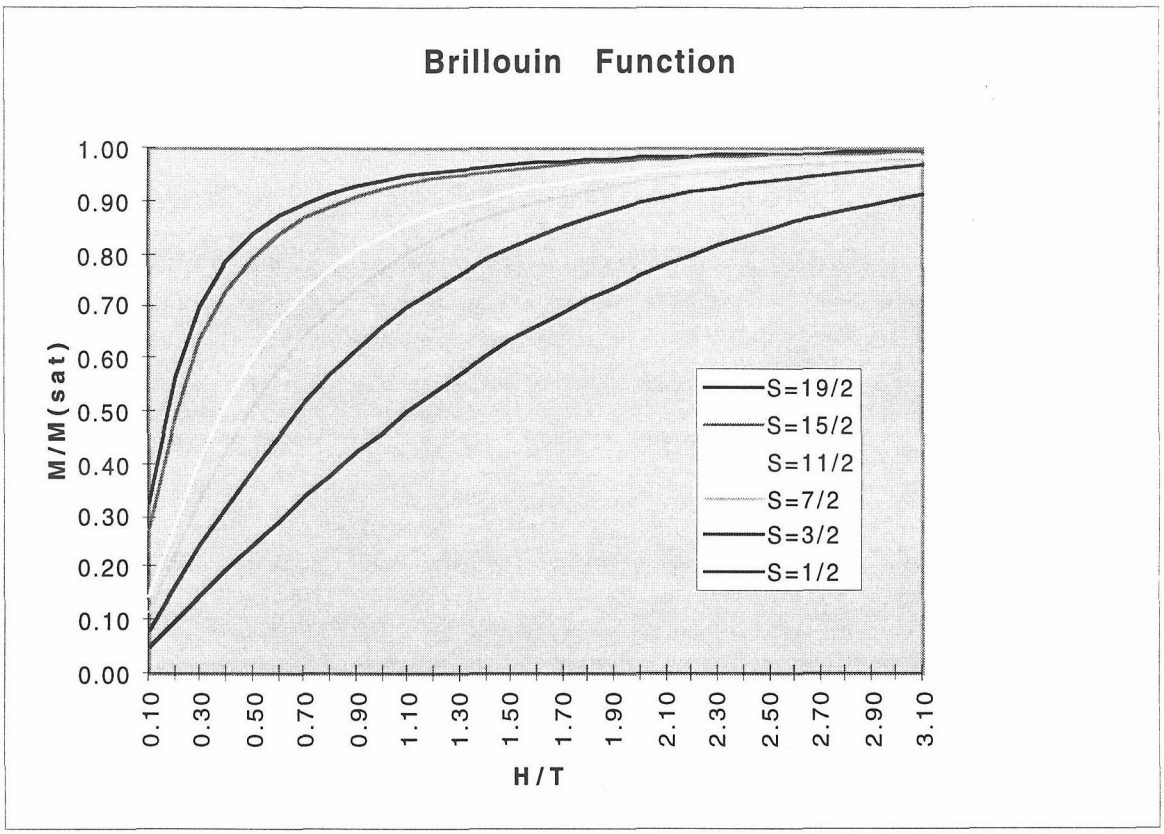

Figure 1-6 Theoretical saturation plots for various S values

The magnetization after saturation gives an accurate count of the total number of unpaired spins in the material. This is where the superiority of the Brillouin treatment becomes clear. Instead of fitting the real moment, an unitless normalized magnetization can be used to fit the Brillouin function. This normalized magnetization is defined as the ratio of magnetization at any given field and temperature to the saturation magnetization, M_{sat}. The procedure enables us to obtain the spin quantum number of any material without knowing their exact chemical composition. This is especially important for the characterization of organic magnetic materials where precise structures can be sometimes difficult to determine[16].

As previously mentioned, the observed magnetization always has a diamagnetic component.

$$M_{obs} = M_{dia} + M_{para} = \chi_{dia}H + Ng\mu_B SB_S(\eta) = \chi_{dia}H + M_{sat}B_S(\eta) \qquad (18)$$

Since diamagnetic contribution exists in any sample, the M_{obs} will always have a linear component. This can lead to an overestimation of spin quantum number, S and is especially obvious for samples with low spin concentrations. Certainly, a three-parameter fit can be conducted to evaluate χ_{dia}, M_{sat} and S simultaneously. However, such fit can sometime give inaccurate χ_{dia}. We find it is preferable to recover the diamagnetic susceptibility from the variable temperature data and Curie plot. The diamagnetic component is then subtracted from the observed moment. The real S and M_{sat} is then determined in a two-parameter fit.

References

[1]Mattis, D. C. *The Theory of Magnetism I*; 2nd Ed.; Springer-Verlag: New york, **1988**; Vol. 17

[2] Josef Neeham, *Science and Civilization in China*

[3] Hurd, C. M. *Contemp. Phys.* **1082**, *23*, 469-493

[4] Miller, J. S.; Esptein, A. J.; Angew. Chem. Int. Ed. Engl. **1994**, *31*, 385-415

[5] Seebach, D *Angew. Chem. Int. Ed. Engl.* **1990**, *29*, 1320-1367

[6] Dougherty, D. A.; Grubb, R. H.; Kaisaki, D. A.; Chang, W.; Jacobs, S. J.; Shultz, D.A.; Anderson, K. K.; Jain, R.; Ho, P. Tp.; Stewart, E. G. In *Magnetic Molecular Materials*; D, Gatteschi, o. Kahn, J. S. Miller and F.

[7] Hurd C. M. *Comtemp. Phys.* **1982**, *23*, 469- 493

[8] Bao, S. Q.; Shen, J. L. *Comm. Theo. Phys.* **1998**, *30*, 27-32

[9] Breslow, R.; Jaun, B.; Kluttz, R. Q.; Xia, C.-Z. *Tetrahedron*, **1982**, 863

Miller, J. S.; Epstein, A. J.; Reiff, W. M. *Science*, **1988**, *240*, 40-47

Miller, J. S.; Epstein, A. J.; Reiff, W. M. *Acc. Chem. Res.* **1988**, *21*, 114

[10] Edited by Weston Thatcher Borden *Diradicals Chapter Two* New York : Wiley, **1982**

[11] Ovchinnikov, A. A. *Theoret. Chim. Acta. (Berl.)* **1978**, *37*, 297-304

[12] Borden, w. T.; Iwamura, H.; Berson J. A. *Acc. Chem. Res.* **1994**, *27*, 109-114

[13] Silverman, S, K.; Dougherty, D. A. *J. Phys. Chem.* **1993**, 97, 13273

[14] Yashizawa, K.; Tanaka, K.; Yamabe, T.; Yamauchi, J. *J. Phys. Chem.* **1992**, 96, 5516-5522

Yashizawa, K.; Chano A.; Ito, A.; Tanaka, K.; Yamabe, T.; Fujita, H.;Yamauchi, J.; Shiro, M. *J. Am. Chem. Soc.* **1992**, *114*, 5994

Tukada, H. *J. Chem. Soc. Chem. Comm.* **1994**, 2293

Rajca,A.; Rajca, S. Desai, S. R. *J. Chem. Soc. Chem. Comm.* **1994**, 2293

Wienk, M. M.; Janssen, R. A. J. *J. Am. Chem. Soc.* **1996**,*118*, 10626-10628

[15] Carlin, R. *Magnetochemistry*; Springer-Verlag: New York, **1986**

Kaisaki, D. A. Ph.D. Thesis, California Institute of Technology, Pasadena, California, 1990

Anderson K. K. Ph.D. Thesis, California Institute of Technology, Pasadena, California, 1990

[16] Sugawara, T.; Bandow, S.; Kimura, K.; Iwamura, H.; Itoh K. *J. Am. Chem. Soc.* **1986**, *108*, 368-371

Iwamura, H. *Pure & Appl. Chem. 1987, 59*, 1595-1604

Iwamura, H.; Koga, N. *Acc.Chem. Res. 1993*, *26*, 346-351

Rajca, A. *Chem. Rev. 1994*, *94*, 871-893

Chapter 2. Magnetic Interaction in Hyperbranched Triphenylmethyl Polyradicals

General Concerns

Two distinct strategies have been employed in developing organic-based ferromagnetic materials. The crystal engineering approach takes advantages of the weak and subtle intermolecular interactions in the solid state. This concept has produced several ferromagnetic pure radical crystals and charge transfer salts[1]. On the other hand, this study focused on the molecular approach that exploits the stronger intramolecular through-bond interactions as a mean to align the spins. The magnetic interaction here is controlled by connecting the radicals through appropriate π-topology. In this molecular approach, it is also easier to introduce minor structural and compositional changes to the material and study their effect on bulk magnetic behavior.

The basic design principle is to conceptually break the molecules or polymers into two compartments, the spin containing units (SC) and the ferromagnetic coupling units (FC) that connect the SCs with high-spin topologies (Figure 2-1).

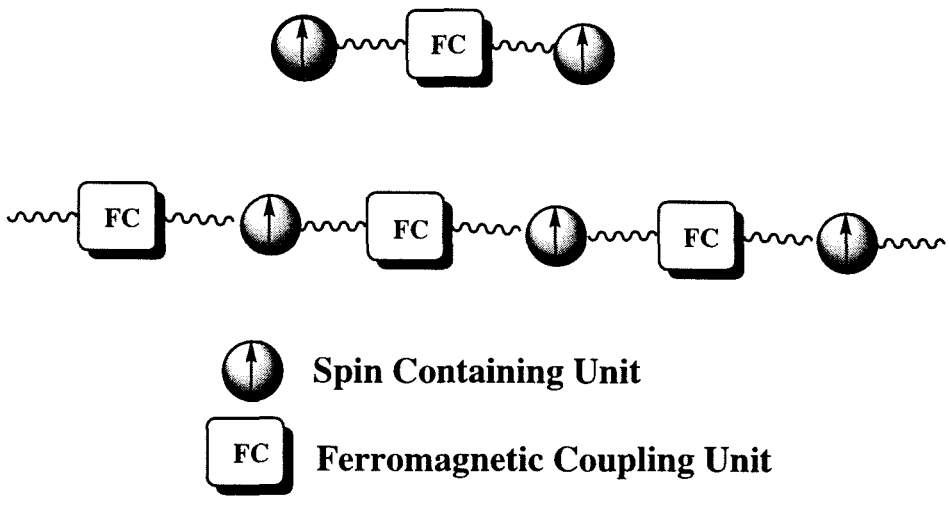

Figure 2-1 Basic scheme for design high-spin polymers

Although this division seems rather simple-minded, the scheme has proved very useful in designing and analyzing high-spin structures[2]. It is equally valid for high-spin inorganic solids, where the bridging ligands between the spin-containing metal atoms can be perceive as FC's[3].

The essential topological feature that enforces high-spin coupling in organic systems have been demonstrated from studying small triplet biradicals. The FC structures are identified as the linkage between the two radical centers. For example, *meta* -phenylene in *meta* -xylylene, 1,1-ethylene in trimethylenemethane (TMM) and the double methylene bridge of 1,3-cyclobutadiyls are all sound FCs.

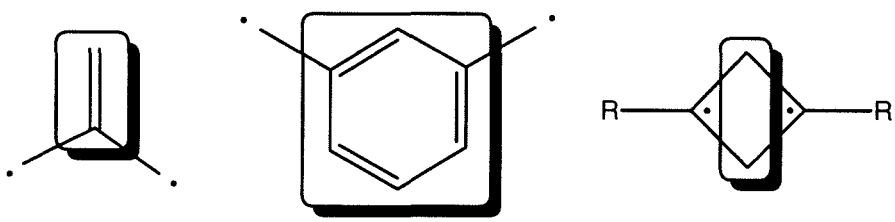

Figure 2-2 FCs in high-spin biradicals

All three biradicals in Figure 2-2 have relatively large singlet-triplet gaps and are considered "robust" triplets[4]. Early study implies *meta* -phenylene to be the ideal FC. With an estimated preference for triplet state of 10 kcal/mol[5], it can ensure high-spin coupling even in some highly twisted and conjugated systems. In addition, the reliable synthetic methods have been developed to incorporate this unit into polymers. Furthermore, this motif is chemically inert enough to endure the sometimes fierce conditions necessary to generate the radicals.

As for SCs, many organic radicals or biradicals have been employed. Trimethylene methane derivatives[6], cyclobutyldiyl[7], triphenyl methyl[8] and

its chlorinated derivatives[9], t-butyl nitroxide[10], carbene[11], nitrene[12] and various radical cations have all proved satisfactory (Figure 2-3).

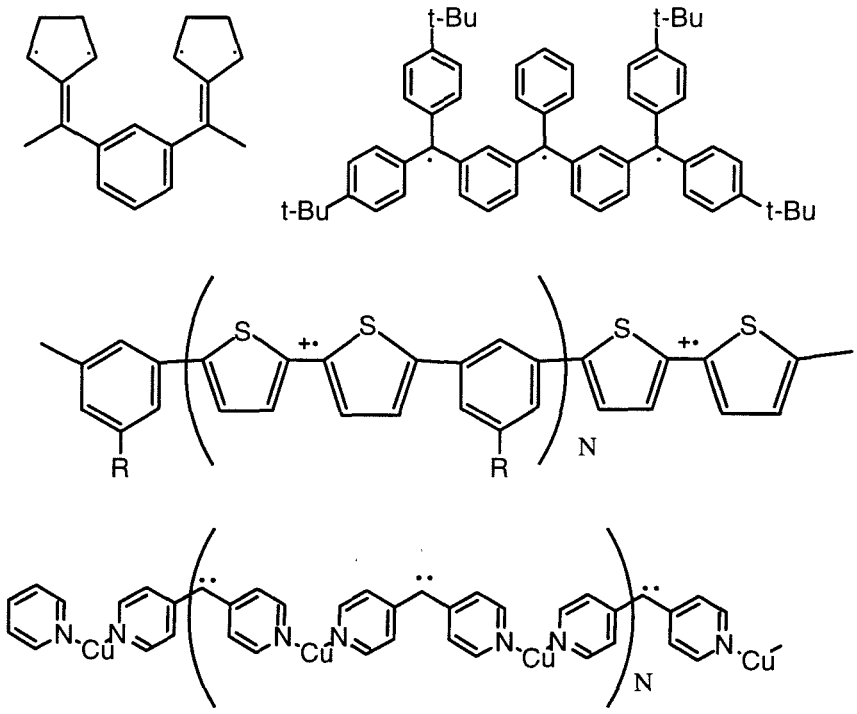

Figure 2-3 Examples of high-spin systems with various SCs and FCs

The pertinence of a potential SCs depends critically on their chemical stability and accessibility. In order to observe the designed high-spin species, the spins must be generated with very high efficiency at a temperature where they are stable. Failing to meet this standard can cause interruptions in the coupling pathway and can greatly diminish the ferromagnetic interaction.

Magnetism in One-Dimensional and Two-Dimensional Systems

Figure 2-3 demonstrated examples of spin alignments in linear arrays. However, real ferromagnetism is a three-dimensional phenomenon and it is necessary to study compounds with higher dimensionality in order to

understand more advanced magnetic behaviors. The scheme in Figure 2-1 is a linear model. However, it can be easily extended to the two-dimensional system as in Figure 2-4.

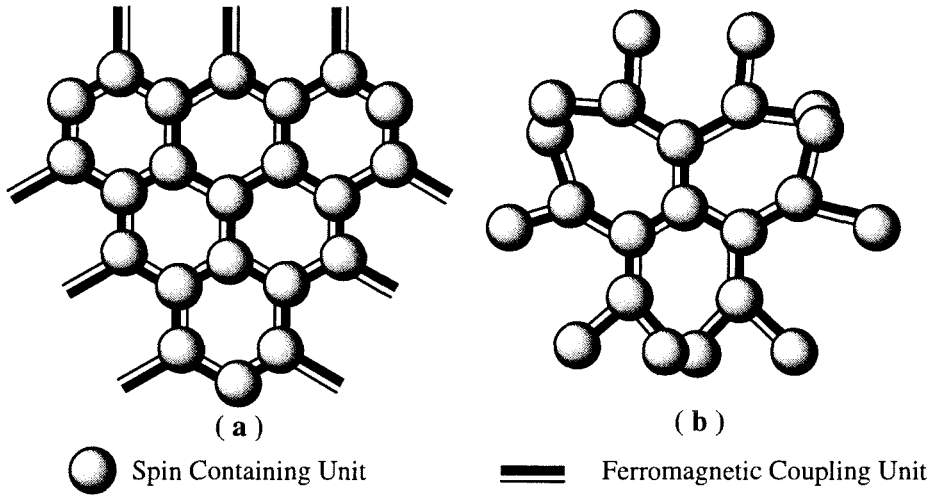

Figure 2-4 Magnetization in two-dimensional molecules

The major advantage of studying magnetism in higher dimension is that the network of high-spin interaction can be preserved in the presence of defects. In the real world, some SCs in the system can lose the spins for various reasons. This is especially true for organic radicals that are usually somewhat unstable. When a defect appears, the system not only misses a spin, but also loses some of the networks that communicate all other sites. In a linear system, this inevitably leads to two isolated fragments each of a lower spin state (Figure 2-5a). In a two-dimensional system, however, most spins can still interact with each other through the cyclic structure and maintain the high-spin coupling through alternative pathways (Figure 2-5b).

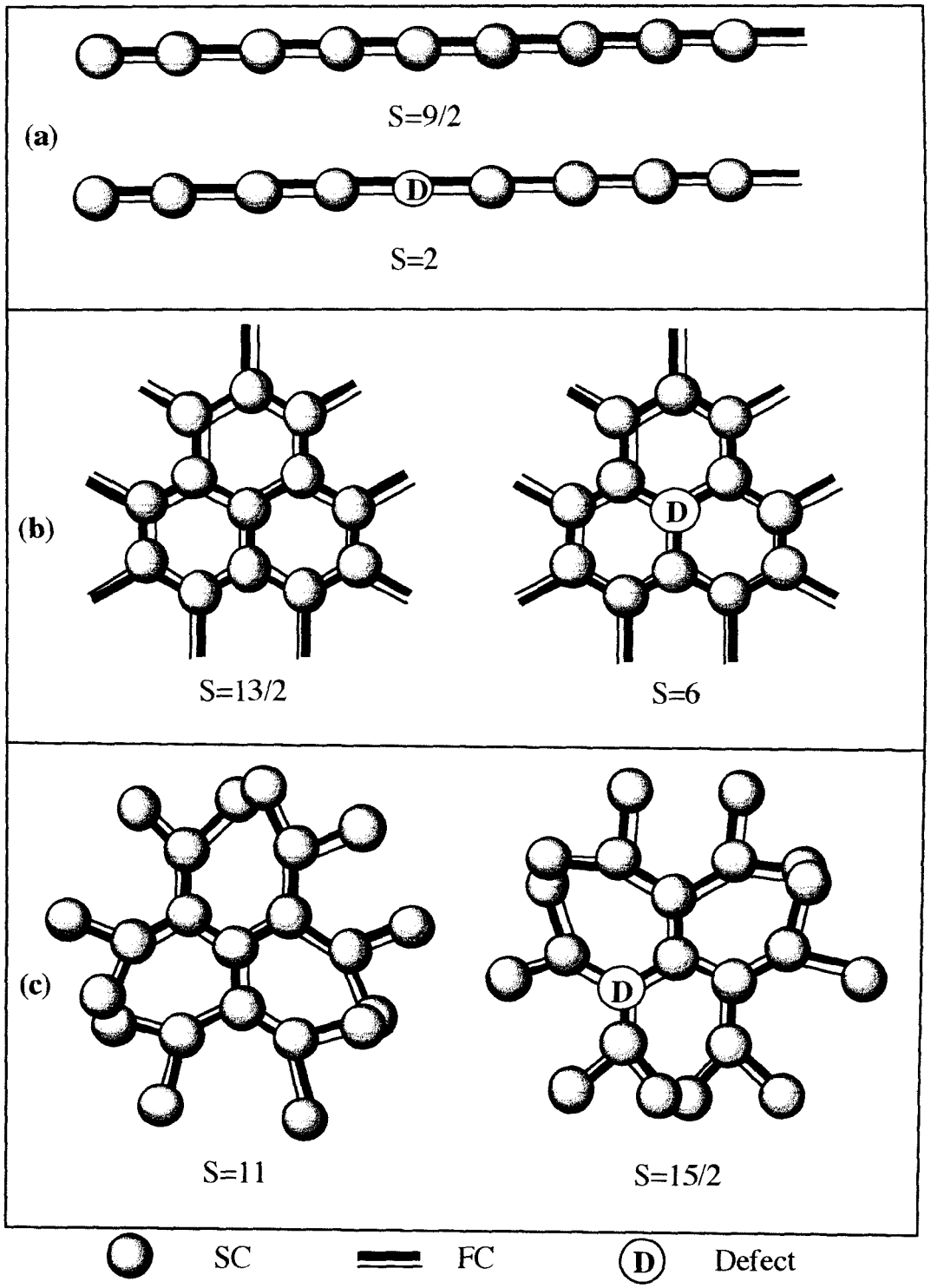

Figure 2-5 The effects of defect in linear and two-dimensional systems

Even without the cyclic arrangement, the branching in network structures alone can lessen the impact of defects. This is best demonstrated in Figure 2-5c. This system has no cyclic structure motif, but it is branched at every site except at the peripheral ones. The importance of a site in conducting the magnetic interaction depends on its location. The outer sites are less important and can become defected without greatly impairing the S value. On the contrary, when a defect happens near or at the center of the spin assembly, the decline in S will be quite dramatic. However, statistically, defects are more likely to happen at peripheral sites. For example, in Fig. 2-5c, the chance of a defect at the core is less than five percent. If a defect arises at the next layer (with approximately 14 percent chance), more than sixty percent of the spins in the system are still high-spin coupled. Other than purely statistical reasons, electronic and steric factors can further protect the center units from becoming defected.

Studying magnetism in these network systems has offered both challenges and opportunities to physical organic chemists. The goal of this project is to synthesize high-spin polyradical with higher dimensionality and hope to gain new insights into magnetic interactions in general.

General Design Criteria

The lack of structural information is one of the major problems in investigating magnetism in organic compounds. Because the paramagnetic nature of the samples, NMR become powerless. EPR and related techniques are only moderately helpful in determining the structure. Indeed, some of the most interesting materials produced in early studies are poorly characterized, intractable or insoluble solids. Notable examples include Torrance's iodine complex of poly(1,3,5 triaminobenezene)[13] and Ota's

COPNA resins[14]. The flaw of these studies is that the polymerization and introduction of spins are achieved in one single step. No diamagnetic precursor polymer of known composition is ever isolated. While the technological significance of these materials can not be overlooked, they provide little insight regarding how magnetic interaction is effected by molecular structure. In this project, a major goal is to isolate pristine diamagnetic polymers and to characteriz them with conventional physical tools to the fullest extent before spins are introduced. In this way, we can be much more confident about the composition and topology of the polymer and therefore achieve a deeper understanding of the structure-property relationships concerning magnetism.

The low solubility of planar conjugated polymers has long plagued the conducting polymer field ever since its beginning. Polyacetylene and polyphenylene, for example, are both insoluble and infusible. Polymer chemists have developed several standard techniques to solve this problem. In preparing magnetic polymers, the solubility is not only necessary for polymer characterization, it is even more important for an efficient spin-generating reaction at a later stage. Therefore, structural motifs that might lead to low solubility, like planarity and rigidity, should be avoided in the design.

As mentioned before, one of the major benefits of a network structure is the cyclic arrangement of spin containing sties. Unfortunately, such crosslinking can dramatically reduce the solubility of a polymer because the extra rigidity imposed by the cyclic structure. Furthermore, the synthesis of polycyclic structures presents a formidable challenge. Rajca recently reported the largest of such compounds, which contains three fused rings and requires ten synthetic steps with less than 0.001 percent

yield. Because the numerous difficulties cyclic structures might invoke, this project focuses on how the branching of a network structure can effect its magnetic behavior.

In the past decade, organic and polymer chemists have developed tactics to make highly branched structures. The name "dendrimer" was given to this class of compounds because of their extensive branching[15]. The standard procedure of making dendrimers is the "convergent" approach developed by Frechet[16] and Moore[17] (Figure 2-6). Some dendrimers are now produced in very large quantity and available from Aldrich. The success of a convergent synthesis lies in a well masked reactive group, a clean unmasking procedure, and a highly efficient coupling reaction. It takes one deprotecting-coupling cycle for the polymer to grow an extra layer. Although the basic concept is quite straightforward, some refinements are always necessary for synthesis of every new type of dendrimers and this usually requires tremendous synthetic effort[18].

The other class of branched polymers is much more synthetically accessible. Instead of using the Frechet-Moore strategy to make well-defined molecular architectures, Webster and Moore have published an approach to make highly branched polymers in one step by polymerizing an A_2B type monomer[19] (Figure 2-7).

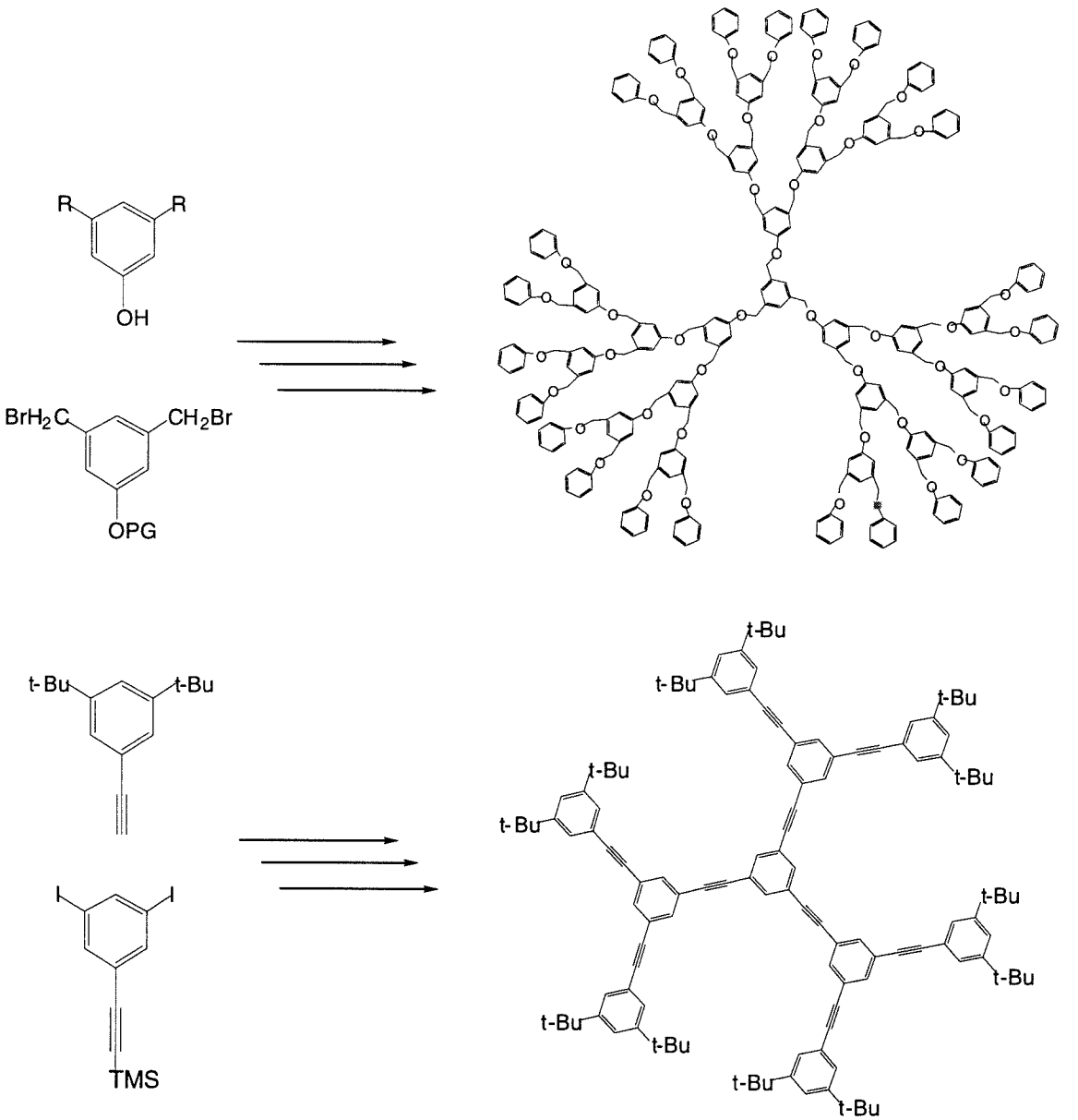

Figure 2-6 The Frechet-Moore convergent approach to dendrimers

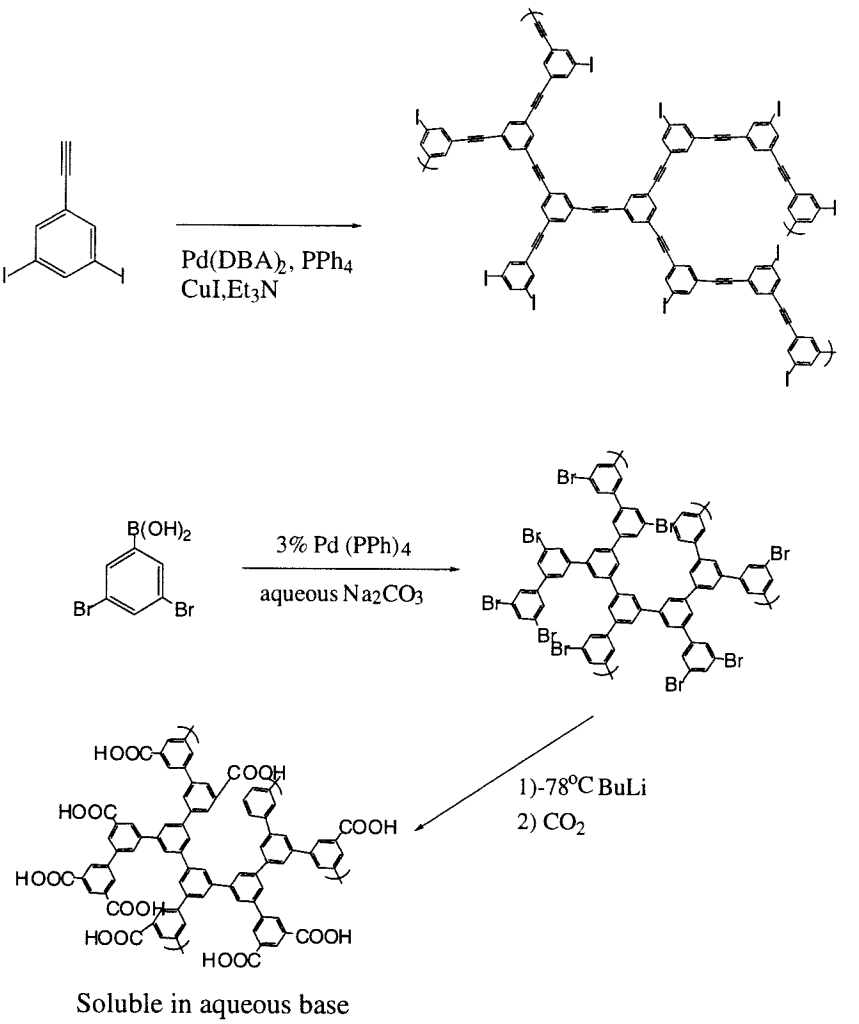

Figure 2-7 Hyperbranched polymer synthesized with one-pot reactions with A_2B monomers

The products of such polymerization are inevitably mixtures of polymer molecules with various degrees of branching. Webster first proposed the nomenclature-"hyperbranched polymer"- to distinguish them from the real dendrimers. This name is now well accepted by polymer chemists[20] and will be used thereafter.

All hyperbranched polymers have three types of topologically distinct sites. Statistically, twenty-five percent of all monomer units are branched

and another twenty-five percent are peripheral. The rest of the sites have the topology just like that in linear polymers. As mentioned earlier, the branching and peripheral sites can reduce the deleterious effect of defects on the ferromagnetic interaction. Therefore, hyperbranched polymers should persevere one of the important benefits that make dendrimeric structures desirable in making magnetic polymers. Yet, their synthesis is obviously much simpler.

As for their solubility, because the A_2B type monomer is used, at no time can more than one B group appear on one polymer molecule during its growth. As a result, intramolecular crosslinking in such systems is kept at a minimum level. Consequently, hyperbranched polymer is generally quite soluble in common organic solvents (tetrahydrofuran, benzene, CH_2Cl_2). This is crucial for their characterization and subsequent reaction to produce radicals. (Although, in principle, similar branching can also be achieved with a A_2+B_3 type bimolecular polymerization, polymers produced in such a way are usually heavily crosslinked and therefore insoluble. We made very little effort to exploit this possibility.) The basic idea in this work is to synthesize the hyperbranched molecular architectures, then transform them into polyradicals and finally explore their magnetic interactions.

Choices of SCs and FCs

The judicious choice of SCs and FCs is pivotal to the success of achieving high S values. Most organic radicals are unstable and usually undergo oxidation, hydrogen extraction or dimerization to give diamagnetic products. Extensive conjugation is frequently employed to stabilize a radical. Steric hindrance can also render protection to radicals

against those decomposition reactions. Although these tactics improve the stability of individual spins, they can dramatically reduce the ferromagnetic interactions between SCs. In the design paradigm (Figure 2-1), the FCs align spins in the SCs as in biradicals. In the real world, the energetic preference for the alignment is factored by the square of spin concentration (or the molecular orbital coefficient) at the connecting point. Therefore, if the SC is extensively conjugated, the ferromagnetic coupling can become very weak. The force can be so weak that it is easily overcome by thermal energy or the natural tendency for electrons to pair up. When bulky groups are incorporated to protect the SCs, the interaction can also be diminished because of the twisting imposed by these sterically demanding substitutions. A very delicate balance must be reached for any system to succeed.

According to Webster's study, the most convenient synthesis of hyperbranched polymers is essentially a one-component polymerization with all three functional groups (A_2B) in one molecule. To achieve maximal degree of branching, it is preferable that all three groups are kept spatially separated and thus react independently. This can be achieved if the monomer actually has three branches. This criteria immediately brought to mind the triphenyl methyl radicals. This class of radicals is among the most stable organic radicals and enormous synthetic and spectroscopic techniques for their study have already been developed[21]. The three reactive groups can be installed at each phenyl rings in a triphenyl methyl ether monomer. After the polymer is synthesized, the ether units can be converted into triphenyl methyl (trityl) radicals by several very well-developed procedures.

With trityl radical as the SC, there can be three choices of FCs (Figure 2-8). The most common one is *meta*-phenylene (Figure 2-8a). This

structure has been used extensively by Rajca and coworkers[22] and will not be exploited here. The other two possibilities, *m,p* -biphenylene and *p,m,p* - terphenylene (Fig. 2-8b and 2-8c), can both be perceived as extended versions of the *m* -phenylene.

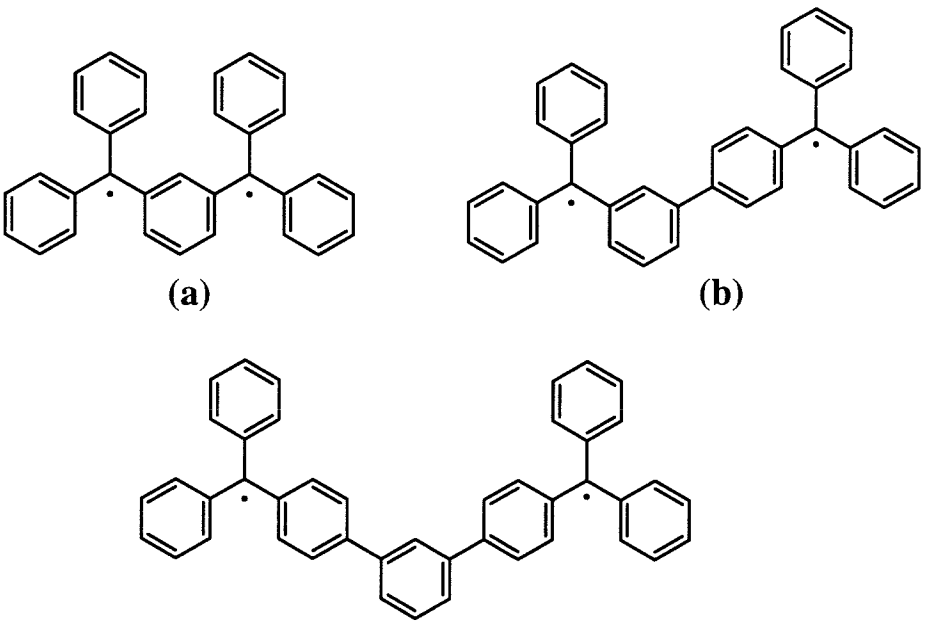

Figure 2-8. Potential ferromagnetic coupling pathway between two trityl radicals

Although experiments and theory have confirmed both structures to be valid FCs[23], *m,p'*-biphenylene is clearly the preferable one for this work. Its shorter coupling pathway ensures a stronger ferromagnetic interaction. From the synthetic point of view, Figure 2-8b can easily be disconnected into two trityl units while 2-8c requires one more phenyl group inserted in. A polymer composed of this structural motif (2-8b) can be synthesized by polymerizing a trityl ether monomer with reactive groups at appropriate positions.

Polymerization Reaction

The essence of this polymerization is to make aryl-aryl bonds with high efficiency and selectivity. The basic idea is shown below.

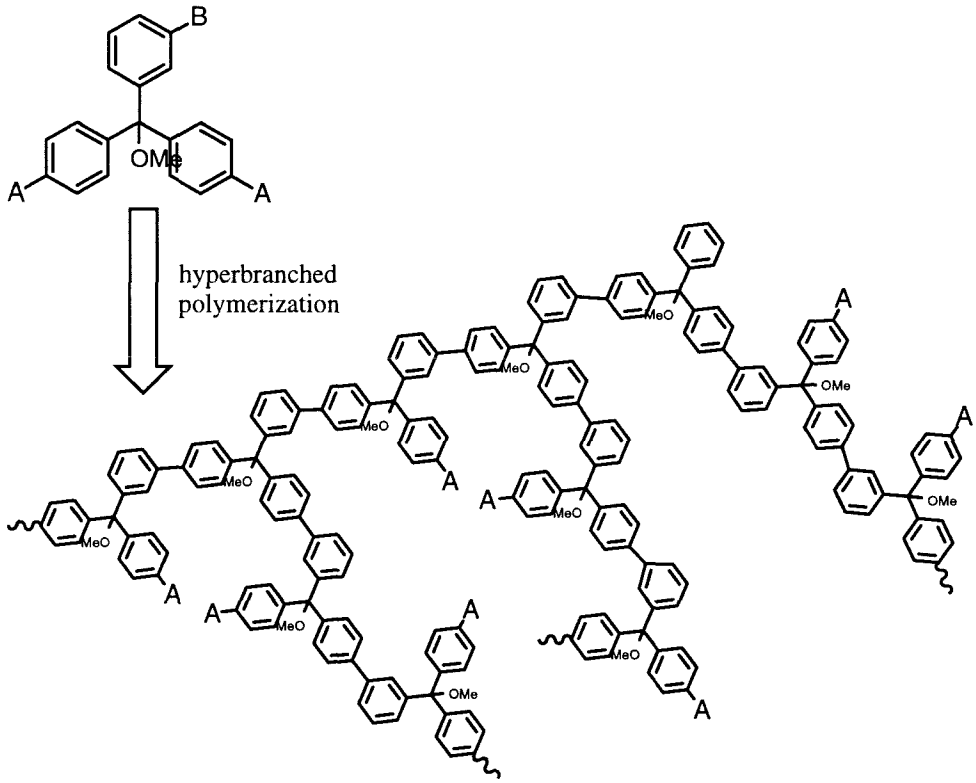

Figure 2-9. Basic synthetic strategy of hyperbranched trityl polymer

In a step-growth system, the degree of polymerization (DP) depends on the yield of reaction (ρ) as shown in Equation 2-1 and Figure 2-10.

$$DP = \frac{1}{1-\rho} \qquad (1)$$

The plot clearly indicates the molecular weight of a step-growth polymer only becomes large when the reaction yield is nearly quantitative.

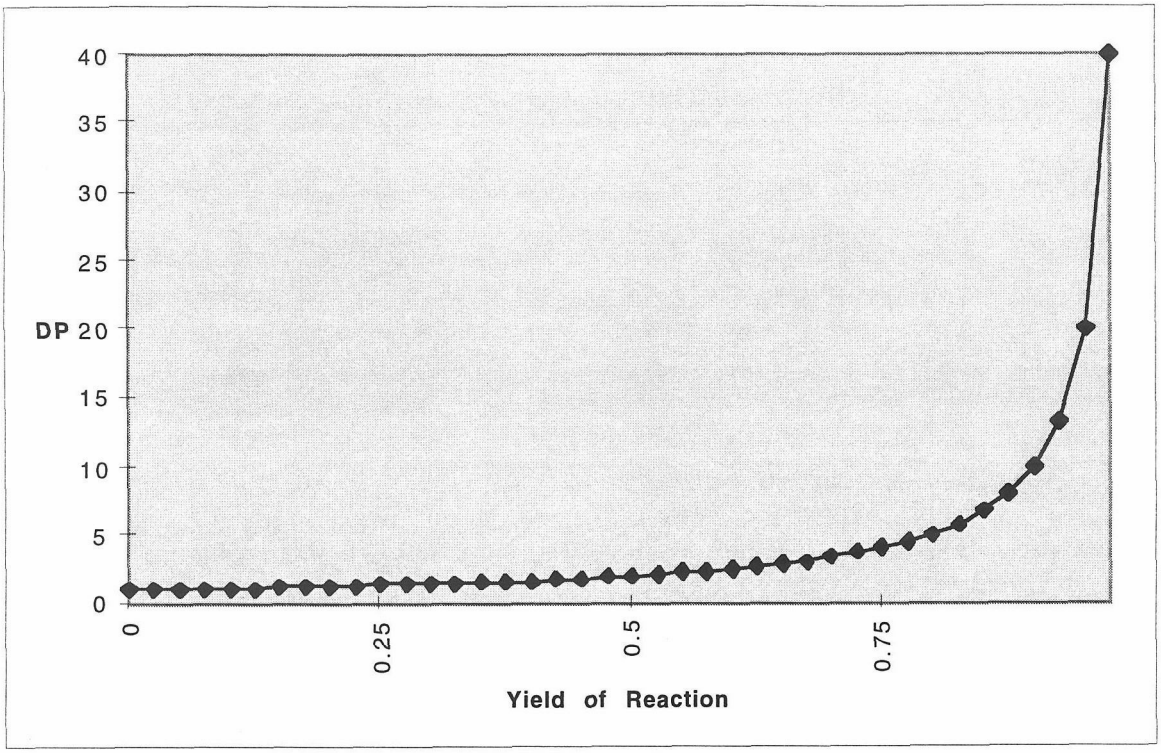

Figure 2-10 Plot of molecular weights versus extent of reaction for step-growth polymerization

In a linear step-growth polymerization, it is also extremely important that both bifunctional monomers are extremely pure. Trace amount of monofunctional impurity leads to early chain termination and the production of low molecular weight oligomers. Hyperbranched polymerization, however, is much less sensitive in this regard. Since one of the coupling partners is intrinsically in excess, the impurity, although inevitably reduces degree of branching, has much less detrimental effect on the DP. This is particularly important if a monomer is hard to purify.

A high reaction selectivity is crucial to ensure the long range ferromagnetic interaction. For example, in Figure 2-9, every time a coupling reaction occurs between two As instead of an A-B pair, a strong antiferromagnetic interaction is introduced into the system. Hence, for this

purpose, any reaction that has the tendency to cause homocouplings should be avoided

Palladium Catalyzed Reaction in Polymer Synthesis

The cross coupling reaction between two aryl groups is one of the most useful synthetic reactions. The earliest example is the nickel catalyzed coupling between aryl halides and aryl Grignard reagents reported by Kumada[24]. Group VIII transition metals, particularly nickel and palladium, are among the most effective catalysts. Variations on reactive partners, reaction conditions and phosphine ligands have all been extensively studied to improve the yield, selectivity and functional group tolerance[25]. The generally accepted catalytic cycle is shown below.

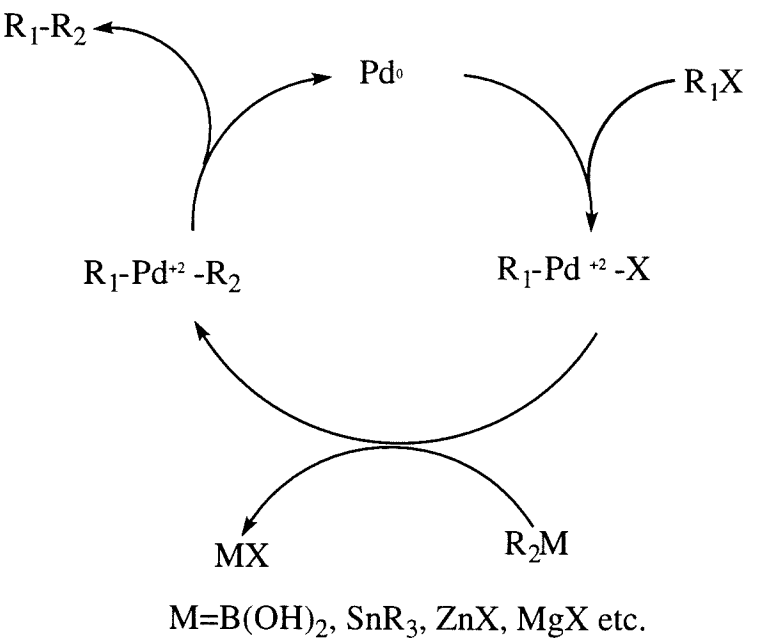

Figure 2-11 General catalytic cycle for Pd-mediated cross-coupling

The oxidative addition of aryl halide to the low valent metal produces an electrophilic metal center. Aryl nucleophile then substitutes the halide to

give a diary metal complex. The reductive coupling then gives the biaryl product and regenerates the low valent metal to complete the catalytic cycle. Aryl bromides or iodides are usually used because they tend to be more reactive in the oxidative addition step. Many organometalic compounds have been employed as nucleophiles. Utilization of organozinc compounds has been extensively investigated by Negishi[26]. Stille elegantly demonstrated the application of organic tin compounds to this purpose[27]. In 1980, Suzuki reported that arylboronic acids can undergo facile cross-coupling with aromatic halides in the present of aqueous base and palladium(0) catalyst[28]. This reaction meets all the standard of a polymerization reaction. Organoboronic acids are moderately stable to moisture and oxygen and thus allows the A_2B monomer to be isolated in pure form. The side product in the reaction, boric acid, is non-toxic and can be easily removed. In the last decade, the protocol has been used in the synthesis of various soluble conjugated polymers with great success. Notable examples include several soluble poly-*p*-phenylenes[29], planarized poly-*p*-phenylenes[30] (Figure 2-12) and dendrimers[31] . Specifically in this project, in order to apply the Suzuki's reaction, functional group A and B in the monomer in Figure 2-9 should be bromides and boronic acid respectively.

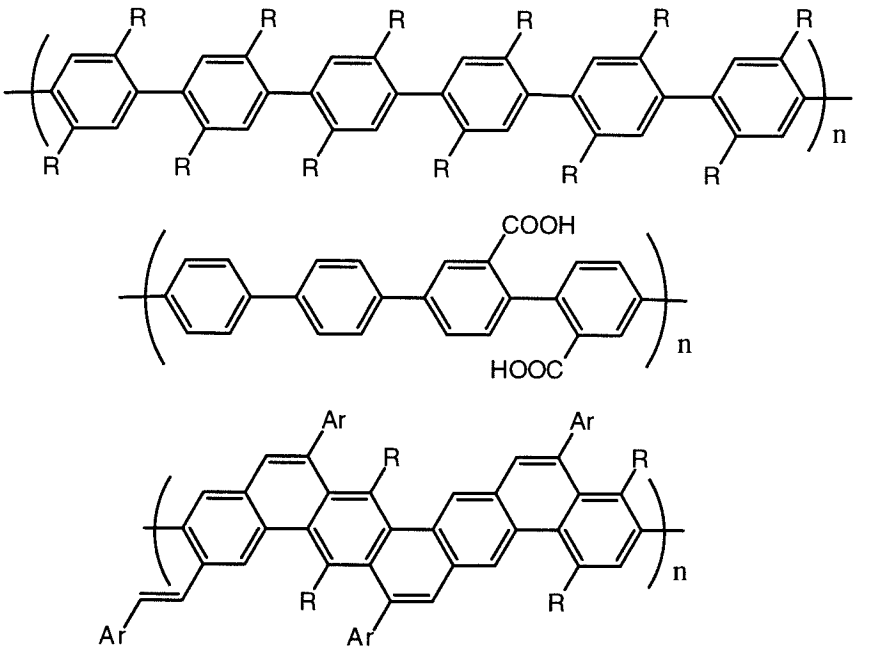

Figure 2-12 Aromatic rod-like polymers synthesized via Suzuki's coupling reaction

Two occasionally overlooked problems in palladium catalyzed polymerization are worth pointing out. Although, in principle, the molecular weight of the polymer increases as the efficiency of the polymerization reaction increases, there are more complicating factors in a real operation. One of the major efforts to improve the coupling reactions has focused on to increase reactivity of palladium catalyst. Several highly dissociative phosphine ligands have been used to facilitate the coordination of substrates to the metal center[32]. Even a ligand-free system of "naked" palladium has been developed[33]. Indeed, these new conditions do give impressive coupling yields for some very unreactive substrates. However, in order to produce high molecular weight product, a catalyst must also be stable in the time scale of polymer growth. Unfortunately, these highly reactive species without supporting ligands do not always meet this

requirement. They sometimes produce only oligmers before the catalyst decomposes.

The major side reaction of Suzuki's coupling is the hydrolytic deboronation which sometimes leads to dismal yields. This problem is elegantly solved by a non-aqueous modification of the original Suzuki condition. In the new procedure, the system is switched from nonpolar solvents (THF or toluene) to polar ones (DMF or dimethoxyl ethyl ether)[34]. Unfortunately, this new condition is not always compatible with polymer chemistry since most conjugated polymers are not very soluble in these polar solvents. The products usually precipitate from the solution long before high molecular weight is reached. Finding the optimal condition for the polymer synthesis thus involves balancing various delicate factors.

Monomer Syntheses

There are two well established procedures to make arylboronic acids. One utilizes highly reactive aryl lithium or Grignard reagents and react them with trialkyl borate[35]. The second one is the metathesis reaction between an aryl trialkyl silane and boron tribromide[36]. It seemed obvious at first that the second approach would have much better functional group tolerance since it does not employ organometalic reagent. However, this fairly general protocol failed to produce any arylboronic acid product when a trityl ether substrate is subjected to the standard condition. Prolonging the reaction time or raising the temperature did not give better results. More surprisingly, when the reaction was quenched with methanol/pyridine mixture, the starting trityl ether silane was recovered in very high yield. Such stability of an aryl silane under the treatment of strong Lewis acid is unprecedented. It is highly probably that the trityl

ether is converted into trityl cation well before the exchange between silyl group and the boron tribromide can take place. It is then conceivable that once the cation is formed, its overwhelming electron withdrawing power reduces the nucleophilicity of silane so much that is becomes completely inert to the metathesis. After this first setback, we directed our effort toward the organometalic approach.

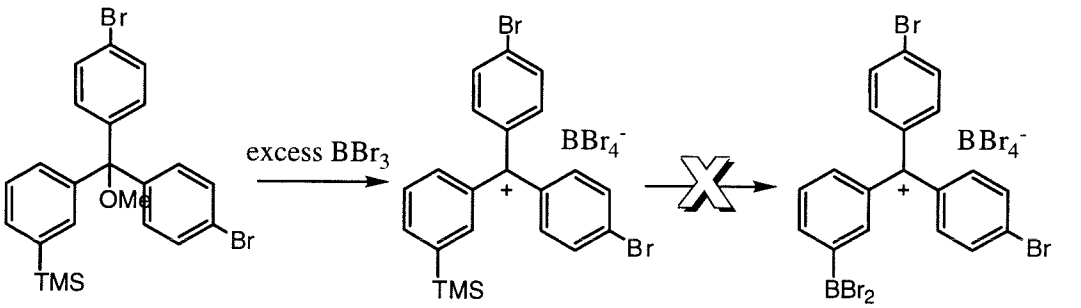

Figure 2-13 Unsuccessful monomer synthesis using the silicon-boron exchange reaction

The synthetic applications of organolithium and Grignard reagents have long been hampered by their incompatibility with other functional groups. Specifically in this monomer synthesis, the problem is how to selectively generate organolithium (or Grignard) reagent at one specific site in the presence of two other aryl bromides. The major concern was the generated aryl lithium can undergo exchange reaction with the aryl bromides. This exchange can lead to the production of undesired isomeric boronic acids which are hard to separate. These impurities can cause topological defects in the hyperbranched polymer by incorporating antiferromagnetic interaction in the network. Although halide-containing aromatic lithium reagents are well documented in the literature[37], most of these compounds carry chlorides and fluorides that are much less reactive towards the

exchange. Also, when both the lithium and bromide are on the same aromatic ring as in those examples, electronic effect usually inhibits the second exchange at low temperature[38]. Yet, the target monomer here does not have this advantage.

To solve this problem, the basic idea is to take advantage of the different reactivities between aryl bromides and iodides towards lithium-halogen exchange reaction. Although the selectivity towards carbon-iodide bond is warranted by thermodynamics, the practical synthetic condition for such an elaborated system has never been documented to the best of our knowledge. Fortunately, the optimal condition for this selective exchange was found to be as following. When the reaction is conducted at -96°C to -98°C in diethyl ether with one equivalent of n-butyl lithium, the desired monoboronic acid can be isolated after the aryl lithium is quenched with 4-5 equivalents of trimethyl borate. This simple condition are also applicable to other similar compounds. It is the key synthetic reaction for this project. On the other hand, the all *meta* isomer **3** and all *para* isomer **4** are synthesized from the tribromide precursors because contamination from isomeric boronic acid is no longer a concern. Figure 2-14 shows the synthetic scheme for all four regioisomers of this monomer.

The strategy is very straightforward. The triaryl methyl alcohol was assembled with a simple double Grignard addition to the ethyl iodobenzoates. The preparation of bromophenyl magnesium bromide has already been reported[39]. (It is worth pointing out that substituting Grignard with aryllithium reagent leads to insoluble polymeric products. Apparently, the lithium-iodide exchange is faster than the addition to the ester group in this case.) The alcohol was converted to methyl ether with a large excess of sodium hydride and methyl iodide. The iodide (or bromide) group was

then transformed into boronic acid with the standard condition in moderate to high yield. Purification can be carried out with simple flash chromatography.

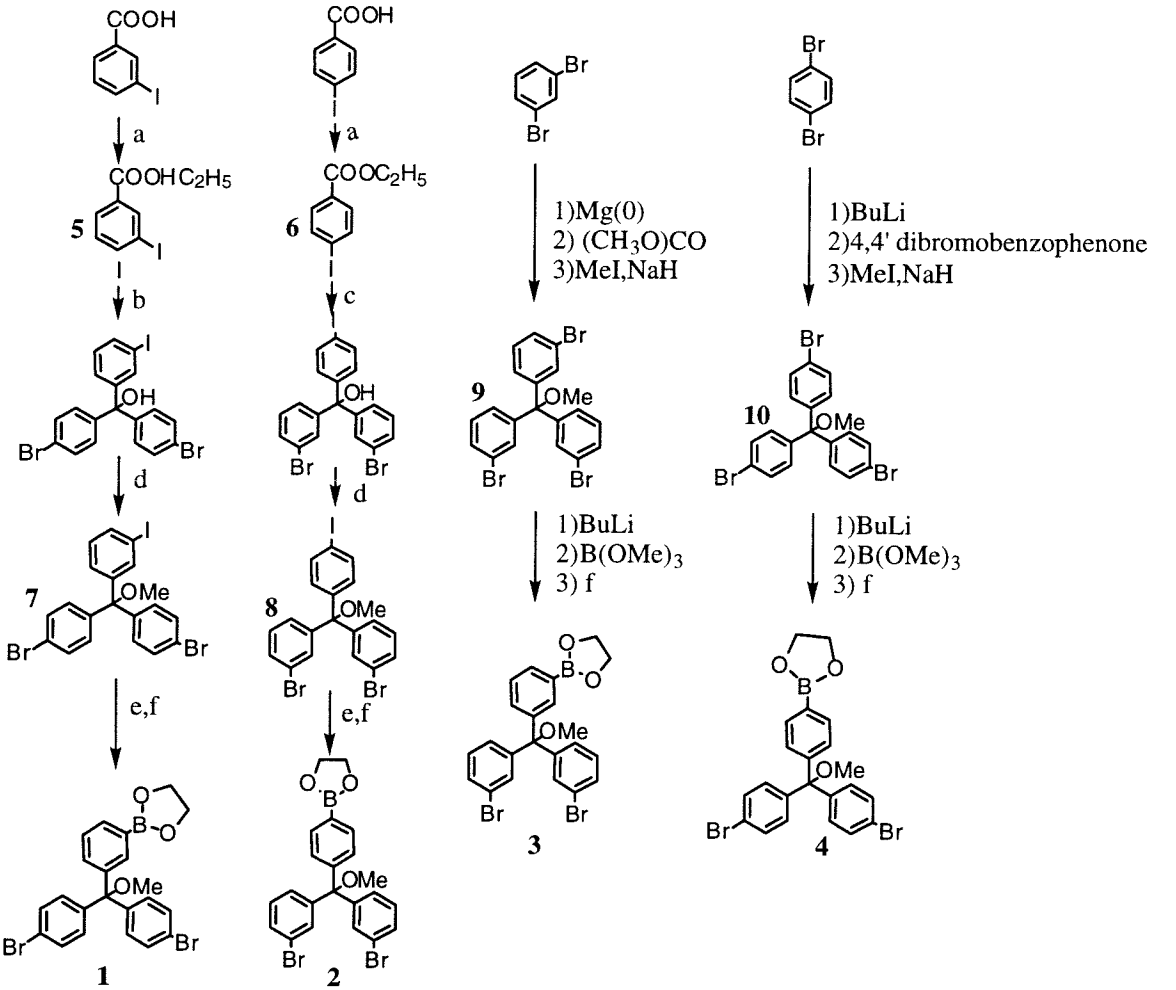

a) C_2H_5OH, cat.H_2SO_4 azeotropic distillation
b) p-bromophenyl magnesium bromide in refluxing benzene-ether
c) m-bromophenyl magnesium bromide in refluxing benzene-ether
d) NaH, MeI
e) 1.05eq n-BuLi added at -98C, 4-5 eq of B(OMe)3 added after 40 min
f) ethylene glycol, benzene azeotropic distillation

Figure 2-14 Syntheses of isomeric trityl monomers for hyperbranched polymerization

It is well known that pure boronic acids tend to form oligomeric anhydrides which sometimes make the characterization difficult. Thus the products were converted to their ethylene glycol esters to avoid such complication. This modification has no effect on the reactivities of boronic acids in subsequent Suzuki's reaction.

Polymer Synthesis and Characterization

As mentioned earlier, to maximize the degree of polymerization (DP) in such a system requires a delicate balance of such factors like the reaction yield, catalyst stability and polymer solubility. Fortunately, the solubility of hyperbranched polymers are generally good and need no optimization. From some early studies[40], it was revealed that tetrakis (triphenylphosphine)palladium (0) in reflux toluene has the sufficient stability for polymer synthesis. The remaining task is obviously to improve the reaction yield. After some trial-and-error effort, it became clear that the determining factor of DP is the monomer concentration. The optimal monomer concentration for the polymerization is 0.5M. The amount of catalyst is unimportant as long as more than 0.02 equivalent is used. The standard reaction time is 48-72 hours. Continuing the reflux beyond this point does not produce polymers with higher molecular weights. On the contrary, longer reaction time tends to decrease the yield because some of the materials become insoluble. Two equivalents of aqueous potassium carbonate is used as the base. The abbreviated nomenclature of the polymers are listed as the following.

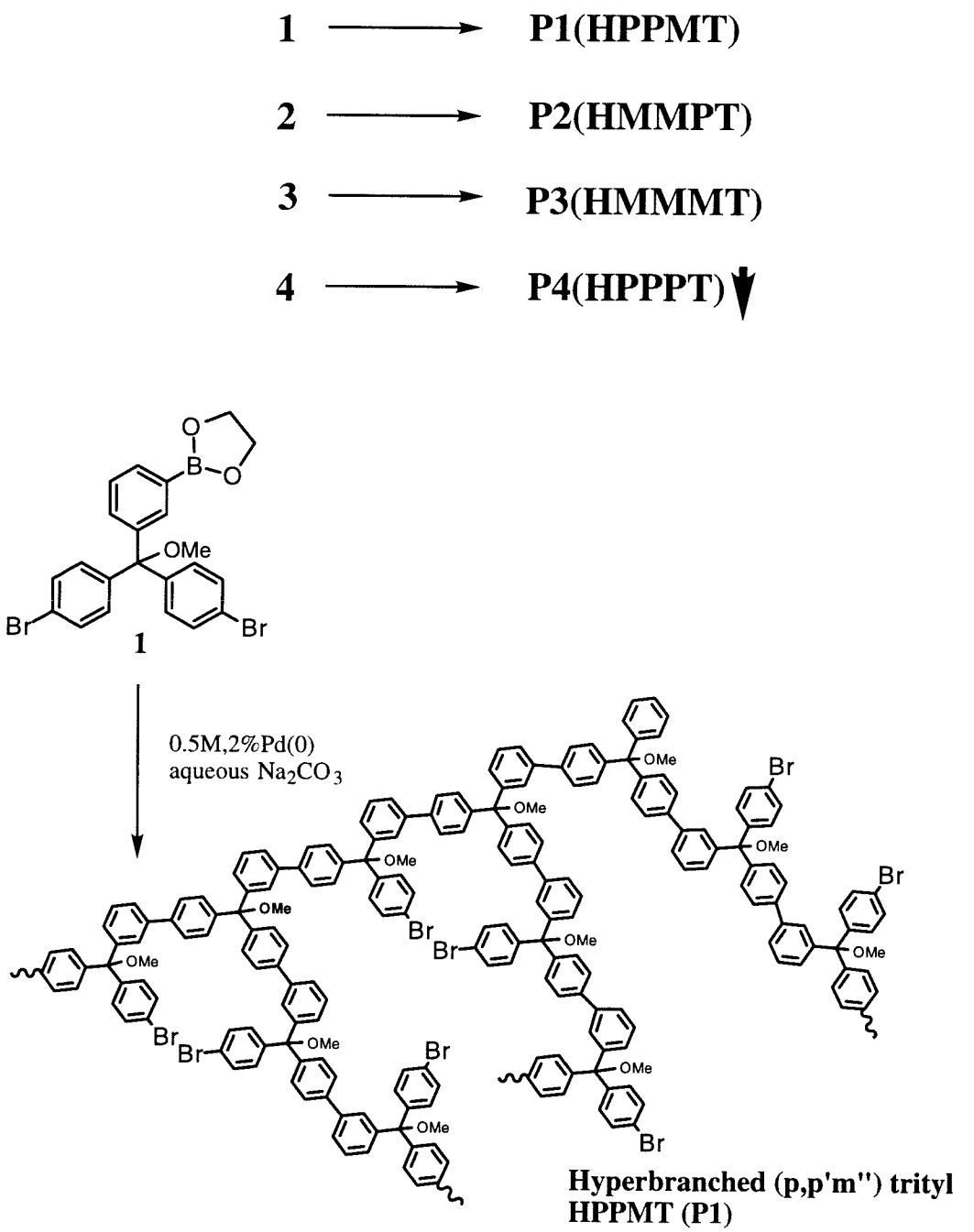

Figure 2-15 Hyperbranched polymerization of **1**

Except for **4**, all monomers give soluble hyperbranched polymers in almost quantitative yields. For the polymerization of **1**, **2** and **3**, the polymers remained at least partially soluble during the reactions. In

contrast, polymerization of **4** led to insoluble precipitation in just 40 minutes. This might be due to the symmetry of *p, p'*-biphenyl structural motif. The product can not be redissolved in any common solvents. Carrying out the polymerization at lower concentrations gives the same result. No further effort was directed towards solublizing this polymer. It is neither characterized nor converted to polyradical.

The proton NMR spectra of all three soluble polymers give very broad peaks due to slow tumbling of the polymer molecules as typically observed for all high molecular weight samples. The broadening might be even more severe in hyperbranched system because of the presence of more structurally distinct sites. Despite the crude feature in the spectra, the absence of boronic acid end group is evident. The lack of contamination from triphenylphosphine oxide and other low molecular weight side product can also be confirmed.

Neither IR nor UV/visible spectroscopy is very informative for characterizing these polymers. The IR spectra shows only C-H stretching absorption typical of any hydrocarbon. Not surprisingly, the UV spectrum of **HPPMT** is almost indistinguishable from that of pure biphenyl. This is expected because the most extensive conjugation in these polymers before doping is exactly the biphenyl system.

In a hyperbranch polymerization, in contrast to the linear ones, one reactive group is in excess of the other. Consequently, at the end of the reaction, the polymer still contains that fuctional group. In the present case, when the DP is large enough, the polymers should carry roughly one bromide per monomer on average. This is confirmed by elemental analyses. However, the actual percentage of bromides is always a little lower than one per monomer. This abnormality can not attribute to a low

degree of polymerization because the oligomers should have a bromide per monomer ratio larger than one. A more reasonable explanation is the reductive debromination catalyzed by the palladium complex. It is well known that phosphine complexes can undergo intramolecular oxidative addition of C-H bonds in phosphine ligands to the metal center[41]. This generates a palladium hydride species which can then reduce C-Br bond. Fortunately, such loss of bromides should not eradicate the design ferromagnetic interaction. Another possible way to account for the loss of bromides is by the intramolecular coupling of two arylbromides. However, such homocoupling reaction is usually catalyzed only by nickel complexes and often requires more than one equivalent of the metal[42].

Gel permeation chromatography (GPC) is the most reliable way to determine the molecular weight and polydispersity of a polymer. The retention time of polymer is indicative of its molecular weight and the polydispersity can be deduced from the width of the elution profile. Polystyrene standards are usually used for the calibration. However, GPC meets its limitation as an analytical tool for hyperbranched polymers. First, the calibration using linear polystyrene might not be valid for a branched system. Second, unlike linear polymers, hyperbranched polymers can have enormous structural variations even for molecules with the same molecular weight. As a result, GPC data inevitably exaggerate the polydispersity of a hyperbranched polymer. Therefore, this technique can only give very rough estimations of the molecular weight at its best.

Unlike the linear polymers, the chromatogram of these hyperbranched polymers give bimodal distributions. **HPPMT**, **HMMPT** and **HMMMT** all show the same peculiar feature in the analyses. (This phenomenon is unique to hyperbranched system. A linear trityl polymer was synthesized as

the control and behaves normally.) This could mean that there are two groups of molecules with very different molecular weights. However, since GPC is a size-dependent chromatography technique, it may as well imply two groups of molecules with distinct shapes. The second explanation seems more plausible to the hyperbranched systems where molecular shapes can be greatly influenced by the degree of branching. More recently, a very similar observation was reported by Moore in hyperbranched polyphenylacetylene[43].

Since GPC usually underestimates the molecular weight of dendrimers[44], it seems more appropriate to use the first peak in the bimodal distribution in calculating the molecular weight. (Also, part of the second peak lies well out of the reliable range of GPC. Employing these figures led to unreasonably small molecular weights that contradicts the line width in NMR experiments.) From such truncated data, the number average molecular weights indicating an average of 50-150 monomer units per polymer network. Admittedly, judged by the standard of polymer chemistry, the polydispersity is unacceptably large[45]. Nevertheless, this is not relevant for the purpose and there was no attempt to improve it.

The branching point is the central feature of this design. Unfortunately, it is quite difficult to determine the degree of branching unambiguously. As mentioned earlier, there are three types of topologically distinct sties in a hyperbranched network. Statistically, one fourth of the sites should be branching points. In the actual reaction, the degree of branching depends on the reactivity of the aryl bromides on different molecules. For the parent polymers, it is not possible to distinguish the three different sites from NMR spectrum. One important clue might come from a cognate polymer which was made independently for a related project (Figure 2-

16). In the NMR spectrum, the methine proton of this polymer appear at 5-6 ppm and clearly divides into three groups. This observation strongly suggests a substantial degree of branching in this system. Although it not yet possible to specify which peak corresponds the branching units, the distribution appears to be roughly statistical.

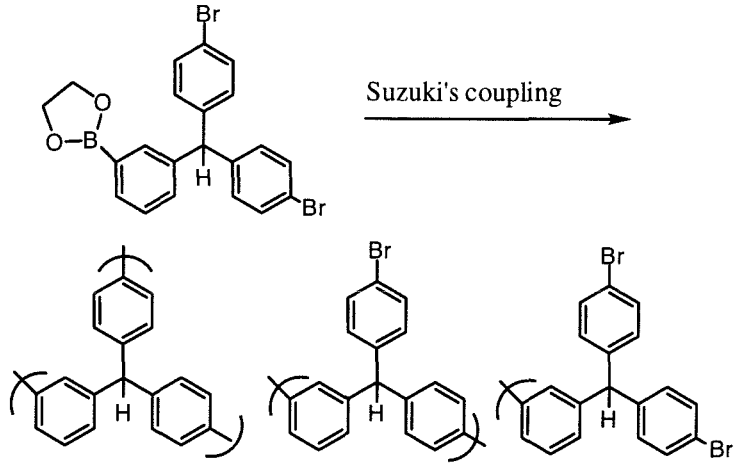

Figure 2-16 Three types of sites distinguishable in NMR spectrum in a model polymer

Conversion of Polymers to Polyradicals

There are many procedures to transform trityl derivatives to trityl radicals ranging from electrochemistry to γ irradiation. However, the purpose of most of these early studies is just to record the EPR spectrum of radical species. Because of the sensitivity of EPR spectroscopy, the yield was never a major concern. In contrast, the procedure to be used here must have very high yield to avoid large number of defects in the polyradicals. The reaction condition must also be carefully adjusted so that the radicals can survive after they are generated. For example, since the radical units can be unstable at elevated temperature, the ideal condition would be, so

long as the yield is good, to keep the sample at low temperature for as long as possible. Three possible protocols are shown below.

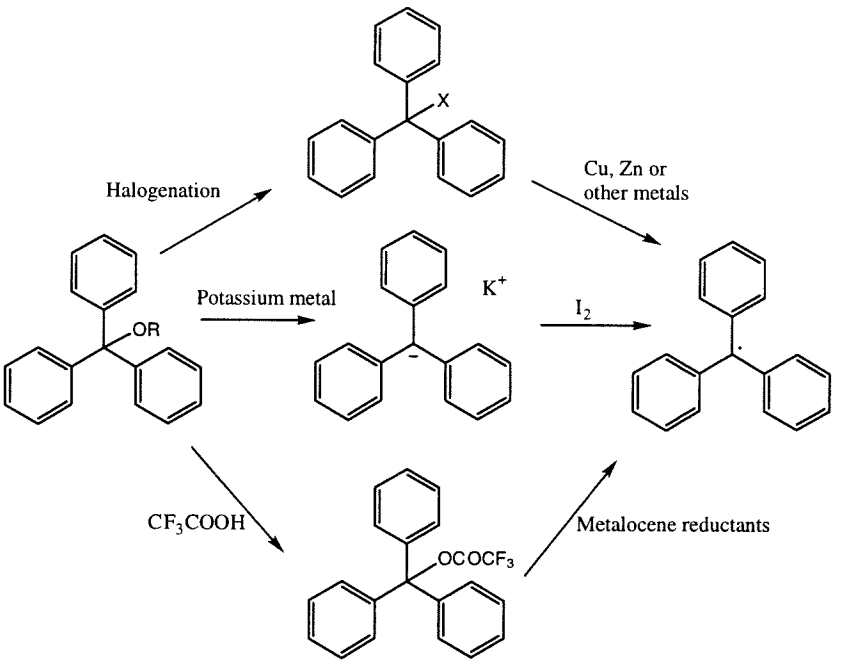

Figure 2-17 Three efficient methodologies to convert trityl ethers into radicals

The first method is the most classical synthesis of trityl radical[46]. The trityl ether is first converted into halide which is then reduced to radical by heterogeneous metal reductants. Zinc and copper are the most common choices. The second way is developed and perfected by Rajca and coworkers[47]. The trityl ether is first reduced to trityl anion with highly reactive alkali metals at room temperature. The anion is then oxidized to radical with I_2 at -100°C. Under careful control, this reaction sequence produces trityl radicals in almost quantitative yield. In the third procedure, the alkoxyl group is first transformed to a leaving group-trifluoroacetate. This intermediate is then reduced by a soluble metalocenen reductant. The

basic concept here is very similar to that of the first approach. However, this method is preferable because of some operative details.

Several difficulties were encountered with the first approach. Since the trityl halides are somewhat water sensitive, it is important that the halogenation step can be worked up with minimal exposure to moisture. For small molecules, this is usually achieved by crystallization. But in a polymeric system, it is hard to remove the side products (phosphoric acid, Lewis acid etc.) without water extraction. Also, due to its heterogeneous nature, the reduction step has to be conducted in reflux benzene and the polyradical might decompose at such temperature.

Rajca's reduction-oxidation approach seems excellent for this purpose. Unfortunately, the reduction step is incompatible with the bromides on the hyperbranched polymers. When **HPPMT** was treated with a large excess of lithium power in THF, the solution first turned blue, indicating the production of trityl anion. But the color dissipated in several hours and a yellow precipitation immediately followed. This yellow solid can not be redissolved in any solvents and therefore can not be readily oxidized. The precipitation is most likely caused by intramolecular crosslinking. The excess bromides still attached to the polymer can certainly undergo Ullmann type intramolecular coupling in the presence of lithium and form macrocycles inside the network. Obviously, this will severely impair polymer solubility.

The third approach was brought to our attention by Dr. Owen Webster[48]. The simplicity in generating the polytrityl trifluoroacetate was its first appeal. In a simple NMR experiment of **HPPMT**, using 1:1 deuterated TFA in chloroform as the solvent, the broad methoxyl peak near 3 ppm disappeared completely and a sharp peak grew in near 4 ppm.

The sharp peak vanished after the sample stood at room temperature for 48 hours. This result is best interpreted by the formation of polytrityl trifluoroacetate and loss of methanol. Equally importantly, there are substantial changes in the aromatic region of the spectrum. Most peaks show significant downfield shift (to 8 ppm) in the mixed solvent. This observation implies at least some of the trityl trifluoroacetate units exist as dissociating ion pairs, which is also consistent with the deep red color of the solution. After the deeply colored solution stood in room temperature for 6-12 hours, TFA and methanol were removed under vacuum and the polytrityl trifluoroacetate was isolated as a purple power. It is also worth pointing out that the NMR spectrum of the polytrityl trifluoroacetate in pure deuterated chloroform no longer exhibited the down field shifts in the aromatic region. This suggests most of the $Ph_3C\text{-}OCOCF_3$ bonds are covalent instead of ionic. The dissociative behavior observed earlier appears to be unique to TFA solvent system and is presumably due to TFA's high dielectric constant. Other hyperbranched polymers investigated here are all soluble in TFA and handled in the same manner.

The choice of metallocene reductants is quite limited. It must have the proper reductive potential range and adequate solubility at appropriate temperature. Although ferrocene itself is not reductive enough for this purpose, decamethyl ferrocene proves to be satisfactory thanks to the electron-donating power of the methyl groups. Indeed, this reagent was initially the choices for the project. But difficulty arises when we try to estimate the spin concentration in the produced polyradicals. The side product in this reaction, decamethyl ferrocenium trifluoroacetate, is a paramagnetic 17-electron species. Since the magnetic measurement does not distinguish contributions from different species, it is very hard to isolate

the magnetic behavior that can be precisely attributed to the polyradicals. The same problem occurs with nickelocene. A superior choice would be a paramagnetic reductant that gives a diamagnetic oxidized product after the reaction. Cobaltocene fits these standards perfectly. This mild 19-electron reductant is reductive enough and is turned into the 18-electron diamagnetic cobaltocenium after the reduction. Because of this preferable property, cobaltocene is used in all the later studies.

All polytrityl trifluoroacetates are moderately soluble in common solvents. The reduction was successfully conducted in methylene chloride, benzene and toluene. From these studies, it was concluded that solvents have little if any effect in the reaction. In each operation, after stirred at room temperature for several hours in an oxygen-free glove box, the reaction solution was poured into a dish to allow the solvent to evaporate. The resulting dark green solid was then subjected to magnetic measurement. Although the procedure is very simple, the polyradical is at ambient temperature through the whole process. It has been reported the S value of a high-spin polyradical decreases considerably after brief exposure to room temperature[49]. In order to keep the polyradical at low temperature during most of the manipulation, the "common" solvents like benzene or toluene were switched to two "unconventional" solvents, dimethyl ether and chloromethane. Both these "solvents" have very low boiling points and must be condensed into the reaction flask at -78°C. The major advantage is that these solvents can be evaporated at -78°C under vacuum and thus allows the polyradicals to stay at that temperature until powder samples are obtained. Although the polymers are barely soluble at -78°C, the progress of reduction is evident from the color change of the reactant. Subsequent measurements confirmed that samples produced by the method do have

higher S numbers and spin concentrations. The nomenclature of the polyradicals are shown as the following. (There is no obvious advantages of one of these solvents over the other. The less costly chloromethane is thus used in all the subsequent experiments.)

P1 ⟶ **PR1(HPPMTR)**

P2 ⟶ **PR2(HMMPTR)**

P3 ⟶ **PR3(HMMMTR)**

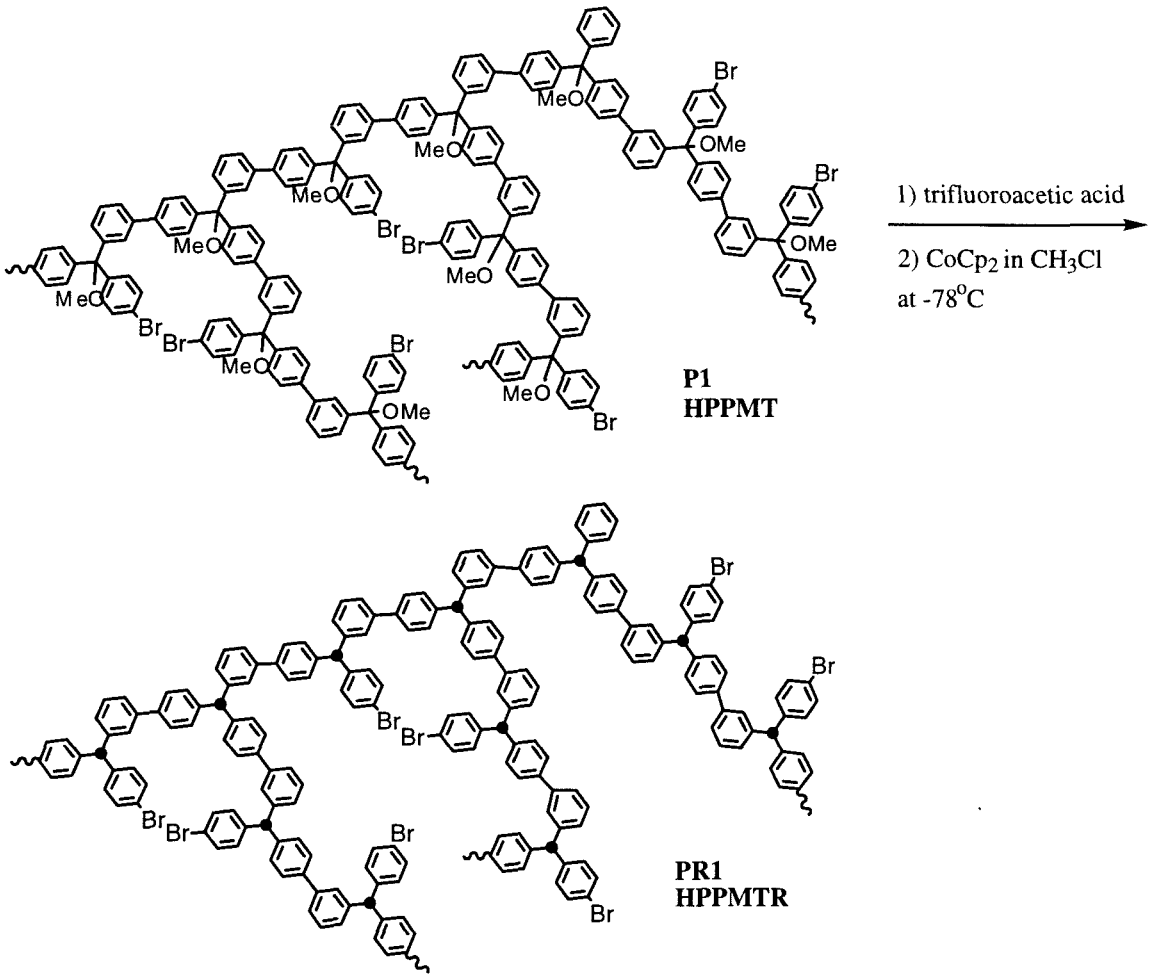

Figure 2-18 Transformation of **P1 (HPPMT)** to **PR1 (HPPMTR)**

Instrumental Concerns

For the last 50 years, EPR has undoubtedly been the most powerful tool for studying high-spin molecules. Because of its high sensitivity, paramagnetic species can be detected at very low concentration. The electron-nuclear hyperfine coupling can often unveil the electronic and molecular structure of the spin-carrying species. Variable temperature data is routinely used to estimate the energy gap between spin states. Despite its great proficiency in studying small molecules and ions, it is of limited use in the polymeric systems discussed here[50]. In a typical EPR experiment, the spin-spin interaction can broaden spectrum line width considerably by shortening the T_2 relaxation time. To avoid this complication, a high-spin sample is usually diluted in a mixed crystal or frozen solution matrix. However, in this study, since the efficiency of radical generation is only moderate, there are usually numerous chemically non-equivalent magnetic centers just in one polymer molecule. These "spin islands" can give rise to a vast array of magnetic transitions, all broadened by mutual exchange interactions. Since such intramolecular interactions can not be removed by dilution, the analysis or simulation of such spectrum would be a formidable challenge. Furthermore, EPR has difficulties detecting long-range spin ordering and distinguishing between very small ferromagnetic and antiferromagnetic interactions because the zero-field splitting parameters in such cases are usually infinitesimally small.

For characterizing small radical molecules, magnetometry, the measurement of magnetic susceptibility, is just a complementary technique to EPR. However, for polyradicals, it is arguably the most important tool in determining the spin multiplicity and spin concentration. This technique is especially valuable in determining the average spin state of complex

mixtures and weakly interacting systems. According to Faraday's Law, the magnetic flux near a closed conductor loop induced by a magnetized paramagnet can cause an electromagnetic field that is measured as voltage. The Quantum Design Magnetic Property Measurement System (MPMS) used in this project is based on this principle. A gradient, second derivative arrangement of superconducting quantum interference device (SQUID) magnetometer is surrounded by a ±5.5 Tesla variable field magnet that provides the external field. The device detects the magnetization inside the coil but rejects the surrounding field because of its superconducting nature. This instrument is based on a Josephson junction that is very sensitive to change in the magnetic flux and is able to measure extremely small magnetic moments (10^{-12} Emu/gram) with high accuracy. The temperature near the sample can be modulated between 1.7 and 400K to achieve variable temperature studies. The measurement starts with moving the sample in the direction of the external field. Any motion that causes a deflection of the flux in any loop will be recorded. The scan provides a trace of the amplified induced voltage as a function of sample holder displacement. The magnetization is extracted from fitting the function to a special equation.

One major difficulty in the measurement is to provide a small homogeneous background signal. This is especially important for the weakly paramagnetic samples in this work. As the field dependent paramagnetic susceptibility is positive and the field independent diamagnetic susceptibility is negative, it is possible that the observed susceptibility may change its sign when the field strength exceeds a certain threshold. When the moment goes near zero, the SQUID trace become uninterpretable by the fitting program. A delrin poly-(formaldehyde)

holder was designed to solve this problem[51]. The tube is magnetically homogeneous except at the sample region. Because the background material is diamagnetic, the empty space appears to the detector as a small "paramagnetic" signal. This ensures the total moment to be always positive regardless of the field strength and greatly simplifies the analysis.

Magnetic Characterization of Polyradicals

This section describes the magnetization behavior of the hyperbranched trityl polyradicals generated under various conditions. To optimize the magnetic property, the reaction condition was adjusted according to the SQUID results from previous runs. The ultimate goal is to find a common condition to achieve maximum S value and spin concentration in these polyradicals.

- **Basic Concept**

In our design, there is no control over intermolecular interactions. Since the nature of these interactions are usually weakly antiferromagnetic, there is little chance that these polyradicals will spontaneously order into ferromagnets. The current study focuses on probing the intramolecular interactions and determining whether the spins act independently (indicated by $S=1/2$) or if some local high/low-spin coupling is present between radical centers (demonstrated by $S>1/2$ or $S<1/2$). As mentioned in the first chapter, the spin state can be determined from a plot of magnetization versus applied field at constant temperature. At low temperature, the induced moment increases as the field increases until all spins are aligned by the field. The S value of a material is decided by examining the rate such saturation is reached. This saturation behavior may be quantitatively modeled by the Brillouin function[52] and both S and saturation

magnetization can be extracted from fitting the experimental data to the function.

If every monomer unit is converted into an infinitely stable radical, the spin concentration would be 100 percent. In reality, the radical-generating steps are probably never quantitative. The spin concentration is further marred by the subsequent radical decomposition through oxidation, hydrogen abstraction or dimerization. The actual spin concentration is therefore the ratio of saturation magnetization and the theoretical magnetization. It reflects of the percentage of monomers that are doped and then survive.

•The Interpretation of Fitted S

In a polyradical with several defects, the molecule surely contains distinct magnetic sites with different S values. The S derived from Brillouin plot fitting procedure is just the average of all S values from these fragments. For example, an S value of 2.0 suggests that the sample consists of ferromagnetially coupled four-spin clusters on average. It should not be interpreted as if every radical is in some four-spin assembly. Actually, fitted S values that significantly deviate from the perfect integer or half integer numbers are very common.

Then how is this empirical S related to the real Ss in the polyradical? From the format of Brillouin equation, the magnetization is the product of Brillouin function and a spin independent factor, $Ng\mu_B$.

$$M = Ng\mu_B S B_s(\eta)$$

and $$B_S(\eta) = \frac{1}{S}\left[(s+1/2)\coth(s+1/2)\eta - \frac{\coth(\eta/2)}{2}\right]$$

where $$\eta = g\mu_B H/kT$$

If there are two non-interacting magnetic fragments with spin number S_1 and S_2 in the sample, the experimental saturation profile should be the sum of two individual functions, $Ng\mu_B S_1 B_{S1}(\eta)$ and $Ng\mu_B S_2 B_{S2}(\eta)$. This summation certainly does not lead to a function that can be exactly fitted by another new function in the form of $Ng\mu_B S' B_{S'}(\eta)$. Some approximation must be made. Mathematically, the Brillouin function behaves like a quadratic equation of S when H/T is small. With large H/T values, on the other hand, the magnetization is directly proportional to S. Accordingly, as observed in the earlier study of polaronic ferromagnets, fitting saturation curve of a mixed system using a single S value will overestimate the magnetization at low field and underestimate the value at high field. Since the S is largely determined by the magnetization data at low field strength, the fitted S inevitably biases toward the higher values. Figure 2-18a illustrates two theoretical saturation curves of doublet and sextet state mixtures with different compositions. In both cases, the observed S numbers are significantly larger than the arithmetic average of the two real Ss. When the S values of two segments are closer as the quartet and sextet in Figure 2-18b, the fitted S falls much closer to their arithmetic average though some deviation is still noticeable. In summary, the single S value Brillouin fit of a mixture system always gives spin numbers larger than the real average of individual spin states.

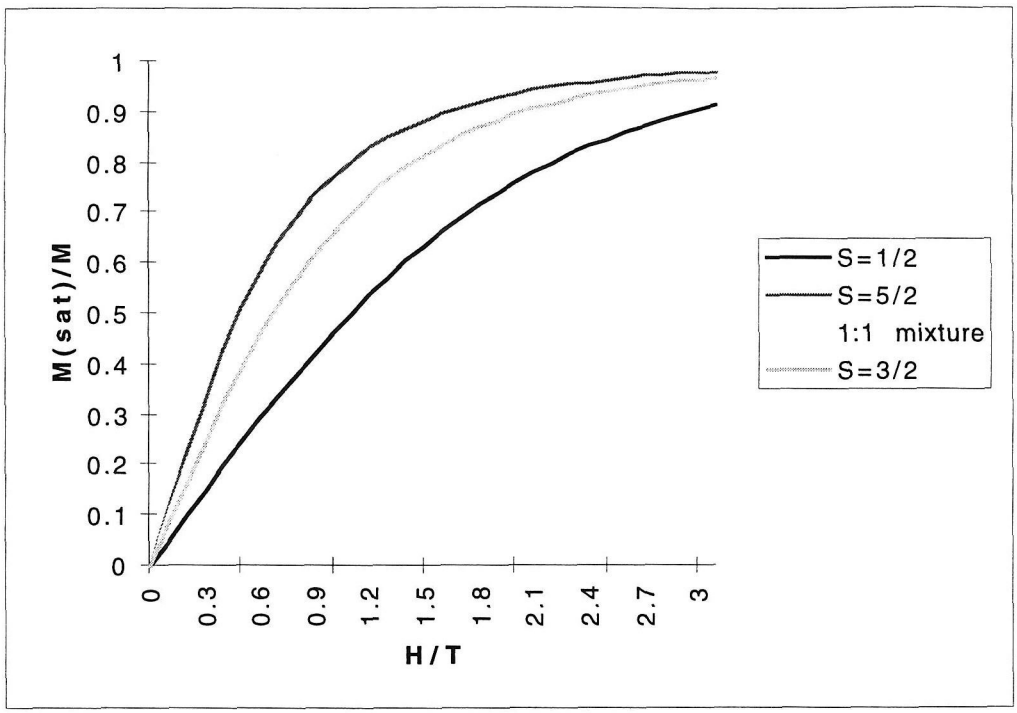

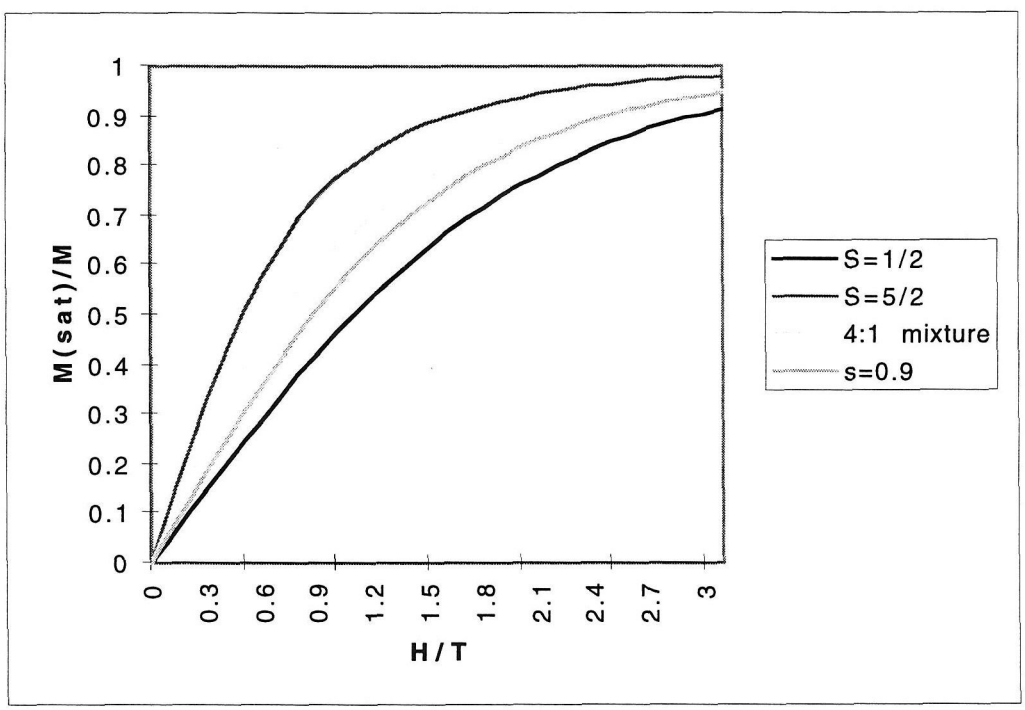

Figure 2-18a Brillouin plot of mixed spin states (S=0.5 and S=2.5)

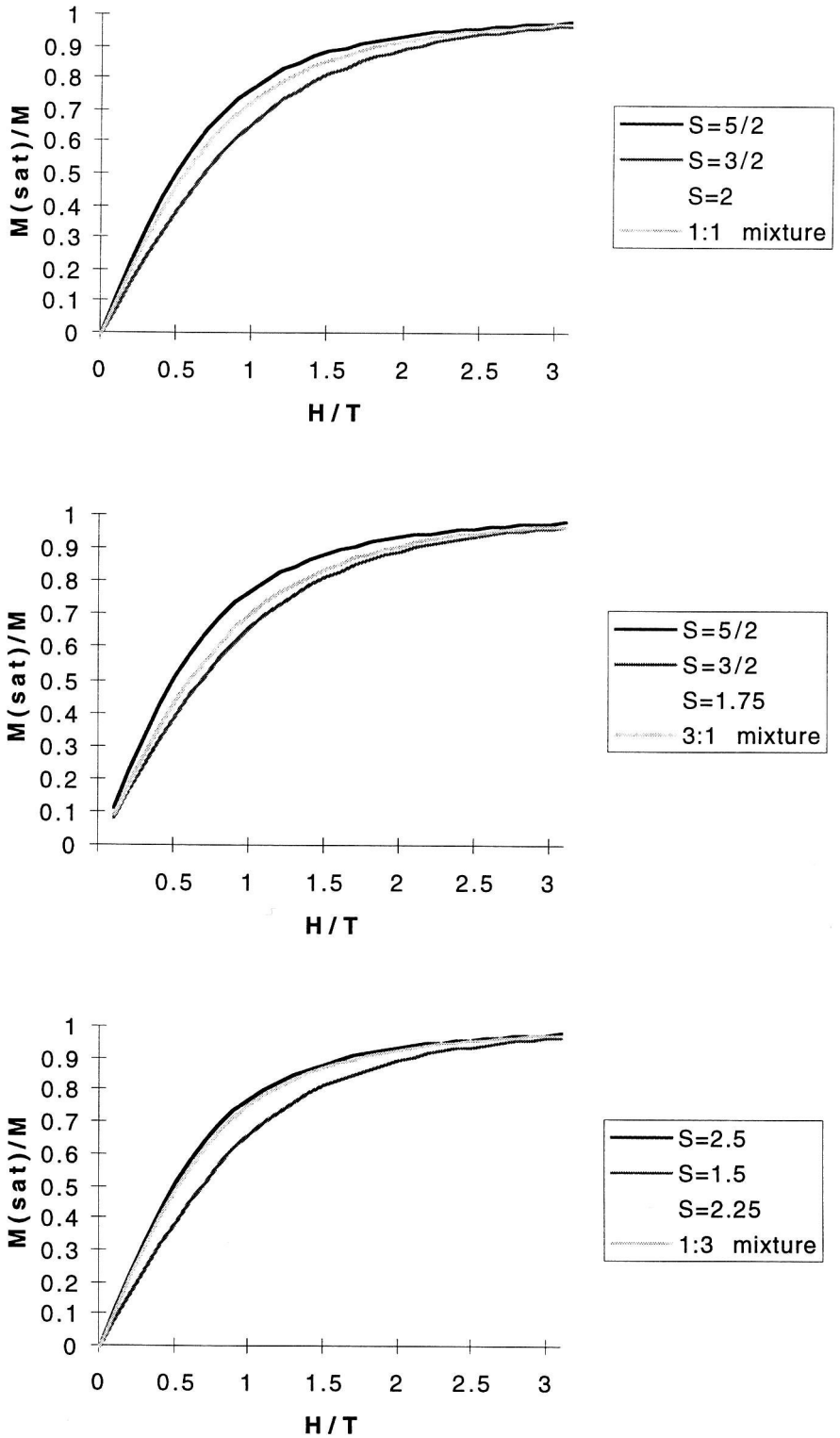

Figure 2-18b Brillouin plot of mixed spin states (S=2.5 and S=1.5)

•Estimation of Diamagnetic Correction

In small organic radicals and inorganic compounds, Pascal's constants are often used to estimate their diamagnetic correction. However, this method is not amenable to systems of unknown composition. Its aptness to atypical structures is also questionable. A superior way is to estimate this residual magnetization from either variable field or variable temperature studies. As mentioned in the first chapter, a diamagnetic correction term can be added to the Brillouin equation. Using this modified equation, a three-parameter fit to variable field data at low temperature should grant a simultaneous assessment of M_{sat}, S and χ_{dia}. Alternatively, a plot of χ_{emp} versus the inverse of absolute temperature gives a straight line in the medium to high temperature regime where the Curie law is valid. The diamagnetic correction can then be evaluated by extrapolating the susceptibility to infinite temperature. The χ_{para} term vanishes at this hypothetical condition because all spin alignments are overwhelmed by the infinite thermal energy.

There is a major flaw in the three-parameter-fit strategy. As mentioned earlier, a mixed system can never be accurately represented by a single Brillouin function. Therefore the diamagnetic contribution from the three-parameter fit always inadvertently includes correction to this intrinsic inadequacy of the operation. This inevitably leads to the overestimation of χ_{dia} and S value while the spin concentration is underrated. When the moment is enormous, the fitted χ_{dia} can sometimes be even larger than the correction observed for the empty sample holder (ordinarily 3-8 $\times$ 10^{-8} emu·G). As mentioned before, this small positive susceptibility corresponds to the "absence" of diamagnetic material at the sample retaining region, adding any substance to this area should decrease the observed diamagnetic

term. Any deviation from this behavior is obviously the artifact of the fitting procedure.

On the other hand, Murray has found the variable temperature data followw the Curie law normally in the 50-200 K range. From the intercept of Curie plot, very reasonable diamagnetic corrections can be obtained[53]. Hence all the diamagnetic terms reported here are from variable temperature plots at constant field.

•Effective Moment Plot

Fitting the saturation curve to the Brillouin function is a powerful tool to determine the spin state of any given material. However, in order to assure the saturation, the temperatures in these experiments are usually very low (T<5K). The fitted S values at such low temperatures are affected indiscriminately by ferromagnetic and antiferromagnetic interactions alike. The magnitude of these couplings can be distinguished to some extent by inspecting the magnetic susceptibility of a sample as a function of temperature. The variable temperature experiment is thereby performed. The field strength in such an operation must be considerably lower than what is used in a saturation experiment in order to detect weak interactions at low temperature. Practically, the onset of different interactions is observed by plotting the relative effective moment (defined in Equation 2-2) versus temperature. The moment is labeled relative because the exact composition of the polyradical is unknown.

$$\mu_{rel.eff} \propto \sqrt{\chi_{para} \times T} \qquad \text{(Eq. 2-2)}$$

This quantity has the unit of moment. It is directly proportional to the molar effective moment at all temperatures. The flat part of effective

moment plot means that no interactions of magnitude comparable to the thermal energy at those temperature are present. This temperature range is also where Curie law is valid. Accordingly, an upturn in the effective moment curve at a particular temperature indicates ferromagnetic interaction of magnitude similar to the thermal energy at that temperature whereas a downturn is characteristic of antiferromagnetic interactions.

Polymer **HPPMT** was the first one to be studied. The optimized condition for it was then used to all other polymers. Sample handling and data manipulation for **HPPMT** will be described in more detail here; other polymers were treated in the same manner.

The initial experiments were all conducted in a glove box at room temperature. Under the conditions tested, neither the polytrityl trifluoroacetate nor the polyradical can be cast as thin films on Teflon block or glass slide. All the reductions were thus performed in the solution phase. One equivalent of metalocene was added to the solution of polytrityl trifluoroacetate and the reaction was stirred for 2-8 hours. The duration of the reaction is inconsequential as long as its purple color no longer persists. After the solvent naturally evaporates, powder samples of different colors were obtained. These results of magnetic measurements are shown in the following figures and table.

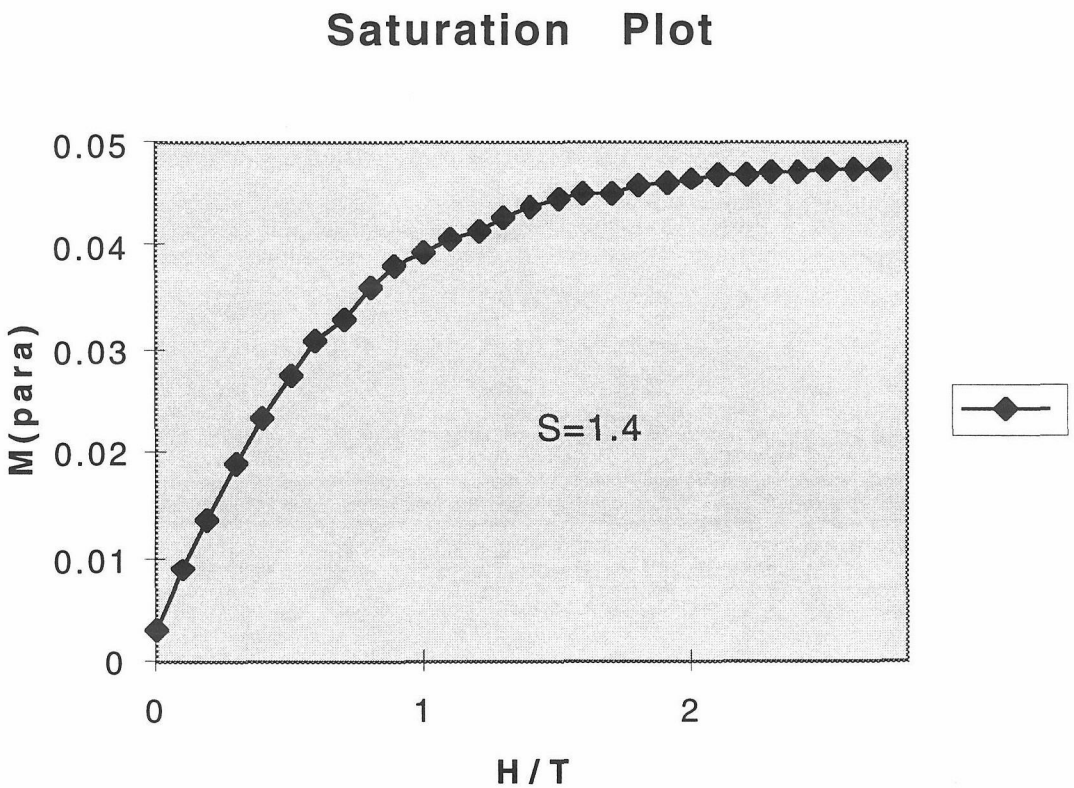

Figure 2-19a: A typical saturation plot of the polyradicals
The S value 1.4 is obtained from the
two-parameter-fitted Brillouin equation

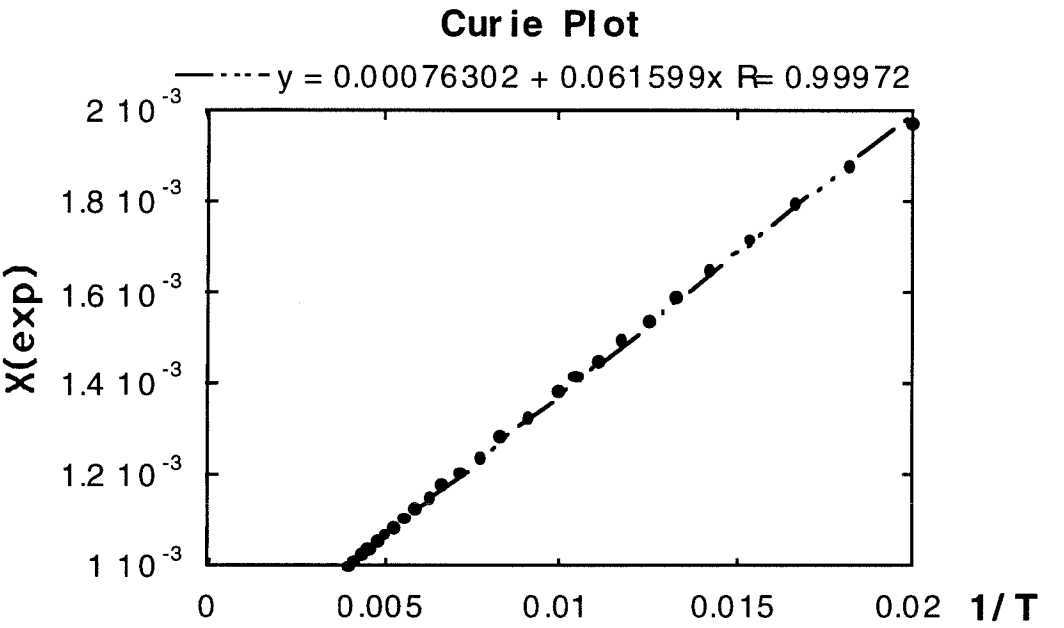

Figure 2-19b: A typical Curie plot of the polyradicals.

The diamagnetic correction of the sample is estimated from the intercept at the Y-axis. This correction typically lies between $5*10^{-4}$ and $8*10^{-4}$ Emu/G.

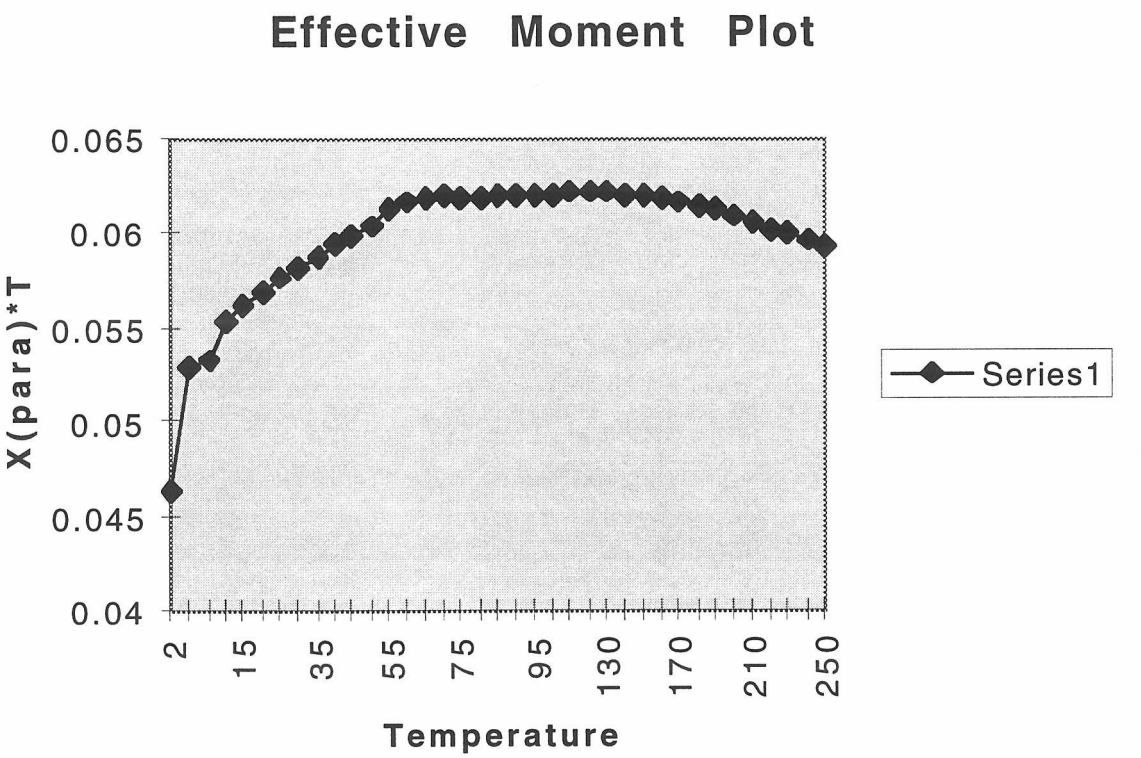

Figure 2-19c: A typical effective moment plot of the polyradicals. Because of the mediocre spin concentration (10%-20%), no clear upturn can be observed in the plot.

	$Fe(Cp^*)_2$ decamethyl ferrocene	$Ni(Cp)_2$ nickelocene	$Co(Cp)_2$ cobaltocene
Color	green	dark green	yellow
S value	1.4	0.6	1.4
spin concentration	10% ?	12% ?	8%

Table 2-1 Magnetic properties of **HPPMTR** from three different reductants

The sample from such a protocol is obviously a mixture of polyradicals and the oxidized metalocene. In the case of cobaltocene, it is also possible that the reduction does not proceed to completion and the unreacted reductant also contributes to the observed moment. No attempt was made to purify the polyradicals for it is very difficult to separate the mixtures without causing the already unstable radical units to decay even further.

The spin concentration of samples from $Fe(Cp^*)_2$ and $Ni(Cp)_2$ reduction can not be determined without some assumption about the degree of reduction and the magnetic behavior of oxidized metalocene. If the reduction is complete and the metaloceniums act as perfect paramagnets, the observed spin concentration will be more than 100%. This is never the case. On the other hand, if the reduction is less than half way complete and metaloceniums behave as before, the spin concentrations of polyradicals should be half of what are observed. The spin concentrations reported in the first and second row of Table 2-1 are based on the latter assumption. It is to be conceded that ferromagnetic or antiferromagnetic interaction can

also occur between produced metalocenium molecules due to intermolecular interactions. The true magnetic properties of these metaloceniums should lie somewhere between the two extremes and therefore the reported spin concentrations should be considered only as the lower limits of real values.

Fortunately, pure cobaltocene powder from Aldrich Co. behaves as an almost perfect paramagnet in the control experiment. The fitted S is very close to 1/2 and the spin concentration is more than 90%. (It is worth pointing out that this behavior is not as general as one might assume. We have encountered cases where the fitted spin concentrations of pure commercial organic radicals are below 70 percent[54].) When mixed with the polyradical, cobaltocene is even less likely to exhibit long range spin ordering for the intermolecular interaction should diminish further upon dilution by the polymer matrix. Because of cobaltocene's superior reductive potential[55], this reduction is assumed to be nearly quantitative. It is also worth pointing out that such reduction is electron transfer in nature. This means the reaction can be quite effective even if the reductants are spatially inaccessible to the sites to be reduced. Therefore, all monomer units are reducible even if they are shielded by some hyperbranched architecture or barely soluble polymer matrix. The assumption of this high efficiency is also corroborated by experimental evidence. The linear diamagnetic component in the saturation plot should be significant if a large amount of monoradical, such as unreacted cobaltocene, is present. However, this was not detected. In all the following discussions, all reductions with cobaltocene are assumed to be nearly quantitative. Under such assumption, the spin concentration actually reflects the survival rate of radical centers after they are generated.

As mentioned earlier, the polyradicals can also be generated in chloromethane solvent at -78°C. One equivalent of cobaltocene was again utilized as the reductant in all cases. The reduction was finished in 12 hours judged by the dissipation of the light purple color from the suspended solution. Pale to murky yellow powder samples were obtained by evaporating the low boiling solvent at the reaction temperature under vacuum for another 12 hours. The sample was then moved into an oxygen-free glove box to be loaded into the delrin sample holder. It has been reported that some polyradicals are more stable in their solid state than in solution presumably because the packed solid matrix provides some natural protections against radical decomposition pathways[56]. (It is also conceivable that the restricted environment might inhibit some radical dimerization.) If this remains true for our system, this handling procedure should furnish the maximum spin survival rate when a powder sample is desired. The suspended polyradical solutions are kept at -78°C and the solid sample is exposed to room temperature only very briefly (about 30 min). At neither state is the radical decay likely to be severe. After this protocol was shown to be suitable for **HPPMT**, **HMMPT** and **HMMMT** were treated in the same manner. The results of their magnetic studies are presented in the table below.

	HPPMTR	HMMPTR	HMMMTR
S Value	1.5-2.0	1.5-2.0	1-1.5
Spin Concentration	15-20%	15-20%	15-20%

Table 2-2 Magnetic properties of three isomeric polyradicals

Despite their heterogeneous nature, all reactions appear to complete within reasonable time spans. The low temperature procedure marginally improves the S value while the increase of spin concentration is more noticeable. This improved radical stability at lower temperature is certainly expected. Besides, the radical centers may be stabilized simply for being kept only partially soluble throughout the reduction as in all these cases.

Even with the low temperature procedure, the spin concentration of the polyradicals are still not high enough to produce collective behaviors. This is evident from the small S values and effective moment plot. Although some gradual upturns are detected in some samples, no drastic rising of effective moment is observed. In our design, only intramolecular covalent interactions are controlled to be ferromagnetic. However, interactions that are through space in nature are usually weakly antiferromagnetic. This is accurately depicted at the low temperature in Figure 2-19c and such behavior is typical of all the polyradicals studied here. These interactions could be between different polymer molecules or, more possibly, spin clusters separated by defects within one polymer molecule or even radical centers in the same spin assembly.

Discussion on Preliminary Results

The results from these first generation polyradicals are certainly encouraging. Evidences of ferromagnetic interaction are seen in all the samples. In the best case, the fitted S suggests that it is the equivalent of a tetraradical with a quintet ground state. It is even moderately stable at room temperature. Although similar high-spin species are also observed in the one-dimensional polaronic ferromagnets, the spin concentration of those cationic polyradicals are typically below one percent[57]. The data processing for such samples can be complicated because the diamagnetic contribution to the low field end of the saturation plot is quite substantial. Statistically, the probability of having four to five uninterrupted doped SC units in such a system is extremely low. Heavy doping raises the spin concentration but also decreases the S values to 1/2 probably because of interchain polymer crosslinking. Such behavior can raise some serious questions about the actual structure of the high-spin radical cluster. On this aspect, hyperbranched trityl polymers exhibit a significant improvement. Especially in the low temperature experiment, the spin concentration can sometimes be higher than 20 percent. Even the samples from room temperature reaction give concentrations near ten percent.

Although the progress is indisputable, apparently, a much higher spin concentration is necessary in order to observe real collective behaviors and huge S values. Despite all the effort to preserve the spins, to our disappointment, the radical centers apparently still decay. As a result, the experimental S is still far from ideal. The most famous decay pathway of triphenylmethyl radical is the dimerization. Historically, triphenyl methyl radical was first prepared by Gomberg as a monomeric intermediate to synthesize hexaphenyl ethane[58]. In his 1900 paper, Gomberg proposed a

equilibrium between the radical and its dimer. It was not until 1968, almost seven decades after Gomberg's first paper, that the real structure of Gomberg's trityl dimer was revealed by NMR to be an α-p' dimer instead of the α-α' dimer originally proposed[59].

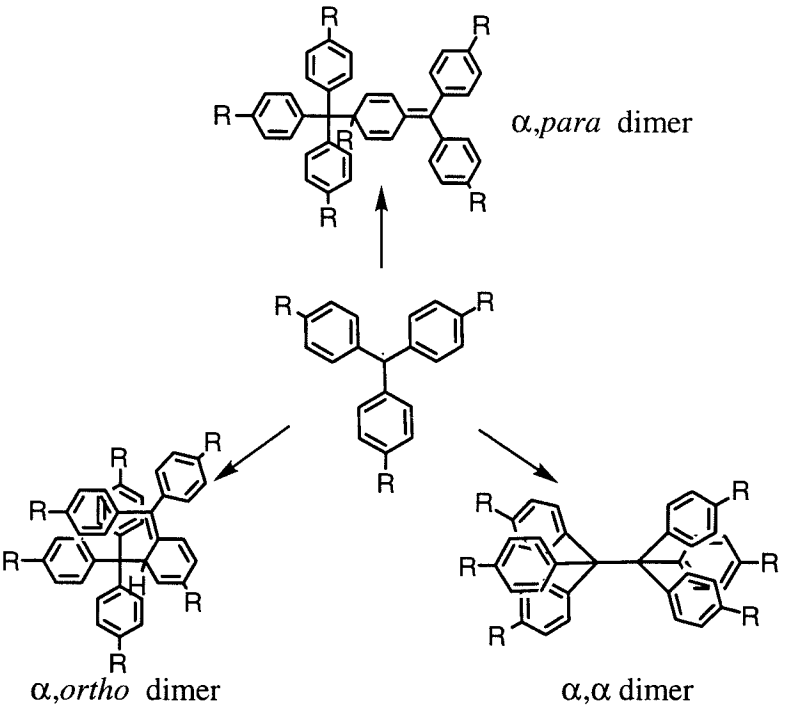

Figure 2-20 Three isomeric trityl radical dimers

Since then, numerous trityl dimers have been prepared and characterized[60]. Even the most elusive hexaphenyl ethane structure has been observed in a crystal lattice[61]. The dimerization should be even more probable in polyradicals where the reaction becomes intramolecular and therefore suffer much less entropy loss. It is well known that the dimer formation is often hampered by various substitutions at the *para* positions. Some *ortho* substitutions have also been shown to block the dimerization mainly for steric reason. In addition, *ortho* substitutions also protect the radicals from oxidation and other decomposition pathways. All these

principles of improving radical stability will be applied to improve our system in the next section.

In the previous section, we found the residual bromides attached to the polymers to be incompatible with a spin generating reaction. It is also known that the *α-p'* trityl radicals dimers carrying *para* halide substitutions can be reduced to form new monoradicals[62] (Figure 2-21). Unlike simple dimerization, this reaction can be even more detrimental to magnetic interaction because it is irreversible. To prevent the formation of such defects, it is essential to remove the excess bromides. An "end capping" strategy will be pursued in the next section.

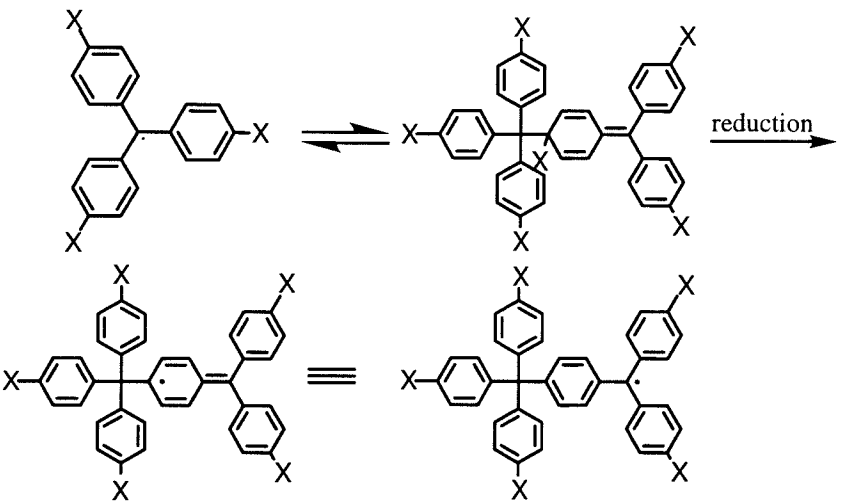

Figure 2-21 Irreversible reductive dimerization of trityl radicals with para halogen substations

It is not surprising that **HPPMTR** and **HMMPTR** show comparable magnetic behaviors. In spite of some trivial structural discrepancies, the FC in both polyradicals is *m,p'*-biphenylene. It is, however, somewhat unexpected that the interaction in **HMMMTR**, although to a lesser extent, are also ferromagnetic. Theory predicts its *m,m'* -biphenylene linkage to

be a disjointed coupling unit[63] (Figure 2-22). Such bridging unit minimizes electron repulsion between SCs and thereby makes the singlet and triplet states nearly degenerate. To determine the ground state of a disjointed system is usually difficult[64]. In several systems where *m,m'*-biphenylene has been tested, it appears that ferromagnetic coupling through this unit is possible but the interaction is so weak that it can easily become antiferromagnetic when the dihedral angle between two phenyl groups changes[65]. At this point, it seems that the ferromagnetic coupling observed in this particular polyradical is purely accidental. However, this view will be challenged by some latter experiments.

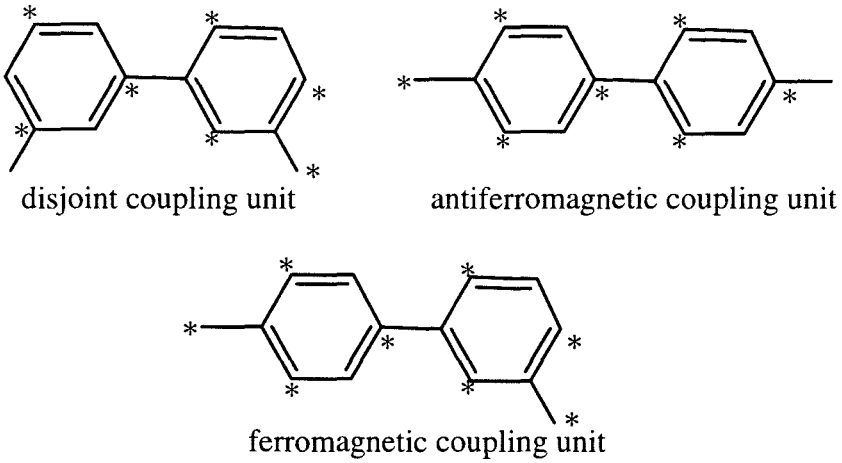

Figure 2-22 Three isomeric biphenylenes as magnetic coupling units

One clear weak link of these preliminary studies is the lack of a control experiment. Although ferromagnetic interactions are observed in both **HPPMTR** and **HMMPTR** as expected, there is no concrete evidence to support that the interaction is actually due to the designed topology. The skepticism is aggravated especially by the displays of a similar interaction

in **HMMMTR**. A more reliable proof would require the comparison between two polyradicals with ferromagnetic and antiferromagnetic coupling units respectively. The only unequivocal antiferromagnetic coupling unit in the biphenylene structure family is the *para-para* isomer[66] (Figure 2-22). Unfortunately the only polymer with this coupling units, **HPPPT**, is completely insoluble despite its hyperbranched structure. All attempts to process this polymer prove futile. Not even the slightest change of color could be observed when it was suspended in pure TFA. One central point of further investigations will be to find a pair of soluble polymers with the two distinct topologies. They can then be transformed into the supposedly high-spin and low-spin polyradicals for comparisons after undergoing the identical radical-generating procedure.

Attempts to Improve the S Value and Spin Concentration

In order to improve the original system, it seems some more elaborated monomer is necessary in order to make the polyradicals more persistent. Indeed, such an approach has proven moderately successful in Rajca's quest for high-spin polyradicals[67]. Since the best known and probably the most stable trityl radical dimer is the *α-p'* isomer, a sensible approach is to synthesize hyperbranched trityl polymers with all their *para* positions on the phenyl rings blocked by some substitutions. According to this idea, methyl substituted version **HMMPT** and **HPPMT** should be the next targeting polymers. The synthetic procedures of two required monomers **11** and **12** are shown in Figure 2-23.

The synthesis of **11** started with a simple addition of mono-lithiated 2,4-diiodo-m-xylene to *p,p'*-dibromo-benzophenone. The extra *ortho* methyl group can render further protection to the radical center.

Unfortunately, for some reasons, the intermediate trityl ether **14** is very insoluble in common solvents. Consequently, the key selective lithium-iodo exchange reaction can not be carried out effectively. This synthesis was not investigated further.

The synthesis of **12** started from 2-bromo-4-nitro-toluene. The nitro group was converted into iodide after a simple reduction and the Sandmeyer reaction via the diazonium salt. The resulting 2-bromo-4-iodotoluene was then transformed into mono-Grignard reagent by the selective insertion of magnesium into the weaker carbon-iodide bond under controlled condition. The organometalic reagent added twice to ethyl 4-iodo-benzoate to furnish the desired trityl alcohol. The following reaction sequences are identical to those used in the synthesis of **1-3** (Figure 2-14) with the key step being the selective lithium-iodide exchange at -98°C. Unfortunately, this monomer is not a good substrate for Suzuki's coupling reaction presumably because of steric hindrance imposed by the extra methyl groups. Judged from GPC and the NMR spectrum, only oligomers ranging from tetramer to octamer are obtained after prolonged reflux in toluene. Suzuki recently published a modified condition which is supposedly less sensitive to steric factors[68]. The reaction is run in DMF or 1,2-dimethoxyethane with barium hydroxide or potassium phosphate as the base. However, this method also proved ineffective not for a poor coupling yield but the solubility of produced polymer. The oligomeric products precipitate out of the solution before the molecular weight reaches the desired range. At this point, we decide to explore other means to improve the system.

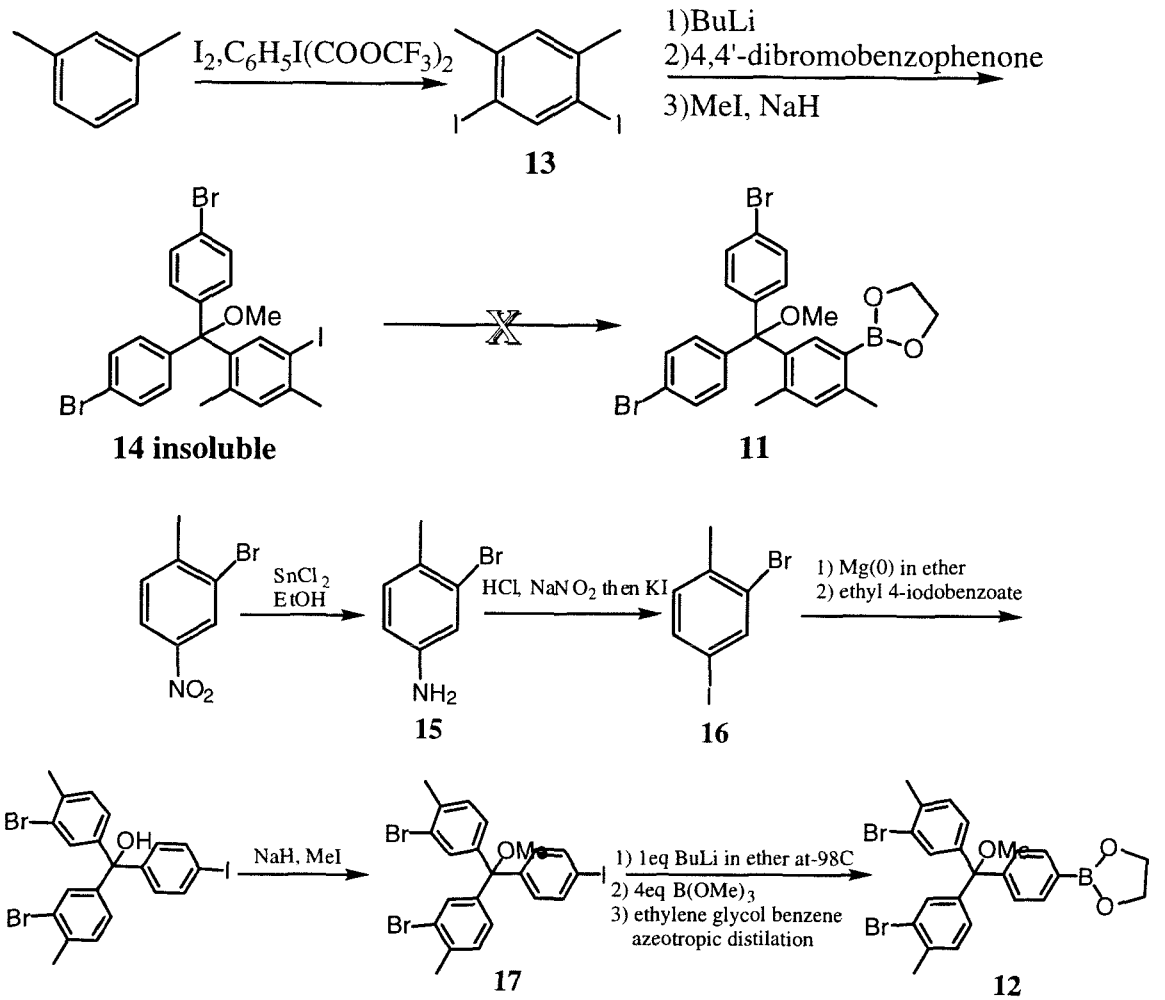

Figure 2-23 Syntheses of *para* substituted trityl monomers **11** and **12**

Another option to improve the magnetic properties of the polyradical is through the functionalization of the parent polymer, more specifically, to transform the excess bromides into some inert functional groups to avoid interference during radical generating steps. Since Rajca's reduction-oxidation protocol (Figure 2-17) is by far the most efficient method to convert trityl ethers into radicals, we decided to aim for a modification that will make the hyperbranched polymer compatible with this procedure. To apply Rajca's protocol, the major problem is the intramolecular cyclization

due to Ullmann type homocoupling when **HPPMT** is treated with lithium metal. The crosslinked polyanion thus produced is insoluble and hence can not be easily oxidized. Furthermore, the newly formed linkage has the strongly antiferromagnetic *para-para* topology. Because of this concern, the functionalization reaction must be nearly quantitative. Otherwise, the designed magnetic property might still be ruined by the newly formed antiferromagnetic coupling units even if the polyanion remains soluble during and after the reduction.

In the first report about hyperbranched polymers, Webster already reported one example where the bromides in a hyperbranched polyphenylene are converted into carboxylic acids. This is achieved by quenching with carbon dioxide the polylithiated polymer generated by lithium-bromide exchange[69]. This produces water-soluble hyperbranched polycarboxylate (Figure 2-7). Unfortunately, this manipulation is not amenable to this project because of solubility problems at low temperature. Furthermore, functional groups that can be conveniently incorporated via organolithiums reagent (esters, amides, acid etc.) are probably still incompatible with lithium metal reduction in Rajca's procedure.

It turns out the best approach to modify **HPPMT** is still the traditional Suzuki's reaction by which the bromide was converted to *p*-tert-butyl phenyl. This bulky substitution should block intramolecular radical dimerization as well as increase the solubility of diamagnetic precursor polymer. At first, there is concern about whether this catalytic system is reactive enough to couple with all the aryl bromides specially those more hindered ones buried inside the hyperbranched architecture. Fortunately, this obstacle is overcome by simply using a large excess of *p* -tert-butyl phenyl boronic acid in the coupling reaction.

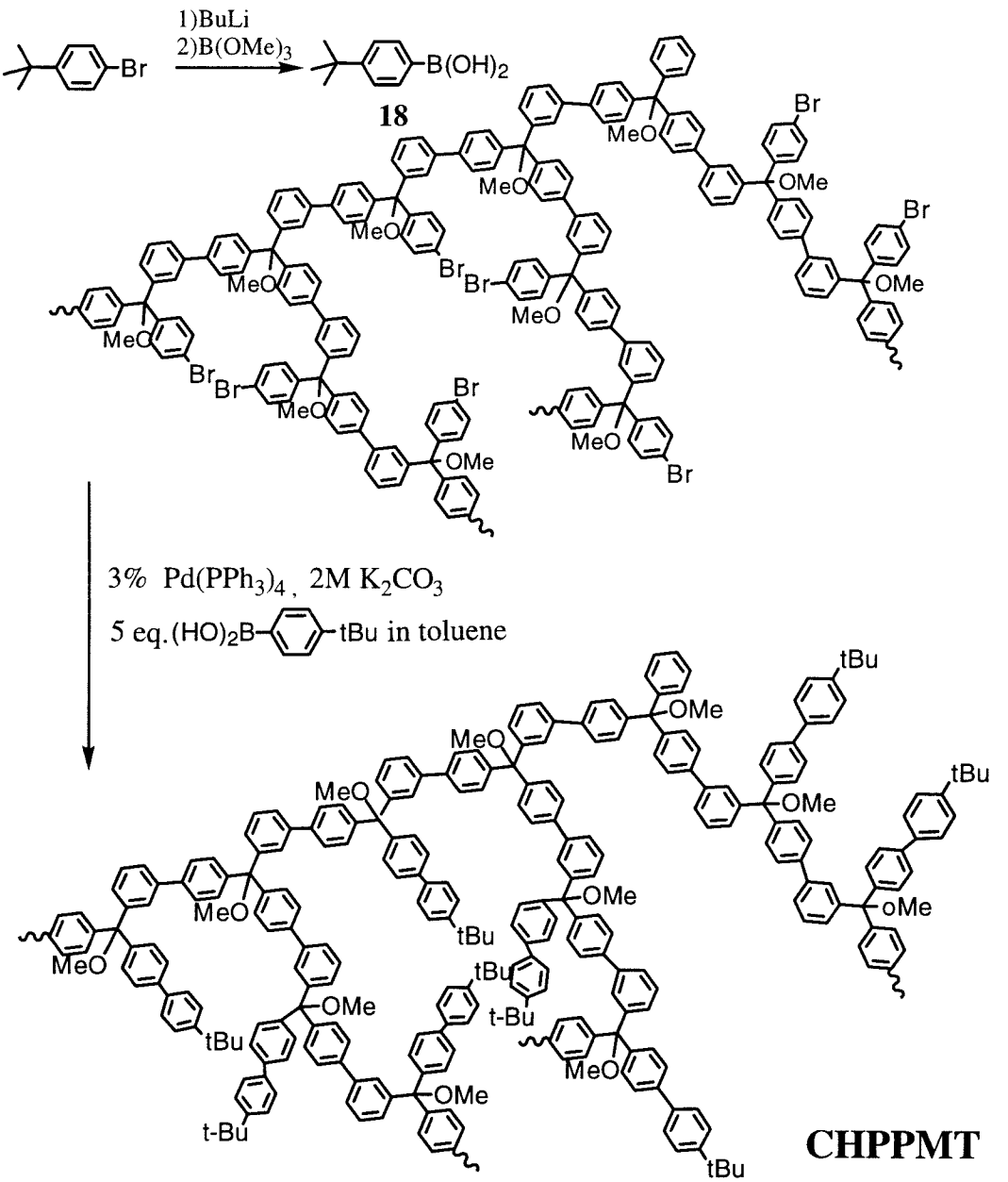

Figure 2-24 End-capping of **HPPMT** to produce **CHPPMT**

The required boronic acid was synthesized in just one step from 4-t-butyl bromobenzene. This "capped **HPPMT**" is named **CHPPMT**. As expected, **CHPPMT** is noticeably more soluble than the uncapped **HPPMT**.

The degree of functionalization can be deduced from proton NMR integration. Although the spectrum of **CHPPMT** is broadened as all polymers, two peaks corresponding to the methyl ether and t-butyl near 3 ppm and 1.3 ppm respectively are clearly distinct. Since a large hyperbranched polymer carries approximately one bromide per monomer unit, the integration ratio of these two peaks should be one to three if the reaction is quantitative. In the actual spectrum, the ratio is between 2.5:1 to 2.7:1. This observation suggests a reaction yield of 80 to 90 percent. Although such efficiency seems far from perfect, it should be remembered that the starting polymer only carries 80 to 90 percent of the theoretical bromides judging from elemental analysis. If the elemental analysis of **HPPMT** accurately depicts its bromide content, this functionalization procedure is indeed nearly quantitative. This assumption is further supported by the result of **CHPPMT**'s elemental analysis which affirms a very low bromide content (Br percentage < 1 %).

The GPC chromatogram of **CHPPMT** looks similar to the starting polymer with a clear bimodal distribution. However, the first peak appears somewhat smaller than before the capping. Since it is very unlikely that the condition of Suzuki's reaction causes the polymer to break down into smaller fragments, we assume **CHPPMT** to have the same degree of polymerization as its uncapped predecessor. The minor change in GPC is probably induced by some alteration of the global molecular shape resulting from some local conformation change imposed by the newly incorporated bulky groups.

To study the effect of capping on radical stability and magnetic coupling, **CHPPMT** is transformed into its corresponding polyradical (**CHPPMTR**) by undergoing the same treatment as **HPPMT**. It was first

dissolved in TFA to afford the polytrityl trifluoroacetate. Both high and low temperature reductive procedures were applied. The changes of colors during the course of the transformation are quite similar to those of **HPPMT**. The SQUID results are shown in Table 2-3.

	Room Temperature Experiment	Low Temperature Experiment
S Value	0.8-1	1-1.5
Spin Concentration	12%	20%

Table 2-3 Magnetic property of **CHPPMTR**

Somewhat disappointingly, compared with the uncapped polymers (Table 2-1 and 2-2), **CHPPMTR** shows no improvement in its magnetic properties. Apparently, either the radical instability in these systems arises for reasons other than simple dimerization or the *p* -t-butyl phenyl group can not effectively block the dimerization. It is not possible to distinguish between the two possibilities with the current data.

The main purpose of making **CHPPMT** is to apply Rajca's procedure to our system. As already mentioned, the removal of bromides is critical to the success of the reduction step. When the tetrahydrofuran solution of **CHPPMT** was vigorously stirred with an excess of lithium powder, the solution gradually became deep blue, indicating the formation of triphenylmethyl anion. The whole operation was conducted in an oxygen-free glove box to protect the intermediate carbanion and produced polyradical from oxidation. The reduction took 48 hours. In contrast to the uncapped **HPPMT**, no precipitation can be observed during the whole

course of the reduction. The clean solution of the polyanion was obtained after a simple filtration to remove the excess lithium powder. The next step of Rajca's recipe is an oxidation with gaseous or crystal iodine at -100°C. However, technical difficulties prevent this methodology from being fully implemented. Alternatively, the oxidation was performed at room temperature using ferrocenium hexafluorophosphate as the oxidant. The side product of this oxidation is the 18-electron diamagnetic ferrocene which surely does not interfere with the magnetic characterization. The solution immediately turned yellow after one equivalent of ferrocenium salt was added. Like previous cases, after the solvent was evaporated naturally, the remaining yellow powder was loaded into the SQUID sample holder. The SQUID measurement outcome, however, is once again disappointing when compared to earlier results. No noticeable improvement in S value can be observed. In fact, it is almost surprising that samples from two completely different operations can exhibit such similar S values.

Judging from this observation, the decay of radical centers is probably intrinsic to the polyradical itself while the effect of radical-generating process is minimal. Since **CHPPMTR** produced by various methods all fail to exhibit any superior magnetic property, the end-cap functionalization is not applied to other polymers.

We once more turned back to the first approach- building new polymers from new monomers. Unsatisfactory results of **CHPPMT** clearly show that radicals can not be effectively stabilized by blocking groups at *para* positions. The other option is to shield the radicals by *ortho* substitutions. In such an approach, the *ortho* groups provide physical barrier directly to protect the radical centers against all decay pathways.

The major trouble of this strategy, however, is the propeller twist around the radical center induced by the substitutions[70]. This conformational change will certainly diminish the already weak ferromagnetic interaction. Its impact, however, can vary widely depending on the type of compounds. For example, in some bis-TMM derivatives, the ferromagnetic coupling survives despite severe twisting[71] while comparable twisting causes *m*-phenylene to become an antiferromagnetic coupling unit in one of Iwamura's bis-nitroxide[72].

At this stage, the factors to be taken into account have become too complicated to allow a fully rational design. Monomer **19** was chosen as the target mainly for its synthetic accessibility rather than any particular theoretical concern. The major difficulty in this synthesis is to assemble the triphenylmethyl ether frame work with all the required halogen substitutions in their right places. Organomagnesium reagent is usually the best choice for this purpose because of its high reactivity towards the carbonyl and inertness to the existing halogen functionality. However, the *ortho* substituted Grignard reagent required for this synthesis is not reactive enough to add to esters. Organolithium reagents usually possess superior reactivity, but they tend to undergo lithium-halogen exchange reactions with other halogens. This side reaction can be especially troublesome when the desired addition pathway is retarded by steric factors as is in this case. This obstacle can be overcome with a reverse addition technique. The optimal condition is to add a newly generated cold organolithium solution to the solution of an appropriately substituted benzophenone at 0°C slowly. A detailed layout of the synthesis is shown below.

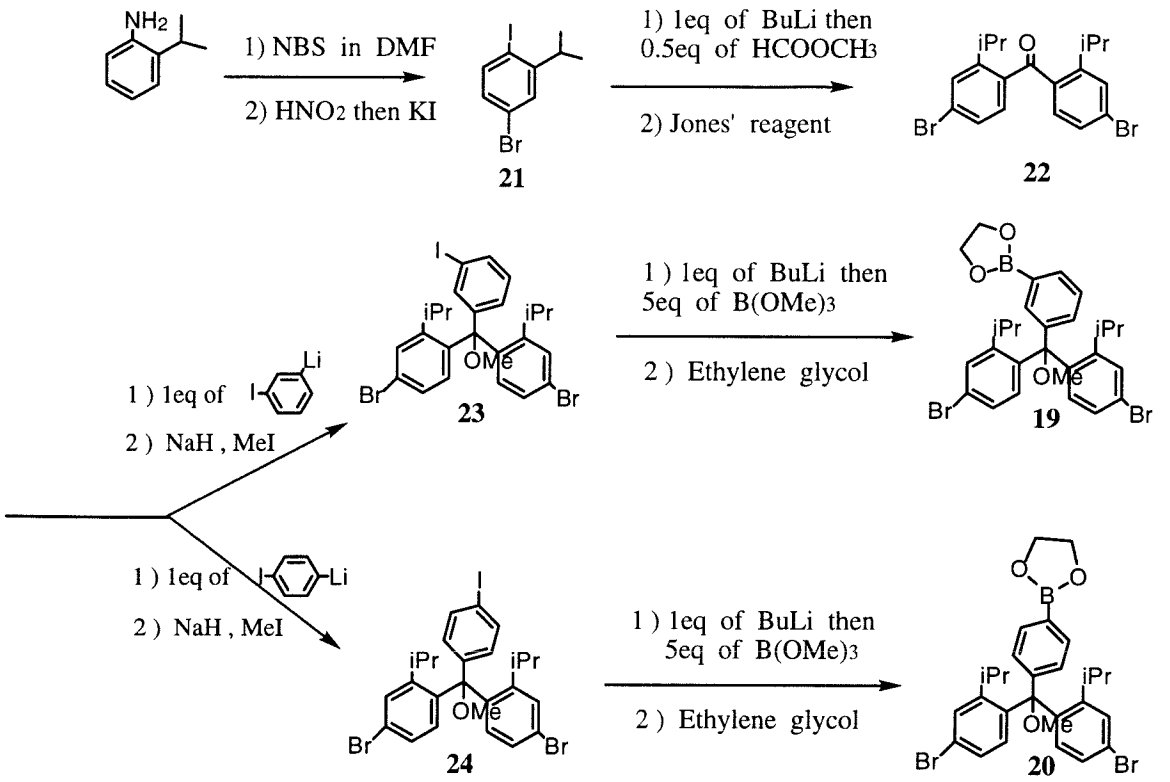

Figure 2-25 Syntheses of isomeric *ortho*-substituted monomers **19** and **20**

The plan started from 2-isopropyl aniline which was brominated under a mild condition to give the mono-brominated *para* isomer. Sandmeyer substitution reaction transformed the aryl amine into an aryl iodide via its diazonium salt. The 4-bromo-2-isopropyl-iodobenzene, **21**, was treated with one equivalent of n-butyl lithium at -78°C in ether to furnish the monolithiated species. Half equivalent of methyl formate was then added at that temperature. Due to the high reactivity of the formate ester, the moderately hindered lithium reagent smoothly added twice to the electrophile to afford the corresponding diphenylmethanol derivative. After a simple Jones oxidation with chromium trioxide, 2,2'-diisopropyl-4,4'-dibromo-benzophenone, **22**, was obtained as a pale orange solid. It is

worth pointing out this substituted benzophenone possesses exceptionally high solubility compared to other benzophenone derivatives. (For example, the solubility of 4,4'-dibromo-benzophenone in THF is only about 0.1 gram/ml while this diisopropyl derivative is infinitely soluble in petroleum ether.) The effect of the *ortho* isopropyl groups is evident yet not well understood. The significance of this greatly improved solubility will be clear later.

m-Diiodobenzene was monolithiated with n-butyl lithium at -78°C. The cold solution of this lithium reagent was slowly transferred to an ether solution of **22** at 0°C. The desired trityl alcohol was obtained in 70 to 80 percent yield without contamination by polymeric products resulting from lithium-bromide exchange. The alcohol was then converted into the methyl ether **23** by the standard condition. Interestingly, the proton NMR spectrum of **23** shows some unusual features in its aliphatic region. First, the four methyl groups appear at relatively high field territory above 1 ppm. This abnormal chemical shift is certainly caused by the shielding effect from the π electrons of phenyl rings[73]. More peculiarly, there are two sets of peaks corresponding to the methyl groups. Each set shows the normal hyperfine splitting into two peaks by the benzylic proton. Clearly, the two methyl groups in isopropyl are not equivalent on NMR time scale presumably due to restricted rotation around the aryl-methine bond. In other words, the two enatiomeric forms of **23** interconvert slowly at room temperature and thus the methyl groups become diastereotropic. This is not surprising considering the steric hindrance around the trityl center. It should also be noted that the NMR spectrum in the aromatic region indicates the two 1,2,4- trisubstituted phenyl rings to be equivalent. Apparently, the rotation around the trityl center still happens at an

appreciable rate. To obtain the target monomer, the methyl ether was then subjected to the standard reaction sequence as in Figure 2-14. Dibromo boronic ethylene glycol ester **19** was obtained accordingly. As expected, **19** also shows the same anomalous NMR characteristic as before indicating that isopropyl groups here are still hindered rotors.

19 underwent polymerization smoothly with exactly the same Suzuki's coupling condition used for **1-3** (Figure 2-15) to produce **HPPMDIT**. The product thus obtained also has broadened NMR spectrum strongly pointing to a high molecular weight polymer. The GPC chromatogram again shows the typical bimodal distribution characteristic of hyperbranched polymers. The molecular weight is a little lower than that of its unsubstituted counterpart, probably due to the larger size of this new monomer. Nevertheless, this reduction in the degree of polymerization should not effect latter experiments and interpretations of data.

When *p*-diiodobenzene was used in place of its *meta* isomer, with otherwise identical reactions, monomer **20** was obtained with similar yield as **19**. The same unusual NMR pattern also appears in this isomer implying analogous stereochemical behavior. When **20** was subjected to the standard Suzuki's polymerization condition, a polymer **HPPPDIT** with low solubility was obtained. Both NMR line width and GPC data affirm its high molecular weight. But more importantly, although its solubility in common solvents is quite low, this limited solubility did prove enough for **HPPPDIT** to undergo the common radical-generating protocol developed previously. Compared to its unsubstituted analogue, **HPPPT**, which is completely insoluble even in pure TFA, the improvement is intriguing. There are at least two explanations for this dramatic change in solubility. The improvement can simply be attributed to the extra isopropyl groups

which offer more surface to solvent molecules than **HPPPT** does. Furthermore, because all monomer units are chiral in **HPPMDIT**, this polymer contains almost infinite numbers of diastereomers. This inevitably makes it more amorphous and thus more soluble. The real significance of **HPPPDIT** is that it is the suitable control system we long for in this study. Previously, **HPPPT**, the only precursor polymer unambiguously possesses antiferromagnetic coupling units, can not be transformed into the corresponding polyradical due to its poor solubility. Together with some equivocal data from the *meta-meta* linked **HMMMTR**, some skepticism was raised in those promising results from **HPPMTR** and **HMMPTR**. Both being soluble, **HPPMDIT** and **HPPPDIT** now represent the first pair of regioisomeric soluble polymers with ferromagnetic and antiferromagnetic coupling units respectively implanted in the network. It is anticipated that, by comparing the magnetic properties of their corresponding polyradicals, it can finally be settled whether the ferromagnetic interactions in these polyradicals are accidental or designed.

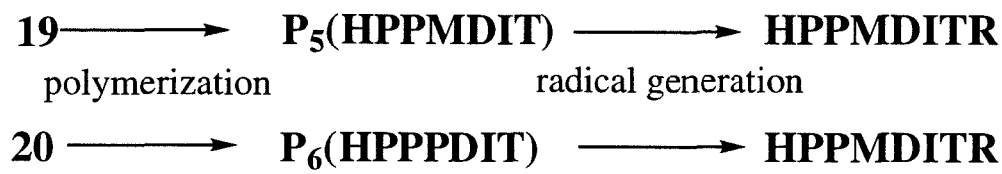

The polyradicals, **HPPMDITR** and **HPPPDITR**, were synthesized with reactions identical to those previously described. In both cases, the reduction step was carried out in suspended solutions of polytrityl trifluoroacetate at -78°C. For **HPPMDIT**, the color changes during the course of the transformation are almost indistinguishable from those of its unsubstituted counterpart **HPPMT**. This is anticipated considering both

polymers have the same pattern of cross conjugated π system. On the other hand, when **HPPPDIT** underwent the same treatment, the colors of the solutions are visibly different from all former instances. The TFA solution **HPPPDIT** is blue compared to the deep red of **HPPMT** (and every other polymer). The powder sample of **HPPPDITR** is green while all other polyradicals are yellow. These color changes are totally consistent with the longer conjugation in **HPPPDIT** as its optical absorption clearly shifts to a longer wave length. It also indicates that some extensive conjugation does exist in the polyradicals. This alleviates some concerns that these systems are actually non-interacting monoradicals linked together covalently. Both **HPPMDITR** and **HPPPDITR** were handled as other polyradicals in the SQUID measurement. The fitted result are in Table 2-4.

	HPPMDITR	**HPPPDITR**
S Value	1.6-2.2	1-1.5
Spin Concentration	20-22%	7-10%

Table 2-4 Magnetic properties of *ortho* substituted polyradicals

The spin concentration is once again disappointing . Although, it seems the spins do have higher survival rate in **HPPMDITR** than **HPPPDITR** (supposing the reduction in both instances have similar efficiency), no clear improvement was observed over the unsubstituted systems in either case. Apparently, even the installation of two bulky isopropyl groups is not adequate to protect the radicals from decomposition.

The S values are even more puzzling. The good news is the twisting imposed by *ortho* substitution apparently does not have much deleterious

effect on the ferromagnetic interaction. Unfortunately, a fitted S definitely larger than one is seen in **HPPPDITR** where it should be no more than 0.5. This means the antiferromagnetically coupled control system exhibits ferromagnetic interactions just a little weaker than the *para-meta* linked designed system. This totally unexpected outcome seems to dismiss all previous results. An immediate conclusion would be that the design strategy is invalid. The observed high-spin species could come from some unintended intermolecular superstructure or even ferromagnetic contamination. Both possibilities must involve unknown interactions (or side reactions) that are much more subtle than the current design has intended. It is thus unlikely that these inadvertent factors can be eliminated by just synthesizing more elaborate new polymers or developing new radical-generating protocols. In the next section, a new mode of ferromagnetic interaction unique to dendrimeric and hyperbranched systems will be introduced to explain the seemingly irreconcilable results.

Discussion

In a practical sense, the effort to "improve" the polymers is in vain. All three new polyradicals show neither higher S values nor higher spin concentrations than their uncapped or unsubstituted counterparts. Nevertheless, these results have provided some valuable information about the nature of the spin carrying species and the interaction that lead to the observed magnetic behavior. This section will first deal with those "normal" results where the design seems to have worked, although not perfectly, sufficiently well. The focus will then be shifted to the more daunting task of resolving the conflicting data from **HPPMDITR** and **HPPPDITR**.

As mentioned earlier, the hyperbranched trityl polymers show significantly improved spin concentrations over the polaronic magnets. This advantage still prevails in the modified systems. With the exception of **HPPPDITR**, spin concentration around 20 percent seems to be the norm for this class of material.

The spin concentration from **CHPPMTR** clearly asserts that *para* halogen substitutions do not effect the radical stability either during or after they are generated. It is also established that how the polyradical is generated does not effect its magnetic property to any substantial degree. Either the capping t-butyl phenyl is totally ineffective as a protecting group or the original polyradical loses its spin via some pathways unrelated to the *para* substitution. Despite the two bulky *ortho* protecting groups, the spin concentration of **HPPMDITR** does not show any improvement either. From simple CPK molecular modeling, it is very unlikely any dimerization can occur at the α position because of the steric hindrance. If it is assumed the effect of substitution on radical stability is general in all polyradicals, the logical conclusion of these results points to a common radical decay mechanism that is intrinsic to trityl type structure other than α dimerization. Possibilities include oxidation and hydrogen atom abstraction. A logical prevention to these decays is using even more hindered monomers. For example, 2,2',2",6,6',6"-hexamethoxyl triphenyl methyl is a well known monomeric radical that is stable even in atmospheric oxygen[74]. However, to make such highly crowded monomer is undoubtedly very challenging synthetically. There also remains the concern that such a system will be so severely twisted around the radical centers that the ferromagnetic interaction will become too small to align a

multitude of spins. This high-risk and labor-consuming direction is thus not seriously pursued.

One puzzling aspect of polyradical chemistry has always been the correlation between spin concentrations and S values. Many polyradicals, including those in this study, have spin concentrations far less than 100 percent. The defects divide the polyradicals into small spin segments which gives much lower Ss. When the spin concentration is as low as 20 percent as in the current cases, about 80 percent of all spin sites should be isolated monoradicals. Furthermore, if the radical distribution is purely statistical, less than one percent of all active sites should be in an interacting tetraradical assembly. This does not seem to be the case. Judged from the saturation plot, considerable percentage of the radicals exists as spin clusters of size around three to four. Rajca has also observed high-spin coupled pentaradical in a tetradecaradical with a defect rate of 60 percent. Murray reported a similar phenomenon in linear polaronic ferromagnets where an S value of 2.5 has been perceived with spin concentration lower than one percent. Apparently, the radical generating or decaying process is far from homogeneous. Murray proposed an inhomogeneous doping model to account for the observed S in lightly doped poly (*m*-phenylene dithiophene). However, this hypothesis is not applicable here because all reductions are performed in the solution phase with exactly one equivalent of metalocene reductants and the reduction appears to be complete. Therefore, this non-uniform distribution of radicals should be attributed to inhomogeneous decay.

There are at least two reasonable explanations for this peculiar behavior. First, the stabilization from an extended π system can reduce its reactivity and hence make it less susceptible to defects. Of course, in a

ferromagnetic coupled system, the π system is not conjugated in the sense that a new Kekule structure can be drawn. Nonetheless, they can still be stabilized as a result of the reduction of electron repulsion by spin correlation. The first defect introduced to a defect-free system can happen at any site. After the original polyradical is broken into two or more non-interacting fragments by the first defect, the following defect can happen at either of these pieces depending on their reactivities. According to this line of argument, the defect will go to the smaller spin clusters as they tend to be more reactive. Thus, the smaller polyradicals will break down into even smaller pieces faster than the larger spin cluster. Although the preference might be very small at each step, the survival rate of larger spin clusters will definitely prevail if the defects happen many times as in the present cases. Figure 2-26 is a schematic representation of how this mechanism works in a dendrimer system. It should be reemphasized that the "average" spin number from fitting a single S value to a mix-spin system always inclines towards the higher Ss (Figure 2-18). Therefore, it is quite probable that this bias of defect formation is at least partly responsible for the observed S.

The second explanation is based on the global structure of hyperbranched polymers. In contrast to what might be perceived in a two-dimensional presentation, molecular modeling studies have repeatedly confirmed that dendrimers are rarely planar[75]. A detailed description of the conformational behavior of dendrimers is beyond the scope and necessity of this work. It is now generally accepted that there are complex intramolecular cavities, channels and other microstructures in a dendrimer molecule. In fact, using dendrimers as host molecules has always been a major pursuit in this field[76]. This leads to the important conclusion that

some monomer units are located in the "outer sphere" of the polymer globe and provide a barrier to protect the "inner sphere" units from physical contact with the environment. A recent report by Diederich has demonstrated how this concept is applied to an iron-porphyrin system functionalized by four leaves of dendrimers[77]. Another late research used a dendrimer as the host to encapsulate small molecules. When the monomer units at surface are functionalized with bulky groups, some guest molecules are permanently trapped inside the dendrimer box[78].

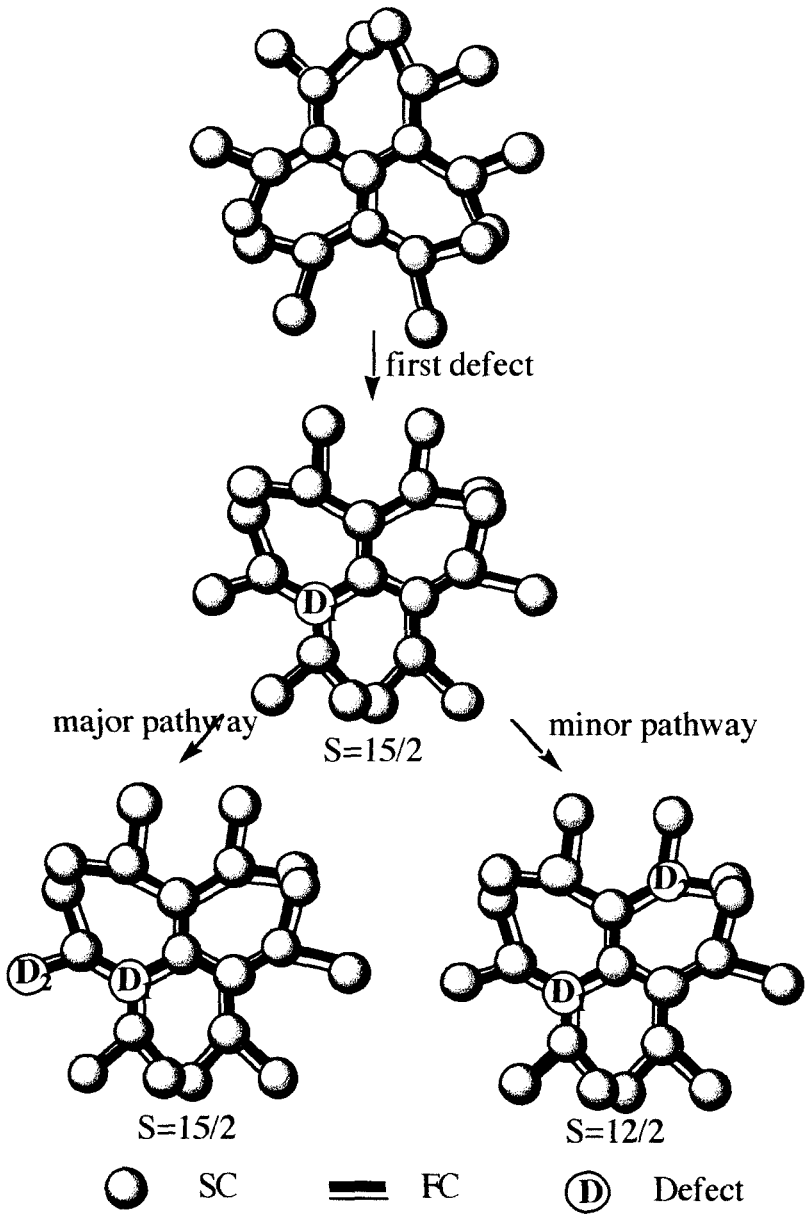

Figure 2-26 Non-statistical defect distribution resulted from radical clusters with distinct reactivities

Are these experiments relevant to the present study? The answer is yes if hyperbranched polymers also have the distinct inner and outer units as dendrimers. Although only perfect dendrimers are modeled by theory, it is hoped the related hyperbranched structure will exhibit similar behaviors at

least qualitatively. The radical decomposition pathways perceived so far all involve some atom or group transfer reactions. Unlike the metalocene reduction step which is electron transfer in nature, such reactions are very sensitive to the distance between the reactants. It is conceivable that the outer units protect the inner ones from oxidation or other types of radical decay by providing a barrier to keep out the defect-causing molecules. Although these outer sites themselves are still susceptible to the damages, the loss of these spins should have only moderate impact on the S value since they are by definition peripheral. Furthermore, the inner radical units are probably protected even better when many surface units become defects. Whenever a defect is introduced, a planar sp^2 radical becomes a tetrahedral sp^3 center. Since the tetrahedral center clearly occupies more space than the planar trigonal one, a layer of surface defects should form a better protecting shell against further decomposition than the surface radicals themselves. If some defects are caused by certain radical dimerization or dioxygen reactions with two trityl units, the resulting surface crosslinking can make this protecting shell even more robust. Figure 2-27 shows this mechanism at work in a hypothetical polyradical.

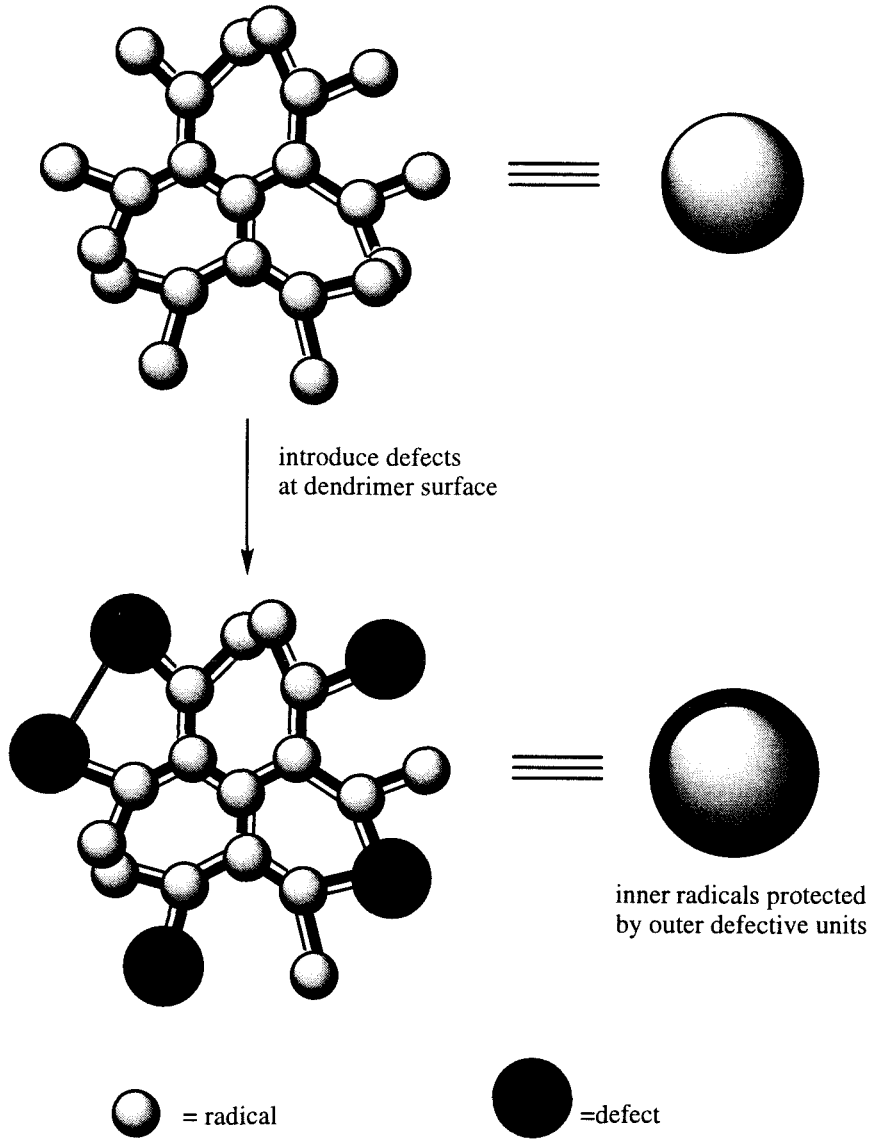

Figure 2-27 Non-statistical defect distribution resulted from global structural feature

It is also quite possible that some intermolecular packing contributed to the stability of inner radical units. This mechanism can be particularly important in this work because all the reductions at low temperature are heterogeneous. These samples probably contain polyradical segments never

exposed to anything other than its surrounding polymer matrix during the whole course of the transformation.

Although the high-spin ground state in these systems is guaranteed on account of the FCs, the effect is factored down by the square of spin densities of SCs at their connecting points. To compare interactions in related systems, since the spin density map for an SC is often not intuitive, it is helpful to consider the coupling strength in terms of number of unpaired electrons and the size of the π system. This concept is derived from the relationship between high-spin coupling and the electron repulsion. When two electrons are confined to a small π system with ferromagnetic topology, the large repulsion leads to a preference for the triplet state. On the contrary, in extensively conjugated diradicals, the two spin states can be nearly degenerate regardless of topology because the electrons would hardly have any chance to interact with each other. The preference for high-spin ground state can be further diminished by the twisting in the π system. Equation 2-3 shows how the interaction is affected by the twisting dihedral angle θ.

$$I=I_{planar}\cos^2\theta \qquad \text{(Eq. 2-3)}$$

I_{planar} = the theoretical interaction at Huckel level

Qualitatively, judged from the S values, the ferromagnetic coupling survives all these challenges. The ferromagnetic coupling unit used here, *m,p'*-biphenylene, is surprisingly robust. All four polymers with this topology show unmistakable high-spin coupling at low temperature regardless of other electronic and steric factors. This is quite remarkable considering how delicate these interactions can be. Therefore, *m,p'*-

biphenylene proves to be another excellent ferromagnetic coupling unit. Although it is conceptually just an extended version of *m*-phenylene, this structure does have some advantages over the more widely used *m*-phenylene. First, as mentioned earlier, the size of the π system ought to be large enough to stabilize the radicals yet small enough to ensure strong magnetic interaction. A proper balance of these two factors is the key to an ideal ferromagnetic coupling unit. *m,p'*-Biphenylene appears to be a promising candidate for further investigation. It extends the smaller *m* -phenylene by one aromatic ring while it maintains the ferromagnetic interactions at a fairly decent level. Synthetically, this unit is more accessible than *m*- phenylene thanks to the numerous transition metal catalyzed aryl-aryl coupling reactions. In fact, Rajca has recently used it to construct a polyradical with a record breaking S value of 10.[79]

In this work, the hyperbranched structure is chosen as the target mainly because its branching points imitate a two-dimensional system. Since the design is only partly successful, the question arises whether the branching structure is advantageous at all. Studying linear controlled polymers will not help to answer this question unless the spin concentrations in the two systems can be controlled at the same level. It has recently been reported that dendrimeric structures might not be particularly beneficial in making high-spin polytrityl[80]. Since a hyperbranched polymer can only have half the branching points of a dendrimer at most, it is not surprising the hyperbranched polyradicals do not exhibit any gigantic S values.

The original expectation is that the hyperbranched system can be more tolerant of defects because it possesses much more "less important" peripheral sites than a linear system (Figure 2-4). Theoretically, the average S of a dendrimeric 46-radical with one defect should retain more

than 90 percent of that of a defect-free system while the same defect rate in a linear system can cause the S to drop by more than 25 percent. However, this notion is valid only when the spin concentration is sufficiently large. Ironically, when nearly 80 percent of all sites are defects as here, a dendrimer or hyperbranched structure can have just the opposite effect. To visualize this down fall, it is helpful to imagine a hypothetical polyradical being constructed by putting radicals into an empty dendrimer skeleton as filling the pigeon holes. By the same argument how defects should have happened mostly at outer sites, the first few radicals to be placed are much more likely to be at the edge of the structure and thus isolated from each other. Such trend continues until at least 25 percent of the sites are filled. The desired "defect-resistant" property comes out only after more than 60 to 70 percent of all sites are occupied. Likewise, in hyperbranched systems, the first 25 percent of radicals are likely to occupy the linear portion of the polymer. In order for the polyradicals to be defect-insensitive, a spin concentration higher than 70 percent is required. Apparently, the spin concentrations of polyradicals discussed here do not even reach the first threshold. Therefore the preservation of high-spin species observed here should not be attributed to the hyperbranched structure. Instead, the more reasonable explanations should be the reactivity and structural factors mentioned before.

The obvious next step is to improve the spin concentration. One such attempt will be presented in the next section. However, it has also been reported that a highly branched systems with spin concentration higher than 80 percent still exhibits only moderate S value[81]. Apparently, polyradicals can be even more sensitive to defects than what is derived from the simple pigeon-hole model.

All the discussions so far have been focused on those "normal" polyradicals where the ferromagnetic interaction is presumably the result of the designed topology. However, at the heart of all these seemingly logical rationales lies a very serious flaw. The result from the control polyradical **HPPPDIT** seems to suggest that the observed ferromagnetic interaction has nothing to do with the designed topology. However, the magnetic property of the linear control polymer, poly(*p*-tert-butyl *p',p"*-triphenylmethyl), seems to suggest otherwise (Figure 2-28).

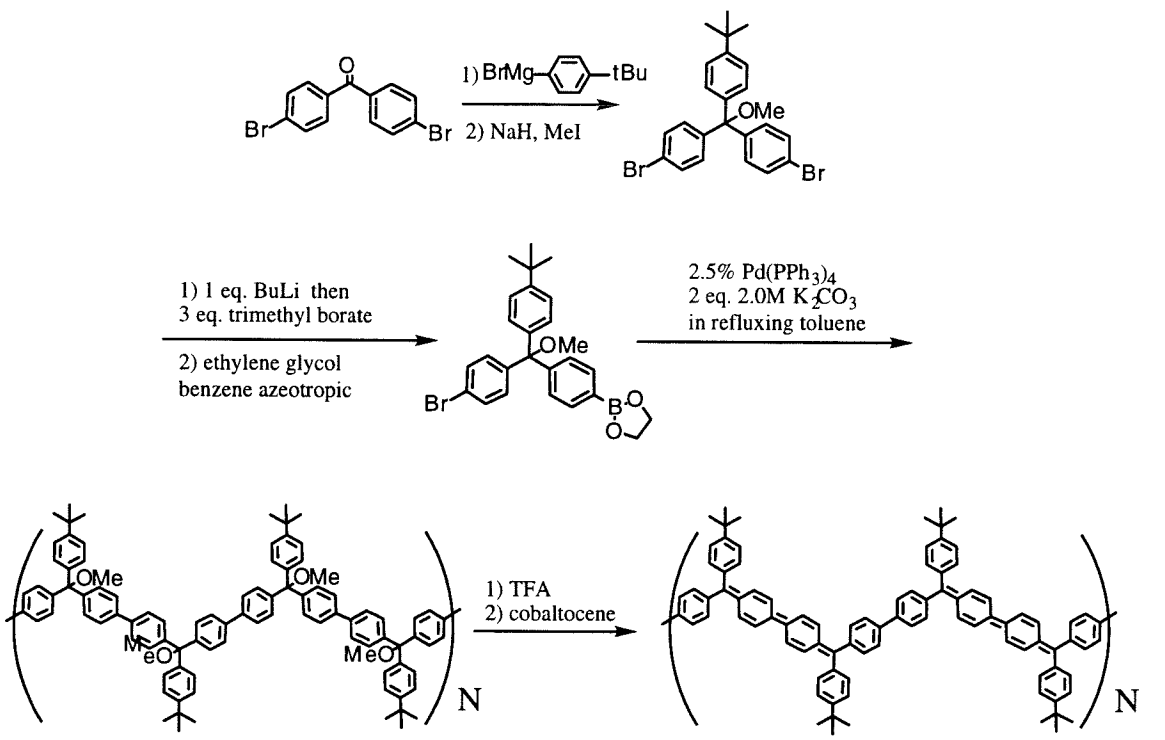

Figure 2-28 Synthesis of a *para* linked linear trityl polyradical

The SQUID measurement reveals this polyradical to be diamagnetic, a strongly indication that this polyradical has a singlet ground state. This control experiment reaffirms *p,p'*-biphenylene to be the antiferromagnetic coupling unit as predicted by theory. It also to some extent discounts the

possibility that the high-spin ground state in **HPPPDITR** is caused by some unintended noncovalent interactions.

In the polaronic ferromagnets investigated earlier, the S value for poly(phenylene octatetraene) unambiguously drop from 2.0 to 0.5 when the ferromagnetic coupling unit, *m*-phenylene, is replaced with *p*-phenylene, an antiferromagnetic one. This observation excludes that the high S value of **HPPPDITR** comes from instrumental problem or the mathematical artifact of the fitting procedure.

The most disturbing possibility is that every high S value in this project comes from some contamination. Although this has not been directly ruled out, there are some circumstantial evidences arguing against it. First, the spin concentration in all samples are relatively high. It is unlikely any high-spin impurity can be consistently introduced at such concentration. Second, the S value for **HPPPDITR** is measurably smaller than for other polyradicals. There is no reason why this particular polyradical should be less prone to contamination. Similarly, the linear control system in Figure 2-28, which was generated by the same procedure as all others, exhibits the physical properties of an antiferromagnent. There is no rationale why it should be immune to contamination. Finally, the effective moment plots of **HPPMTR** and **HPPPDITR**, though neither exhibits clear cut upturn temperature, are visibly different. This observation strongly argues against a common contaminant being responsible for the magnetic behavior in all the samples.

After some evaluation of various factors, we are forced to face the possibility that the S value does come from **HPPPDITR** itself. The challenge then is to develop a physically sound model which explains how

net ferromagnetic interaction can result from neighboring anti-ferromagnetic interactions.

To reevaluate the dilemma we start from the five fundamental types of magnetism introduced in Figure 1-1. In these phenomena, the origin of ferrimagnetism bears the closest resemblance to what is required for the new model. In a ferrimagnet, there are two kinds of SCs with different S values coupled antiferromagnetically. A net bulk moment in such a sample is guaranteed because two moments of different magnitudes can never cancel each other completely. The similarity to **HPPPDITR** lies in the sense that antiferromagnetic neighboring interactions result in a high-spin ground state. However, since there is obviously only one type of radical, namely trityl, in **HPPPDITR**, what is observed here can not be real ferrimagnetism. After all, at least some interactions in a ferrimagnet within one SC are still ferromagnetic in order to produce the two S values. **HPPPDITR**, on the other hand, does not have such luxury.

A more likely scenario is that, for some reason, **HPPPDITR** has two non-equivalent sets of sites. If the number of sites in these two sets are not equal, a residual moment would naturally result from the incomplete cancellation of the opposite spin angular momenta. This can happen even when the adjacent interaction is strongly antiferromagnetic as imposed by *p,p'*-biphenylene. This explanation, in a certain sense, is very similar to ferrimagnetism. In both models, unpaired electrons are divided into two groups of unequal populations and net bulk moments arise from the incomplete cancellation of the opposing moments. In ferrimagnetism, such division comes from the two chemically distinct SCs. In **HPPPDITR**, on the other hand, the assorting can take place naturally from its

hyperbranched structure which, as mentioned before, always has more peripheral units than central ones.

Under this hypothesis, we reexamine the spin ground state in some perfect dendrimeric polyradicals with antiferromagnetic coupling units as simulative systems to **HPPPDITR** (Figure 2-29).

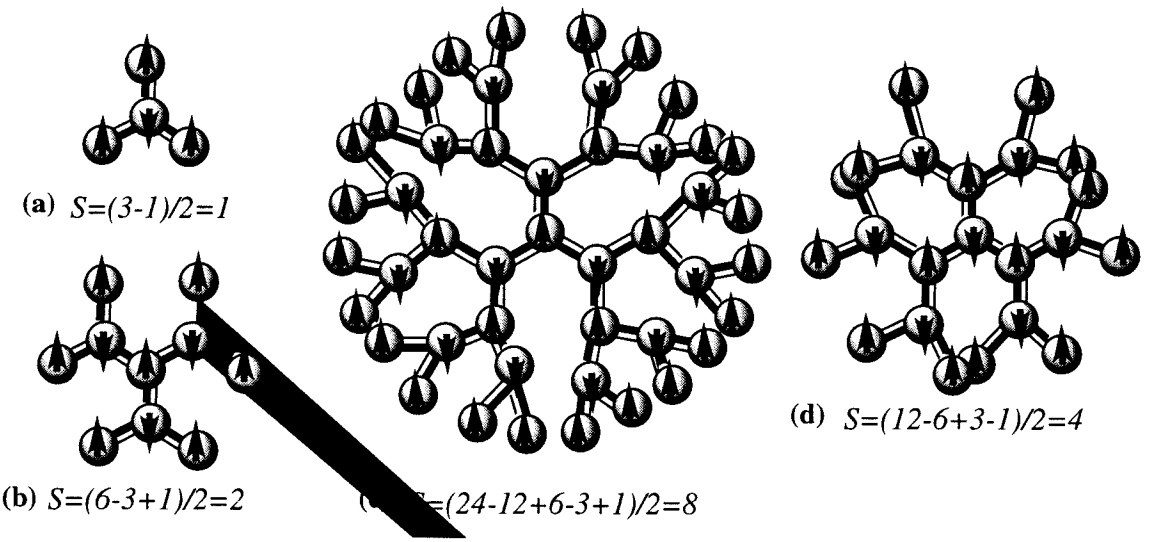

Figure 2-29 Hypothetical high-spin polyradicals with antiferromagnetic coupling units

At first, to our great surprise, all the hypothetical dendrimeric polyradicals have high-spin ground states despite the antiferromagnetic interactions between all adjacent sites. The spin orientation of radical units alternate between the dendrimer layers as the antiferromagnetic interaction requires. However, every layer has at least two times as many units as its immediate inner layer. The "two sets" of spins hence are divided between the even-number and odd-number layers. The population of the two groups can never be equal and therefore results in the incomplete cancellation depicted in the last paragraph.

Upon a closer inspection, we realize this anomalous ferromagnetic coupling should have been anticipated all along. Actually, the origin of this oddity is closely related to the spin polarization model for diradicals proposed by McConnel[82]. This simple model states that the spin wave function at every atom in a diradical is slightly polarized by the unpaired electrons. The diradical will have a triplet ground state if the net result of this polarization produces excessive spins in one direction or otherwise the ground state will be singlet (Figure 2-30).

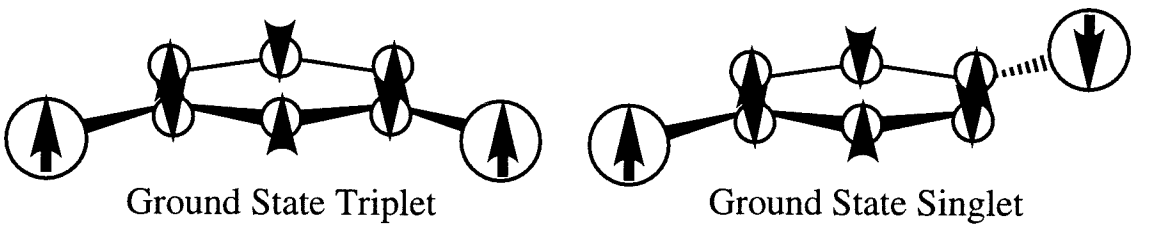

Figure 2-30 McConnel's model of predicting ground state spin multiplicity

This is a restatement of Ovchinnikov-Borden in a physicist's language. Compared to the systems in Figure 2-29, the antiferromagnetic coupling is analogous to the polarization and the incomplete cancellation is similar to the non-zero net polarization. In fact, two well-known triplet biradicals, TMM and Yang's biradical, can just be perceived as tetraradicals with neighboring antiferromagnetic interaction as in Figure 2-29a.

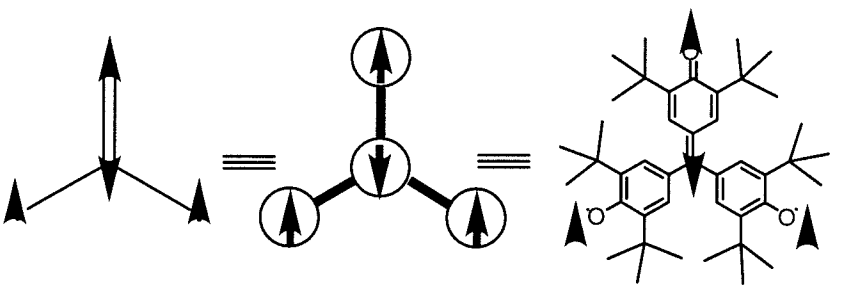

This concept can be easily adapted to hyperbranched systems. About half of the sites in a hyperbranched polymer have dendrimer like topology while the other half behave like linear polymers. The linear portion of **HPPPDITR** is not expected to carry much measurable moment because of the antiferromagnetic coupling. The dendrimeric segments, on the other hand, should have high-spin ground states as the model systems in Figure 2-29. For **HPPPDITR**, the S value can arise from a dendrimeric seven-radical cluster. This cluster size is, while it remains reasonably close to those in other polyradicals, a little larger. In contrast to **HPPMTR** and **HMMPTR** where the branching structure appears nonessential to conduct the ferromagnetic interaction, branching points play a crucial role in the magnetic property of **HPPPDITR**.

With this new model, not only the magnetic behavior of **HPPPDITR** is rationalized, it also helps to clarify the ambiguous S value of **HMMMTR**. In the preliminary discussion, the high-spin ground state in **HMMMTR** depends entirely on that the *m,m'*-biphenylene unit behaves as a weak ferromagnetic coupling unit. Now, it becomes clear that **HMMMTR** can possess high-spin ground state segments even if the *m,m'*-biphenylene is an antiferromagnetic coupling unit. The smaller S of **HMMMTR** rightly reflects the more equivocal nature of *m,m'*-biphenylene as a coupling unit.

Admittedly, there is no conclusive evidence yet that this new model is the actual mechanism working in **HPPPDITR**. Because of the complexity of the system, no further control experiments were performed. There are, however, two observations that strongly support this idea. First, in spite of the resulting high-spin ground states, all polyradicals in Figure 2-29 still lose substantial amount of moment due to the antiferromagnetic interaction. For example, the decaradical (2-29b) has a quintet ground state, which could have been undecet if the interaction were ferromagnetic. In other words, sixty percent of spins annihilated each other. Figure 2-31 is a side-by-side comparison of two otherwise identical dendrimers with ferromagnetic and antiferromagnetic coupling units respectively. Depending on the size of the system, 60 to 75 percent of the spins cancel each other in 2-31b. If the polyradical is very large, the survival rate of the spins will be about one third.

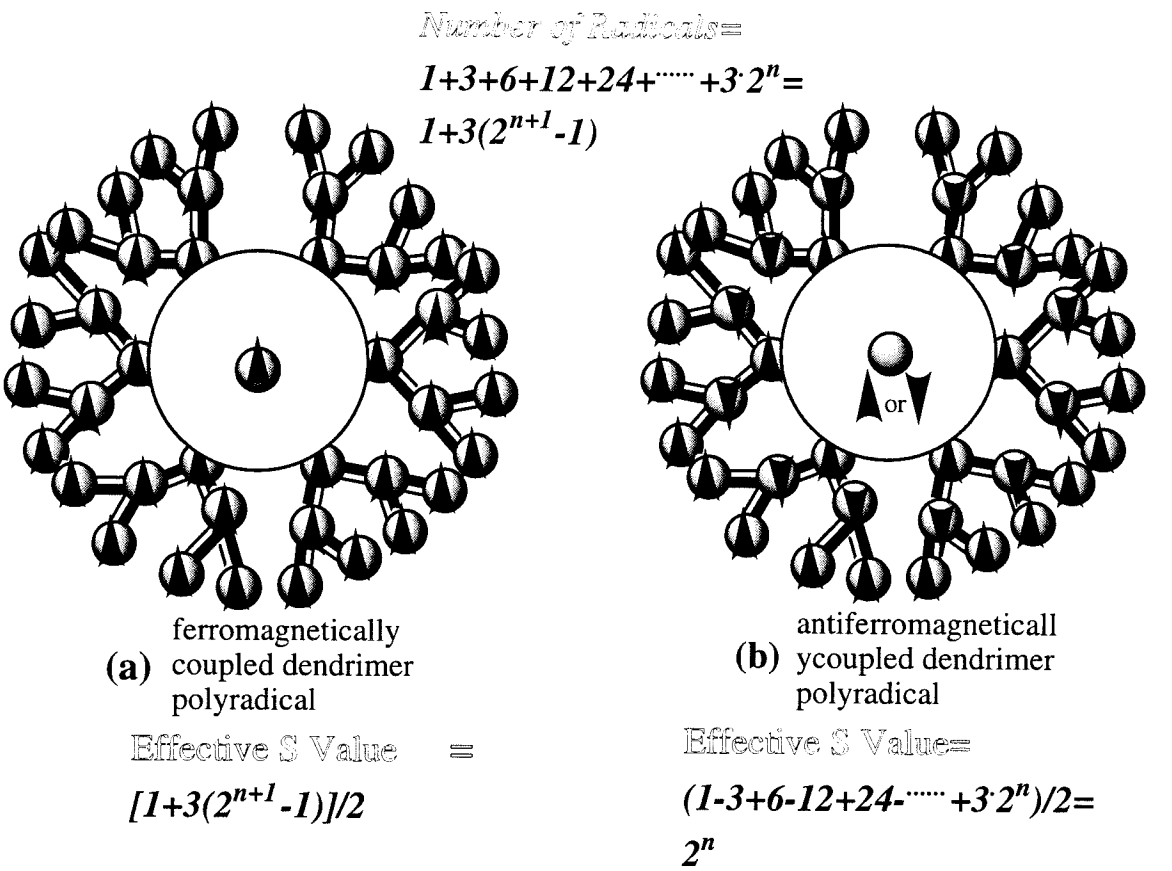

Figure 2-31 The theoretical S values of hypothetical polyradicals

The antiferromagnetic interactions are often too strong for the external field to overcome. If the spins in polyradicals with different coupling units have similar stability, the molar saturation moment of **HPPPDITR** should be only half to one third that of **HPPMDITR**. The observations fit this prediction very well (Table 2-4). Without employing this new model, the smaller spin concentration of **HPPPDITR** would be hard to justify.

The second evidence comes from a dendrimeric tetraradical cation. Clites synthesized a first-generation dendrimer composed of four triphenyl amine moieties. Oxidative doping with nitrosonium tetrafluoroborate furnished tetraradical cation **25** (Figure 2-32)[83]. **25** is obviously

topologically related to TMM type system in 2-29a. Its SQUID measurement indicates a S value around 0.8, again points to ferromagnetic interaction.

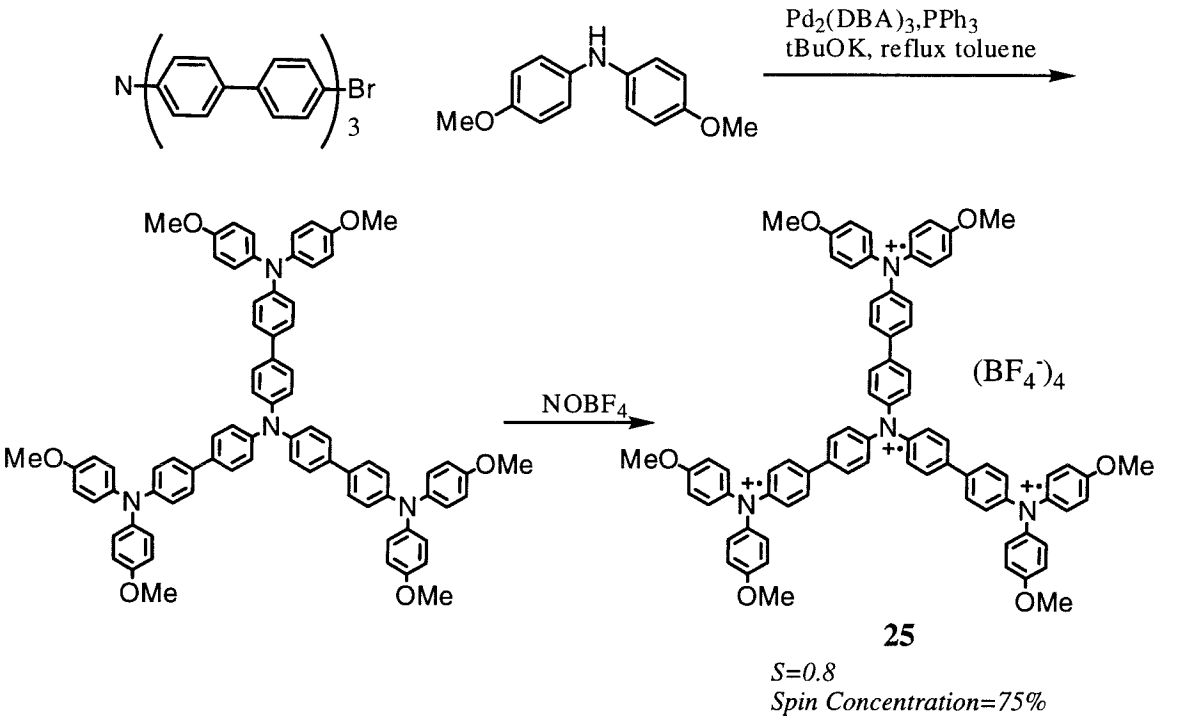

Figure 2-32 Tetra-(triaryl amine) radical cation with triplet ground state

This outcome signifies the validity of our new model in a closely related system. Compared to trityl radical, the unpaired spins in triphenyl amine radical cation should be much more localized because of its cationic nature. As a consequence, the singlet-triplet gap of **25** must be substantially smaller than its tetratrityl analogue. Therefore, as a definitive sign of high-spin coupling is observed in **25**, it is only reasonable to assume similar interaction also occurs in **HPPPDITR**.

Finally, if the model is correct, the spin clusters in **HPPPDITR** seem to be a little larger than those in other polyradicals. This small difference can be attributed to extra radical stability resulting from the all *para*

topology. As mentioned previously, the *para* position of a trityl is the place where a lot of radical decomposition reactions take place. In **HPPPDITR**, every *para* position is protected by a phenyl group or a bromide. For every other polyradical studied here, at least one of the *para* positions in the radical units is unsubstituted and thus more susceptible to certain defects. Again, its low solubility also contributes to the stability as explained before. Finally, unlike **HPPMTR** and **HMMPTR**, **HPPPDITR** can have numerous stable Kekule structures which can stabilize the system by resonance. Several examples in a hypothetical decaradical are shown below.

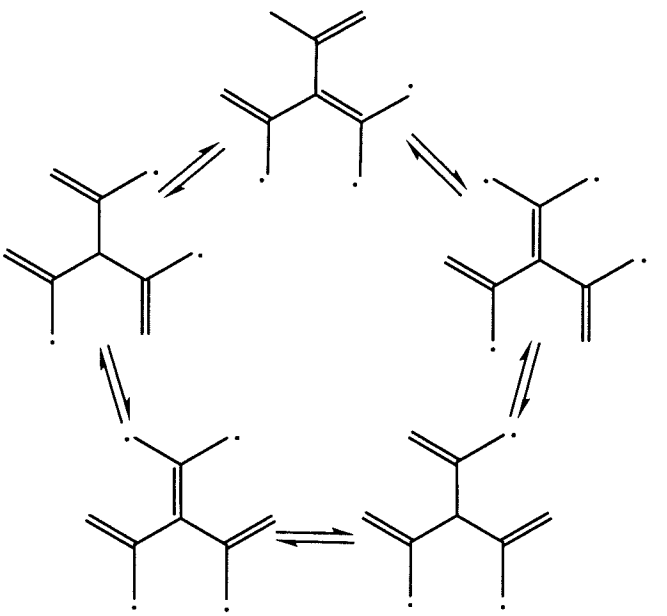

Figure 2-33 Resonance structures of a decaradical with S=2

Conclusion

A preliminary understanding of magnetism in hyperbranched polymers has been drawn from these studies. A number of important conclusions are summarized as followed.

• Trityl based hyperbranched polymers with substantial degrees of branching can be made reliably by employing a unimolecular polymerization with bifunctional monomers. A selective lithium-halogen exchange reaction was developed for the synthesis of monomers. As for the polymerization, Suzuki's cross-coupling reaction by far offers the most satisfactory molecular weights for unhindered substrates. The reaction conditions are mild and the yields are generally excellent. A similar reaction condition was even used to functionalize a polymer with high efficiency.

• The trityl ether units were transformed into trityl radicals by first treating the polymers with TFA. The produced polytrityl trifluoroacetate was then reduced by cobaltocene at low temperature. This procedure is relatively convenient and also applicable to all the polymers studied here. Other methodologies suffer solubility, reactivity or technical problems.

• S values of the all polyradicals are noticeably greater than 0.5 which indicates ferromagnetic interactions between the spins at least at low temperature. These results further extend the validity of our design paradigm to hyperbranched systems. Weak antiferromagnetic interactions are seen in all the samples in variable temperature plots. Judged by their magnitudes, these interactions should be through space in nature. Yet, it is not clear whether these interactions are intermolecular or intramolecular.

• The polyradicals are stable at room temperature for finite periods of time. Their spin concentrations are generally around 20 percent. This

represents a significant improvement over the earlier polaronic ferromagnets.

- The most intriguing finding from these studies is that a hyperbranched polyradical, **HPPPDITR**, appears to have a high-spin ground state although all the interactions between adjacent spins are antiferromagnetic. This unanticipated phenomenon is explained by a new model very similar to McConnel's spin polarization model. The new model thus reveals a novel strategy in designing magnetic material that is not hitherto widely recognized.

Some notable limitations of this design have also been exposed.

- Despite the hyperbranched structure, one polymer is completely insoluble in any common solvent.
- The stability of radicals does not improve any further by removing the excessive bromides or surrounding the radical centers with bulky groups. The radical decay appears quite insensitive to these structural modifications.
- The spin concentration, despite some improvement, is not high enough to ensure very large S as desired.
- There is no clear-cut control experiment that can unambiguously disclose the effect of hyperbranched topology and various coupling units.

The second and the third problems listed above are clearly interrelated. Although Rajca's success in similar systems seems to discount the concern for radical stability, the results here lead us to question whether such polyradicals are intrinsically fragile. However, some minor difference between Rajca's protocol and what is used here should be noted. In Rajca's procedure, the polyradicals are kept at low temperature at all times and the sample is measured in THF or MeTHF frozen solution. On the contrary,

our samples are briefly exposed to room temperature and powder samples are used in most cases. The temperature factor could be especially decisive. Rajca's tetradecaradical has been reported to lose 60 to 90 percent of its spins after standing at room temperature for 30 min to 24 hour. This is very consistent with our results. Structurally, Rajca's polyradicals are built on a rigid scaffold that tends to keep the radicals spatially separated. The hyperbranched polymerization, however, can not provide such structural control. It is thus quite probable that hyperbranched systems lose radicals through some intramolecular reactions between the units. How these radicals decay is still not clear because none of the decay products have been characterized. Therefore, it is quite difficult to rationally design a more defect-resistant system.

Future Directions

Instead of making systems with increasingly hindered radical centers, electronic factors are also worth exploiting as a mean to stabilize the radicals. Triaryl amine radical cation and 2,6-di-t-butyl-fuchsone radical anion are two classes of charged radicals structurally closed related to triphenyl methyl. Because of the presence of heteroatoms, these two charged radicals are much more stable than trityl itself and therefore both are suitable candidates as SCs for examination. One tetraradical composed of triaryl amine radical cations was already made (Figure 2-33). Some possible applications of this radical unit will be discussed in more detail later.

Besides being exceptionally stable, 2,6-di-t-butyl-fuchsone radical anion is also easily accessible by electrochemistry. This favorable property makes it the SC of choice in Anderson's synthesis of linear high-spin

polyradicals[84]. In that study, an unambiguous correlation between S values and spin concentration is observed for the first time. Equally significantly, the onset temperatures of ferromagnetic interaction shows moderate correlation with the extent of reductive doping. Both results are hints of collective behavior.

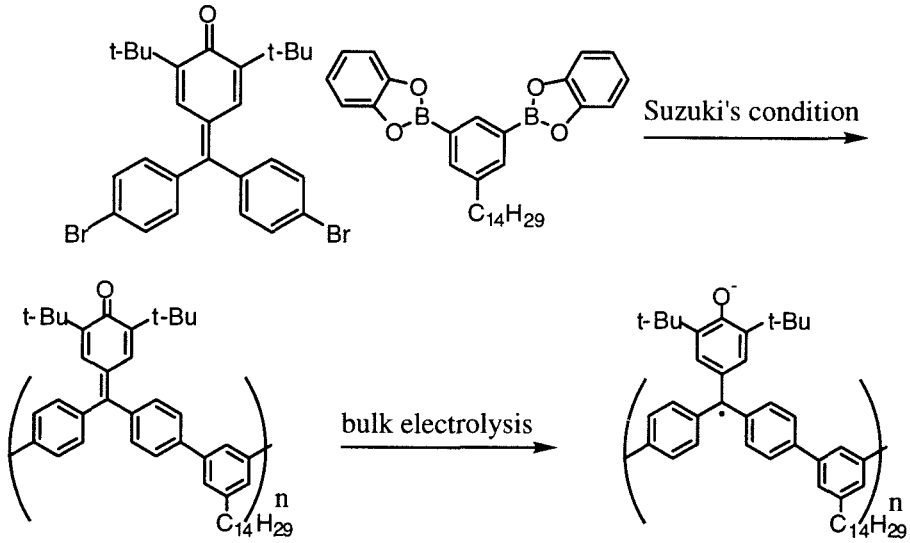

Figure 2-34 Anderson's approach to high-spin polyradical

This breakthrough is attributed to both the well controlled electrochemical doping and the suppression of intermolecular antiferromagnetic interactions. The author also points out that in otherwise identical systems, diradicals composed of radical anions should have larger singlet-triplet gaps than those containing neutral or cationic SCs[85]. The rationale is again that electron repulsion should be stronger in an anionic system because there is much less space for electrons to avoid each other. This implies, as SCs, radical anions may have some intrinsic advantages over the cationic and neutral radicals.

A sensible step following this success is to make hyperbranched poly-fuchsone and wish that the branching structure will cause even stronger collective behaviors. The synthesis can be easily achieved with the familiar unimolecular A_2B type polymerization. The synthesis of a suitable monomer and the polymerization procedure are shown below.

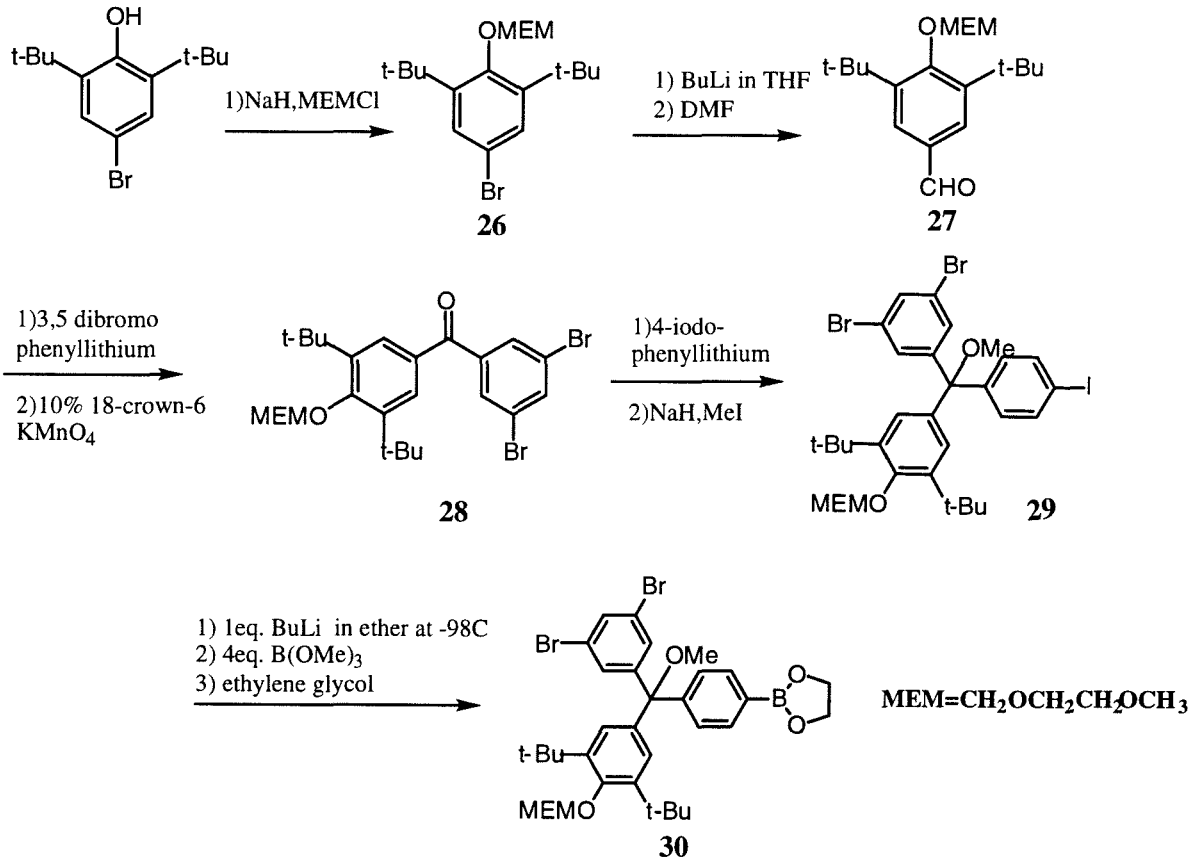

Figure 2-35a Synthesis of monomer **30**

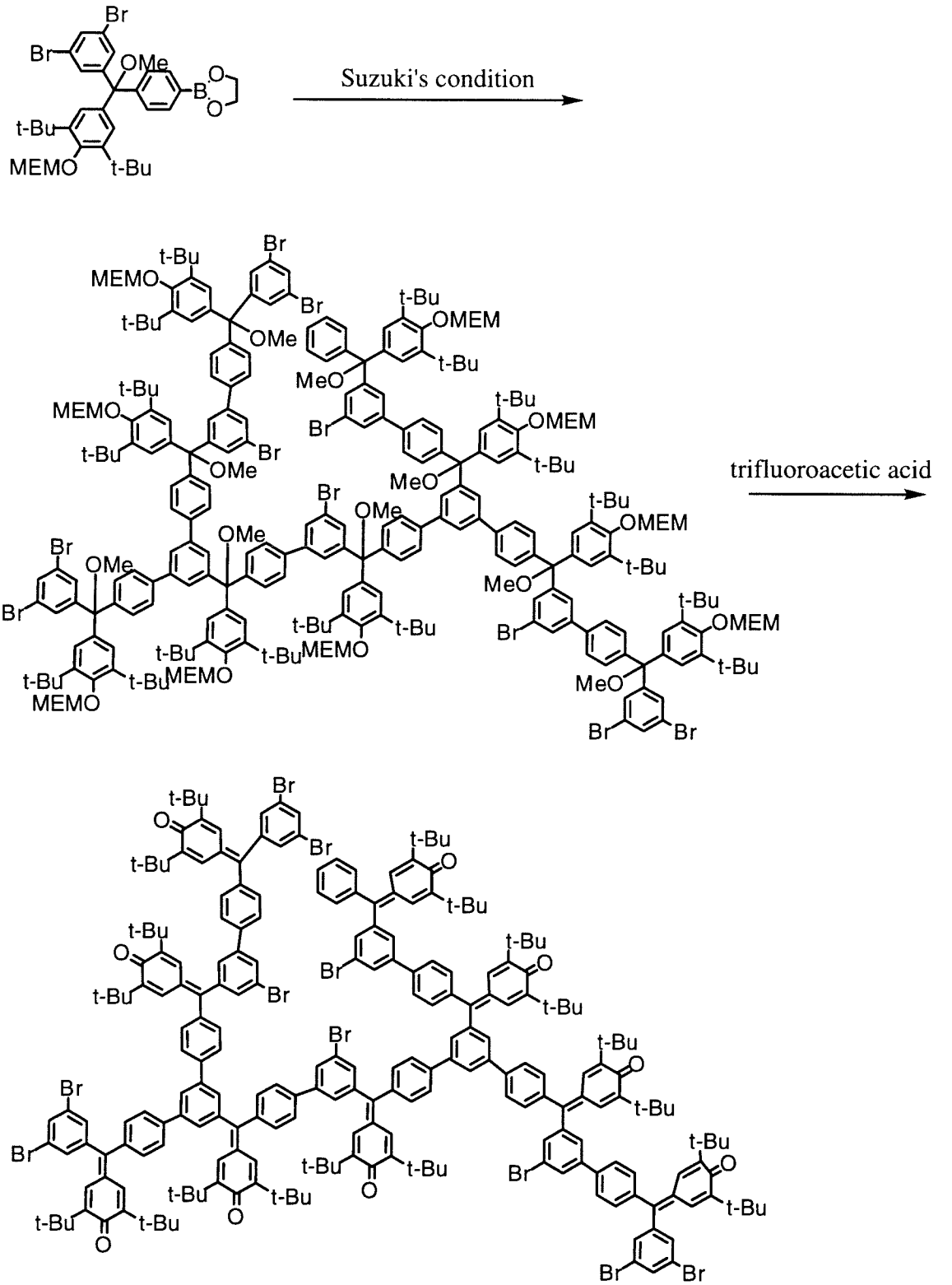

Figure 2-35b Synthesis of hyperbranched fuchshone

The strategy is quite straightforward. The hydroxyl of 2,6-di-t-butyl-4-bromophenol was first protected with a methoxyl ethoxyl methyl (MEM) group. The bromide was then converted into an aldehyde **27** via the aryllithium intermediate. 3,5-Dibromo phenyl lithium then added to the aldehyde to furnish the diphenyl methanol derivative that was immediately oxidized to benzophenone **28** by potassium permanganate under phase transfer condition. This neutral oxidation condition is essential to keep the MEM group intact. The second aryllithium addition incorporated the iodide functionality necessary for the selectivity in the next step. The boronic acid was then installed through the same selective lithium-iodide exchange reaction sequence for all other trityl monomers. Suzuki's coupling was again employed for polymerization. By dissolving the resulting polymer in pure TFA, the MEM protecting group and the methyl ether were simultaneously removed to produce the desired polyfuchsone structure. The last transformation is quite clean judged by NMR spectrum. MEM group is chosen specifically to guarantee the efficiency of this finally step. (When a methyl group was used instead, it stayed intact after the TFA treatment.) Unlike Anderson's original system, the fuchsone units are linked through the *m,p'*- biphenylene unit here. In a bis-fuchsone radical anion with this linkage, Huckle level calculation predicts the triplet state is stabilized by about 160 cal/mol. The corresponding onset temperature for such interaction is around 80 K, well within the detectable range of the variable temperature experiment. For the reduction, chemical or electrochemical doping should both be applicable. It is hoped that higher S value and more conspicuous collective behavior can be observed. Unfortunately, time constrains did not permit further work on this interesting polymer.

The hyperbranched structure is chosen for this study because its branching resembles a two-dimensional system. Since the present S values are not completely satisfactory, making the current systems more "two-dimensional like" should be the another judicious step to improve the S. The fundamental difference between a hyperbranched and a real two-dimensional system is the crosslinking that incorporates loops in the network. The benefit of the loop structures is that it provides alternative communicating pathways between the spins when defects are present (Figure 2-4). Rajca and coworkers claim to observe this effect in one of their systems[86]. Unfortunately, the original synthetic strategy of hyperbranched polymers is specifically designed to avoid intramolecular cyclization to keep the products soluble. In an attempt to make a crosslinking polymer, an A_2+B_3 type bimolecular polymerization was performed. Unfortunately, as expected, the product is very insoluble.

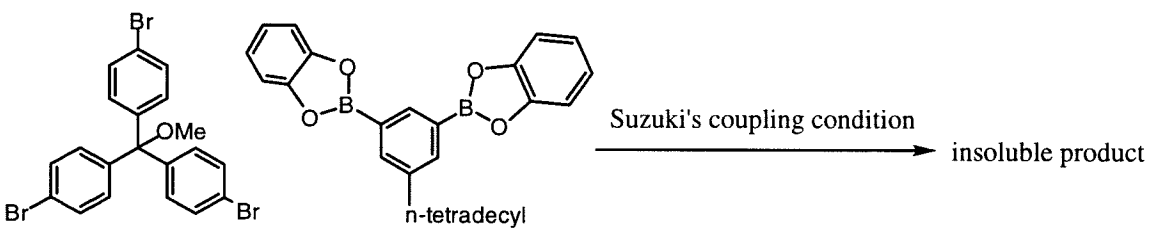

Here, we propose two strategies to introduce crosslinking into the polyradical in a more controllable fashion so that the favorable solubility may survive after the modification. The problem of the A_2+B_3 polymerization is that pairs of A-B are often attached to the polymer when it is still growing. This inevitably leads to extensive intramolecular cyclization and insoluble products. In the A_2B type polymerization employed in this work, only one boronic acid is present on the growing

polymers and therefore very few crosslinks can occur. An "end capping" cyclization reaction might combine the benefits of both strategies (Figure 2-36).

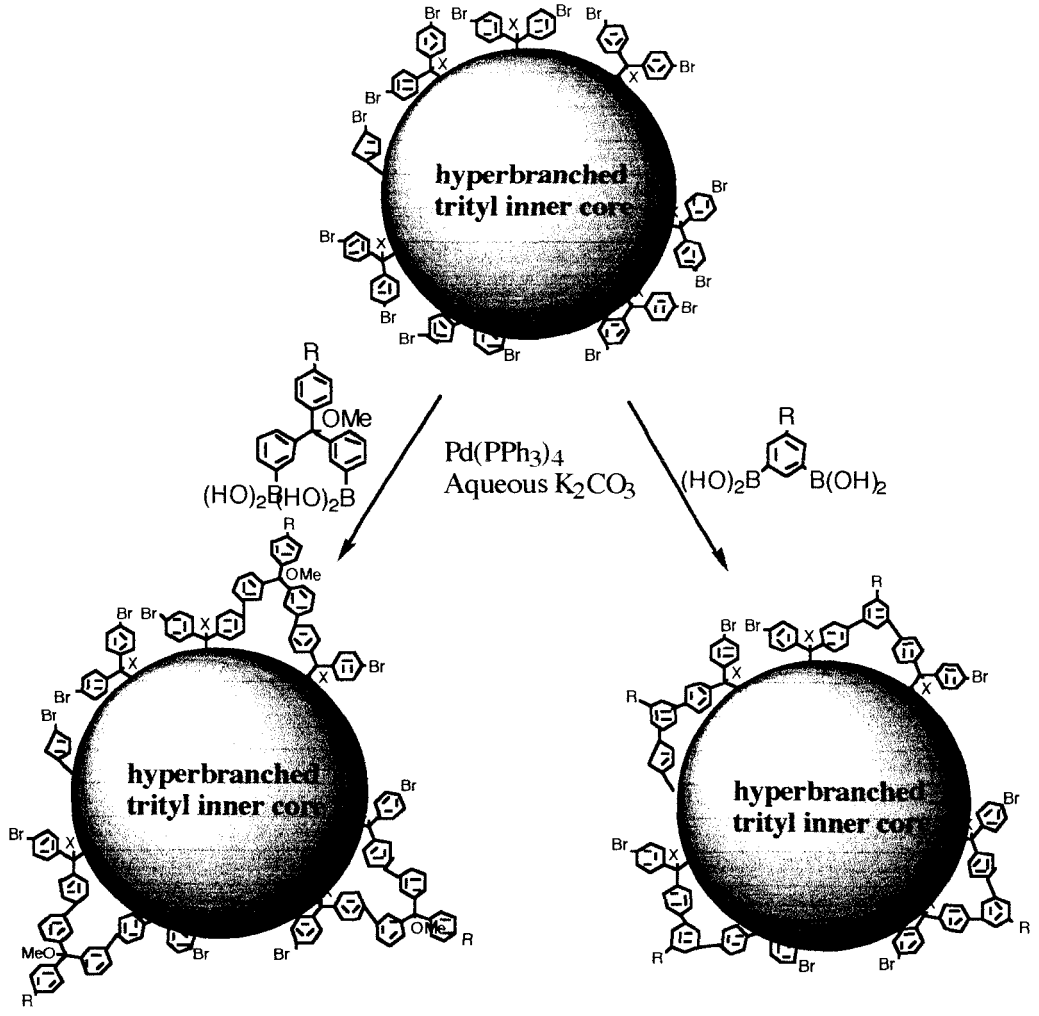

Figure 2-36 The "end capping" cyclization strategy to crosslinked **HPPMT**

Just like in the capping of **HPPMT** where the bromides couple with aryl boronic acids under Suzuki's condition, bis-boronic acids with appropriate topologies can be used in the capping. Some intramolecular cyclization should take place with the second boronic acid and furnish the

desired crosslinking. This method is superior to the A_2+B_3 polymerization because the degree of crosslinking can be modulated by equivalents of bis-boronic acid used. The goal is to maximize crosslinking while maintaining the solubility. However, not every coupled bis-boronic acid necessarily leads to crosslinking. Therefore this method does not provide a direct control over the exact degree of crosslinking and it is quite difficult to determine this value experimentally. It should also be pointed out that the S value of the antiferromagnetically linked **HPPPDIT** will not necessarily benefit from crosslinking. Depending on the size of the cyclophane formed, its S can sometimes decrease because of the capping.

The shortcomings of the first approach result from the lack of acute synthetic methods to modify polymers. Alternatively, incorporation of loop structures can also be achieved with more elaborated monomers already containing cyclic structures. Figure 2-37 shows one example of this strategy.

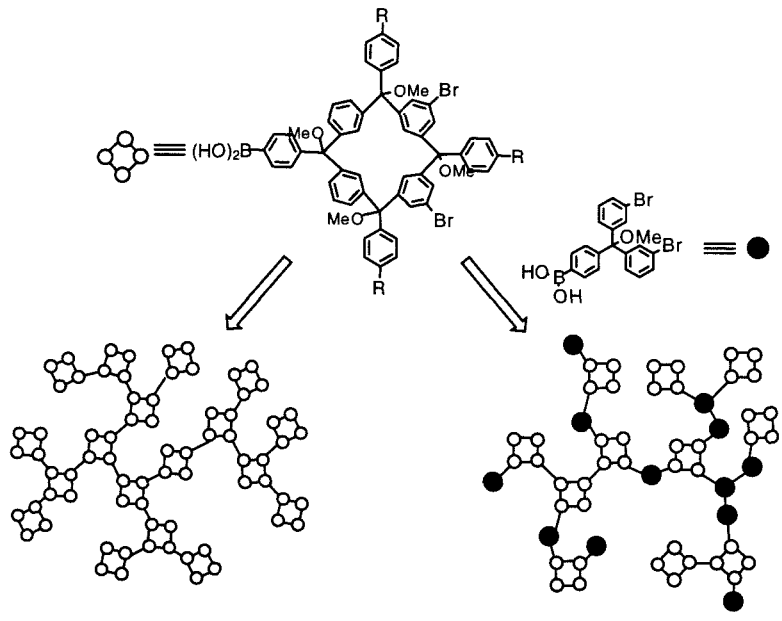

Figure 2-37 Using cyclic monomer to achieve crosslinking

The [4]-calixarene type cyclophanes have already been used as a crucial structural motive in Rajca's polyradicals. Their general syntheses have also been developed by the same author[87]. With this protocol, the degree and mode of crosslinking can be precisely controlled by copolymerizing cyclic monomer and acyclic one in different ratios. This offers the real opportunity to systematically study how well crosslinking can lessen the effect of defects.

The greatest disadvantage of hyperbranched molecules is arguably their diversity in compositions. Not only do the products from a hyperbranched polymerization have diverse molecular weight, but almost infinite structural possibilities also exist for polymers with the same degree of polymerization. Even structural features on an average scale are very hard to determine with the currently available spectroscopic techniques. In all the rationale given in this work, it is assumed that hyperbranched molecules and perfect dendrimers behave similarly, at least qualitatively. Although this hypothesis might seem very intuitive, it still lacks any solid experimental validation. Deeper and more adamant insights about magnetism in branched systems should be gained from studying structurally well defined dendrimeric polyradicals made by the convergent strategy.

Dendrimeric high-spin molecules have been studied with carbenes as the SCs. The results from such investigations appeared quite promising[88]. However, Rajca's dendrimeric polytrityl exhibits S values far lower than anticipated[89]. All these investigations used the conventional design paradigm where the spin alignment is enforced by ferromagnetic coupling units. The novel concept of making high-spin systems through antiferromagnetic interactions proposed in this work should also be tested in this regard.

Ultimately, such a project is necessary to verify this new model. After all, the model is really derived in the context of dendrimeric, not hyperbranched, structure. In addition to the necessity of a scientific process, this new class of polyradicals also have the great potential to exhibit unique physical and material properties that traditional high-spin systems can not possess. Therefore this pursuit will be of great interest to both pure and applied science.

As the way to produce high-spin dendrimers, the new model does give certain advantages. As mentioned previously, the radicals in an all *para* linked system appear to be more stable for both electronic and steric reasons. The spins are expected to be even more persistent in a fully capped, more spherical dendrimer. The other benefit is related to product characterization. The real challenge of dendrimer research is sometimes, instead of the synthesis, to confirm the structure of the polymer products. This task becomes even more dreadful if the monomer units do not contain some elements of symmetry. Indeed, symmetric monomers are always used in this field to simplify the characterization. This problem can be more devastating for our target systems because the monomer unit is larger than those in other researches. In the regard, the *p,p'*- biphenyl linkage is clearly superior to the *p,m* -biphenylene because of its symmetric geometry.

Admittedly, about two thirds of the radicals can not contribute to the observed S directly because of the antiferromagnetic coupling units. However, this annihilating interaction can also lead to some fascinating optical and electronic properties that are unique in these new systems. In the first chapter, it was mentioned that one favorable material property for organic magnets is optical transparency. In the traditional design, no two

radicals are in real conjugation with each other because all FCs have cross conjugated topology. This means that the optical absorption of this type of polyradical should be roughly identical to that of its monomer units regardless of its size. In other words, the optical excitations in such systems tend to be quite localized. Consequently, the photophysical properties these materials can display will be rather limited. On the contrary, the absorption spectrum of an antiferromagnetically linked system should shift to longer wave length as the molecular size increases. This will greatly improve the versatility of these magnetic materials as optical devices. When compared to their ferromagnetically linked counterparts with the same molecular weight, these new polyradicals should have much more optical absorption corresponding to conjugated segments of various lengths. This provides the opportunity to explore some wave length dependent photophysics in these system. In a more technological language, this system may have interesting wave-length-dependent magneto-optical switching properties.

Analogous to optical properties, the new polyradicals should also be very interesting electronic materials. In a linear system, a polyradical is classified to be either "conductive" or "magnetic" depending on its topology[90]. In a conducting polymer, all radical centers are in conjugation with each other. The redox chemistry behavior of such systems depends largely on its length[91]. A polymer becomes a conductor when the conjugation is long enough that its band gap approaches zero. On the contrary, the magnetic topology by definition prohibits the conjugation of radicals. In other words, the unpaired electrons in a magnetic polymer behave much more independently than in conducting polymers. This foretells that their redox behavior should always resemble that of their

monomer units. Therefore magnetic polymers, in practical terms, are insulators. However, this simple dichotomy breaks down in the world of dendrimeric polyradicals. As demonstrated in Figure 2-29, a polyradical can certainly be a conductor while having a high-spin ground state. These two-dimensional polyradicals are of great scientific and practical interest simply on the grounds of their conducting property. With the newly proposed magnetic property, another interesting prospect can now be added to their possible applications. According to the model, it is conceivable that the magnetic property of a conducting dendrimeric system can be effected by an external electric field. In other words, it might lead to a magnet switchable by applied voltage.

Some preliminary experiments aimed at synthesizing real dendrimeric polyradicals with antiferromagnetic coupling units have already been performed. With several synthetic intermediates for making **19** and **20** at hand, a simple approach was designed according to the concept of convergent synthesis proposed by Frechet and Moore (Figure 2-6). The peripheral unit **32** is made from *p,p'*-di-t-butylbenzophenone and lithiated **21** through the standard reaction sequence. 4,4'-Dibromobenzophenone is employed with the hope that its ketone functionality can serve as a masked site for latter dendrimer extension. A triiodo core unit **35** is synthesized by a triple lithium-bromide exchange on tribromide **34** to facilitate the latter coupling reaction. Unfortunately, all the oligomers have unusually complicated NMR spectra partly because of hindered rotation at every trityl center. This makes their purification and characterization extremely difficult. Even more disappointingly, the yield of the key coupling is only moderate. Clearly, this particular Suzuki's coupling condition has met its limitation. The reactivity is expected to drop further as the reactants

become larger in size. When the coupling yield for the first generation molecule is already at such a mediocre level, the reaction is clearly not suitable for making even higher generation molecules.

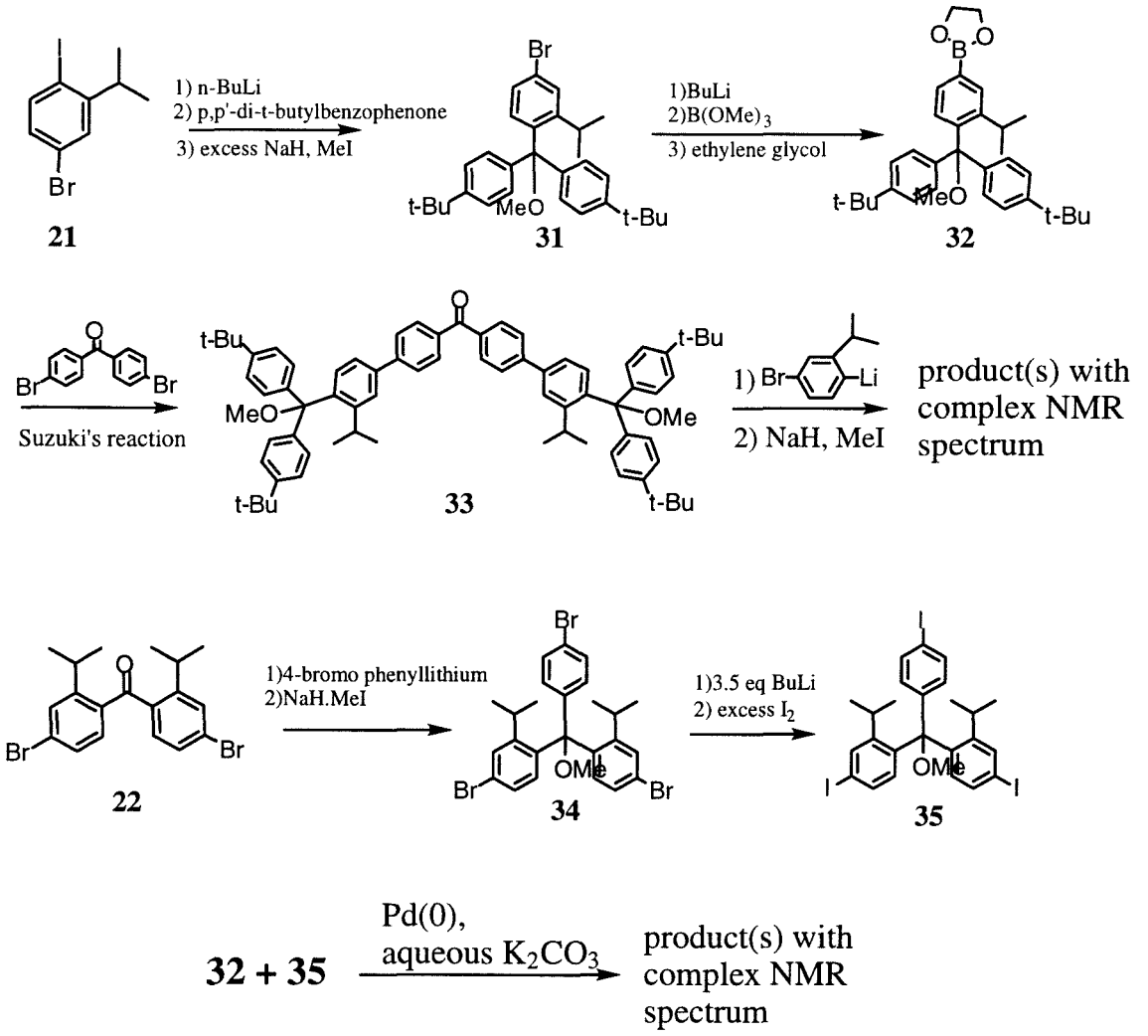

21 31 32 33 22 34 35

Figure 2-38 Attempted synthesis of trityl dendrimer

Furthermore, even if the coupling yield can be optimized, no convenient method has been developed to generate and mask aryl boronic acids with enough efficiency for dendrimer synthesis. Today, the best way to make aryl boronic acid is to quench aryl lithium reagent with trialkyl

borate. The yield for this process is only fair and is expected to drop even further in larger molecules. This is probably the reason why Suzuki's coupling reaction is seldom used in real dendrimer synthesis[92]. This approach is thus put on hold until more efficient synthetic reactions are developed.

A more standard methodology to make dendrimers with conjugated backbones was developed by Moore[93]. The highly efficient alkyne-aryliodide coupling reaction is the key step. The greatest advantage of this strategy is that terminal alkynes can be easily protected with trialkyl silyl groups. The deprotection can be conveniently carried out under mild conditions. A synthetic scheme analogous to Moore's strategy is shown in Figure 2-39a. The reaction condition here is a little different from the earlier Suzuki's coupling. This will be discussed in more detail in the next chapter. The drawback of this approach, however, is that triple bonds are not as chemically robust as aryl groups. The compatibility of alkynes with the subsequent spin-generating reactions must always be considered.

An attractive alternative to trityl radicals as spin sources is the radical cation of triaryl amines. They can be generated by chemical or electrochemical doping[94]. These radicals sometimes dimerize irreversibly under oxidative conditions[95]. However, when their *para* positions are blocked by appropriate substitutions, these radical cations are among the most persistent spin sources known. Some of them are commercially available. Bushby and colleagues have utilized such favorable stability to produce hyperbranched poly(triaryl amine) radical cation with a moderate S value near 2[96]. In the all *para* linked target dendrimers, every *para* position is naturally protected and therefore the radical stability should be properly secured. The syntheses can be carried out in parallel to the

polytrityl systems using Suzuki's coupling (Figure 2-39b). Still, the main obstacle in this approach is the generation and masking of boronic acids.

More recently, a palladium catalyzed coupling reaction between amines and aryl halides has been developed by Buchwald and Hartwig[97]. The new reaction generally affords superior yields and its condition is much milder than the traditional Cu(0) catalyzed Ullmann coupling. Hartwig has already published some pioneering experiments to make dendrimers using this new reaction with very promising results[98]. The same idea should also be applicable here. The synthetic scheme is shown in Figure 2-39c. In order to ensure that every unit in the dendrimer is readily oxidizable to the corresponding cation, *p*-biphenylene is chosen as the bridging unit instead of *p*-phenylene. The benefit of this approach, compared to Suzuki's coupling, again lies in the simple protecting and deprotecting of the diaryl amines. As already mentioned, Cliteshas carried out some preliminary experiments in this direction[99] (Figure 2-32).

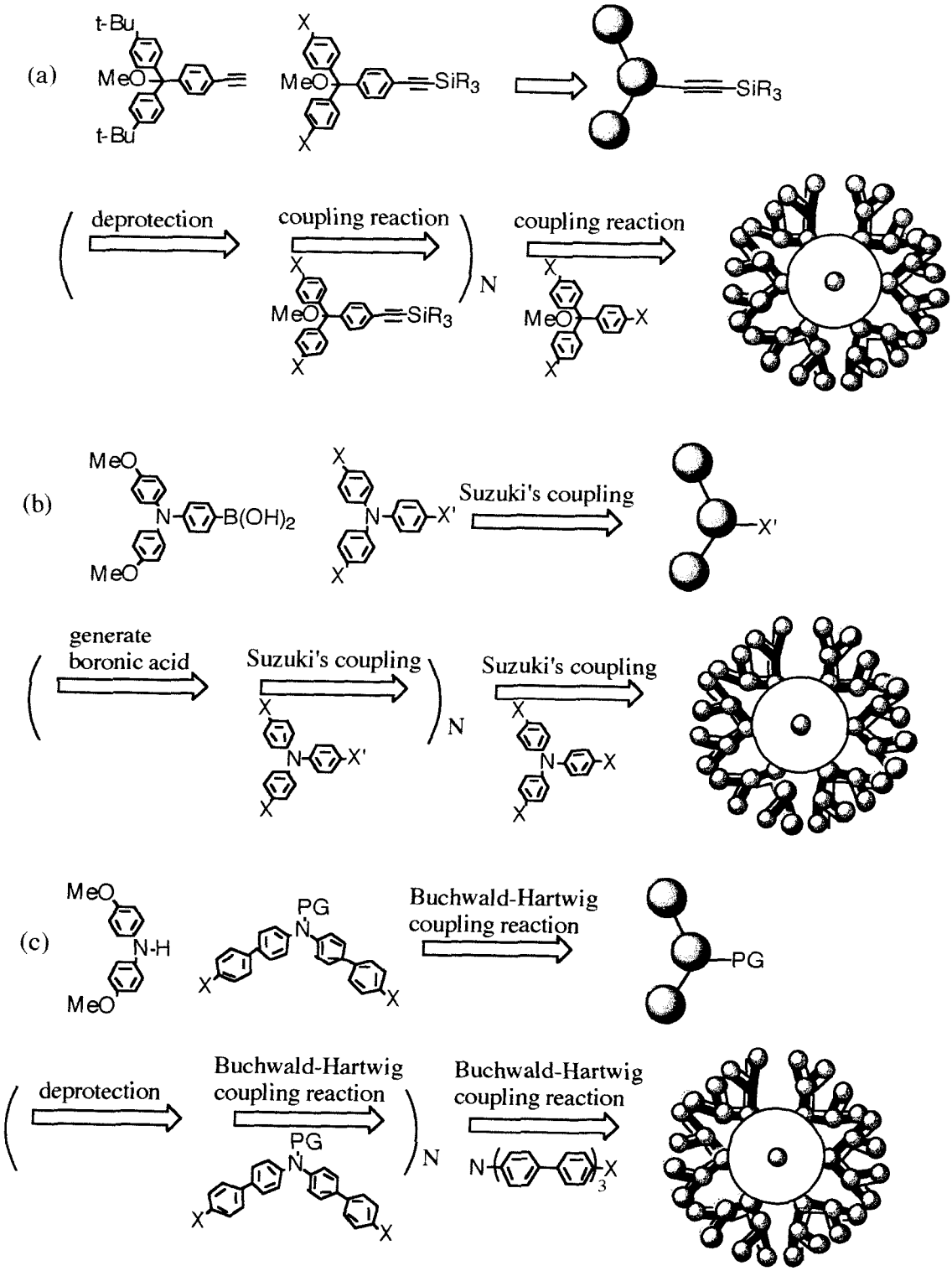

Figure 2-39 Synthetic strategies to various dendrimers

References

[1] Lappas, A.; Prassides, K.; Vavekis, K.; Arcon, D.; Blinc, R.; Cevc, P.; Amato, A.; Feyerherm, R.; Gygax, F. N.; Schenck, A. *Science*, **1995**, *267*, 1799-1802

Chiarelli, R.; Novak, M. A.; Rassa, T. A.; Tholence, J. L. **Nature**, *1993*, *363*, 147-149

Cirujeda, J.; Mas, M.; Molins, E.; Depanthou, F. L.; Laugier, J.; Park, J. G.; Paulsen, C.; Rey, P.; Rovira, C.; Veciana, J. *J. Chem. Soc. Cem. Comm.* **1995**, 709

[2] Dougherty, D. A. *Acc. Chem. Res.* **1991**, *24*, 88

Iwamura, H.; Koga, N. *Acc. Chem. Res.* **1993**, *26*, 346

Yoshizawa, K.; Hoffmann, R. *Chem.-Eur. J.* **1995**, *1*, 403-413

[3] Sano, Y.; Tanaka, M.; Koga, N.; Matsuda, K.; Iwamura, H.; Rabu. P.; Drillon, M. *J. Am. Chem. Soc.* **1997**, *119*, 8246

Karasawa, S.; Sano, Y.; Akita, T.; Koga, N.; Itoh, T.; Iwamura, H.; Rabu, P.; Drillon, M. *J. Am. Chem. Soc.* **1998**, *120*, 10080-10087

[4] Wasserman, E,; Schueller, K.; Yager, W. A.; **Chem. Phys. Lett**. *1968*, *2*, 259-260

Dowd, P. *Acc. Chem. Res.* **1972**, *50* ,1251-1259

Jain, R.; Sponsler, M. B.; Coms, F. D.; Dougherty, D. A.; *J. Am. Chem. Soc.* **1988**, *110*, 1356-1366

[5] Kato, S.; Morokuma, K.; Felelr, D.; Davidson, E. R.; Borden, W. T. *J. Am. Chem. Soc.* **1983**, *105*, 1791-1795

Wenthold, P. G.; Squires R. R.; Lineberger, W. C. *J. Am. Chem. Soc.* **1998**, *120*, 5279-5290

[6] Jacobs, J. S.; Shultz, D. A.; Jain, R.; Novak, J.; Dougherty, D. A. *J. Am. Chem. Soc.* **1993**, *114*, 1744-1753

[7] Dougherty, D. A.; Jacobs, S. J. *Angew. Chem. Int. Ed. Engl.* **1995**, *34*, 240

[8] Rajca, A.; Utamapanya, S.; Thayumanavan, S.; *J. Am. Chem. Soc.* **1992**, *114*, 1884

[9] Veciana, J.; Rovira, C.; Ventosa, N.; Crespo, M. I.; Palacio, F. *J. Am. Chem. Soc.* **1993**, *115*, 57-64

[10] Fujita, J.; Matsuoka, Y.; Matsuo, K.; Tanaka, M.; Akita, T.; Koga, N.; Iwamura, H. *J. Chem. Soc. Chem. Comm.* **1997**, 2393

[11] Nakamura, N.; Inoue, K.; Iwamura, H. *Angew. Chem. Int. Ed. Engl.* **1993**, *32*, 872-874

[12] Minato, M.; Lahti, P. M.; Vanwilligen, H. *J. Am. Chem. Soc.* **1993**, *115*, 4532-4539

[13] Torrance, J. B.; Oostra, S.; Nazzal, A. *Synthetic Metals* **1987**, *19*, 709

[14] Ota, M.; Otani, S.; Igarashi, M. *Chem. Lett.* **1989**, 1183-1186

[15] Tomalia, D. A. *Sci. Am.* **1995**, *272*, 62-66

Tomalia, D. A.; Esfand, R. *Chem. Ind-London* **1997** 416-420

[16] Frechet, J. M. J. *Science* **1994**, 263, 1710-1715

Wooley, K.L.; Hawker, C. J.; Frechet, J. M. J. *Angew. Chem. Int. Ed. Engl.* **1994**, *33*, 82-85

[17] Xu, F.; Moore, J. S. *Macromolecules* **1991**, *24*, 5893

Xu, F.; Moore, J. S. *Angew. Chem. Int. Ed. Engl.* **1993**, *32*, 246

Xu, F.; Moore, J. S. *Angew. Chem. Int. Ed. Engl.* **1993**, *32*, 1354

[18] Miller, T. M.; Neenan, T. X.; Zayas, R.; Bair, H. E. *J. Am. Chem. Soc.* **1992**, *114*, 1081

[19]Kim, Y. H.; Webster, O. W. *Macromolecules* **1992**, *25*, 5561-5572

Kim, Y. H.; Webster, O. W. *J. Am. Chem. Soc.* **1990**, *112*, 4592-4593

Bharathi, P.; Moore, J. S. *J. Am. Chem. Soc.* **1997**, *119*, 3391-3392

[20] Johansson, M.; Malmstrom, E.; Hult, A. *Trends Polym. Sci.* **1996**, *4,* 398-403

Voit, B. I.; Turner, S. R. P. *Angew. Makromo. Chemie.* **1994**, *233*, 13

[21] Gomberg, M. *Chem. Revs.* **1925**, *1*, 91

Sholle, V. D.; Ronzantsev, E. G.; *Russ. Chem. Rev.* **1973**, *42*, 1011

MacBride J. M. *Tetrahedron* **1974**, *30,* 2009-2022

Ballester, M. *Acc. Chem. Res.* **1985**, *18*, 380

[22] Rajca, A. *Chem. Rev.* **1994**, *92*, 871-893

[23] See Reference 6-12

[24] Kumada, M.; Tamo, K.; Sumitani, K. *Org. Synt.* **1978** ,*58*, 127

[25] Bringmann, G.; Walter, R.; Weirich, R. *Angew. Chem. Int. Ed. Engl.* **1990**, *29*, 977-991

Stanforth, S. P. *Tetrahedron* **1998**, *54*, 263-303

[26] Negishi, E.; King, A. O.; Okukado, N. *J. Org. Chem. 1977, 42*, 1821

Negishi, E.; Takahashi, T.; King, A. O. *Org. Synt.* **1987**, *66*, 67

[27] Stille, K. J. *Angew. Chem. Int. Ed. Engl.* **1986**, *25*, 508

Mitchell, T. *Synthesis* **1992**, 803

[28] Miyuara, N.; Yanagi, T.; Suzuki, A. *Synt. Comm.* **1981**, *11*, 513

Miyuara, N.; Suzuki, A. *Chem. Rev.* **1995**, *95*, 2457

[29] Rehahn, M.; Schulter, A.-D.; Wegner, G.; Feast, W. J. *Polymer* **1989**, *30*, 1060-1062

Wallow, T. I.; Novak, B. M.; *J. Am. Chem. Soc.* **1991**, *113*, 7411-7412

[30] Goldfinger, M. B.; Swager, T. M. *J. Am. Chem. Soc.* **1994**, *116*, 7895

Lamba, J. J. S.; Tour J. M. *J. Am. Chem. Soc.* **1994**, *116*, 11723-11736

[31] Miller, T. M.; Neenan, T. X.; Zayas, R.; Bair, H. E. *J. Am. Chem. Soc.* **1992**, *114*, 1081

[32] Farina, V.; Krishnan, B. *J. Am. Chem. Soc.* **1991**, *113*, 9585-9595

[33] Wallow, T. I.; Novak, B.M. *J. Org. Chem.* **1994**, *59*, 5034-5037

Goodson, F. E.; Wallow, T. I.; Novak, B. M. *Org. Synt.* **1998**, *75*, 61

[34] Watanabe, T.; Miyaura, N.; Suzuki, A. *Synlett.* **1992**, 207-210

Ohe, T.; Miyaura, N.; Suzuki, A. *J. Org. Chem.* **1993**, *58*, 2201

[35] Chen, G. J.; Tambroski, C. *J. Organometal. Chem.* **1983**, *251*, 149

[36] Haubold, W.; Herdtle, J.; Gollinger, W.; Einholz, W. *J. Organomet. Chem.* **1986**, *315*, 1

Miller, T. M.; Neenan, T. X. *Chem. Mater.* **1990**, *2*, 346

[37] Wakefield, B. J. *Organolithium Methods* London : Academic Press **1988**

[38] Klusener, P. A. A.; Hanekamp, J. C.; Brandsma, L.; Schleyer, P. V. *J. Org. Chem.* **1990**, *55*, 1311-1321

[39] Schiemenz, G. P. *Org. Synt. Col. V* **1973**, 496

[40] Murray, M. M.; Kaszynski, P.; Kaisaki, D. A.; Dougherty, D. A. *J. Am. Chem. Soc.* **1994**, *116*, 8152-8161

[41] Guss, J. M.; Mason, R. *J. Chem. Soc. Chem. Comm.* **1971**, 58

Barr, N.; Dyke, S. F. *J. Organometal. Chem.* **1983**, *243*, 223

[42] Zembayashi, M.; Tamao, K.; Yoshida, Y.; Kumada, M. *Tetra. Lett.* **1975**, *16*, 3375

Colon, I.; Kelly, D. R. *J. Org. Chem.* **1986**, *51*, 2627

[43] Bharathi, P.; Moore, J. S. *J. Am. Chem. Soc.* **1997**, *119*, 3391-3392

[44] Hawker, C.; Frechet, J. M. J. *J. Am. Chem. Soc.* **1990**, *112*, 7638

Visscher, G. T.; Bianconi, P. A. *J. Am. Chem. Soc.* **1994**, *116*, 1805

Callstrom, M. R.; Neenan T. X.; Whitesides, G. M. *Macromolecules* **1988**, *21*, 3528

[45] Edited by Brandrup, J.; & Immergut, E. H. *Polymer Handbook* New York : Wiley, **1998**

[46] Gomberg, M. *J. Am. Chem. Soc.* **1900**, *22*, 757

Gomerberg, M. *Ber. Dtsch. Chem. Ges.* **1900**, *33*, 3150

Neumann, W, P.; Uzick, W.; Zarkadis, A. K. *J. Am. Chem. Soc.* **1986**, *108*, 3762-3770

[47] There are some variations in reaction conditions. For a recent example, see Rajca, A.; Wongsriratanakul, J.; Rajca, S. *J. Am. Chem. Soc.* **1997**, *119*, 11674-1686

[48] Owen Webster, Personal communication

[49] Rajca, A.; Lu, K.; Rajca, S. *J. Am. Chem. Soc.* **1997** *119*, 10335-10345

[50] Wertz. J. E.; Bolton, J. R. *Electron Spin Resonance: Elementary Theory and Practical Application* Chapman and Hall: New York, London **1986**

[51] Jacobs, J. S. Ph.D. Thesis, California Institute of Technology, Pasadena, California, **1993**

[52] Carlin, R. L. *Magnetochemistry*; Springer-Verlag: New York **1986**

Rajca, A.; Utamapanya, S. *J. Am. Chem. Soc.* **1993**, *115*, 10688-10694

[53] Murray, M. M. Ph.D. Thesis, California Institute of Technology, Pasadena, California, **1996**

[54] Besides ferrocenium hexafluorophosphate, two other commercially available radicals [radical cation of tris(*p*-bromophenyl)amine and bis(1,3-2,2'-biphenylene)-2-phenyl allyl radical] also show similar intermolecular antiferromagnetic interactions indicated by low saturation moments.

[55] Robbins, J. L.; Edeltein, N.; Spencer, N.; Smart, J. C. *J. Am. Chem. Soc.* **1982**, *104*, 1882-1893

Koelle, U.; Khouzami, F. *Angew. Chem. Int. Ed. Engl.* **1980**, *19*, 640-640

[56] Rajca, A.; Utamapanya, S. *J. Am. Chem. Soc.* **1993**, *115*, 2396-2401

[57] Murray, M. M.; Kaszynski, P.; Kaisaki, D. A.; Dougherty, D. A. *J. Am. Chem. Soc.* **1994**, *116*, 8152-8161

[58] See reference 46

[59] Lankamp., H.; Nuata, W. Th.; MacLean, C. *Tetra. Lett.* **1968**, 249

Staab, H. A.; Brettshneider, H.; Brunner, H. *Chem. Ber.* **1970**, *103*, 1101

For this history, See McBride, J. M. *Tetrahedron* **1974**, *30*, 2009

[60] Neumann W. P.; Penenory, A.; Stewen U.; Lehnig M. *J. Am. Chem. Soc.* **1989**, *111*, 5845-5851

Dunnebacke D.; Neumann W. P.; Penenory, A.; Stewen U. Chem. Ber. 1989, 122, 533-535

Neumann, W. P.; Uzick, W.; Zarkadis, A. K. *J. Am. Chem. Soc.* **1986**,*108*, 3762-3770

[61] Kahr, B.; Van Engen, D.; Gopalan, P. *Chem. Mater.* **1993**, *5*, 729-732

[62] Gombergm M,; Cone, L.H. *Ber. Dtsch. Chem. Ges.* **1906**, *39*, 3274

Gomberg, M.; Blicke, F. F *J. Am. Chem. Soc.* **1923**, *45*, 1765

[63] Schmidt, R.; Brauer, H.-D. *Angew. Chem. Int. Ed. Engl.* **1971**, *10*, 506

Schmidt, R.; Brauer, H.-D. *Z, Natorforsch.* **1972**, *B27*, 1363

[64] Reynolds, J. H.; Berson, J. A.; Kumashiro K. K.; Duchamp J. C.; Zilm, K. W.; Scaiano J. C.; Berinstain A. B.; Rubello, a.; Vogel, P. *J. Am. Chem. Soc.* **1993**, *115*, 8073-8090

Hrovat, D. A.; Borden, W. T.; *J. Am. Chem. Soc.* **1994**, *116*, 6327-6331

[65] Rajca, A.; Utamapanya, S.; Smithhisler, D. J. *J. Org. Chem.* **1993**, *58*, 5650-5652

[66] Montgomery, L. K.; Huffman, J. C.; Jurczak, E. A.; Grendze, M. P. *J. Am. Chem. Soc.* **1986**, *108*, 6004

Sugimoto, T.; Sakaguchi, M.; Ando, H.; Tanaka, T.; Yoshida, Y.; Yamauchi, Y.; Kai, Y.; Kanehisa, K.; Kasai, N. J. Am. Chem. Soc. 1992, 114, 1893-1895

[67] Rajca, A.; Utamapanya, S.; Xu, J. T. *J. Am. Chem. Soc.* **1991**, *113*, 9235-9241

[68] See reference 35

[69] Kim, Y. H.; Webster, O. W. *J. Am. Chem. Soc.* **1990**, *112*, 4592-4593

[70] Mislow, K. *Acc. Chem. Res.* **1976**, *9*, 26

[71] Silverman, S. K.; Dougherty, D. A. *J. Phys. Chem.* **1993**, 97, 13273

[72] Kanno, F.; Inoue, K.; Koga, N. Iwamura, H. *J. Am. Chem. Soc.* **1993**, *115*, 847-850

[73] William Kemp *Organic Spectroscopy* New York : W.H. Freeman, **1991**

[74] Sabacky, M. J.; Johnson, C. S. Jr.; Smith, R. G.; Gutowsky, H. S.; Martin, J. C. *J. Am. Chem. Soc.* **1986**, *89*, 2054

Martin, J. C.; Smith, R. G. *J. Am. Chem. Soc.* **1964**, *85*, 2252

Jang S. H.; Lee, H. I.; McCracken J;.; Jackson J. E. *J. Am. Chem. Soc.* **1993**, *115*, 12623, 12624

[75] Ashton P. R.; Anderson D. W.; Brown, C. L.; Shipway, A. N.; Stoddart, J. F.; Tolley, M. S. *Chem. Europ. J.* **1998**, *4*, 781-795

Amabilino, D. B.; Ashton. P. R.; Balzani, V.; Brown, C. L.; Credi, A.; Frechet , J. M. J.; Leon, J. W.; Raymo, F. M.; Spencer, N.; Stoddart, J. F.; Venturi, M. J. Am. Chem. Soc. 1996, 118, 12012-12020

[76] Narayanan, V. V.; Newkome, G. R. *Top. Curr. Chem.* **1998**, *197*, 19-77

Wallimann, P.; Seiler, P.; Diederich, F. *Helv. Chem. Acta.* **1996**, *79*, 779

Stevelmans, S.; van Hest, J. C. M.; Jansen, J. F. G. A.; van Boxtel, D. A. F. J.; van den Berg, E. M. M. D; Meijer, E. W. *J. Am. Chem. Soc.* **1996**, *118*, 7398-7399

[77] Miklis, P.; Cagin, T.; Goddard, W. A. *J. Am. Chem. Soc.* **1997**, *119*, 7458-7462

[78] Dandliker, P. J.; Diederich F.; Gross M.; Knobler C. B.; Louati A.; Sanford, E. M. *Angew. Chem. Int. Ed. Engl.* **1994**, *33*, 1739

Mattei, S.; Wallimann, P.; Kenda, B.; Amrein, W.; Diederich, F. *Helv. Chim. Acta* **1997**, *80*, 2391-2417

[79] Rajca, A.; Wongsriratanakul, J.; Rajca, S.; Cerny, R. *Angew. Chem. Int. Ed. Engl.* **1998**, *37*, 1229-1232

[80] Rajca, A.; Utamapanya, S. *J. Am. Chem. Soc.* **1993**, *115*, 10699-10694

[81] See reference 85

[82] McConnell, H. M. *J. Chem. Phys.* **1963**, *39*, 1910

McConnellm H. M. in *Proc. R. A. Welsh. Foun. Conf.;* **1967**, pp144

[83] Jeffery A. Clite, Clifornia Institute of Technology, unpublished result

[84] Anderson, K. K.; Dougherty, D. A. *Adv. Mater.* **1998**, *10*, 688-692

[85] Anderson, A. A. Ph. D. Thesis California Institute of Technology, Pasadena, California **1996**

For an example of a high-spin radical dianion, see Rajca, A.; Rajca, S.; Desai, S. R. *J. Chem. Soc. Chem. Comm.* **1995**, 1957-1958

[86] Rajca, A.; Rajca, S.; Padmakumar, R. *Angew. Chem. Int. Ed. Engl.* **1994**, *33*, 2091-2093

Rajca, A.; Rajca, S.; Desai, S. *J. Am. Chem. Soc.* **1995**, *117*, 806-816

[87] Rajca, A.; Padmakumar, R.; Smithhisler, D. J.; Desai, S. R.; Ross C. R.; Stezowski, J.J. *J. Org. Chem.* **1994**, *59*, 7701

Rajca, A.; Lu, K.; Rajca, S. *J. Am. Chem. Soc.* **1997**, *119*, 10335-10345

[88] Matsuda, K.; Nakamura, N.; Inoue, K.; Koga, N.; Iwamura, H. *Chem.-A Europ. Journ.* **1996**, *2*, 259-264

Nakamura, N.; Inoue, K.; Iwamura, H. *Angew. Chem. Int. Ed. Engl.* **1993**, *32*, 872-874

[89] Rajca, A.; Utamapanya, S. *J. Am. Chem. Soc.* **1993**, *115*, 10688-10694

[90] Ouahab, L. *Coordin. Chem. Rev.* **1998**, *180*, 1501-1531 Part 2 Gomezgarcia, C. j.; Gimenezsaiz, C.; Triki, S.; Coronado, E.; Lemagueres, P.; Ouahab, L.; Ducasse, L. Sourisseau, C.; Delhaes, P. *Inorg. Chem.* **1995**, *34*, 4139-4151

Yoshizawa, K.; Hoffmann, R. *Chem.-Eur. J.* **1995**, *1*, 403-413

[91] Tour, J. M. *Chem. Rev.* **1996**, 96, 537-553

Roncali, J. *Chem. Rev.* **1997**, *97*, 871

[92] Miller, T. M.; Neenan, T. X.; Zayas, R.; Bair, H. E. *J. Am. Chem. Soc.* **1992**, *114*, 1018-1025

[93] See reference 17

[94] Oyama, M.; Okada, M.; Okazaki, S. *J. Electroanal. Chem.* **1993**, *346*, 281-190

Oyama, M.; Nozaki, K.; Okazaki, S. *Anal. Chem.* **1991**, *63*, 1387-1392

Oyama, N.; Ohsaka, T. *Synt, Met.* **1987**, *18*, 375-380

Liu, Y. C.; Liu, Z. L.; Wu, L. M.; Chen, P. *Tetra. Lett.* **1985**, *26*, 4201

For the oxidation of Polytriphenylamine, see Ohsawa, Y.; Ishikawa, M.; Miyamoto, T.; Murofushi, Y.; Kawai, M. *Synt, Met.* **1987**, *18*, 317

[95] Debrodt, H.; Heusler, K. E. *Z. Phys. Chemie Neue Forge* **1981**, *125*, 35

Seo, E. T.; Nelson, R. F.; Fritsch, J. M.; Marcoux, L. S.; Leedt, D. W.; Adams, R. N. *J. Am. Chem. Soc.*, **1966**, *88*, 3498

[96] Bushby, R. J.; McGill, D.R.; Ng, K. M.; Taylor, N. *J. Mater. Chem.* **1997**, *7*, 2343-2354

Bushby, R. J.; Gooding, D. *J. Chem. Soc. Perk. 2* **1998**, 1069

[97] Hartwig, J. F. *Angew. Chem. Int. Ed. Engl.* **1998**, *37*, 2047-2067

Wolfe, J.P.; Wagaw, S.; Marcoux, J. F.; Buchwald, S. L. *Acc. Chem. Res.* **1998**, *31*, 805-818

Guram, A. S.; Rennels, R. A.; Buchwald, S. L. *Angew. Chem. Int. Ed. Engl.* **1995**, *34*, 1348-1350

Paul, f.; Patt, J.; Hartwig, J. F. *J. Am. Chem. Soc.* **1994**, *116*, 5969

[98]Yamamoto, T.; Nishiyama, M.; Koie, Y. *Tetra. Lett.* **1998**, *39*, 2367

Louie, J.; Hartwig, J. F.; Fry, A.J. *J. Am. Chem. Soc.* **1997**, *119*, 11695

See an example of linear oligomer synthesis, Sadighi, J.P.; Singer, R. A.; Buchwald, S.L. *J. Am. Chem. Soc.* **1998**, *120*, 4960-4976

[99] Clites, J. A. California Institute of Technology, unpublished results

Experimental Section

•Material

Tetrahydrofuran and diethyl ether were distilled from sodium/ benzophenone in a nitrogen atomsphere. Toluene, benzene and methylene chloride were distilled from CaH_2. For radical-generating step and polymerization reactions, the solvents were degassed with freeze-pump-thaw cycle five times. All other starting material are commercially available from Aldrich or Lancaster Co. and were used as received. The freshness of trimethyl borate and tetrakis(triphenylphosphine) palladium can be crucial for excellent yields in the reactions where they were used. In some instances, a new bottle of reagent made all the difference.

Unless otherwise noted, all reactions were run under an atmosphere of dry argon in oven or flame-dried glassware. A magnetic stir bar of appropriate size was always used to make the reaction solution well-mixed. Thin layer chromatography was performed on 0.25 nm silica pre coated glass plates and visualized with UV light. Flash chromatography was performed with 230-400 mesh silica gel from Merck.

•Instrumentation

Proton and ^{13}C NMR spectra were recorded on a GE-300 spectrometer in $CDCl_3$ at room temperature and referenced to residual protons unless specified otherwise. EI mass spectra, 70 eV, for small volatile molecules were obtained on a Hewlett-Packard 5890/5970 GC/MS. machine. Other compounds and all FAB mass and high resolution exact mass measurement were performed at the Center of Mass Spectrum at University of Nebraska. UV/visible spectra were recorded on a Beckman Instruments DU-640 continuous wave spectrometer. Elemental analyses were determined at Atlantic Microlab at Norcross Georgia, Galbraith Laboratories at

Knoxville Tennessee or Quantitative technologies Inc. At Whitehouse New Jersey. Gel permeation chromatography was performed on a home made instrument employing either three Shodex size Styyrgel columns, (KF 803, KF 804 and KF 805) or an American Polymer Standard 10-μm mixed-bed column, an Altex model 110A pump, a Knauer differential refractometer and a Kratos UV detector. Methylene chloride was used as the eluant at a flow rate of 1 ml/min. Molecular weights were reported relative to narrow polystyrene standards. The common concentrations for polymer were between 0.4 to 0.6 mg/ml. The solutions were passed through a 0.5μm filtration pad before injection.

•Magnetization Studies

Initially, the glassware used in the radical-generating reactions were rinsed in EDTA solution and the polyradical samples were handled with a Teflon-coated spatula. These precautions were taken to avoid contamination from transition metals. However, neither were necessary as revealed by latter control experiments. Variable field and temperature measurements were performed on a Quantum design MPMS SQUID Magnetometer. Weighed samples were loaded into the delrin screw-cap holders in an oxygen-free glove box. The diamagnetic correction of sample and holder, χ_{dia}, was determined from a plot of magnetic susceptibility, χ_e, versus the inverse of absolute temperature. The corrections were estimated from the intercept as the extrapolation at infinite temperature. This variable temperature behavior was measured between 2 and 300 K at constant field (usually 10000 gauss). To obtain the correction, only susceptibilities at temperature higher than 50 K were used because data at lower temperature no longer obey the Curie Law. The variable field magnetization was measured between 0 and 55000 gauss at constant temperature (1.8K). The

measurement started from high field. Every time after a desired field strength was reached, a proper delay time was necessary for the system to achieve saturation. The average spin state of a material, namely S value, was determined from a two-parameter Brillouin fit that simultaneously evaluates both S and the paramagnetic saturation moment M_{sat}.

The spin concentrations were most conveniently estimated from the variable field plot as follows: the empirically determined saturation moments expressed in emu•G/g can be converted into molar quantities when being multiplied by the effective molecular weight (M^r). Assuming the sample is homogeneous, this factor should be the sum of the molecular weight of monoradical unit and cobaltocenium trifluoroacetate (or other oxidized metalocene).

$$M^m_{sat}\,(\text{emu•G/mol}) = M^w_{sat}\,(\text{emu•G/g}) \times M^r\,(\text{g/mol})$$

The saturation moment for a mole of electrons was described by:

$$M^e_{sat}\,(\text{emu•G/mol}) = Ng\mu_B S \;(S=1/2)$$

where N is Avogardo's number, g is the Lande splitting factor and μ_B is the Bohr magneton. Given $g \approx 2$, this formula is simplified to:

$$M^e_{sat}\,(\text{emu•G/mol}) = 5585$$

$$\text{Spin Concentration} = (M^m_{sat} / 5558) \times 100$$

- **Monomer Syntheses**

General procedure for esterification of iodobenzoic acid-synthesis of 5 and 6:

In a 500 ml flask, 25 g of *meta* or *para* iodobenzoic acid was suspended in 200 ml of absolute ethyl alcohol. 2-3 ml of sulfuric acid was added as the catalyst. The flask was connected to a Dean-Stark trap and a condenser to facilitate the removal of the produced water. The suspended solution becomes clear after 12 hours of reflux. The solution was then neutralized with saturated sodium bicarbonate solution. After the solvent was removed on a rotary evaporator, lightly brown opaque liquid was obtained. This liquid was dissolved in ether and the solution was washed by 10% sodium bicarbonate solution and water and then dried over anhydrous sodium sulfate. 23-25 g of ethyl iodobenzoates were obtained as yellow oils after the solvent was evaporated (yield 88-90%). Both compounds showed identical proton NMR spectrum as authentic commercial samples and were pure enough for the next step without further distillation.

General procedure for the syntheses of unsymmetrical trityl alcohol and trityl methyl ether:

15 g of *meta* or *para* dibromobenzene was dissolved in 140-150 ml of diethyl ether. The solution was put in an addition funnel that was connected to a 500 ml three-necked flask also equipped with a condenser. In the flask were placed 1.5 g of fresh magnesium turns (one equivalent), 10-20 ml of ether, and a few bits of iodine crystal. 5-10 ml of the dibromobenzene solution was first added at once to initiate the Grignard reaction. The reaction should begin in several minutes after the color of iodine faded away. If the reaction does not start after five minutes, a heating mantel can be applied. The mantel was removed once a gentle reflux was achieved. The success of the initiation is indicated by a

continuous bubbling from the magnesium surface even after the heating is discontinued. Once the reaction began, the rest of the solution was added dropwise at such rate that a very gentle reflux was maintained. After all the dibromobenzene was added (in about 40 minutes), the heating mantel was again employed to sustain the reflux for twenty more minutes. In another 500 ml flask, 7.2 g of ethyl iodobenzoate (0.4 equivalents) was dissolved in 150 ml of THF or benzene. The bromophenyl magnesium bromide solution was transferred into the second flask via canula under a slightly positive pressure. There was a dash of blue color at the first contact of the two solutions but it quickly dissipated. The mixed solution was refluxed under argon for 6 to 8 hours. The resulting cloudy yellow solution was immersed in an ice water bath and saturated ammonium chloride solution was added to quench the reaction. The solvent was removed under vacuum and the residual material was redissolved in 150 ml of methylene chloride. The solution was washed with 3M HCl and water, dried over sodium sulfate, and concentrated to give a viscous residue that mainly consists of the corresponding triphenyl methanol judged by its NMR spectrum. Pure trityl alcohol can be isolated at this stage by flash column (50% methylene chloride/petroleum ether). However, this purification was quite difficult and unnecessary for the next step. The crude triphenyl methanol was thus directly subjected to the next methylation step.

The crude trityl alcohol was dissolved in 150 ml of THF and the solution was cooled to 0°C. 2-2.5 g of sodium hydride (60% suspended in mineral oil, 2-2.5 equivalent of the benzoate) was added in several portions. Every portion was added only after the hydrogen gas evolution from the previous addition subsided. 3-3.5 ml of iodomethane (1.9-2.2 equivalent) was added to the cloudy alkoxide solution. After stirring overnight at room temperature, the solution was again cooled to 0°C and

the excess NaH was quenched by saturated ammonium chloride solution. The THF was evaporated and the residual mixture was redissolved in ether. The solution was washed several times, dried over sodium sulfate and concentrtated. The crude products were purified on a silica gel flash column (20% methylene chloride in petroleum ether). 10-11 g of trityl methyl ethers (69-76% yield based on ethyl iodobenzoate used) were obtained as pale yellow viscous liquids.

1,1-bis(4-bromophenyl)-1,(3-iodophenyl) dimethyl ether (7): ^{1}H NMR δ 3.04 (s, 3H), 7.04 (dd, J=8 Hz, 8 Hz, 1H), 7.28 with a small set of doublet hidden beside (d, J=8 Hz, 4H) 7.46 (d, J=8 Hz, 4H), 7.60 (dd, J=8 Hz, 2 Hz, 1H), 7.83 (dd, J=2 Hz, 2 Hz, 1H) ^{13}CNMR δ 52.81, 87.47, 94.94, 122.34, 128.30, 130.45, 130.97, 131.88, 137.05, 137.50, 142.41, 146.30 FABMS, m/z molecular ion peak was not observed, 529 (M-OCH_3, ^{81}Br ^{81}BR,50%); 527 (M-OCH_3, ^{79}Br ^{81}BR,100%); 525 (M-OCH_3, ^{79}Br ^{79}BR, 50%); 479 (7%); 401 (60 %); 355 (40 %); 183 (28%); 154 (65%); HRMS 555.8533 AT 0.2 ppm, calculated for $C_{20}H_{15}{}^{79}Br_2O$ 555.8534

1,1-bis(3-bromophenyl)-1,(4-iodophenyl) dimethyl ether (8): ^{1}H NMR δ 3.03 (s,3H), 7.12 (d, J=8 Hz, 2H), 7.17 (dd, J=8 Hz, 8 Hz, 2H), 7.27 (dd, J=8 Hz, 2 Hz, 2H), 7.39 (dd, J=8 Hz, 2 Hz, 2H), 7.59 (dd, J=8 Hz, 2 Hz, 2H), 7.65 (d, J=8 Hz 2H) ^{13}C NMR δ 52.84, 87.10, 94.25, 122.98, 127.77, 130.25, 131.16, 131.27, 131.75, 137.83, 1442.81, 145.94; FABMS, m/z 558 (M, 3%); 527 (M-OCH_3, 37%); 401 (24%); 356 (12%); 307 (45%); 289 (25%); 154 (100%); HRMS 555.8523 at 2.1 ppm, calculated for $C_{20}H_{15}{}^{79}Br_2O$ 555.8534

General procedure for the syntheses of boronic acids and their ethylene glycol ester:

In a 500 ml flask, 8 g of the dibromo-iodo trityl methyl ether was dissolved in 200-220 ml of diethyl ether. The solution was then cooled

down to -98°C with a methanol/liquid nitrogen bath. (The temperature of this bath can be somewhat unstable and thus it is necessary to monitor the fluctuation constantly. A new portion of liquid nitrogen must be added about every fifteen minutes to maintain the low temperature.) One equivalent of BuLi (9 ml of 1.6 M solution in hexane) was added dropwise in about ten minutes via a syringe. The reaction was left at -98°C for another hour during which some white suspending solid started to form. After the lithium-iodo exchange was completed, 6.5-8 ml of newly opened trimethyl borate (4-5 equivalent) was slowly added via a syringe. The flask was then warmed back to room temperature and left for another 8-10 hours. The reaction was quenched with water and the solution was washed several more times with water until the aqueous layer became neutral. The ether layer was dried over sodium sulfate or magnesium sulfate and concentrated under vacuum to give a yellow liquid. After flash chromatography on a silica gel column (30% diethyl ether in methylene chloride), boronic acid was isolated as a white opaque paste. The NMR spectrum of boronic acids are always complicated by various degree of oligomerization. The acids were thus converted to their ethylene glycol esters to simplify the characterization.

The pure boronic acids were dissolved in 150 ml of benzene in a 250 ml flask. 5-10 ml of ethylene glycol was added to the solution. The flask was then equipped with a Dean-Stark trap and a condenser. The esterification was carried out at reflux temperature (azeotropic distillation) for 8-10 hours. After the benzene was removed on a rotary evaporator, the residual liquid was dissolved in methylene chloride and washed with water several times to remove the excess glycol. The solution was dried on sodium sulfate and then concentrated. 5 g of boronic ester (≈70% of yield

in two steps) was isolated as white amorphous solid after the residual solvent was removed on vacuum line.

1,1-bis(4-bromophenyl)-1,(3-1,3,2-dioxaborole-phenyl) dimethyl ether (1): ^{1}H NMR δ 3.02 (s, 3H), 4.35 (s, 4H), 7.29 (d, J=8 Hz, 4H), 7.43 (dd, J=8 Hz, 8 Hz, 1H), 7.42 (d, J=7 Hz, 4H), 7.49 (d, J=8 Hz, 1H), 7.72 (d, J=7 Hz, 1H), 7.84 (bs, 1H) ^{13}C NMR δ 51.82, 65.80, 86.08, 121.09, 127.52, 130.07, 130.84, 130.89, 131.39, 133.66, 134.41, 142.37, 142.42

1,1-bis(3-bromophenyl)-1,(4-1,3,2-dioxaborole-phenyl) dimethyl ether (2): ^{1}H NMR δ 3.03 (s, 3H), 4.35 (s, 4H), 7.17 (dd, J=8 Hz, 8 Hz, 2H), 7.29 (d, J= 8 Hz, 2H), 7.35 (d, J=8 Hz, 2H), 7.37 (d, J=8 Hz, 2H), 7.60 (bs, 2H), 7.78 (d, J=8 Hz, 2H) ^{13}C NMR δ 52.84, 66.65, 122.85, 127.90, 128.79, 130.13, 130.98, 131.81, 135.21,146.33

1,1-bis(3-bromophenyl)-1,(3-iodophenyl) dimethyl ether (9): The *m*- bromophenyl magnesium bromide was generated from *m*-dibromobenzene and magnesium turn as described in the synthesis of **7**, **8**. A solution of dimethyl carbonate in THF (0.25 equivalent) was added to this Grignard reagent. The mixture was refluxed for 12 hours before it was quenched by saturated ammonium chloride. The solvent was removed under vacuum and the residual was redissolved in ether. The organic layer was washed several times, dried over sodium sulfate and concentrated. The crude alcohol was methylated with the standard condition (excess NaH/MeI in THF). Pure **9** was isolated after flash chromatography (30% methylene chloride in petroleum ether) in about 50% yield. ^{1}H NMR δ 3.04 (s, 3H), 7.20 (dd, J=8 Hz, 8 Hz, 3H), 7.27 (ddd, J=8 Hz, 2 Hz, 2 Hz, 3H), 7.42 (ddd, J=8 Hz, 2 Hz, 2 Hz, 3H), 7.59 (dd, (J=2 Hz, 2Hz, 3H) ^{13}C NMR δ 52.03, 85.61, 122.16, 127.07, 129.40, 130.42, 131.01, 144.86 FABMS, m/z

molecular ion peak was not observed, 479 (M-OCH_3, in a set containing three bromides, 15%); 355 (7%); 307 (32%); 154 (100%);

1,1,1 tris(4-bromophenyl) dimethyl ether (10): In a 250 ml flask, 6 g of 1,4- dibromo benzene was dissolved in 80 ml of THF. The solution was cooled to -78°C with a dry ice acetone bath. One equivalent of n-BuLi (10 ml of 2.5 M hexane solution) was added slowly and the exchange reaction was allow to proceed at low temperature for 45 minutes. In another 250 ml flask, 8.2 g of 4,4'-dibromobenzophenone (0.95 equivalent) was dissolved in 100 ml of THF and the solution was cooled to 0°C in a ice bath. The bromophenyl lithium solution was transferred to the dibromobenzophenone solution via a canula under a slightly positive pressure. The solution turned blue at first but faded to light orange quickly. The reaction was warmed back to room temperature and was stirred for four more hours. After the reaction was quenched with saturated ammonium chloride, the solvent was evaporated on a rotary evaporator. The residual material was redissolved in ether and the solution was washed with water three times. Crude trityl alcohol was obtained after the solvent was evaporated under vacuum. No major side product can be detected from NMR spectrum. Without further purification, the alcohol was converted to methyl ether under the methylation condition identical to what was used for **7, 8**. 10 g of the ether **10** (83% yield in two steps) was isolated after flash chromatography (30% methylene chloride in petroleum ether). ^{1}H NMR δ 3.04 (s, 3H), 7.27 (d, J=8.Hz, 6H), 7.45 (d, J=8 Hz, 6H) ^{1}H NMR δ 51.88, 85.83, 121.37, 129.97, 130.95, 141.85 FABMS, m/z 510 (M, ^{79}Br, ^{79}Br, ^{81}Br, 12%); 478.8 (M-OCH_3, in a set containing three bromides, 100%), 431 (25%); 401 (22%), 355 (67%); 183 (27%); 154 (57%); HRMS 507.8668 at 0.9 ppm, calculated for $C_{20}H_{15}{}^{79}Br_2O$ 507.8673

1,1-bis(3-bromophenyl)-1,(3-1,3,2-dioxaborole-phenyl) dimethyl ether (3): 8 g of **9** was dissolved in 200 ml of THF and the solution was cooled to -78°C. The following reaction sequences were almost identical to those used for the synthesis of **1**, **2**. The solution was first treated with n-butyl lithium solution and the lithium reagent was then quenched with 3.5 ml of trimethyl borate (two equivalents). The boronic acid was purified on a flash column and then converted to its glycol ester. However, the yield (40%) was much lower than before due to the contamination from bis(boronic acid) and starting material. ^{1}H NMR δ 3.03 (s, 3H), 4.36 (s, 4H), 7.17 (bs, 1H), 7.30 (d, J=8 hz, 2H), 7.34 (dd, J=8 Hz, 8 Hz, 1H), 7.36 (d, J=8 Hz, 2H), 7.44 (ddd, J= 8 Hz, 2 Hz, 2 Hz, 1H), 7.62 (dd, J=2 Hz, 2 Hz, 2H), 7.75 (d, J=8 Hz, 1H), 7.85 (dd, J=2 Hz, 2 Hz, 1H) ^{13}C NMR δ 52.65, 66.62, 86.83, 122.87, 127.93, 128.32, 129.52, 130.09, 130.92, 131.78, 132.56, 134.66, 135.41, 142.28, 146.57, 146.68

1,1-bis(4-bromophenyl)-1,(4-1,3,2-dioxaborole-phenyl) dimethyl ether (4): Starting from **10,** exactly the same procedure as used for **3** was followed. The starting tribromide is not totally soluble in THF in low temperature but the efficiency of the reaction is still good enough (33% yield). ^{1}H NMR δ 3.03 (s, 3H), 4.36 (s, 4H), 7.27 (d, J=8 Hz, 4H), 7.43 with one other set of doublet hidden under (d, J=8 Hz, 4H), 7.77 (d, J=8 Hz, 2H) ^{13}C NMR δ 51.87, 64.88, 87.10, 121.17, 121.34, 129.99, 130.07, 130.82, 134.33, 142.20, 145.77

1,3-diiodo-4,6-dimethyl benzene (13): 5 g of *m*- xylene and 12 g (two equivalents) of iodine crystal were dissolved in 120 ml of methylene chloride in a 250 ml flask. The purple solution was chilled to 0°C and 22 g of bis(trifluoroacetoxy)iodo benzene (2.15 equivalents) was added in several portions through a plastic funnel. Under vigorous stirring, the reaction was allowed to proceed at room temperature for 8 hours under

argon. After the solution was transferred to a separatory funnel, saturated sodium carbonate solution was slowly added to quench to side product trifluoroacetic acid and excess iodine. The purple color faded to yellow after the base wash and the organic layer was further washed with 3M HCl and water before it was dried over sodium sulfate and concentrated. 16 g of diiodo compound (94% yield) was isolated as a white powder after its solution is passed through a short silica gel column with hexane as the eluant. The product has an identical NMR spectrum as reported in the literature. ^{1}H NMR δ 2.35(s, 6H), 8.21 (s, 2H)

1,1-bis(4-bromophenyl)-1-(4,6-dimethyl-3-iodophenyl) dimethyl ether (14): 6 g of **13** was dissolved in 200 ml of THF in a 500 ml flask. The solution was cooled to -78°C with a dry ice acetone bath and 11.5 ml of 1.6 M n-BuLi solution (1.1 equivalent) was added dropwise via a syringe to generate the mono-lithiated species. The rest of the operation was totally analogous to that used in the synthesis of **4.** The lithium reagent was transferred to a cold solution of 4,4'-dibromobenzophenone. The produced trityl alcohol was then methylated with excess NaH and MeI. Purification was performed on a flash column (15% methylene chloride in petroleum ether) to furnish a white powder with the expected spectroscopic features yet unexpected low solubility. ^{1}H NMR $CDCl_3$ δ 1.88 (s, 3H) 2.42 (s, 3H) 3.08 (s, 3H), 7.07 (s, 1H) 7.28 (d, J=7 Hz, 4H), 7.42 (d, J=7 Hz, 4H) 7.78 (s, 1H)

3-Amino-6-methyl-bromobenzene or 3-bromo-*p*-toluidine (15): in a 500 ml flask, 10 g of 3-nitro-6-methyl-bromobenzene was dissolved in 200 ml of absolute ethyl alcohol and 21 g of tin (II) chloride dihydrate (two equivalents) was added to the solution. The suspended solution was refluxed for 12 hours with vigorous stirring. The ethanol was removed on a rotary evaporator. 200 ml of petroleum ether was added

and the inorganic by-products were removed from the solution by a simple filtration. The solid was washed several times with petroleum ether until no organic solute can be detected with UV lamp on a TLC plate. The combined filtrate was dried over sodium sulfate and concentrated under vacuum to give 8.4 g of light brown liquid (97% crude yield). The crude product was used directly in the next step without further purification. ^{1}H NMR δ 2.27 (s. 3H) 3.42 (bs, 2H), 6.55 (dd, J=7 Hz, 2Hz, 1H), 6.89 (d, J=2 Hz, 1H) 6.98 (d, J=7Hz, 1H)

3-Bromo-6-methyl-iodobenzene (16): 8 g of 3-bromo-*p*-toluidine was added to 200 ml of concentrated HCl (13.6 M) slowly under mild stirring. The suspended solution was cooled to 0°C in an ice bath. To this chilled solution was added a solution of 3.8 g of sodium nitrite (1.3 equivalents) in 10 ml of water. The addition rate must be controlled to minimize the procuction of NO_2. Also, the flask should be protected from light. The diazonization was accomplished in 45 minutes. In another Elymeyer flask, a solution of 75 g of potassium iodide in 300 ml of water was heated to 70°C. The cold red diazonium salt solution was added in several portions under vigorous stirring. The temperature was maintained for another 30 minutes after all visible evolution of nitrogen gas ceased. After the excess HCl was neutralized with sodium carbonate, the solution was extracted with petroleum ether four times. The combined organic layer was dried over sodium sulfate and concentrated. The dark brown liquid was passed through a short silica gel column (hexane as eluent) and 8.6 g of pure product (67% yield) was isolated as a pale orange oil. 2.31 (s, 3H), 6.96 (d, J=7 Hz, 1H) 7.50 (dd, J=7 Hz, 2 Hz, 1H) 7.86 (d, J=2 Hz, 1H)

1,1-Bis(4-methyl-3-bromophenyl)-1-(4-iodophenyl) dimethyl ether (17): 8.5 g of **16** was dissolved in 50 ml of ether. The solution was placed in an addition funnel and it was connected to a 3-necked 250 ml

flask equipped with a condenser. 0.68 g of magnesium turns (one equivalent), small amount of iodine and 5 ml of ether were placed in the flask. The Girgnard reagent was generated with the identical procedure as that used in the synthesis of **7**, **8** and **9.** The organomagnesium reagent then was transferred to another flask containing 3.6 g of ethyl iodobenzoate (0.9 equivalent) and 80 ml of THF via a canula. The addition reaction was completed after 8 hours under reflux. The reaction was cooled down to room temperature and was quenched with saturated ammonium chloride solution. The solvent was evaporated and the residue was redissolved in ether and the solution was washed with water. The organic layer was dried over magnesium sulfate and concentrated. This gives the crude trityl alcohol which was immediately converted into its methyl ether with the standard methylation condition. After flash chromatography (20% methylene chloride/ petroleum ether), **17** was isolated in 66% yield (5 g opaque viscous liquid) based on the benzoate used. 2.38 (s, 6H), 3.03 (s, 3H), 7.16 (d, J=7 Hz, 2H), 7.18 (two overlapping singlet) 7.60 (bs, 2H) 7.67 (d, J=7 Hz, 2H)

1,1-Bis(4-methyl-3-bromophenyl)-1-(4-1,3,2-dioxaborole phenyl) dimethyl ether (17): The synthesis procedure was essentially identical to that used to make **1**, **2** and **3.** 5 g of **16** was dissolved in 100 ml of ether and underwent the selective lithium-iodo exchange reaction and the lithium reagent was quenched by five equivalents of trimethyl borate. The boronic acid was first purified by flash chromatography and esterified with ethylene glycol under azeotropic condition. About 3 g (65% yield) of boronic ester was isolated as a white powder. 2.38 (s, 6H), 3.05 (s, 3H), 4.38 (bs, 4H), 7.18 (d, J=7 Hz, 2H), 7.21 (dd, J=7 Hz, 2Hz, 2H) 7.43 (d, J=7 Hz, 2H) 7.63 (d, J=2Hz, 2H), 7.78 (d, J=7 Hz, 2H)

3-Isopropyl-4-amino-bromobenzene: In a 250 ml Elymeyer flask, a solution of 15 g of 2-isopropyl aniline in 100 ml of DMF was cooled down to 0°C in an ice bath. In another flask, 20.5 g of N-bromo-succinimide (1.02 equivalents) was dissolved in 80 ml of DMF. With the chilled solution well stirred and protected from light, the NBS solution was added manually through a pipette at such rate that the solution temperature did not exceed 4°C. After the addition was completed (in about 30 minutes), the solution was kept in the ice bath for four more hours. The resulting dark brown mixture was poured into a separatoy funnel which already contained 200 ml of petroleum ether. The biphasic mixture was washed with water five times to remove the DMF and succinimide. The organic layer was dried over sodium sulfate and concentrated to give 22.8 of brominated product as a black viscous liquid (96% yield). The crude bromide can be used in the next step with further purification. ^{1}H NMR δ 1.22 (d, J=7 Hz, 6H), 2.84 (heptet, J=7 Hz, 1H), 3.66 (bs, 2H), 6.55 (d, J=8 Hz, 1H), 7.10 (dd, J=8 Hz, 2 Hz, 1H), 7.22 (d, J=2 Hz, 2H) ^{13}C NMR δ 21.83 (2C), 27.56, 110.60, 117.03, 128.11, 128.92, 134.51, 142.18

4-Bromo-6-isopropyl-iodobenzene (21): An Elymeyer flask containing 200 ml of concentrated HCl (13.6 M) was immersed in an ice bath. To this chilled well-stirred acid, 20 g of **20** was added manually with a pipette at such rate that a suspended solution of granular chloride salt was formed. A spatula could also be used to break large lumps whenever they formed. A sodium nitrite solution (8.3 g in 20 ml of water, 1.3 equivalents) was added slowly to minimize the evolution of red NO_2. After the addition was completed, the deep red solution was kept at 0°C for 40 more minutes. (The solution should be protected form light during this whole operation.) In another Elymeyer flask, a solution of potassium iodide (160 g in 300 ml of water, 10.5 equivalents) suspended with 0.5 g of

copper powder was heated to 70°C. The diazonium salt solution was added to the second flask in several portions. After the nitrogen gas evolution ceases, the darks green solution was kept at 70°C for 40 more minutes. The reaction was cooled to room temperature and the excess HCl was neutralized with sodium carbonate. The heterogeneous mixture was extracted with petroleum ether four times and the combined organic phase was dried over sodium sulfate. After the solvent was evaporated, the residual dark liquid was purified on a flash column with pure petroleum ether as the eluant. 21.6 g (72% yield) of iodide was isolated as a lightly orange liquid. ^{1}H NMR δ 1.23 (d, J=7 Hz, 6H), 3.14, (heptet, J= 7 Hz, 1H), 7.02 (dd, J=8 Hz, 2 Hz, 1H), 7.35, (d, J=2 Hz, 1H), 7.66 (d, J=8 Hz, 1H) ^{13}C NMR δ 22.70 (2C), 37.95, 98.70, 122.79, 129.00, 130.52, 140.46, 152.30

2,2'-Diisopropyl-4,4'-dibromobenzophenone (22): In a 1000 ml flask, 20 g of **21** was dissolved in 250 ml of diethyl ether. The solution was cooled down to -78°C in a dry ice-acetone bath and 26 ml n-BuLi solution (2.5 M in hexane, or 1.05 equivalents) was added dropwise via a syringe. The selective exchange proceded under the bath temperature for 45 minutes before 1.8 ml (0.47 equivalent) of methyl formate was slowly added through a syringe. The solution was then warmed back to room temperature and left stirred overnight. The reaction was quenched with saturated ammonium chloride and the aqueous portion of the mixture was discarded. The ether solution was concentrated to give the crude alcohol product as a gray solid. The success of this reaction was confirmed by NMR spectrum of the crude mixture. No further purification was necessary before the next oxidation step. ^{1}H NMR δ 1.08(d, J=7 Hz, 6H), 1.32 (d, J=7 Hz, 6H), 3.07 (heptet, J=7 Hz, 2H), 6.37 (d, J=6 Hz, 1H), 7.16 (d, J=8 Hz, 2H), 7.35 (dd, J=8 Hz, 2 Hz, 2H), 7.49 (d, J=2 Hz, 2H)

The solid was dissolved in 150 ml of acetone and the solution was cooled down to 0°C with a ice bath. The Jones reagent was prepared with sulfuric acid and chromium trioxide according to the published procedure. The chromiun reagent was added to the well stirred solution slowly to keep the internal temperature below 5°C. The addition continued until the yellow-orange color of chromium (VI) visibly persisted. The reaction was stirred at room temperature for another hour. 20 ml of isopropyl alcohol was then added to scavenge the excess chromium (VI). After the solvent was evaporated on a rotary evaporator, the residual dark viscous liquid was dissolved in ether and the solution was washed with water (four times). The ether layer was dried over magnesium sulfate and concentrated. The residual brown liquid was purified on a silica gel flash column (30% methylene chloride in petroleum ether). The newly isolated benzophenone was a pale orange oil which solidified slowly after prolonged standing at room temperature. The combined yield through the two steps was 73% based on the methyl formate used (9.3 g isolated product). ^{1}H NMR δ 1.22 (d, J= 7 Hz, 12H), 3.43 (heptet, J=7 Hz, 2H) 7.05 (d, J=8 Hz, 2H), 7.30 (dd, J=8 Hz, 2 Hz, 2H), 7.57 (d, J=8 Hz, 2H) ^{13}C NMR δ 24.51, 30.01, 126.93, 129.00, 130.55, 132.07, 137.83, 151.89, 199.85 FABMS, m/z 425 (M+H, 100%); 344 (8%); 409 (8%); 381 (28%); 225 (20%); 154 (44%); HRMS 420.9797 $(M-H)^{+}$ within 1.4 ppm, calculated for $C_{19}H_{19}{}^{79}Br_2O$ 420.9802

***m*-Diiodobenzene:** diiodobenzene was made from 3-Iodo-aniline through its diazonium salt with the identical Sandmeyer condition used in the synthesis of **21**. The diazonization was carried out in concentrated HCl with slight excess of sodium nitrite. The diazo group was substituted by iodide with ten equivalents of KI. The crude product was purified with a short silica gel column eluted by hexane to give a colorless oil. The diiodobenzene crystalized as long rod after extended standing at room

temperature. The NMR spectrum of the product (obtained in 70% yield) was identical to the literature value.

1,1-Bis(2-isopropyl-4-bromophenyl)-1-(3-iodophenyl) dimethyl ether (23): 6 g of *m*- diiodobenzene was dissolved in 120 ml of THF and the solution was cooled to -78°C in a dry ice acetone bath. 1.1 equivalents of n-BuLi solution (12.5 ml of 1.6M hexane solution) was added in about 15 minutes via a syringe. The exchange reaction was allowed to proceed for 45 minutes in the cold bath. The resulting mono-lithiated species was transferred to another flask (immersed in 0°C ice bath) containing the ether solution of **22** (6 g in 100 ml of diethyl ether, 0.77 equivalent to the lithium reagent) via a canula under a positive pressure. Blue color was first observed on the contact of the two solutions, but it quickly dissipated. This addition reaction was left at room temperature for another eight hours before it was quenched by saturated ammonium chloride solution. After the solvent was removed under vacuum, the remaining solid was redissolved in ether and washed with water three times. The organic layer was then dried over sodium sulfate and concentrated. The resulting crude trityl alcohol was subjected directly to the standard methylation procedure described previously. The crude methyl ether was purified on a silica gel flash column (10% methylene chloride in petroleum ether) and 6.4 g of pure product (72% yield based on the benzophenone used) was isolated as a white powder. ^{1}H NMR δ 0.84 (d, J=7 Hz, 6H), 0.96 (d, J=7 Hz, 6H), 3.08 (s, 3H), 3.21 (heptet, J=7 Hz, 2H), 7.02 (dd, J=8 Hz, 8 Hz, 1H), 7.16 (d, J= 8 Hz, 2H), 7.24 with another of doublet hidden beside (dd, J=8 Hz, 2 Hz, 2H), 7.45 (d, J=2 Hz, 2H), 7.55 (dd, J=8 Hz, 2 Hz, 1H), 7.64 (dd, J=2 Hz, 2 Hz, 1H) ^{13}C NMR δ 23.19, 23.94, 29.48 (2C), 53.51, 88.58, 93.40, 122.32, 127.81, 128.03, 129.23, 130.44, 131.14, 135.55, 136.90, 138.21, 144.60, 151.23 FABMS m/z, 641

(M, 5%), 612 (M-OCH_3, 53%); 569 (7%); 443 (40%), 439 (30%); 307 (37%); 154 (100%); HRMS 638.9401 at -1 ppm, calculated for $C_{26}H_{26}{}^{79}Br_2O$ 638.9395

1,1-Bis(2-isopropyl-4-bromophenyl)-1-(4-iodophenyl) dimethyl ether (24): The synthetic process was almost identical to what was used for **23** except that it started with *p*- diiodobenzene instead of the *meta* isomer. 5 g of *p*- diiodobenzene was dissolved in 150 ml of THF and underwent lithium-iodo exchange after the solution was cooled to -78°C. After 45 minutes, the white suspended 4-iodophenyl lithium solution was transferred via a canula to the solution of **22** prepared in advance (5 g of **22** in 100 ml ether). Some large lumps in the solution had to be broken down so that they would not block the canula. The work-up, methylation and purification procedures are all the same as that used for **23**. 5.1 g of methyl ether was isolated as a pale yellow powder after flash chromatography (67% yield). ^{1}H NMR δ 0.85 (d, J=7 Hz, 6H), 0.91 (d, J=7 Hz, 6H), 3.07 (s, 3H), 3.28 (heptet, J=7 Hz, 2H), 7.05 (d, J=8 Hz, 2H), 7.10 (d, J=8 Hz, 2H), 7.21 (dd, J=8 Hz, 2 Hz, 2H), 7.43 (d, J=2 Hz, 2H), 7.62 (d, J=8 Hz, 2H) ^{13}C NMR δ 23.28, 24.19, 30.17, 54.39, 88.87, 93.12, 123.05, 128.52, 131.25, 131.40, 131.97, 137.35, 139.55, 142.42, 152.01 FABMS, m/z 609 (M-OCH_3, 14%); 549 (12%); 445 (9%); 369 (10%); 307 (30%); 154 (100%); HRMS 638.9413 $(M-H)^+$ within 2.8 ppm, calculated for $C_{26}H_{26}O^{79}Br_2O$ 638.9395

1,1-Bis(2-isopropyl-4-bromophenyl)-1-(3-1,3,2-dioxaborole phenyl) dimethyl ether (19): In a 250 ml flask, 5 g of **23** was dissolved in 100 ml of ether and the solution was cooled down to -98°C in a methanol-liquid nitrogen slurry. 5.4 ml of n-BuLi (1.6 M in hexane, 1.1 equivalents) was added slowly in ten minutes. The bath temperature was kept below -96°C during the next 45 minutes with several more addition of

liquid nitrogen. After the exchange reaction was completed, 4.5 ml of trimethyl borate (5 equivalents) was slowly added. The solution was then warmed back to room temperature and left stirred for twelve more hours. The reaction was quenched with water and the organic layer was washed with water four times before dried over sodium sulfate. The solvent was evaporated and the residual viscous liquid was purified on a silica gel flash column (30% diethyl ether in methylene chloride). Pure boronic acid (judged by TLC) was isolated as a pale yellow liquid.

The boronic acid was then esterified with ethylene glycol in benzene under the same azeotropic distillation condition described before. A Dean-Stark trap was utilized to collect the water removed from the system. 3.2 g of dibromo-boronic-ester trityl ether (70% yield) was isolated as a white amorphous powder. ^{1}H NMR δ 0.81 (d, J=7 Hz, 6H), 0.90 (d, J=7Hz, 6H), 3.09 (s, 3H), 3.30 (heptet, J=7 Hz, 2H), 4.32 (s, 4H), 7.17 (d, J=8 Hz, 2H), 7.22 (dd, J=8 Hz, 2 Hz, 2H), 7.30 (dd, J=8 Hz, 8 Hz, 1H), 7.42 with another smaller set of doublet hidden under (d, J=2 Hz, 2H), 7.66 (dd, J=8 Hz, 2 Hz, 1H), 7.77 (dd, J=2 Hz, 2 Hz, 1H) ^{13}C NMR δ 24.13, 24.47, 30.21, 54.37, 66.60, 89.96, 122.82, 127.90, 128.45, 131.44, 131.78, 132.58, 133.88, 135.73, 139.88, 141.97, 152.14

1,1-Bis(2-isopropyl-4-bromophenyl)-1-(4-1,3,2-dioxaborole phenyl) dimethyl ether (20): Starting from **24**, exactly the same procedure used for synthesizing **19** was employed to produce this *para* isomer. Starting from 4.8 g of **24**, after selective exchange, metathesis and esterification, the protocol produced 2.8 g (63% yield) of **20** as a lightly yellow amorphous powder. ^{1}H NMR δ 0.84 (d, J=7 Hz, 6H), 0.91 (d, J=7 Hz, 6H), 3.10 (s, 3H), 3.31 (heptet, J=7 Hz, 2H), 4.35 (s, 4H), 7.15 (d, J=8 Hz, 2H) 7.22 (dd, J=8 Hz, 2 Hz, 2H), 7.34 (d, J=8 Hz, 2H), 7.43 (d, J= 2 Hz, 2H), 7.74 (d, J=8 Hz, 2H) ^{13}C NMR δ 24.19, 24.47, 30.19, 54.45,

66.62, 90.20, 122.89, 128.42, 128.88, 131.46, 131.85, 134.77, 135.59, 139.97, 145.91, 152.15

1-(2,6-di-t-butyl-4-bromo-phenoxyl)methoxyl-2-methoxyl-ethane (26): 10.5 g of 2,6-di-t-butyl-4-bromophenol was dissolved in 150 ml of THF and the solution was placed in an addition funnel. The funnel was connected to a 500 ml flask containing 2 g of sodium hydride (60% mixture with mineral oil, 1.4 equivalents), 6 g of methoxyl ethoxyl methyl chloride (1.3 equivalents according to phenol) and 50 ml of THF. The flask was cooled to 0°C and the phenol solution was added dropwise. The reaction was left in the ice bath for eight more hours until it was quenched with saturated ammonium chloride solution. The solvent was removed under vacuum and the residual oil was redissolved in ether. The ether layer was washed four times and dried over sodium sulfate and concentrated. This produced 12.1 g of orange liquid (87% crude yield) also containing some dark solid. Judged by NMR, this mixture was more than 90% pure. The crude product can be used directly in the next step without further purification. Pure sample can be obtained as a yellow oil after flash chromatography (40% methylene chloride in petroleum ether). ^{1}H NMR δ 1.41 (s, 18H), 3.41 (s, 3H), 3.64 (dd, J=7 Hz, 7 Hz, 2H), 3.95 (dd, J=7, Hz, 7 Hz, 2H), 4.97 (s, 2H), 7.34 (s, 2H) ^{13}C NMR δ 31.55, 35.64, 58.77, 68.80, 71.39, 99.34, 116.69, 129.28, 146.41, 153.27

1-(2,6-Di-t-butyl-4-formyl-phenoxyl)-methoxyl-2-methoxyl ethane (27): 10 g of the crude protected bromophenol **26** was dissolved in 150 ml of THF and the solution was cooled to -78°C in a dry ice-acetone bath. 11.5 ml of n-BuLi solution (2.5M in hexane, 1.1 equivalents) was added dropwise via a syringe and the exchange reaction was allowed to proceed for 90 minutes. 6 ml of anhydrous DMF (3 equivalents) was then added via the syringe slowly to quench the lithiated species. The mixture

was warmed back to room temperature and stirred overnight before it was quenched with water. The organic phase was washed several more times and then dried over sodium sulfate. After the solvent was evaporated, the residual oil was purified with a silica gel flash column (50%-60% methylene chloride in petroleum ether). 6.6 g of pure aldehyde (75% yield based on crude starting material) was isolated as a pale yellow oil. ^{1}H NMR δ 1.47 (s, 18H), 3.42 (s, 3H), 3.64 (dd, (J=7 Hz, 7 Hz, 2H), 3.97 (dd, (J=7 Hz, 7 Hz, 2H), 5.03 (s, 2H), 7.80 (s, 2H), 9.91 (s, 1H) ^{13}C NMR δ 32.54, 36.10, 59.58, 69.72, 72.05, 100.31, 119.32, 128.96, 146.14, 192.58

3,5-Dibromo-3',5'-di-t-butyl-4'-(methoxyl-ethoxyl-methoxyl) diphenyl methanol: 6.2 g of 1,3,5-tribromobenzene was dissolved in 120 ml of THF and the solution was cooled to -78°C. 13.5 ml of n-BuLi solution (1.6 M in hexane, 1.1 equivalents) was added to the solution slowly. The exchange reaction was allowed to proceed for 90 minutes to produce a suspended solution. To the lithium reagent was added a solution of **27** (6 g of **27** in 30 ml of THF, 0.95 equivalent) via a syringe slowly. The reaction was warmed back to ambient temperature and stirred for four more hours before it was quenched with saturated ammonium chloride solution. The solvent was removed under vacuum and the remaining liquid was redissolved in ether. The solution was washed with water several times before it was dried over sodium sulfate and then concentrated. The NMR spectrum indicated this crude product was mainly composed of the desired diphenyl alcohol. No further purification is necessary before the next step. ^{1}H NMR δ 1.41 (s, 18H), 3.42 (2, 3H), 3.63 (dd, J=7 Hz, 7 Hz, 2H), 3.97 (dd, J=7 Hz, 7 Hz, 2H), 4.99 (s, 2H), 5.68 (s, 1H), 7.19 (s, 2H), 7.48 (d, J=2 Hz, 2H), 7.55 (t, J=2 Hz, 1H)

3,5-Dibromo-3',5'-di-t-butyl-4'-(methoxyl-ethoxyl-methoxyl) benzophenone (28): The crude product from the last step

and 0.6 g of 18-crown-6 (0.1 equivalent with respect to potassium permanganate) were dissolved in 150 ml of methylene chloride. 3.5 g of potassium permanganate (1.2 equivalents according to the aldehyde used in the last step) was also added in. The solution slowly turned purple indicating the solubilization of permanganate ion. The reaction was stirred vigorously at room temperature for twelve hours during which maganese dioxide precipitates as a brown solid. 10 ml of isopropyl alcohol was added and the stirring was continued for two more hours to destroy the excess oxidant. The maganese dioxide was then removed from the suspended solution with a simple filtration. The solid was washed with three small portions of methylene chloride. The combined methylene chloride solution was dried and concentrated to furnish a dark brown solid. The crude product was purified on a silica gel flash column (40%-50% methylene chloride in petroleum ether). 7.2 g of pure ketone was isolated as a pale yellow powder (70% yield according the aldehyde used in the last step). ^{1}H NMR δ 1.43 (s, 18H), 3.41 (s, 3H), 3.64 (dd, J=7 Hz, 7 Hz, 2H), 3.99 (dd, J=7 Hz, 7 Hz, 2H), 5.03 (s, 2H), 7.69 (s, 2H), 7.82 (t, J=7 Hz, 2H) 7.85 (t, J=2 Hz, 1H) ^{13}C NMR δ 31.56, 35.72, 58.90, 69.10, 71.35, 99.58, 122.67, 128.87, 130.65, 131.31, 136.97, 140.74, 141.39, 144.82, 182.59

1-(3,5-Dibromo)-1-[3',5'-di-t-butyl-4'-(methoxyl-ethoxyl-methoxyl phenyl)]-1-(4"-iodophenyl) dimethyl ether (29): 4 g of *p*- diiodobenzene was dissolved in 100 ml of THF. The solution was cooled to -78°C and underwent mono-lithiation reaction as described before in the synthesis of **23**. The generated lithium reagent was added slowly to a ketone solution (6.5 g of **28** in diethyl ether, 0.95 equivalents) via a canula. The crude alcohol was isolated after the typical work-up procedure. Methylation was carried out under the NaH/MeI treatment as previously described. The pure ether **29** was isolated after a flash chromatography

(40% methylene chloride in petroleum ether) as a pale yellow amorphous powder (6.8 g, 76% yield). ^{1}H NMR δ 1.36 (s, 18H), 2.99 (s, 3H) 3.42 (s, 3H) 3.64 (dd, J=2 Hz, 2 Hz, 2H), 3.97 (dd, J= 2 Hz, 2 Hz, 2H), 5.00 (s, 2H) 7.14 (d, J=8 Hz, 2H) 7.16 (s, 2H), 7.51(s, 3H), 7.65 (d, J=8 Hz, 2H)

1-(3,5-Dibromo)-1-[3',5'-di-t-butyl-4'-(methoxyl-ethoxyl-methoxyl phenyl)]-1-(4"-1,3,2-dioxaborole phenyl) dimethyl ether (30): The first part of this synthesis involves the selective exchange and the trimethyl borate quenching of the generated lithium reagent. All operations were the same as described before. The boronic acid was isolated as a yellow viscous liquid after flash chromatography (40% methylene chloride in ether). An easier operation for esterification was employed. The boronic acid was dissolved in a heterogeneous mixture of methylene chloride and ethylene glycol. The solution was stirred at room temperature for twelve hours before the glycol was removed with four water washes. The organic layer was then dried over sodium sulfate and concentrated. After the residual solvent was removed on a vacuum line, the pure boronic ester was isolated as a yellow amorphous powder. Starting from 6 g of **30**, 2.9 g was obtained (52% yield). ^{1}H NMR δ 1.36 (s, 18H), 3.01 (s, 3H), 3.42 (s, 3H), 3.64 (dd, J=2 Hz, 2H), 3.97 (dd, J=2 Hz, 2H), 4.37 (s, 4H), 5.00 (s, 2H), 7.18 (s, 2H) 7.42 (d, J=7 Hz, 2H) 7.50 (t, J=2 Hz, 1H) 7.54 (d, J=2 Hz, 2H), 7.77 (d, J=6 Hz, 2H)

[Note: Both **29** and **30** slowly decompose in $CDCl_3$ to the corresponding substituted fuchsone. The NMR spectrum of these fuchsones are shown below.]

29⇒ ^{1}H NMR δ 7.05 (d, J=3 Hz, 1H) 7.01 (d, J=3 Hz, 1H), 6.92 (d, J=8 Hz, 2H), 7.28 (d, J=2 Hz, 2H), 7.69 (t, J=2 Hz, 1H), 7.78 (d, J=8 Hz, 2H), 1.21 (s, 9H), 1.20 (s, 9H)

30⇒ ^{1}H NMR δ 1.20 (s, 9H), 1.25 (s, 9H), 4.41 (s, 4H), 7.08 (d, J=3 Hz, 1H), 7.10 (d, J= 3 Hz, 1H), 7.23 (d, J=8 Hz, 2H), 7.18 (d, J=2 Hz, 2H), 7.71 (t, J=2 Hz, 1H), 7.86 (d, J=8 Hz, 2H) ^{13}C NMR δ 30.02, 36.12, 67.44, 95.04, 119.54, 122.74, 131.62, 131.70, 132.22, 132.27, 134.10, 134.99, 135.20, 144.82, 149.18, 187.23

4, 4'-Di-t-butyl benzophenone: In a 500 ml flask, 20 g of 4-t-butyl bromobenzene was dissolved in 250 ml of THF. The solution was cooled to -78°C in a dry ice-acetone bath and 40 ml of 2.5 M n-BuLi (in hexane, 1.05 equivalents) was added dropwise via a syringe. The exchange reaction was allowed to proceed for 45 minutes before 2.6 ml of methyl formate was added to the lithium reagent all at once. The mixture was warmed back to room temperature and stirred for another four hours before it was quenched by saturated ammonium chloride. After the THF was removed under vacuum, the residual oil was redissolved in ether and the solution was then washed with water. The organic phase was dried over sodium sulfate and concentrated. The resulting crude diphenyl alcohol was oxidized with Jones' reagent as in the synthesis of **22**. 9.5 g of benzophenone product (77% yield) was isolated as a white solid after flash chromatography (50% methylene chloride in petroleum ether). The ^{1}H NMR spectrum of the product was identical with the authentic sample.

1,1-Bis(4-t-butylphenyl)-1-(2-isopropyl-4-bromophenyl) dimethyl ether (31): 8.5 g of **21** was dissolved in 150 ml of ether. The selective lithiation was carried out according to the same procedure in the synthesis of **22**. To this chilled lithium reagent, a solution of 4,4'-di-t-butyl benzophenone (6.2 g in 30 ml of THF, 0.8 equivalent) was added and the mixture was then warmed to ambient temperature and stirred overnight. The reaction was quenched with saturated ammonium chloride and the solvent was evaporated. The reamining solid was redissolved in ether and

the solution was washed, dried over sodium sulfate and concentrated. The crude alcohol is converted into methyl ether **31** with the standard condition. 8 g of ether product is isolated by falsh chromatography (15% methylene chloride in petroleum ether) as a white solid. ^{1}H NMR δ 0.72 (d, J=7 Hz, 6H), 1.31 (s, 18H), 3.08 (b, vaguely heptet, 1H), 3.12 (s, 3H), 7.31 (two overlapping singlets with another set of doublet hidden under, 9H), 7.41 (d, J=2 Hz, 1H), 7.50 (d, J=8 Hz, 1H)

1,1-Bis(4-t-butylphenyl)-1-(2-isopropyl-4-1,3,2-dioxaborole phenyl) dimethyl ether (32): Starting from **31**, the reaction sequence employed was identical to the synthesis of **23** and **24**. One equivalent of n-BuLi was added to the cooled THF solution of **31** and the generated lithium reagent was then quenched by excess trimethyl borate. After the standard purification (flash column on 30% diethyl ether in methylene chloride) and esterification procedure, the boronic ester was isolated as a white amorphous powder in 65% yield. ^{1}H NMR δ 0.78 (d, J=7 Hz, 6H), 1.29 (s, 18H), 3.12 (singlet with a small broad peak hidden under, 3H), 4.39 (s, 4H), 7.28 (d, J=8 Hz, 4H), 7.35 (d, J=8 Hz, 4H), 7.62 (dd, J=8 Hz, 2 Hz, 1H), 7.69 (d, J=8 Hz, 1H), 7.79 (d, J=2 Hz, 1H)

33: 4 g of **32** and 1.24 g of 4,4'-dibromobenzophenone were dissolved in 25 ml of freshly distilled toluene in a 100 ml flask. 0.21 g of tetrakis(triphenylphosphine) palladium (5% with respect to dibromobenzophenone) and 20 ml of 2 M potassium carbonate solution were also added to make a yellow heterogeneous mixture. With vigorous stirring, the biphasic mixture was refluxed for 48 hours during which the solution darkened and some black precipitate formed. The reaction was then diluted with ether and quenched by 0.5 M HCl. The organic phase was washed with 5% sodium bicarbonate solution and water (two times) and then dried over sodium sulfate. After the solvent was removed, the residual

dark solid was subjected to flash chromatography (50% methylene chloride in hexane) to furnish 2.24 g of pure product (62% yield according to **22**) as a white amorphous solid. ^{1}H NMR δ 0.82 (d. J=7 Hz, 12H), 1.33 (s, 36H), 3.18 (singlet with a broad peak hidden under, 6H), 7.33 (d, J=8 Hz, 8H), 7.38 (d, J=8 Hz, 8H), 7.48 (dd, J=8 Hz, 2 Hz, 2H), 7.63 (d, J=2 Hz, 2H), 7.74 (d, J=8 Hz, 2H), 7.78 (d, J=8 Hz, 4H), 7.96 (d, J=8 Hz, 4H)

1,1-Bis(2-isopropyl-4-bromophenyl)-1-(4-bromophenyl) dimethyl ether (34): Starting from *p*- dibromobenzene and **22**, this compound was synthesized again with identical procedures as used for **23**. The tribromo ether was isolated with a simple flash chromatography (15% methylene chloride in hexane) as a light orange powder in 71% yield. ^{1}H NMR δ 0.89 (d, J=7 Hz, 6H), 0.99 (d, J=7 Hz, 6H), 3.14 (s, 3H), 3.32 (heptet, J=7 Hz, 2H), 7.16 (d, J=8 Hz, 2H), 7.22 (d, J=8 Hz, 2H), 7.29 (dd, J=8 Hz, 2 Hz, 2H), 7.46 (d, J=8 Hz, 2H), 7.49 (d, J=2 Hz, 2H)

1,1-Bis(2-isopropyl-4-iodophenyl)-1-(4-iodophenyl) dimethyl ether (35): 5 g of **34** was dissolved in 100 ml of THF in a 250 ml flask. 18.5 ml of n-BuLi solution (1.6 M in hexane, 3.5 equivalents) was added slowly after the solution was cooled to -78°C. The solution gradually became cloudy and the triple exchange was allowed to proceed for 2.5 hours at low temperature. After the exchange was completed, a solution of 8.5 g iodine in 80 ml of THF (4 equivalents) was slowly added to the perlithiated species. The solution was then warmed back to room temperature and stirred for eight more hours. Sodium sulfite solution was added until the purple color from the excess iodine was no longer visible. The aqueous portion was removed then the organic layer was diluted with ether and washed with water several times. The solution was then dried over sodium sulfate and concentrated. The remaining solid was purified on a silica gel flash column (15% methylene chloride in petroleum ether).

3.85 g of triiodide (62% yield) was isolated as a lightly orange solid. ^{1}H NMR δ 0.82 (d, J=7 Hz, 6H), 0.94 (d, J=7 Hz, 6H), 3.08 (s, 3H), 3.23 (heptet, J=7 Hz, 2H), 6.97 (d, J=8 Hz, 2H), 7.06 (d, J=8 Hz, 2H), 7.41 (dd, J=8 Hz, 2Hz, 2H), 7.62 (two overlapping doublets, J=8 Hz and 2 Hz respectively, 2H each)

Polymer Syntheses

Except for **CHPPMT**, all hyperbranched trityl polymers were made with the same Suzuki's polymerization protocol described as following. The 2 M base solution was prepared by dissolving 27.6 g of potassium carbonate in a minimal amount of deionized water then the viscous liquid was diluted to 100 ml. Argon gas was bubbled through the solution for eight hours. The toluene solvent was distilled from calcium hydride and then degassed through five freeze-thaw cycles. 2 g of monomer was placed in a 25 ml flask. This flask was moved into an oxygen-free glove box. 0.11-0.13 g (2.5-3% equivalent) of tetrakis(triphenylphosphine) palladium and 8 ml of degassed toluene were added to the flask to form a yellow solution with monomer concentration of about 0.5 M. The flask was then connected to a condenser (with a septum at the top) and moved out of the glove box. The base solution was added through the top of the condenser and the heterogeneous mixture was refluxed for 72 hours under argon with vigorous stirring. (Aluminium foil was used to protect the system from light. The flask must be well sealed to prevent the solvent from evaporating. Otherwise the oligomers can precipitate before high molecular weight is reached.) After the reaction was cooled to room temperature, the organic phase was diluted by methylene chloride and washed four times with water before it was dried over sodium sulfate. Some insoluble polymer and impurity (presumably decomposed catalyst)

were removed by simple filtration together with the drying agent. The filtrate was concentrated and the remaining solid was redissolved in a small amount of methylene chloride (< 5 ml). 30-40 ml of acetone was added to the viscous solution dropwise and the flask was shaken occasionally to ensure homogeneous mixing. The solution was left undisturbed overnight to allow the polymer to precipitate. The polymer was isolated as a white powder after filtration and two further washes with petroleum ether. The yields (1.4-1.2 g, 100% to 86% yield) were excellent in all instance.

M1 (HPPMT): ^{1}H NMR δ 3.08 (broad, 3H), 7.2-7.7 (broad, 12H); Elemental Anal. Calculated for $(C_{20}H_{15}BrO)_n$:C, 68.37%; H, 4.27%; Br 22.79%. Found: C, 67.37%; H, 4.45%; Br, 18.05%

M2 (HMMPT): ^{1}H NMR δ 3.02 (broad, 3H), 7.0-7.8 (broad, 12H); Elemental Anal. Calculated for $(C_{20}H_{15}BrO)_n$:C, 68.37%; H, 4.27%; Br 22.79%. Found: C, 71.23%; H, 4.58%; Br, 17.28%

M3 (HMMMT): ^{1}H NMR δ 3.02 (broad, 3H), 7.0-7.7 (broad, 12H); Elemental Anal. Calculated for $(C_{20}H_{15}BrO)_n$:C, 68.37%; H, 4.27%; Br 22.79%. Found: C, 75.57%; H, 5.74%; Br, 10.38%

HPPMDIT: ^{1}H NMR δ 0.75 (broad with small shoulder. 12H), 3.1-3.2 (two broad peaks, 6H), 3.3-3.6 (two broad peaks, 2H), 7.1-7.6 (broad multiplets, 10H); Elemental Anal. Calculated for $(C_{26}H_{27}BrO)_n$:C, 71.72%; H, 6.2%; Br 18.4%. Found: C, 72.19%; H, 6.42%; Br, 15.86%

HPPPDIT: ^{1}H NMR δ 0.82 (borad, 12H), 3.0-3.2 (borad peak with a shoulder, 3H), 3.3-3.6 (two broad peaks, 2H), 7.1-7.7 (broad multiplets, 10H); Elemental Anal. Calculated for $(C_{26}H_{27}BrO)_n$:C, 71.72%; H, 6.2%; Br 18.4%. Found: C, 75.43%; H, 6.6%; Br, 11.32%

4-t-Butyl-benzeneboronic acid (18): 20 g of 4-t-butyl bromobenzene was dissolved in 300 ml of THF and the solution was

cooled to -78°C. 40 ml of n-BuLi solution (2.5 M in hexane, 1.06 equivalents) was slowly added to the cold solution via a syringe. After the exchange reaction was allowed to proceed for 45 minutes, 20 ml of trimethyl borate (1.9 equivalents) was added all at once via a syringe. The mixture was warmed back to room temperature and left for eight more hours. The reaction was then quenched with water and this mixture was washed until the aqueous layer became neutral. The organic phase was dried over sodium sulfate before the solvent was removed on a rotary evaporator. The remaining 14 g of viscous liquid (judged by NMR and TLC) was a mixture of 4-t-butyl-benzene and various boronic anhydrides. This mixture can be used directly in the subsequent Suzuki's coupling without further purification.

CHPPMT: Crude 4-t-butylbenzene boronic acid was generated from 6 g of 4-t-butyl-bromobenzene according to the procedure already mentioned. 2 g of **HPPMT** was dissolved in 40 ml of toluene in a 100 ml flask already containing the crude boronic acid (4-5 equivalents to bromide based on the assumption that each monomer unit containing one bromide on average). 0.33 g of tetrakis(triphenylphosphine) palladium (5% equivalent to bromide) and 20 ml of 2M potassium carbonate solution were also added to the flask. The heterogeneous soltion was refluxed with vigorous stirring for 48 hours. (The color of the solution turned from yellow to black.) After the reaction was completed, it was diluted with methylene chloride and the organic phase was washed three times before it was dried over sodium sulfate and concentrated. The residue was redissolved in a little methylene chloride (<4 ml) and the polymer was precipitated from the viscous solution by slow addition of methanol (about 30 ml). The suspended solution was left undisturbed overnight before the polymer powder was isolated by filtration. After the polymer was further

dried on a vacuum line, 2.2 g of black amorphous solid (96% yield) was obtained. ^{1}H NMR δ 1.37 (broad), 3.16 (broad) integration ratio of the two peaks 2.5-2.7:1, 7.2-7.7 (broad); Elemental Anal. Calculated for $(C_{30}H_{28}O)_n$:C, 82.95%; H, 6.45%; Br trace. Found: C, 77.22%; H, 6.07%; Br, <0.5%

All the polymers were converted into polytrityl trifluoroacetate as described earlier. Due to their instability, these polymers were not thoroughly characterized. Nevertheless, they can be detected in NMR spectrum with 1:1 $CDCl_3/CF_3COOH$ as the solvent.

M1 (HPPMT): ^{1}H NMR in $CDCl_3/CF_3COOH$ δ 7.4-8.2 (broad multiplets); in CD_2Cl_2 δ 7.0-7.6 (broad)

M2 (HMMPT): ^{1}H NMR δ 7.2-8.2 (broad multiplets)

M3 (HMMMT): ^{1}H NMR δ 7.2-8.4 (broad multiplets)

HPPMDIT: ^{1}H NMR δ 1.18 (broad, 12H), 2.4-3.0 (broad, 2H), 7.4-8.2 (broad multiplets, 10H)

HPPPDIT: ^{1}H NMR δ 1.0 (broad peak with a small shoulder, 12H), 2.2-2.8 (broad, 2H), 7.2-8.3 (Broad multiplets, 10H)

The hyperbranched fuchsone precursor polymer was also synthesized through Suzuki's coupling with some modifications in the condition. In a typical polymerization, 1 g of the monomer, 0.58 g of potassium carbonate (three equivalents) and 53 mg of tetrakis(triphenylphosphine) palladium (3% equivalent) were placed in a Shlenk tube. 6 ml of freshly distilled toluene and 3 ml of water were added to make the biphasic mixture. The monomer concentration in the organic layer was 0.21 M while the base concentration was 1.2 M. The tube was connected to a vacuum line and the heterogeneous mixture was degassed through freeze-thaw cycle five times. The mixture was then heated in a 100°C oil bath under vigorous stirring for 48 hours during which some polymer precipitation occurred. (The system was protected from light during all these operations.) After the

reaction was cooled back to room temperature, the solution was diluted by methylene chloride and the organic phase was washed four times and dried over sodium sulfate. Some insoluble products were removed by filtration together with the drying agent. After the solvent was evaporated, the residual solid was redissolved in a small amount of methylene chloride and the polymer was precipitated by addition of methanol. White polymer powder was obtained through filtration after the suspended solution stood unperturbed overnight. ^{1}H NMR δ 1.36 (bs, 18H), 3.02 (bs, 3H), 3.37 (bs, 3H), 3.81 (bs, 2H), 3.95(bs, 2H), 4.96(bs, 2H), 7.0-7.8 (broad multiples, 9H); Elemental Anal. Calculated for $(C_{32}H_{36}BrO_4)_n$:C, 68.08%; H, 6.38%; Br 14.18%. Found: C, 67.25%; H, 6.89%; Br, 10.93%

The polymer was converted into polyfuchsone when dissolved in pure TFA. The deep orange solution was stirred at room temperature for twelve hours. TFA was then removed on a vacuum line and the polyfuchsone was obtained as a orange powder. ^{1}H NMR δ 1.22 (bs, 18H), 6.90-8.1 (broad multiples, 9H)

Polyradical Synthesis

- **Room Temperature Polyradical Synthesis**

50 to 100 mg of polymer was placed in a 100 ml flask with a vacuum-adaptable side arm. The flask was then moved into an oxygen-free glove box. 15-20 ml of trifluoroacetic acid was added to the polymer and the resulting solution was deep red. The solution was left in the box under vigorous stirring. Occasionally, lumps of polymer solidifies at the inner surface and need to be washed back into the solution by gently shaking the flask. After twelve hours, the flask was moved out of the glove box and the TFA was evaporated on a vacuum line. (The evaporated TFA was condensed in a second trap.) After nearly all the solvent was removed, the

flask was connected directly to the line for an additional 4-8 hours. The resulting polytrityl trifluoroacetate was a dark purple powder.

With the polytrityl trifluoroacetate still under vacuum, the flask was moved back into the box and 20 ml of solvent (methylene chloride, toluene or benzene) was added. To this suspended solution, one equivalent of reducing metalocene was then added. (The average molecular weight of the monomer unit was approximately that of a trityl ether with one residual bromide attached. For example, in **HPPMT**, an average monomer unit contains $(C_6H_4)_2(C_6H_4Br)C\text{-}OMe$ and thus the average weight is 351.) The deep purple color of the solution changed slowly to deep murky green. After eight hours, the solution was poured into a glass dish or on a Teflon plate. After solvent evaporated naturally, polyradical samples were obtained as brittle solids mixed with the oxidized metallocene. About 20-30 mg of this mixture was loaded into the SQUID sample holder and subject to measurement immediately.

For the **CHPPMT**, Rajca's procedure was modified to suit the circumstances. The whole operation was performed in a glove box. 50 to 100 mg of polymer was dissolved in THF and large excess of lithium powder was added. The solution was stirred vigorously for 48 hours during which the blue color slowly developed. The excess lithium was then removed by filtration through a glass filter. One equivalent of ferrocenium tetrafluoroborate was added to the blue solution and the mixture was stirred for an additional two hours. A yellow powder sample was then obtained after the evaporation of THF as described before. The magnetic measurement was also carried out accordingly.

•Low Temperature Polyradical Synthesis

The synthesis of polytrityl trifluoroacetate was identical as before except a flask with two side arms had to be used. All polymers/TFA solution are deep red except for **HPPPDIT** which showes blue color. After the TFA was removed under vacuum, the flask was moved back to the glove box where one equivalent of cobaltocene was added. Moved outside of the box again, the flask was connected to a lecture bottle of chloromethane (or dimethyl ether) through one side arm. The other arm was hooked to a vacuum line. The whole system was evacuated and refilled with argon three times. After the flask was cooled down to -78°C in a dry ice-acetone bath, the valve of the lecture bottle was opened to allow the condensation of gaseous "solvent" into the flask. Every time the bubbling in the dry ice bath started to intensify, the valve was closed temporarily to keep the system at relatively low temperature. This process was repeated for a few times until 15 to 20 ml of solvent was transferred (according to a premade mark). Judged by the light brown color of the solution, the polytrityl trifluoroacetates are barely soluble at such low temperature. This color did not change significantly during the whole course of the reaction. On the other hand, the color changes of the suspended powder were substantial. Starting from deep purple, it first turned gray at the surface. This thin layer of gray color slowly developed into pale yellow throughout the sample. Again, the only exception was **HPPPDIT.** The color changes were from blue to gray then finally to green. After twelve hours, the flask was once again attached to vacuum line and the solvent was removed in another eight to twelve hours with the flask still in the low temperature bath. The flask was then moved back to the glove box with the vacuum still maintained inside. 20-35 mg of powder was loaded into the sample holder

which was immediately immersed in liquid nitrogen bath before the tube was inserted into the SQUID probe.

Chapter 3 Evaluation of Magnetic Interactions Through the Conducting Backbone in a Hyperbranched System

The Role of Defects

Research aimed at synthesizing very high-spin organic molecules by using intramolecular through-bond interaction is depicted in the last chapter. Such a project has revealed new types of magnetism that is hard to study with metal-based systems. Despite the numerous advantages of studying organic systems[1], the most troublesome flaw of organic radicals remains their low stability. This unavoidably leads to defects which are arguably the major obstacle for most organic polyradicals to exhibit really high S values. Of course, spin persistency is also crucial should an organic magnet find some technological application some day.

Theoretically, a design that invokes crosslinking or hyperbranched structures described in the last chapter has great potential to reduce the damaging effects of defects. However, since only few systems have really been tested in these regards, the effectiveness of this approach in real systems remains questionable. In a recent report by Nishide, the S value only improves marginally when a linear system is modified to contain various degrees of branching[2]. To prevent the formation of defects and to minimize their deleterious effect are the two main challenges for the physical organic chemists in this field.

In most polyradicals, including those in Chapter Two, every radical center is a part of the pathway (or network) to conduct the ferromagnetic interactions through the whole system. Thus the most serious problem caused by defects, instead of the loss of spin angular momentum, is the interruption of high-spin coupling among the remaining radical centers. This connecting pattern and its consequence resemble the series connection in a simple electric circuit; namely, the damage at an individual site can shut down the electricity in the whole system. Alternatively, radical sites can also be connected in a parallel fashion where all radical centers are

attached to a π-conjugated polymer backbone without being a part of the coupling pathway. In such a system, with some subtle designs, defects can only diminish the magnitude of magnetic interaction, but it remains ferromagnetic nonetheless. In other words, this design paradigm might lead to a true "defect-insensitive" system that cannot yet be achieved with hyperbranched structures alone. This chapter presents the effort to combine the advantage of this new concept and hyperbranched approach to continue the quest for organic polyradicals with very high-spin ground state.

Magnetic Interactions Through Conducting Backbones

The hypothetical polyradicals of Figure 3-1 can help to visualize a high-spin system where all radicals are attached to a conjugated backbone.

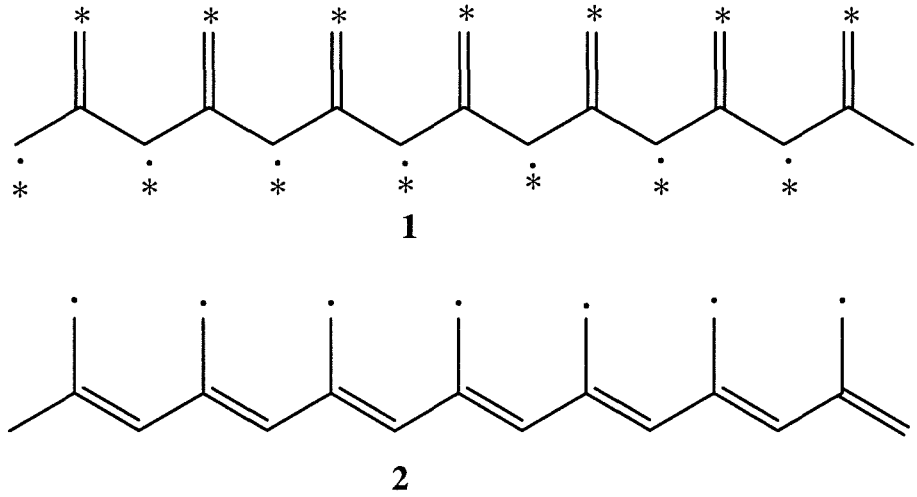

Figure 3-1: A hypothetical polyradical and its defect-insensitive resonance form

In structure **1**, the polymer can be analyzed according to the more conventional design paradigm (Figure 2-1). The ferromagnetic coupling

unit is 1,1-ethylene and the spin containing unit is simply a trivalent carbon. As expected, any defect in the chain reduces the S value at least in half. However, **1** can also be represented in its resonance structure **2** where every radical is connected to a polyacetylene backbone. Both structures should possess the same high-spin ground state as predicted by the Ovichinnikov-Borden theory. But in **2**, the ferromagnetic interactions between the radicals are transmitted through the polymer backbone as depicted in the last section. Theoretically, any two radical centers in **2** are ferromagnetically coupled regardless of the status of all other sites. This exemplifies a real "defect-insensitive" polyradical. However, the magnitude of ferromagnetic interaction still decreases as the rate of defects increases. For example, all the coupling units in **2** consist of three SP^2 carbons if no defects are present. With a single defect, the coupling between the two sites next to the defect is still ferromagnetic yet the coupling unit now has five SP^2 carbons. This inevitably reduces the interaction due to a longer coupling pathway. In a practical level, the diminished interaction can be too small to impose long range spin ordering.

Of course, **1** and **2** are merely two of many resonance structures for this system. By simply examining two resonance structures, it is not possible to predict how the real system will behave one way or the other. However, the system can be modified to favor type **2** structure over other resonance forms by some radical-stabilizing substitutions. For example, if the exo-methylene groups in **2** are substituted by two phenyl groups, the radical should be much more localized at the pendant carbons instead of the polyacetylene chain (Figure 3-2).

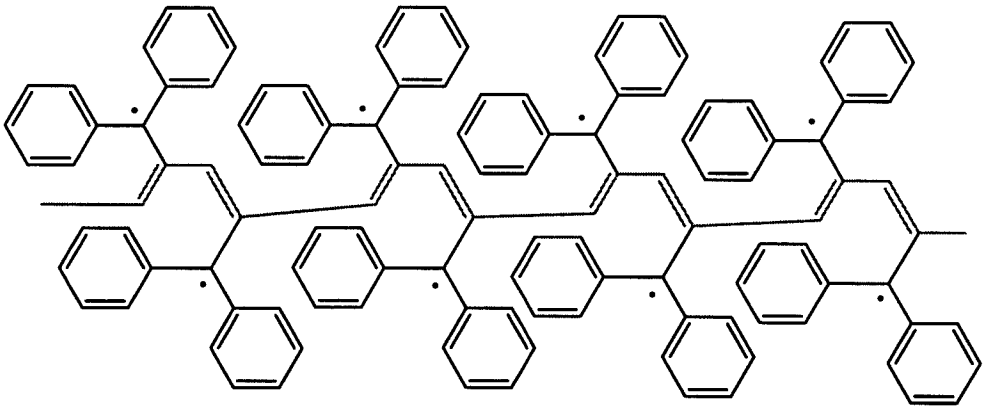

3

Figure 3-2 : Defect-insensitive resonance form stabilized by phenyl substitutions

Based on the structure **3**, Jacobs made some attempts to synthesize a less substituted version via a highly regioselective ring-opening metathesis polymerization of cyclobutene derivatives[3]. Unfortunately, the precursor polymer cannot be converted to the target polyradical under various conditions.

As mentioned in the last chapter, a linear polyradical can usually be classified as either magnetic or conducting according to its connecting pattern. Conducting polyradicals have the conjugated topology as *p*-phenylene or 1,2-ethylene while the magnetic ones possess the cross-conjugated topology as *m*- phenylene or 1,1-ethylene. Polyradicals **2** and **3** appear to be the exceptions to the simple dichotomous rule. The most interesting feature of their topology is that the ferromagnetic interaction is conducted by the polyacetylene backbone. Such a conducting topology is usually considered to cause antiferromagnetic interactions. However, the ferromagnetic coupling can still arise if the regiochemistry of the pendant radicals is carefully controlled with sophisticated synthetic tactics. The

principle should also be applicable to other conducting polymers. With some proper design, high-spin polymers can be made with radicals attached to polyphenylene, polyphenylene vinylene, or polythiophene skeletons at appropriate positions. The magnetic behavior of this type of polyradical has been the subject of numerous theoretical studies since the late 70's[4].

Figure 3-3 outlines the new synthetic paradigm using a conducting polymer backbone to align pending SCs. In order to ensure that all the interactions between adjacent radical sites are ferromagnetic, the polymerization reaction must be highly selective to produce the head-to-tail regioisomer. A head-to-head (or tail-to-tail) defect results in an antiferromagnetic interaction. This will cause the cancellation of spin angular momenta between two high-spin fragments and lead to bulk antiferromagnetism.

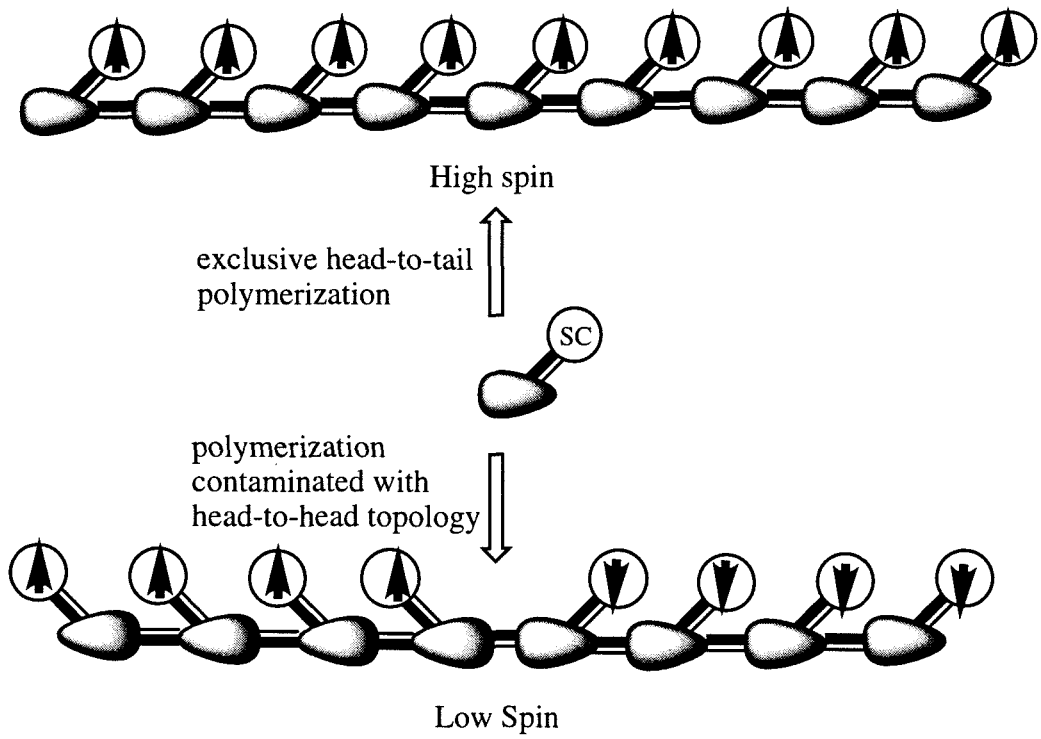

Figure 3-3: Synthetic scheme for defect-insensitive polymer

Despite the "defect-insensitive" property this topology is supposed to induce, it should be emphasized that the concept is by no means a new one. As shown in Figure 3-1, the magnetic behavior of **2** can be simply rationalized with the conventional Borden-Ovichinnikov theory. The reason why such systems might be less sensitive to defects is simply because of spin localization. In contrast to the design in Figure 2-1, the SCs and coupling pathway in such polyradicals are distinct structural motifs; namely, the loss of the former does not interfere with the latter. Another example is shown in Figure 3-4. The more realistic resonance structure of the high-spin polybenzyl polyradical is certainly the one with the polyphenylene backbone and pending radicals instead of the other one resembling **2.** As in **2** and **3**, the radical sites are not in the conducting pathway and therefore defects should have only a minimal effect on the S value. In summary, the major effort in designing these systems is to choose more localized spin sources and incorporate them into a conducting polymer in a regioselective manner.

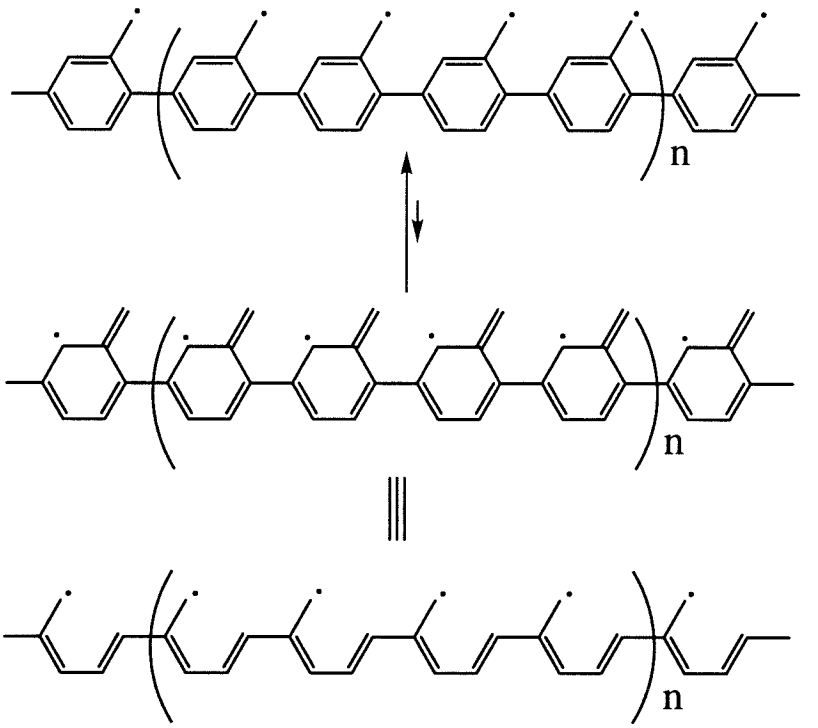

Figure 3-4: High-spin poly (benzyl radical) and its resonance structure

Linear "Defect-Insensitive" Systems

Since confinement of the spin density is the essence of this new design, highly localized radicals has always been utilized by earlier researchers as SCs in such pursuit. Notable examples include Nishide's poly-t-butyl-phenyl nitroxide[5] and poly-nitronyl nitroxide synthesized by Iwamura and Ito[6]. From EPR experiments, the spin densities of these radicals mainly localizes on the hetreoatoms[7].

Typically, the syntheses start with the polymerization of a terminal acetylene monomer that contains a radical precursor. The regioselective polymerization is usually carried out with a transition metal catalyst to furnish a regioregular polyacetylene backbone. Cationic rhodium complexes by far give the most satisfactory results[8]. The diamagnetic polymers with pendant radical precursors are then converted to

polyradicals with some oxidation or hydrogen abstraction chemistry after they are fully characterized.

Due to the high radical stability, these materials usually possess very high spin concentrations. However, the expected ferromagnetic interaction is not observed in any of these early experiments, not to mention the desired defect-insensitive property. Even at very low temperature (1.8 K), all these materials are perfect paramagnets with S=1/2 from SQUID experiments. This lack of collective behavior indicates that the interaction conducted by the polyacetylene backbone is extremely small. These failures are usually attributed to the twisting in the system[9]. It is well known that when substations are introduced, polyacetylene becomes nonplanar and thus an inferior conductor[10]. Clearly, the pendant radicals can force the conducting backbone to adopt a nonplanar geometry. Similarly, the radicals themselves and the backbone cannot be coplanar. Nishide thereby proposes that the infinitesimal coupling resulted from twisting induced by pending radicals.

It is also quite probable that the localization of spins also contributes to these disappointing results. Although such localization is the central point of the design, it can reduce the exchange interaction between the unpaired electrons because they are restricted to their individual spaces. This inevitably leads to nearly degenerate states and the observed paramagnetic behavior. Therefore, the ideal SC for this study should be localized enough to preserve the integrity of the conducting backbone yet still allow the electrons certain degrees of freedom to interact with each other: a delicate balance must be matched.

More recently, Nishide scored the first success in this class of polyradicals[11]. The author uses 2,6-di-t-butyl phenoxyl radical as the SC. The linear precursor polymer is synthesized with a step-growth

unimolecular polymerization reaction. After the polymer is transformed to polyradical, the expected high-spin ground states are observed while the spin density remains fairly localized at the oxygen. Although the S values in these polyradicals are only moderate (S=1-2.5), this constitutes the first experimental evidence that ferromagnetic interaction can be transmitted through a conducting backbone.

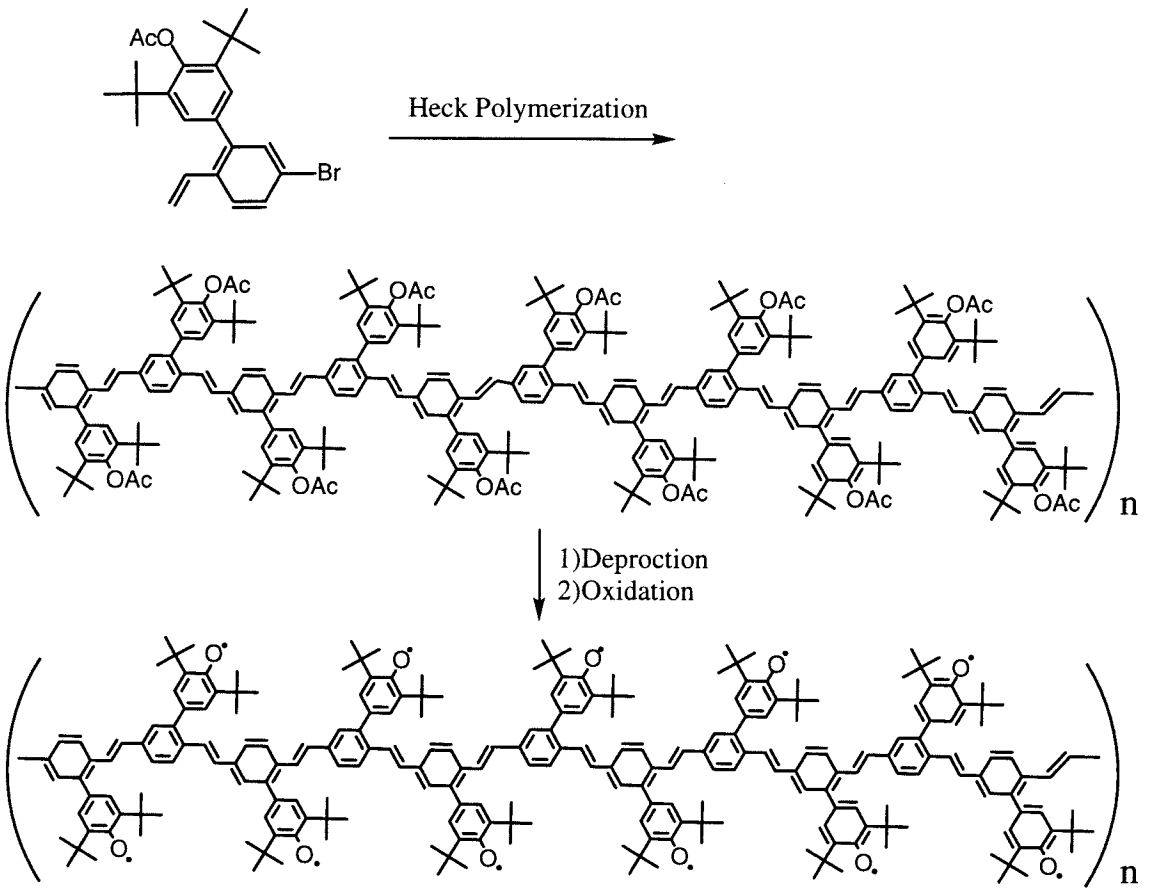

Figure 3-5: Nishide's approach to defect-insensitive poly-phenoxyl

This breakthrough can be partly attributed to the radical unit of choice. Unlike nitronyl-nitroxide or nitroxide, the spin in phenoxyl radical is supported by only one heteroatom. When employed as SCs, it should lead to larger exchange interactions and therefore a greater preference for

high-spin ground states. Furthermore, when the spin is carried by a single atom, the delocalization of the radicals cannot be diminished by the twisting angle between the heteroatom and phenyl groups as in the nitroxide. The utilization of polyphenylene vinylene as the backbone could also be an important factor for success. It is clearly more chemically robust than polyacetylene and therefore more likely to survive some harsh reaction conditions for radical generation.

This chapter describes the attempt to improve Nishide's system by incorporating phenoxyl radicals into a hyperbranched conducting polymer. The basic concept is to make the system even less sensitive to defects by taking advantage of polymer branching as described in the last chapter. The ultimate goal is again to produce organic polyradicals with very high S values and novel magnetic behavior.

Design of a Hyperbranched "Defect-Insensitive" System

In his latest paper, Nishide has modified the original system to produce a lightly branched polyradical[12]. The new polymer is synthesized by copolymerizing a similar monomer and 1,3,5-triiodobenzene (Figure 3-6). Because the carbon-iodine bonds are weaker, the vinyl group should couple with the triiodobenzene selectively until it is nearly all consumed. This furnishes a branching unit the polymer can continue to grow on and brings about the desired topology in the end. Although the rate of branching points (controlled by the equivalent of triiodobenzene used) is less then two percent, this modification does improve the S value moderately from 2 to 3.5 over the linear system. However, judged from the molecular weight of the polymer, this S value is still much smaller than what should be expected if the system is really defect-insensitive. (DP as high as 70 is deduced from GPC.)

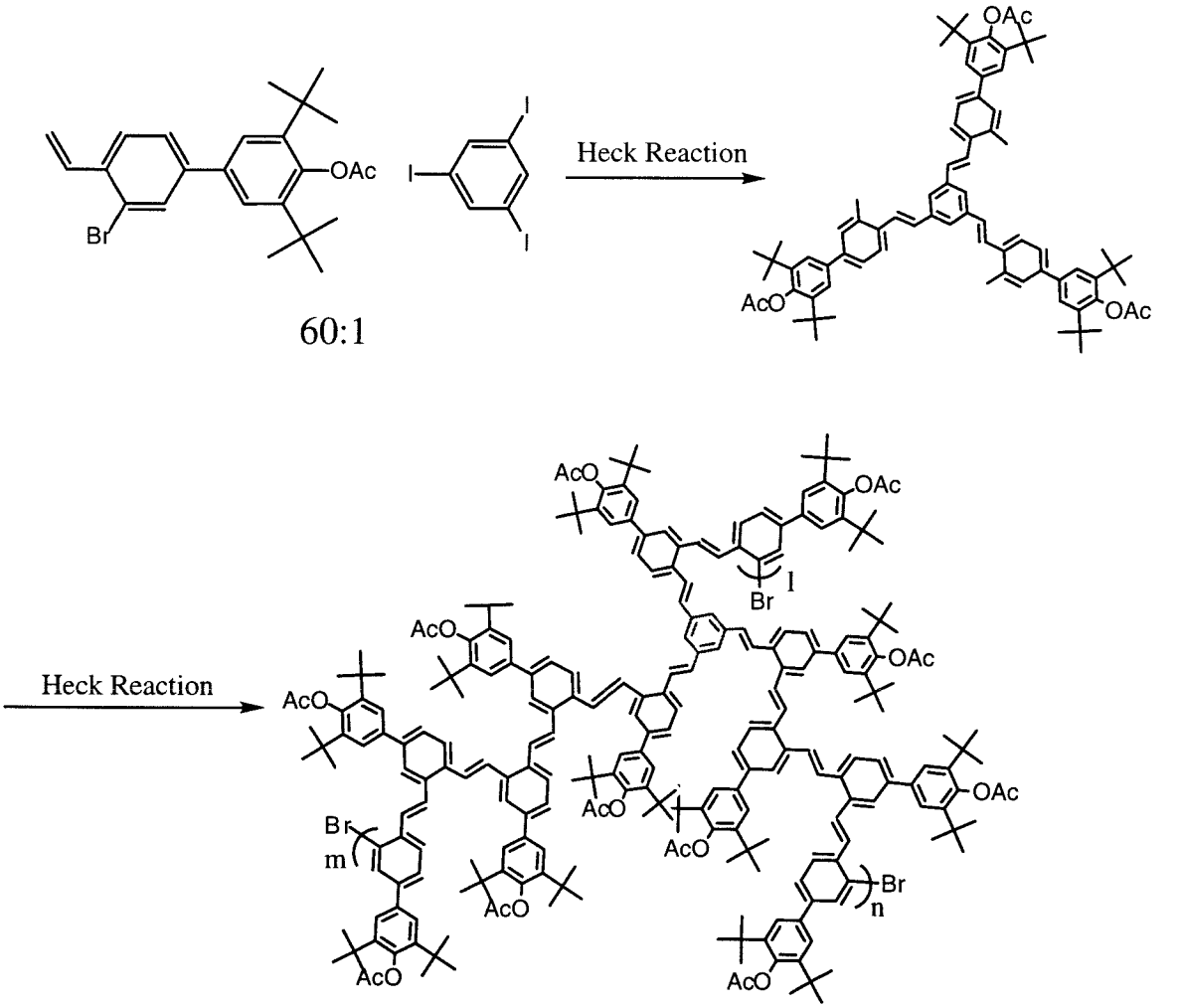

Figure 3-6: Nishide's copolymerizing approach to branched polymer

That the S value can be improved as a result of branching is certainly encouraging and proves this strategy is worth further investigation. In Nishide's study, only polymers with relatively low degrees of branching are investigated presumably because of the concern on polymer solubility. A hyperbranched approach seems to be an excellent remedy for this problem. As demonstrated in the last chapter, hyperbranched polymers are usually quite soluble regardless of their structure features. Statistically, 25 percent of all sites in a hyperbranched polymer are branched. This is more than ten times that of the Nishide's polymer. It is hoped that higher S

values and more definitive collective behaviors will be manifested by this amplification of branching points.

The most convenient synthesis of hyperbranched polymer is the unimolecular polymerization of an A_2B monomer. To achieve the highest degree of branching, the three functional groups in the monomer should be spatially separated. Since the essence of the new design is to remove the SCs from the conducting backbone, the new monomer should contain four compartments, three functional groups for polymerization and the remaining one as the SC precursor. This leads to a primitive concept of monomer design; namely, four groups should be attached to a conjugated framework. The simplest molecular motif that fits this criterion is a tetrasubstituted ethylene. Figure 3-7 shows several possible monomers of this type.

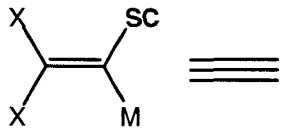

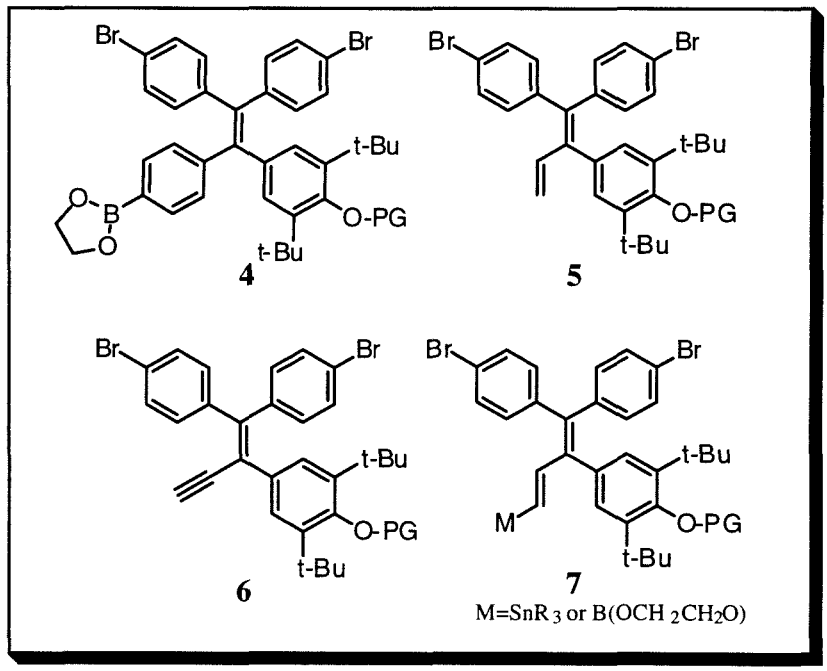

Figure 3-7: Monomers that may lead to defect-insensitive polyradicals

The prototype structure can be developed into several variations. Proved effective in Nishide's work, di-t-butyl-phenol is the SC precursor in all monomers. The palladium catalyzed coupling reactions remain the most reliable polymerization protocol for this purpose. The halogen groups are installed on the extra phenyl rings because the hindrance around the tetrasubstituted ethylene will impair their reactivity and thus minimize the degree of branching. The additional phenyl group should also make the polymer backbone more chemically robust. This improvement can be crucial for the latter characterization and radical generation. **4** can be polymerized with Suzuki's reaction to furnish a hyperbranched version of polystilbene. **5** and **7** should lead to the same polymer composed of phenyl butadiene units. **5** can be polymerized with a Heck reaction as in Nishide's report while Suzuki's-type or Stille's-type coupling should be used for **7**. For polymerization of **6**, the highly efficient palladium catalyzed Stephans-Castro (abbreviated as PSC) coupling between an alkyne and an aryl halide should be employed to produced a hyperbranched polymer composed of phenyl butene-3-yne units.

Both Heck and PSC reactions belong to the same class of palladium catalyzed cross coupling reaction as Suzuki's and Stille's coupling and both have been applied to the synthesis of conjugated polymers with very promising results[13]. However, because of the substrates involved, there are some small differences in reaction mechanisms and conditions for these two reactions. Like the organoboron (or organotin) reagents used in Suzuki's (or Stille's) coupling, neither alkenes nor alkynes by themselves are reactive enough as the nucleophiles in the catalytic cycle. Therefore, both reactions are performed in amine solvents to facilitate the coupling. Although some details are still subject to debate, the general mechanisms for these reactions are pretty well established[14] (Figure 3-8).

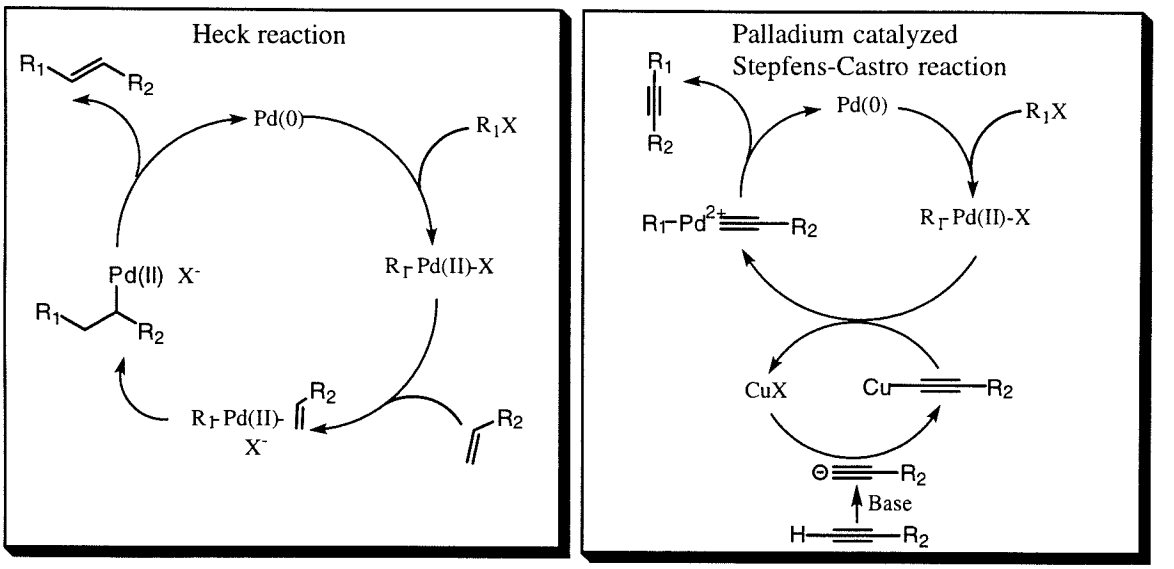

Figure 3-8: Catalytic cycles of Heck reaction and PSC reaction

Identical to the mechanism described in Figure 2-11, the oxidative coupling of aryl halides with the metal center initiates the catalytic cycle. In the Heck reaction, the alkene then coordinates to the palladium. The new carbon-carbon bond is formed in a migratory insertion reaction of the aryl group into the palladium-alkene bond. This step is usually regioselective towards the formation of 1,2-disubstituted ethylene and this selectivity is pivotal to the construction of high-spin topology. The resulting σ palladium complex immediately undergoes elimination in the presence of amine solvent to furnish the coupling product and regenerate the Pd(0) species. In the PSC coupling, low concentrations of alkylydine are first generated through deprotonation of the terminal alkyne by the amine solvent. The anion is then trapped as an organocopper reagent *in situ* by catalytic copper(I) to serve as the nucleophile. A transmetalation reaction then leads to an aryl-alkynyl-palladium species which can undergo reductive elimination to give coupling product.

Synthesis of Monomer

The major challenge of synthesizing monomers in Figure 3-8 is to form the moderately crowded ethylene skeleton regioselectively. The most straightforward disconnection should be a two-component reaction to form the central double bond. Because of the steric hindrance in the product, Wittig type reaction is probably impractical for this purpose. An alternative is to assemble the molecule with the reductive dimerization reaction of two appropriate ketones. The titanium(0)-mediated McMurray coupling is arguably the best established of such reactions[15]. A model coupling reaction was carried out between **9** and a large excess of 4,4'-dibromobenzophenone according to a known procedure[16]. Unfortunately, it appears that the aryl halide groups are labile under such highly reductive condition. This approach is thus aborted without further exploration.

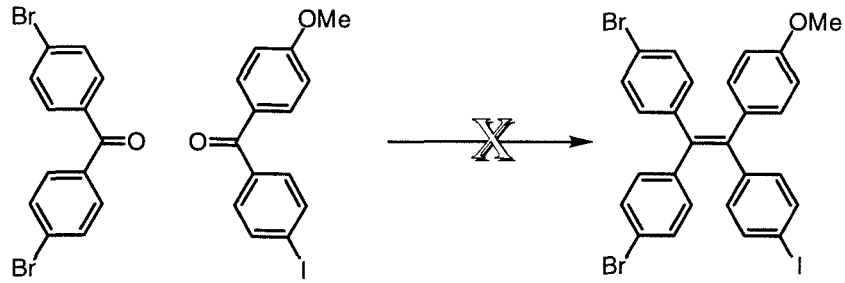

8 **9** **7**

Another excellent way to construct an olefin is through traditional aldol reaction. In the conventional aldol condensation, enolates can undergo addition reaction with ketones to give the β-hydroxy carbonyl compounds. Under certain conditions, this type of substrate can easily dehydrate to give the α,β-unsaturated carbonyl compounds. Based on this concept, a simple retrosynthetic analysis is shown below.

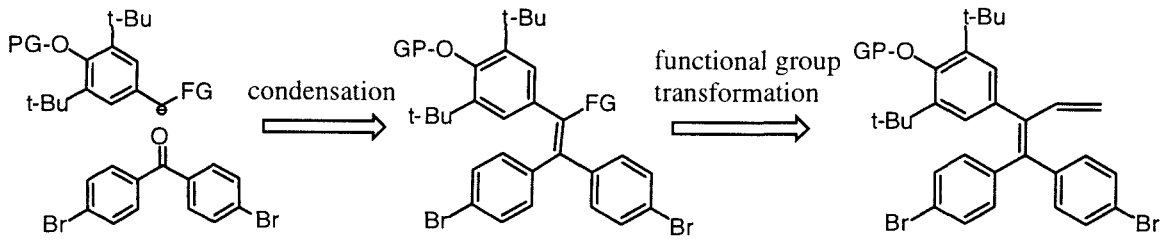

In the current study, for both steric and electronic reasons, the benzophenone electrophile is quite inert. Therefore, the reactivity of the carbanion becomes crucial for an efficient condensation step. Usually, the reactivity of a carbanion roughly correlates with the pK_a of the carbonyl compound it is generated from. [For example, the enolate of acetone (pK_a= 20) is more reactive than that of 2,4-pentanedione (pK_a= 9) yet both are inferior to that of ethyl acetate (pK_a= 24.5).] The main concern here is that the presence of the extra aromatic ring in the carbanion component can render the condensation reaction extremely sluggish. Not only has the carbanion become more hindered upon such substitution, but the electron affinity of the phenyl ring also reduces the pK_a of the parent compound and thus impairs the reactivity of the anion. Not surprisingly, in model studies, enolates originated from ketone or ester groups are not reactive enough to furnish any desired condensation product. On the other hand, compared to the α protons of carbonyls, those of nitrile compounds are much less acidic. (The pK_a of acetonitrile is 31 while those of simple ketones are around 20.) The small size of the cyano group should also be beneficial to the reactivity in the addition step. Indeed, the condensation between benzophenone and phenyl acetonitrile is well documented[17]. In model studies, the only carbanion that gives any olefin product at all is generated from 4-methoxy phenylacetonitrile. Even when a large excess of benzophenone is used, the yield for olefin product is rather poor (30-40%). Nevertheless, this is enough for our purpose.

The road map of monomer synthesis is then to make a protected 3,5-di-t-butyl-4-hydroxy phenylacetonitrile and condense its anion with dibromobenzophenone. The actual procedures are shown in Figure 3-9. The required phenylacetonitrile derivative is synthesized with an unusual substitution reaction between the tosyl hydrazone **10** and potassium cyanide in refluxing ethanol with loss of nitrogen gas[18]. With this procedure, the protection of the phenolic hydroxyl group is not necessary and the highly labile benzyl halide required for the more intuitive SN_2 approach can also be avoided. This improves the yield and simplifies the whole operation considerably.

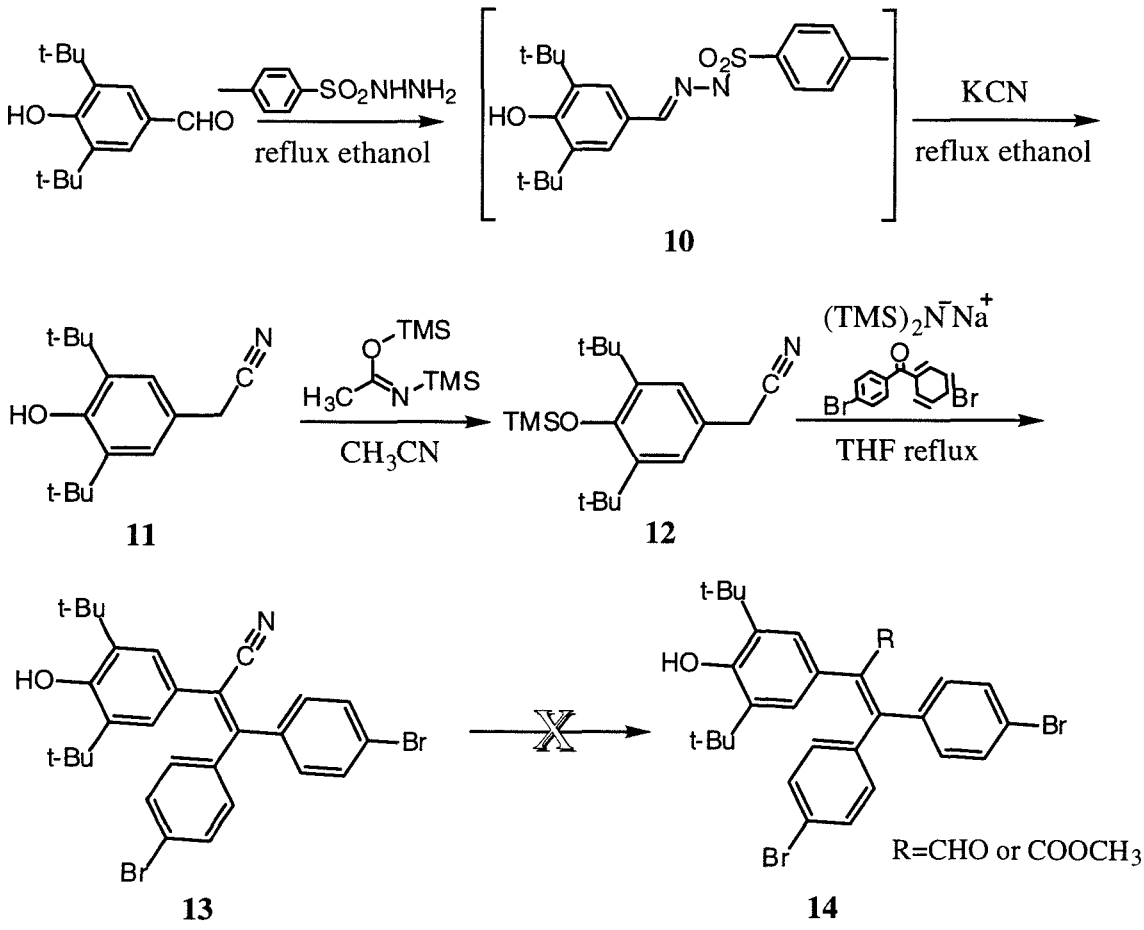

Figure 3-9: Attempt synthesis of monomer **5**

When **11** is employed directly in the condensation step, no olefin product can be detected. In such instance, the phenolate anion certainly forms first and probably cannot be deprotonated any further to give the essential dianion. To ensure that the required carbanion can be easily generated with a common organic base, the hydroxy nitrile **11** is first converted to silyl ether **12** by treating it with N,O-bis(trimethylsilyl) acetamide in refluxing acetonitrile. This highly reactive silylating reagent is especially useful for protecting hindered alcohols. Of course, the reactivity of this special reagent cannot be justified simply by its structure. It is proposed that the imido nitrogen is first protonated *in situ* to generate the actual active species[19].

Several bases were examined for the condensation reaction, and the most satisfactory result comes from sodium bis(trimethylsilyl)amide. This base is sufficiently strong yet still stable enough to allow the reaction to be performed at reflux condition which is crucial for the formation of the double bond. Not surprisingly, the TMS protecting group does not survive this strongly basic condition. As in the model study, the deprotected olefin **13** is isolated in low yield (20%).

The downfall of this approach comes at the seemingly routine functional group transformation. In model compounds, the cyano group cannot be converted to aldehyde or ester with the standard reagents (Dibal-H and HCl/methanol) for such transformation. Even under some quite vigorous conditions, this nitrile group remains completely inert. Judged from such poor reactivity, this cyano group is obviously in an unusually crowded environment. Even if the current obstacle can be overcome with some more elaborated reaction conditions, the next step, which is probably even more sensitive to steric hindrance, is still doomed for the same

reason. Because of all these uncertainties, this strategy is not explored any further.

The setbacks made us reevaluate the original plan in which the hindered olefin is formed in a single step. Such approach, though straightforward, probably requires the development of some highly elaborated reactions that are far beyond the scope of this project. An alternative strategy is to make an allyl alcohol first, the diene unit can be installed latter with a simple dehydration reaction. Figure 3-10 depicts this retrosynthetic analysis.

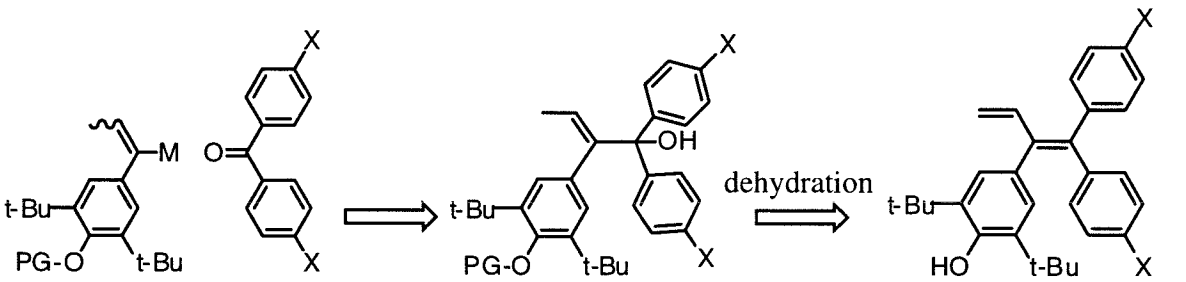

Figure 3-10: New synthetic plan for monomer **5**

In this new plan, the focus of the synthesis is turned from double bond to single bond formation. This can be achieved through an addition reaction of an appropriate organolithium (or Grignard) reagent to a substituted benzophenone. The actualization of this strategy is shown in Figure 3-11.

It is first assumed that the best way to generate the required organometallic reagent is through a lithium-halogen exchange reaction with a proper alkenyl halide. However, it is soon discovered from the model studies that the synthesis of such precursor compound is far too laborious to be practical. Bonds has reported that alkenyl lithium reagents can be obtained from treating 2,4,6-triisopropyl-benzenesulfonyl hydrazones of ketones with two equivalents of n-BuLi[20]. Unfortunately, this Shapiro-type

reaction also proves impractical because the intermediate hydrazone is unstable and cannot be easily purified.

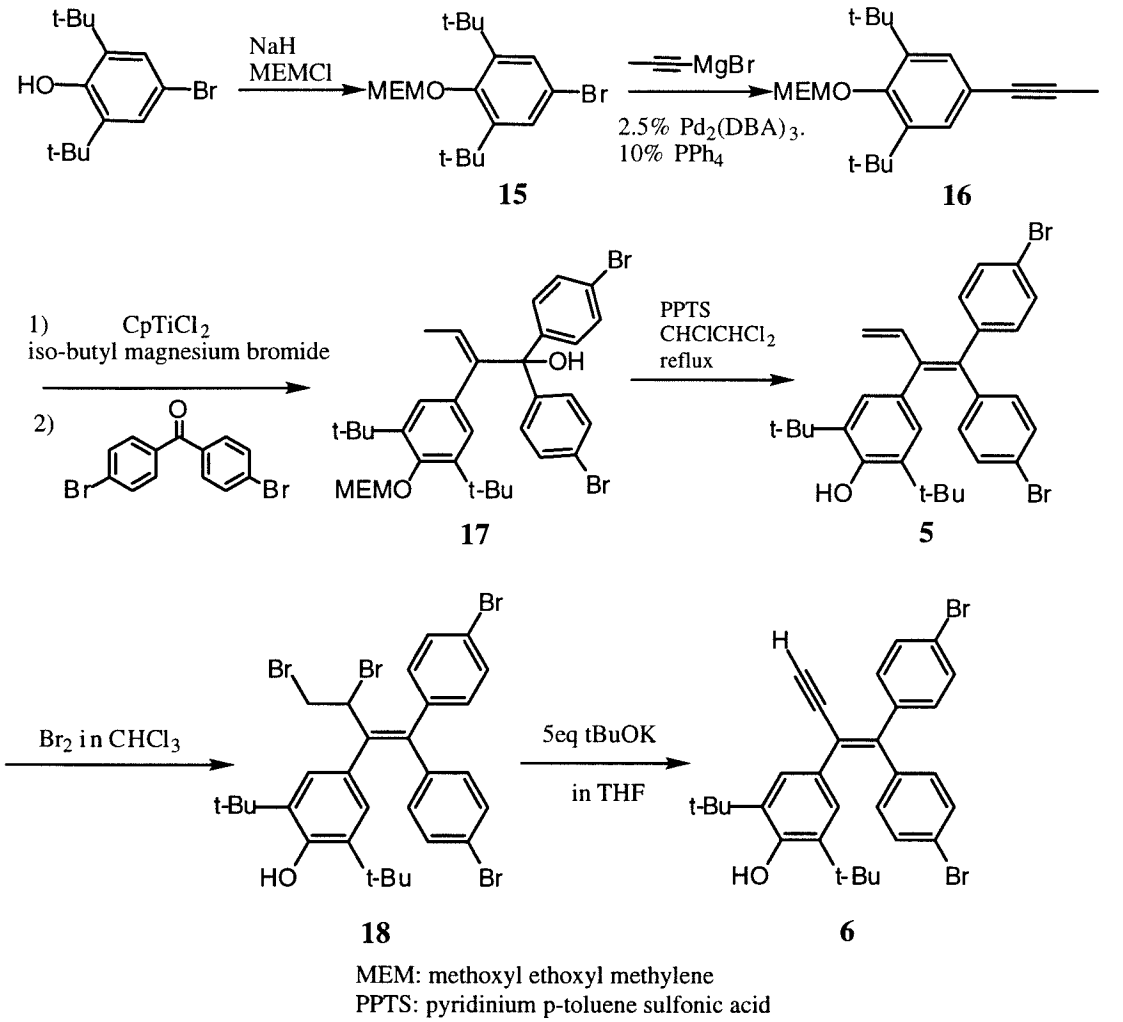

Figure 3-11: Synthesis of monomer **5** and **6**

For this project, it was discovered that the most convenient way to generate the alkenyl metal reagent was the hydromagnesiation of an alkyne[21]. This reaction catalyzed by bis(cyclopentadiene) titanium dichloride with stoichiometric amount of isobutyl magnesium bromide as the source of magnesium and hydrogen. The catalytic cycle starts with a substitution reaction at the metal center to generate the titanium-isobutyl σ

complex. The metal complex immediately undergoes β-elimination to form the titanium hydride and give off isobutene. The metal hydride then adds to the alkyne substrate. The resulting titanium-alkenyl σ complex then undergoes a metathesis reaction with another isobutyl magnesium bromide molecule to produce the desired Grignard reagent and regenerate the titanium-isobutyl complex to complete the catalytic cycle. To produce the required Grignard reagent, the addition reaction must be regioselective to an unsymmetrical substrate such as **16**. Fortunately, in a similar compound (1-phenyl propyne), Sato has found that the selectivity for the desired isomer is more than ninety percent presumably for electronic reasons[22].

To apply this protocol to the present system, the precursor alkyne **16** is synthesized. The phenolic hydroxyl group first is protected with methoxyl ethoxyl methoxyl (MEM) by treating the bromophenol with MEMCl and sodium hydride. The three-carbon unit in **17** is then installed with a palladium catalyzed coupling between the aryl bromide **15** and propynylide magnesium bromide. As expected, **17** undergoes regioselective hydromagnesiation to give the desired Grignard reagent which then reacts with 4,4'-dibromobenzophenone to produce the allyl alcohol. The dehydration and deprotection steps can be carried out in a one-pot procedure with the mild organic acid, pyridinium *p*- toluene sulfonate (PPTS), to give monomer **5.** The combined yield for the two consecutive steps is rather poor (25%) and not optimized. Yet, enough material can be produced for further investigation. The terminal double bond is converted into an alkyne with the most straightforward method, a bromination followed by an exhaustive dehydrobromination[23]. The extent of bromination is controlled by performing the reaction at low temperature. The two-stage elimination is accomplished in one pot with a large excess of

potassium t-butoxide. The two-step combined yield for eneyn **6** is about 50% from **5**.

Polymer Synthesis

Supposedly, a hyperbranched polymer can be made from **5** under the Heck reaction condition reported by Nishide.

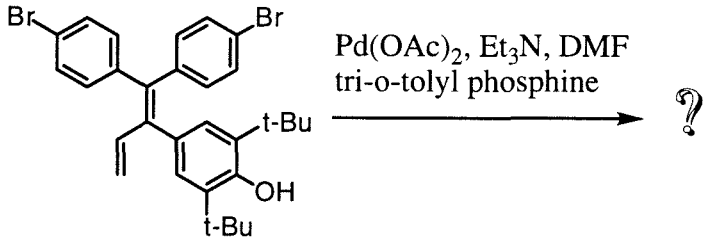

However, upon examining some more examples of polymer synthesis with Heck reaction, it soon becomes clear this approach has little chance to produce the polymer needed for this project. Meier has attempted to synthesize conducting polymers containing anthracene moieties with Heck reaction[24]. The author found that this synthesis can easily be accomplished with 9,10-dibromoanthracene but not with 9,10-divinylanthracene and the rationale is as follows. In the catalytic cycle (Figure 3-8), the rate determining step is, instead of the oxidative addition, the migratory insertion. Mullen proposes that the steric hindrance at the 9 position of anthracene prevents the palladium to move near that site. This leads to the inhibition of migratory insertion and thus the termination of the reaction cycle. In this study, the vinyl group in **5** is doubtlessly in an even more crowded position than that in 9-vinylanthracene. Therefore, more than likely, it will be very hard to improve its reactivity with new variations of reaction conditions. This approach is thus not given any further investigation.

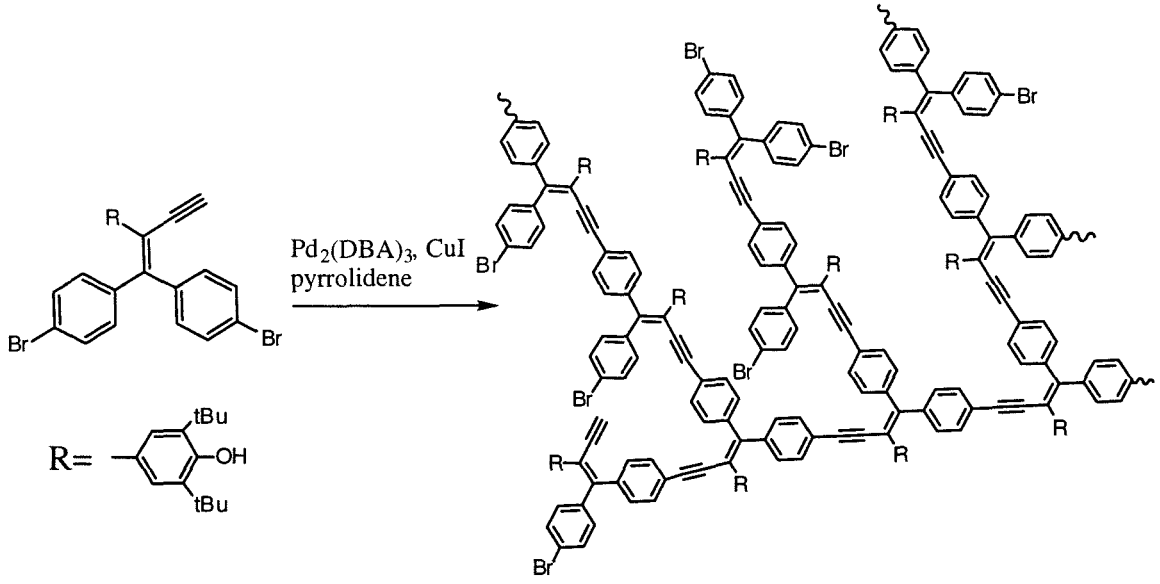

Figure 3-12: Hyperbranched polymerization of **6** to produce **HDPDBOB**

Unlike what is predicted for polymerizing **5** with Heck reaction , the hyperbranched polymerization of **6** with PSC reaction proceeds successfully to give polymer of a decent molecular weight. The difference is probably that the alkyne forms a σ complex with the palladium in contrast to the π-type complex in the Heck reaction (Figure 3-8). Therefore, the crowdness at the other end of the alkyne does not effect the reactivity very much. The reaction is performed under a modified version of PSC reaction used by Moore in the synthesis of hyperbranched phenylacetylene[25]. The catalyst is generated *in situ* with tris(dibenzylideneacetone) dipalladium(0) and triphenylphosphine. This catalytic system is particularly stable and thus very suitable for polymer synthesis. Pyrrolidine is known to accelerate the coupling reaction dramatically presumably because of its basicity[26]. A high monomer concentration (0.5 M) is also important to ensure a high molecular weight.

The polymer **HDPDBOB** [**H**yperbranched 1,1-**D**i-**P**heny-2-(3,5-**D**i-t-**B**utyl-**O**xyphenyl) **B**utene3-yne] is isolated in nearly quantitative yield as a brick red powder. Both the line width of the NMR spectrum and gel permeation chromatography confirm that the molecular weight is large. Again, a bimodal distribution typically seen for other hyperbranched polymers is observed in the GPC. With poystyrene as the standard, the average molecular weight is about 15000, which corresponds to a DP around 30.

Polyradical Synthesis and Magnetic Characterization

Nishide's protocol is first employed to convert the precursor polymer **HDPDBOB** into the corresponding polyradical. The polyphenol is first deprotonated with tetrabutyl ammonium hydroxide to produce the polyphenolate. This polyanion is then oxidized with a large excess of aqueous K_3 [$Fe(CN)_6$] in its THF solution. The polyradical is isolated from the organic layer after the solvent is evaporated.

Alternatively, the oxidation step can be performed with ferrocenium hexafluorophsphate. The advantage of this type of oxidant is already discussed in Chapter Two. First, the reduced oxidant is the diamagnetic ferrocene which does not interfere with magnetic characterization. Also, in contrast to aqueous K_3 [$Fe(CN)_6$], ferrocenium is a homogeneous oxidant and therefore allows the reaction to be performed at low temperature with relatively high efficiency. Again, an unconventional solvent, chloromethane, is used as the solvent and the resulting polyradical is kept at -78°C until a powder sample is obtained.

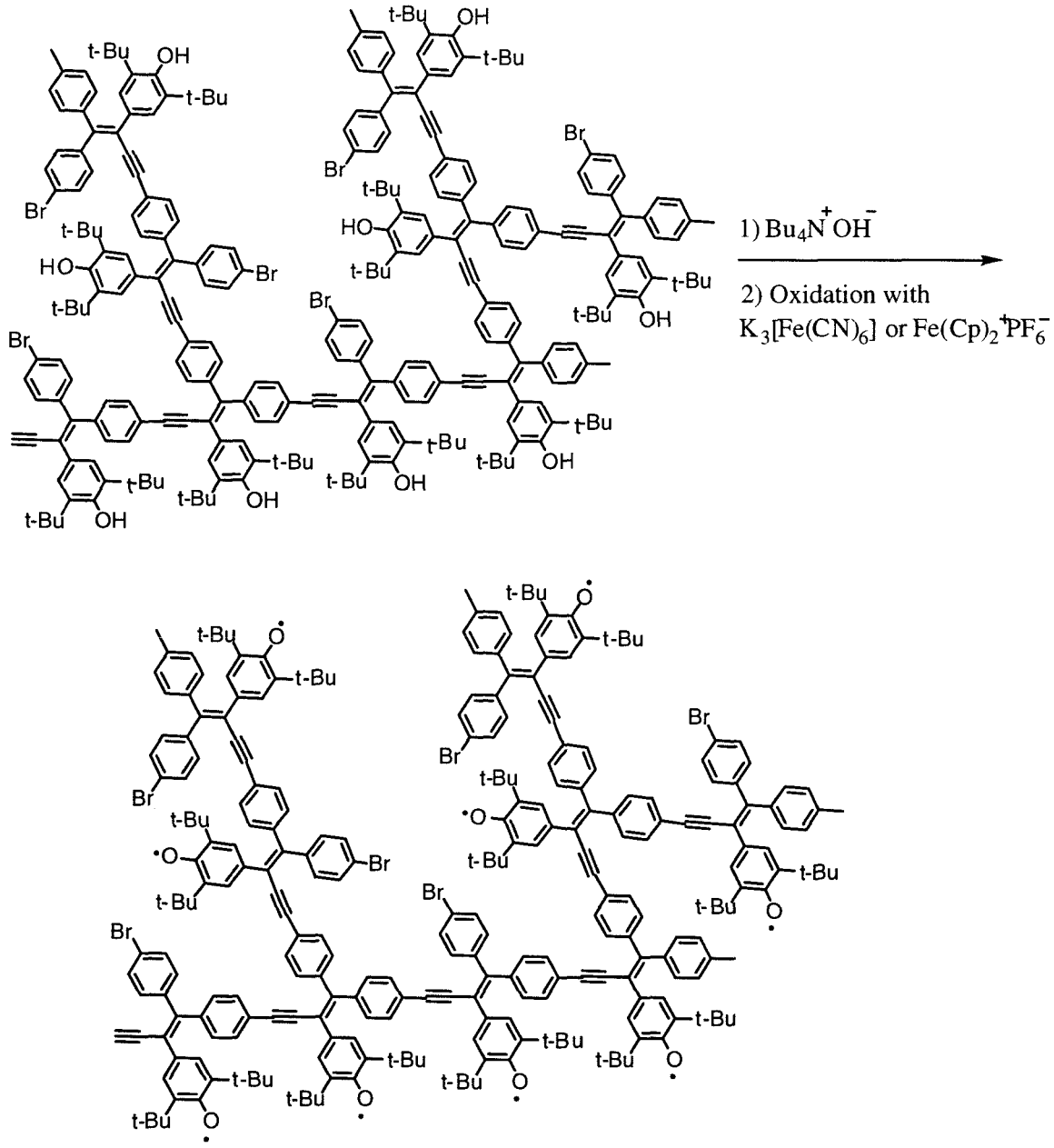

Figure 3-13: Transformation of **HDPDBOB** into polyradical

Polyradical from both protocols can be isolated as a red orange powder. The samples are loaded into the SQUID sample holder in an oxygen free glove box. The magnetic measurements and data processing are performed with the same protocol as those used in Chapter Two. The results are listed in Table 3-1.

	$K_3[Fe(CN)_6]$ as oxidant	$Fe(Cp)_2^+PF_6^-$ as oxidant
Spin Concentration	**68%**	**78%**
S value	**0.8**	**1.3**

Table 3-1: Magnetic properties of polyradical from **HDPDBOB**

The spin concentrations in both instances are comparable to those obtained in Nishide's systems (80%). Compared to the polytrityl in the last chapter, these significant improvement clearly result from the stability of the phenoxyl radical. Similar to what is observed in the polytrityl systems, the spin concentration is higher for the sample from low temperature oxidation. However, the "improvement" can also be attributed to residual ferrocenium because of incomplete oxidation. The S values, on the other hand, are again disappointing. Although the interactions between radicals are unmistakably ferromagnetic, the S values remain moderate at best.

Discussion and Future Directions

The results in Table 3-1 clearly demonstrate that even with the advantage of an extremely stable spin source and hyperbranched topology, the S value falls far short of expectation. Evidently, the defect-insensitive property supposedly guaranteed by the design does not appear even at 1.8 K. Although the magnetic properties might be improved at some lower temperature, such experiment is not performed for both instrumental limitation and time restriction. The few encouraging conclusions from this study are the persistency of di-t-butyl phenoxyl radical and the tiny yet

unmistakably ferromagnetic interaction. This section outlines several intrinsic problems in the design and possible ways to solve them.

First is the polymerization reaction itself. The PSC reaction is arguably the most reliable reaction in the synthesis of conjugated polymers. It has been used extensively by Moore[27] and Swager[28] to make structurally defined polymers. However, since its discovery, the dimerization of terminal alkynes has always been an annoying side reaction. This oxidative dimerization needs a stoichiometric oxidant, presumably oxygen, and copper ion as catalyst[29]. However, in the past studies, the dimer products can only be reduced but never completely eliminated even when oxygen is excluded. In small molecule syntheses, such side product can usually be separated with traditional techniques. However, in a polymer synthesis, the dimerization reaction results in tail-to-tail topological defects that are permanently implanted in the polymer framework. Statistically, even if the probability of this side reaction is only two percent at each single step, about half of the 30-mer molecules will contain at least one diacetylene linkage.

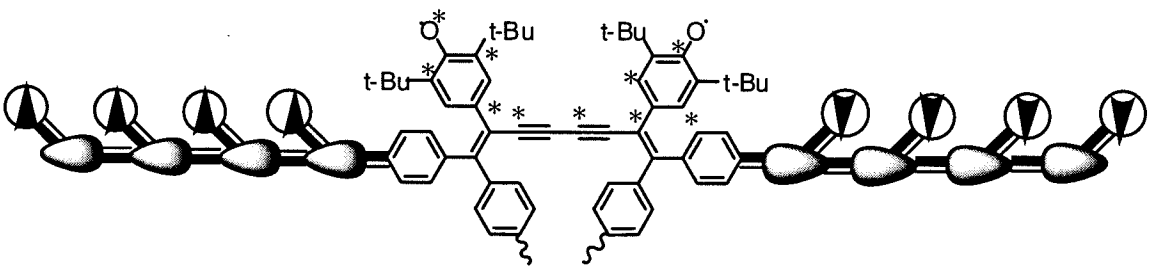

Figure 3-14: Detrimental effect of head-to-head defect on a hypothetical polyradical

As shown above, the diacetylene formation results in a disjoint coupling unit according to the Borden-Ovinchinnikov theory. This means the

polyradicals are really just small weakly interacting spin clusters. This partly explains why the S value is dismal in this system while the spin concentration is still very high.

The problem can be overcome by making the polymer with other more selective coupling reactions. The Suzuki's coupling is the most reliable choice in this regard. Monomer **7** (Figure 3-7) is specifically designed for this purpose. It can be synthesized simply by a hydroboration of **6** by catecholborane.

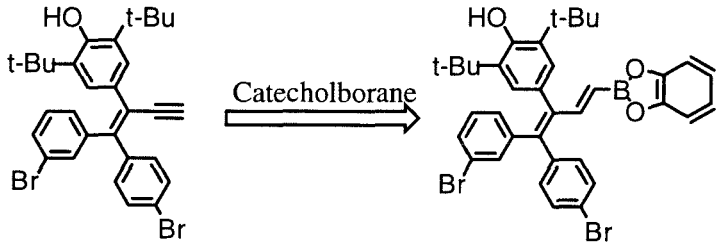

As mentioned earlier, the design principle in this type of system is to localize the radicals so that the SCs and the coupling pathway become structurally independent. However, the observation of ferromagnetic behavior requires the delocalization of electrons so that they can interact with each other. With these two factors conflicting with each other, the magnetic interactions in such systems are intrinsically weak. In most of the early research, no evidence of any interaction is observed at all. Even in Nishide's reports, the interaction strength between neighboring radicals in his system is only about 40 cm^{-1}. In the presence of defects, the coupling pathway is lengthened (at least by six carbons) and the interactions retain only one tenth of the defect-free magnitude. In such a case, the interaction is probably too weak to align long range ordering even at 1.8 K.

In this project, in order to install the hyperbranched network, the coupling pathway is intrinsically extended by two carbons (totally nine

carbons) compared to those in Nishide's polyradicals. This inevitably leads to diminished ferromagnetic interactions and predictably even lower S values. Furthermore, if a spin defect is inserted between two SCs, the coupling pathway is now lengthened to 17 carbons. Even if the interaction remains ferromagnetic, its magnitude is unquestionably too small to impose any spin alignment at 1.8 K.

To gain a more qualitative picture, Closs and Forbe's studies of long-range through-bond interaction may provide some useful insights[30]. They found the coupling strength of two radicals through σ bond framework lose about half of its magnitude when the pathway was extended by one carbon-carbon bond. Although this conclusion is obtained from saturated model compounds, it should still be applicable to the present case because the phenoxyl radical is highly localized. Indeed, Nishide's results (both experimental and computational at AM1-CI level)[31] can be qualitatively predicted with this decay factor of two per carbon-carbon bond. When applied to our system, it predicts a coupling strength of 15 cm^{-1} at most. With any defects present, the interaction can be as small as 1 cm^{-1} if it remains ferromagnetic at all. With such small interactions, it is not at all surprising that neither a large S value nor any defect-insensitive property can be observed.

The already weak interaction could be further attenuated by the steric and delocalization factors already mentioned in Chapter two. In Nishide's system, molecular modeling has demonstrated (UFF force field) that, although the SCs are not co-planar with the polyphenylene vinylene backbone, the conducting main chain is quite planar in its most stable conformer. Such planarity is especially important for maintaining the high-spin coupling in a weakly interacting system. In this project, in order to build the hyperbranched structure, the tetrasubstituted ethylene skeleton is

employed in the monomer design. Unfortunately, because of the crowdedness, this structural motif is considerably twisted. This problem, that already makes the monomer synthesis unusually complicated, can be a detrimental factor concerning the magnetic interaction. From CPK models, not only is the SC is twisted out of plane with the polymer backbone, but the backbone itself is also twisted to avoid the clashing of the phenyl groups. Assuming the latter twisting angle to be 40 degrees, according to Equation 2-3, the interaction can be further reduced by 40 percent.

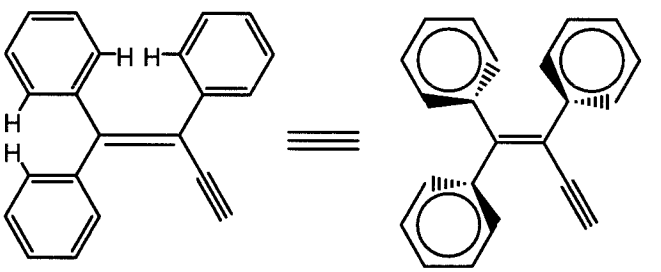

Other than causing steric crowdedness, the extra phenyl ring can also impair the magnetic interaction by diluting the spin density. Compared to that in Nishide's systems, spins here are less confined. This means the unpaired electrons have less chance to contact with each other. It follows that the Columbic repulsion between electrons becomes smaller and therefore the very small preference for high-spin ground state is further lessened.

It is clear from this study that magnetic interaction that is transmitted by a conducting polymer backbone can be extremely delicate. Unlike in the conventional design where high-spin coupling is exceedingly robust, minor structural modifications in such systems can easily eradicate the designed ferromagnetic interaction. The dilemma is between radical delocalization,

which is crucial for strong interaction, and localization, which is essential for the polyradical to be defect-insensitive. The past researches mainly focus on localizing SCs to segregate them from the conducting backbone. However, when localizing the spin sources renders the interaction so weak, there is little chance the defect-insensitive property to ever be detected. Therefore, to improve the system, a more delocalized SC should be employed, even at the price that the S value of the resulting polyradical becomes more defect-sensitive.

It is well accepted that the electronegativity of heteroatoms is the prime cause for the localization of some organic radicals. Notable examples include nitroxide and nitronyl nitroxide. In other words, delocalized radicals are generally carbon-based. With the monomer synthesis and hyperbranched polymerization conditions already developed, the next sensible target polyradical should have the same conducting backbone with pendant carbon-centered radicals. Figure 3-15 shows two such potential monomers.

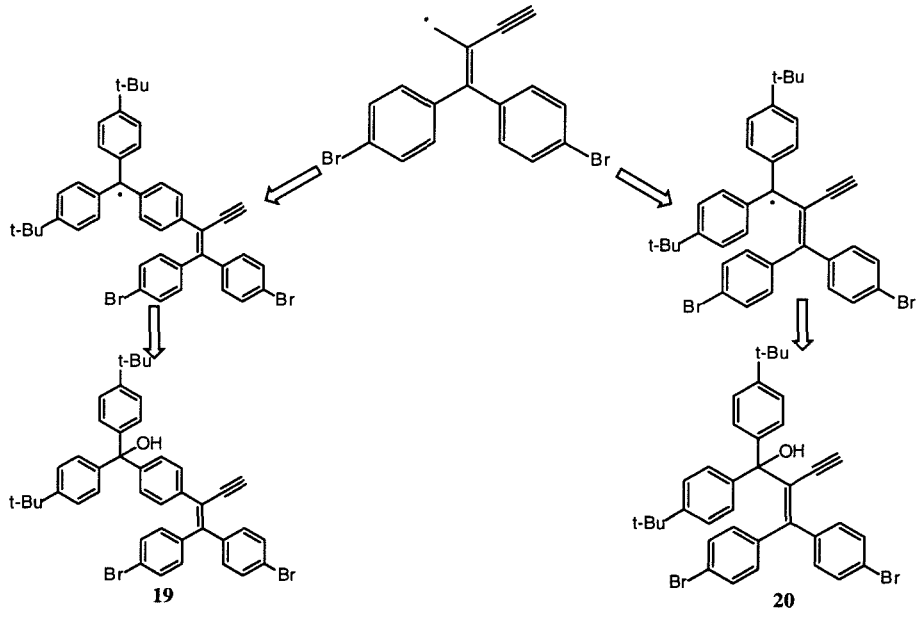

Figure 3-15: The designing logic of two new monomers

Nominally, the SCs in **19** and **20** are trityl radical and diphenyl methyl radical respectively. However, this certainly does not mean the radical stability in polyradical derived from **20** resembles that of simple diphenyl methyl. In contrast, on examining the resonance structures, the radical should be at least as persistent as tetraphenyl allyl radical. This resonance not only ensures the radical stability, but also fulfills the purpose of this new design by allowing the unpaired electrons to delocalize into the backbone. In comparison, the polyradical made from **19** should be much more localized because of the intrinsic stability of trityl. It follows that, of these two potential monomers, **20** should lead to the polyradical with stronger ferromagnetic interaction and is chosen for further study. An tentative synthesis is shown in Figure 3-16.

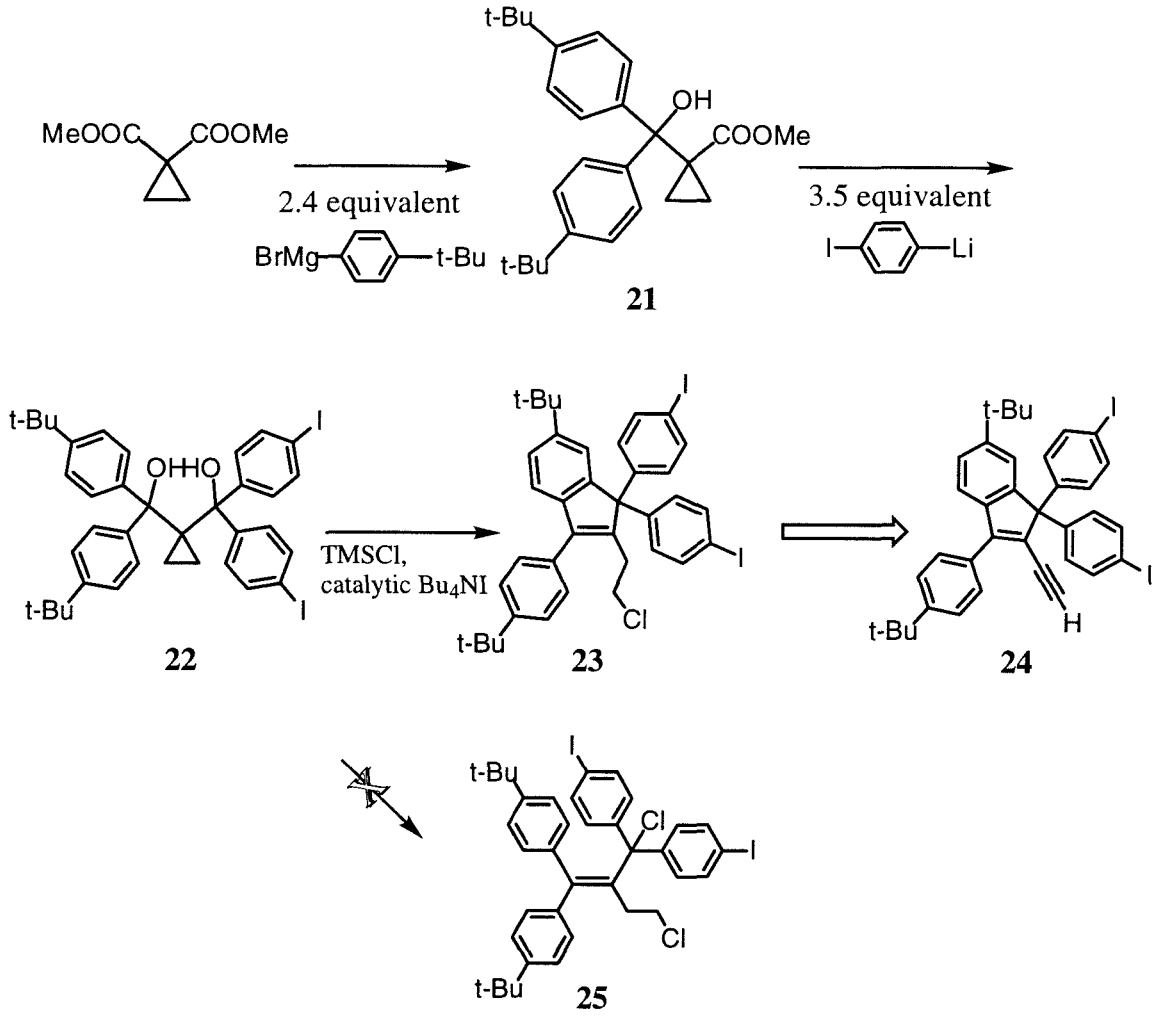

Figure 3-16: Attempt to synthesize monomer **20**

The major obstacle in the synthesis of **20** is again the steric hindrance around the double bond. Following the strategy developed for making **7**, this compound should be made with a dehydration of the corresponding allyl alcohol. Unfortunately, various efforts fail to produce this precursor, presumably also for steric reasons. An alternative way to make a tetra-substituted olefin is the acid-catalyzed rearrangement of cyclopropanol. This method was developed by Julia and Johnson in the early 70's[32] and has since been successfully used in several syntheses of natural products[33]. The

rearranged product is a homoallylic halide which can be easily converted into a diene and ultimately to the desired enyne.

The first task in this synthesis is to make the cyclopropanol substrate for rearrangement with all four appropriately substituted phenyl groups. The most straightforward approach to the diphenylmethyl structure is a double addition of organometallic reagent (Li or Mg) to an ester. However, to make the diol **22**, the two sequential addition reactions must be carefully controlled to furnish the right regioisomer. The optimal procedure is to use a Grignard reagent in the first step followed by a lithium reagent addition to the remaining ester. The order is essential because only with the less reactive Grignard reagent can the reaction be stopped after the first two additions. The rearrangement reaction can be carried out in methylene chloride with a mild Lewis acid, pure iodotrimethylsiane. However, it is more convenient to generate this highly sensitive reagent *in situ* with chlorotrimethylsilane and a catalytic amount of tetrabutyl ammonium iodide[34]. Without further purification, the rearranged product is directly subjected to the elimination step to produce the diene. An enyne is then obtained with the bromination-elimination reaction sequence described earlier (Figure 3-9).

Although both the ring opening and the subsequent functional group transformation are successful, it becomes unfortunately clear only at this last stage that the rearrangement reaction does not lead to the expected product. Based on NMR and mass spectrum, the actual product is the cyclic **23**. This type of cyclization is well known for tetraphenyl allyl cation[35]. Clearly, under this reaction condition, a secondary cation is generated after the initial rearrangement takes place. This cation then undergoes facile intramolecular cyclization to give the cyclic product.

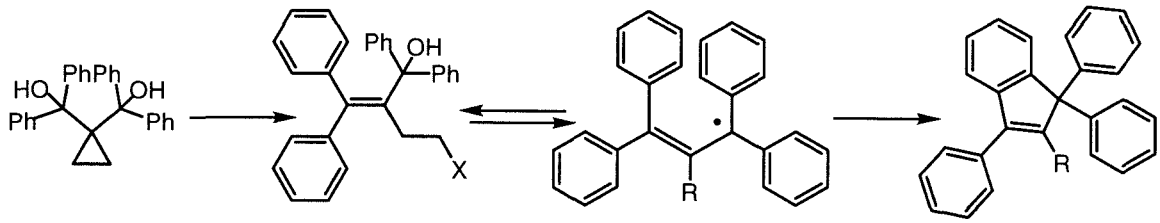

Despite the disappointment, the ring opening reaction does prove quite effective and should remain a prime choice for making other hindered olefins in the future. The problem arises because, under this reaction condition, the rearrangement product inevitably leads to the cation which then undergoes cyclization. Even if this monomer synthesis can be achieved through another route, this intramolecular cyclization can still cause difficulty in the radical generating step where polycation might be an intermediate. A sensible way to avoid this problem is to destabilize the second cation. As shown in the scheme below, this can be accomplished by incorporating a fluorenyl structure. Compared to similar systems, the fluorenyl cation is quite unstable because of its antiaromatic character. Similar strategy has been employed in the synthesis of a very stable organic radical[36]. It is hoped that the synthesis and radical generation can be achieved without the annoying cyclization with this modified substrate under milder acid treatment.

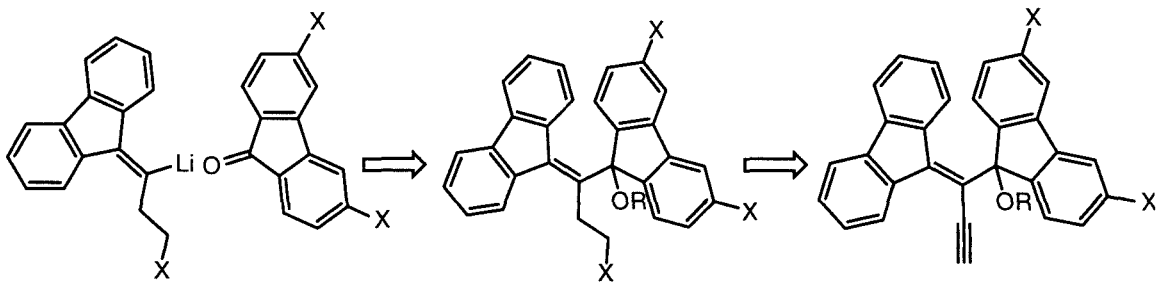

Conclusions

A number of important conclusions have emerged from this study.

- Hyperbranched polymer can be made from an A_2B type monomer that is built on a tetrasubstituted olefin scaffold. Some difficulties arising from steric hindrance are encountered in the monomer synthesis. The obstacle is finally overcome by assembling the necessary component first as an allyl alcohol. A titanium catalyzed regioselective hydromagnesiation reaction is used to generate an essential Grignard reagent. The palladium catalyzed Stephans-Castro coupling reaction perfected by Moore furnishes a soluble polymer in high yield under mild condition.

- The polymer is converted to polyphenoxyl radical in a two-step reaction sequence. The phenol units are first deprotonated to produce the polyphenolate. Subsequent oxidation is performed with two oxidants.

- Thanks to the stability of the SC, the resulting polyradical has a very high spin concentration. The S value, on the other hand, is far lower than anticipated for a polyradical of such size. The designed defect-insensitive property is not observed either. The hyperbranched structure appears to have no beneficial effect.

- Based on this study and other similar researches, it is evident that ferromagnetic interaction transmitted through a conducting polymer backbone is generally very weak. This indicates that the basic strategy of making defect-insensitive systems by localizing the SCs is not compatible with the fundamental requirement of magnetization, radical delocalization.

- To make the system more delocalized, another polyradical with diphenyl methyl as SC is proposed. However, the monomer synthesis is hampered by an unexpected intramolecular cyclization reaction.

Although this study failed to produce any polyradicals with outstanding magnetic properties, it does reveal some hitherto understated problems

concerning this approach to magnetism and monomer syntheses. It is hoped that these new insights can improve the design and synthesis of organic-polymer-based magnetic material in the future.

References

[1] Miller, J. S., Dougherty, D. A., Eds.*Mol. Crys. Liq. Crys.* **1989**, 176.
Dougherty, D. A., *Acc. Chem. Res.* **1991**. *24*, 88

[2] Nishide, H.; Miyasaka, M.; Tsuchida, E. *Angew. Chem. Int. Ed. Engl.* **1998**, *37*, 2400

[3] Jacobs, J. S. Ph.D. Thesis, Chapter Five, California Institute of Technology, Pasadena, California, 1993

[4] Ovchinnikov, A. A. *Theor. Chim. Acta.* **1978**, *47*, 297
Klein, D. J.; Nelin, C. J.; Alexander, S.; Masten, F. A. *J. Chem. Phys.* **1982**, *77*, 3101
Tyutyulkov, N. N.; Karabunarliev, S. H. *Chem. Phys.* **1987**,*112*, 293
Yoshizawa, K.; Hoffmann, R. *J. Am. Chem. Soc.* **1995**, *117*, 6921

[5] Nishide, H.; Yoshioka, N.; Inagaki, K.; Tsuchida, E.; *Macromolecules* **1988**, *21*, 3119
Nishide, H.; Yoshioka, N.; Kaneko, T.; Tsuchida, E.; *Macromolecules* **1990**, *23*, 4487
Nishide, H.; Kaneko, T.; Yoshioka, N.; Akiyama, H.; Igarashi, M.; Tsuchida, E. *Macromolecules* **1993**, *26*, 4567

[6] Fujii, S.; Ishida, T.; Koga, N.; Iwamura, H. *Macrocolecules* **1991**, *24*, 1077
Miura, Y.; Matsumoto, M.; Ushitani, Y. Y.; Teki, Y.; Takui, T.; Itoh, K. *Macromolecules* **1993**, *26*, 6673

[7] Edited by Kochi K. J. *Free Radicals* New York, Wiley: **1973**

[8] Kishimoto, Y.; Itou, M.; Miyatake, T.; Ikaryia T.; Noyori, R. *Macromolecules* **1995**, *28*, 6662

Kishimoto, Y.; Miyatake, T.; Ikariya, T.; Noyori, R. *Macromolecules* **1996**, *29*, 5054

[9] Nishide, H.; Kaneko T.; Igarashi, M.; Tsuchid E.; Yoshioka, N.; Lahti, P. M. *Macrocolecules,* **1994**, *27*, 3082-3086

[10] Skotheim, T. A.; Elsenbaumer, R. L.; Reynolds J. R. *Handbook of Conducting Polymers 2nd ed.* Marcel Dekker: New York, **1998**

Hari Singh *Nalwa Handbook of Organic Conductive Molecules and Polymers*: *Wiley*: Chichester ; New York, **1997** Vol. 2,3

[11] Nishide, H.; Kaneko, T.; Nii, T.; Katoch, K.; Tsuchid E.; Yamaguchi, K. *J. Am. Chem. Soc.* **1995**, *117*, 548

Nishide, H.; Kaneko, T.; Nii, T.; Katoch, K.; Tsuchid E.; Yamaguchi, K.; Lahti, P. M. *J. Am. Chem. Soc.* **1996**, *118*, 9695

[12] Nishide, H.; Miyasaka, M.; Tsuchid E. *J. Org. Chem.* **1998**, *63*, 7399

[13] Heck, R. F. *Org. React. (N.Y.)* **1982**, *27*, 345

Greiner, A.; Heitz, W. *Makromol. Chem. Rapid Commun.* **1988**, *9* , 581

Miyaki, N.; Tomita, I.; Kido, J.; Endo, T.; *Macromolecules* **1997,** *30,* 4504

Zhang, J. S.; Moore, J. S.; Xu, Z. F.; Aguirre, R. A. *J. Am. Chem. Soc.* **1992**, *144*, 2373

Schumm, J. S.; Pearson, D. L.; Tour, J. M.; *Angew.Chem.Int. Ed. Engl.* **1944**, *33*, 1360

[14] Heck, R. F. *Palladium Reagents in Organic Syntheses* Academic Press: London ; Orlando [Fla.], **1985**

Jiro Tsuji *Palladium Reagents and Catalysts: Innovations in Organic Synthesis* ; Wiley & Sons: Chichester, England; New York **1995**

[15] McMurry, J. E. *Acc. Chem. Res.* **1974**, *7*, 281

McMurry, J. E,; *Chem. Rev.* **1989**, *89* , 1513

[16] Gauthier, S.; Mailhot, J.; Labrie, F. *J. Org. Chem.* **1996**, *61*, 3890

[17] Wawzonek, S.; Smolin, E. M. *Org. Synt. Col. Vol. IV* **1963**, 387

[18] Reid, J. R.; Dufresne, R. F.; Chapman, J. J. *Org. Synt.* **1996**, *74*, 217

[19] Young, S. D.; Buse, C.T.; Heathcock, C. H. *Org. Synt. Col.* **1990**, *7*, 381

Tanabe, Y.; Murakami, M.; Kitaichi, K.; Yoshida, Y. *Tetra. Lett.* **1994**, *35*, 8409

[20] Chan, T. H.; Baldassarre, A.; Massuda, D.; *Synthesis*, **1976**, 801

Bonds, F. T.; DiPietro, R. A.; *J. Org. Chem.* **1981**, *46*, 1315

Adlington, R. M.; Barrett, A. G. M. *Acc. Chem. Res.* **1983**, **16**, 55

[21] Sato, F. *Tetra. Lett.* **1983**, *24*, 1041

Sato, F.; Kobatashi, Y. *Org. Synt. Col.* **1993**, *8*, 507

[22] Sato, F.; Ishikawa, H.; Sato, M. *Tetra. Lett.* **1981**, *36*, 2285

Sato, F. *Org. Synt.* **1990**, *69*, 106

[23] Wilcox, C. F. Jr.; Weber, K. A. *J. Org. Chem.* **1986**, *51*, 1088

Wong, H. N. C.; Man, Y. M.; Mak, T. C. W. *Tetra, Lett.* **1987**, *28*, 6359

[24] Scherf, U.; Mullen, K. *Synthesis-Stuttgart* **1992**,*(1-2),* 23

Meier, H.; *Angew.Chem. Int.Ed. Engl.* **1992**, *31*, 1399

[25] Xu, Z. F.; Moore, J. S. *Angew.Chem.Int. Ed. Engl.* **1993**, *32*, 246

Xu, Z. F.; Moore, J. S. *Angew.Chem.Int. Ed. Engl.* **1993**, *32*, 1354

Xu, Z. F.; Moore, J. S. *Macromolecules* **1991,** *24*, 5893

[26] Alami, M.; Ferri, F.; Linstrumelle, G. *Tetra. Lett.* **1993**, *34*, 6403

[27] Moore, J. S. *Acc. Chem. Res.* **1997**,*30*, 402

[28] Zhou,Q.; Swager, T. M. *J. Am. Chem. Soc.* **1995**, *117*, 12593

Yang, J. S.; Swager, T. M. *J. Am. Chem. Soc.* **1998,** *120* , 5321

[29] Rutledge, T. F. *Acetylene Chemistry*, Reinhold Book. Co., New York, **1968**

Campbell, I. D.; Eglinton, G. *Org. Synt. Col Vol. V* **1973,** 517

[30] Closs, G. L.; Miller, J. R. *Science* **1988**, *240*, 440-447

Closs, G. L.; Calcaterra, L. T.; Green, N. J.; Penfield, K. W.; Miller, J. R. *J. Phys. Chem.* **1986**, *90*, 3673

Closs, G. L.; Forbes, M. D. E.; Piotrowiak, P. *J. Am. Chem. Soc.* **1992**, *114,* 3285

Forbes, M. D. E.; Ball J. D.; Avdievich N. I. *J. Am. Chem. Soc.* **1996**, *118*, 4707

[31] Nishide, H.; Kaneko, T.; Nii, T.; Katoch, K.; Tsuchid E.; Yamaguchi, K. *J. Am. Chem. Soc.* **1995**, *117*, 548

Nishide, H.; Kaneko, T.; Nii, T.; Katoch, K.; Tsuchid E.; Yamaguchi, K.; Lahti, P. M. *J. Am. Chem. Soc.* **1996**, *118*, 9695

[32] Julia, M.; Johmson, W. S. *Acc. Chem. Res.* **1974**, *2*, 147

[33] Johnson, W. S. *J. Am. Chem. Soc.* **1968**, *90*, 6224

Andersen, K. E.; Braestrup, C.; Gronwald, F.C.; Jorgensen, A. S.; Nielsen, E. B.; Sonnewald, U.; Sorensen, P. O.; Suzdak, P. D.; Knutsen, L. J. S. *J. Med. Chem.* **1993**, *36*, 1716

[34] Olah, G. A.; Husain, A.; Balaram Gupta, B. G.; Narang, S. C. *Angew.Chem.Int. Ed. Engl.* **1981**, *20*, 690

Olah, G. A.; Narang, S. C.; Balaram Gupta, B. G.; Molhotra, r. *J. Org. Chem.* **1979**, *44*, 1247

[35] Koelsch, S. F. *J. Am. Chem. Soc.* **1932**, *54,* 3384

Koelsch, S. F. *J. Am. Chem. Soc.* **1932**, *54,* 4744

[36] Koelsch, S. F. *J. Am. Chem. Soc.* **1957**, *79*, 4439

Experimental Section

Solvents in the synthetic reactions were distilled before use as described in Chapter Two. All starting materials were commercially available from either Aldrich or Lancaster Co. and were used as received without further purification.

Unless otherwise noted, all reactions were run under an atmosphere of dry argon in oven- or flame-dried glassware. Magnetic stir bar of an appropriate size was always used to make the reaction solution well mixed. Thin layer chromatography was performed on 0.25 nm silica pre-coated glass plate and visualized with UV lamp. Flash chromatography was performed on 230-400 mesh silica gel from Merck. All the instrumentation and data process were identical to those described in Chapter Two.

Monomer Synthesis

4-Hydroxyl-3,5-di-t-butyl-phenylacetonitrile (11): 20 g of 3,5-di-t-butyl-4-hydroxylbenzaldehyde was suspended in 250 ml of absolute ethanol in a 500 ml flask. The mixture was slightly heated on a mantle until all the solid was dissolved. 16 g of *p*-toluene sulfonyl hydrazine (1.01 eqivalent) was added through a funnel in several portions. The flask was then equipped with a Dean-Stark trap and a condenser and the suspended solution was refuxed. The first 50 ml of solvent collected in the trap was discarded. The reaction was heated for twelve more hours to furnish a clear yellow hydrazone solution. The tosyl hydrazone **10** crystallizes as white pallet after the solution was cooled to room temperature. The hydrazone intermediate can be isolated at this stage in nearly quantitative yield. However, it was more convenient to subject it to the next step directly.

16.5 g of potassium cyanide (about 3 equivalents to the starting aldehyde) powder was added to the solution in small portions. After the evolution of nitrogen gas subsided, the mixture was refluxed for another 18 hours under vigorous stir. The resulting dark green solution was first concentrated (in a well ventilated hood) and 200 ml of diethyl ether was added to the residual solid. The insoluble solid (mainly composed of excess sodium cyanide) was removed by filtration and disposed. The ether solution was then washed with 1 M HCl and two times with water. The organic phase was dired over sodium sulfate before concentrated. The crude product was purified on a silica gel flash column (40% methylene chloride in petroleum ether) to give the 8.6 g of pure nitrile prduct (41 % yield over two steps) as a white solid. ^{1}H NMR δ 1.45 (s, 18H), 3.67 (s, 2H), 5.28 (s, 1H), 7.11 (s, 2H)

4-Trimethylsiloxyl-3,5-di-t-butyl-phenylacetonitrile (12): In a 250 ml flask, 8 g of phenyl nitrile **11** and 13 g of bis(trimethylsilyl) acetamide (two equivalents) were dissolved in 150 ml of acetonitrile and the solution was refluxed for 18 hours. After the solvent was removed on a rotary evaporator, the residual oil was redissolved in ether and the solution was washed three times with water. The organic layer was dried over magnesium sulfate and concentrated. The remaining oil was purified with flash chromatography (30% methylene chloride in petroleum ether). 9.6 g of protected phenol (94% yield) was isolate as a white flaky powder. ^{1}H NMR δ 0.43 (s, 9H), 1.42 (s, 18H), 3.64 (s, 2H), 7.19 (s, 2H)

3,3-Bis(4-bromophenyl)-2-(4-hydroxyl-3,5-di-t-butyl-phenyl) arylonitrile (13): In a 500 ml flask, 8 g of protected phenol **12** and 17.2 g of dibromobenzophenone (two equivalents) were dissolved in 250 ml of THF. Cooled in an ice bath, the solution was chilled to 0°C before 50 ml of sodium bis(trimethylsilyl) amide solution (1 M in THF

from Aldrich, two equivalents to the nitrile) was added slowly via a syringe. The solution turned blue purple after the addition presumably because of the benzophenone ketyl radical. The solution was then refluxed for 15 hours before it was quenched with saturated ammonium chloride solution. The deep purple color of organic phase faded immediately. THF was evaporated on a rotary evaporator before 250 ml of methylene chloride was added to the mixture. The organic layer was then washed with 3 M HCl, 10% sodium bicarbonate and finally water (two times). The solution was then dried over sodium sulfate and concentrated. The residual solid was purified on a silica gel flash column (50% methylene chloride in petroleum ether) and 3.2 g of deprotected olefin product (22% yield) was isolated as a pale yellow powder. ^{1}H NMR δ 1.24 (s, 18H), 7.88 (d, J=8 Hz, 2H), 7.04 (s, 2H), 7.33 (d, J=8 Hz, 2H), 7.28 (d, J=8 Hz, 2H), 7.57 (d, J=8 Hz, 2H)

1-(2,6-Di-t-butyl-4-bromo-phenoxyl)methoxyl-2-methoxyl-ethane (15): A solution of 10.5 g of 2,6-di-t-butyl-4-bromophenol in 150 ml of THF was placed in an addition funnel. The funnel was connected to a 500 ml flask containing 2.2 g of sodium hydride (60% mixture with mineral oil, 1.5 equivalents to the phenol), 6 g of methoxyl ethoxyl methyl chloride (1.3 equivalents according to the phenol) and 50 ml of THF. The flask was cooled to 0°C and the phenol solution was added dropwise under vigorous stirring. The reaction was left in the ice bath for another eight hours before it was quenched by saturated ammonium chloride solution. The solvent was removed under vacuum and the residual oil was redissolved in ether. The solution was washed four times and dried over sodium sulfate and concentrated. This produced 13.2 g of an orange liquid (95% crude yield) suspended with some dark solid. Judged by NMR, this mixture was more than 90% pure. The crude product can be used directly

in the next step without further purification. Pure sample can be obtained as a yellow oil after flash chromatography (40% methylene chloride in petroleum ether). ^{1}H NMR δ 1.41 (s, 18H), 3.41 (s, 3H), 3.64 (dd, J=7 Hz, 7 Hz, 2H), 3.95 (dd, J=7, Hz, 7 Hz, 2H), 4.97 (s, 2H), 7.34 (s, 2H) ^{13}C NMR δ 31.55, 35.64, 58.77, 68.80, 71.39, 99.34, 116.69, 129.28, 146.41, 153.27 EIMS. m/z Molecular ion peak was not observed, 286 (5%); 269 (35%); 255 (30%); 241 (31%); 115 (80%); 59 (100%)

1-(3,5-Di-t-butyl-4-methoxyl ethyl methoxyphenyl) propyne (16): In a 500 ml flask, 10 g of **15** and 1.23 g of tetrakis(triphenyl phosphine) palladium (0.04 equivalent) were dissolved in 150 ml of THF. The yellow solution was chilled to 0°C in an ice bath before 34 ml of 1 M propynylide magnesium bromide solution in ether (1.3 equivalents to **15**, the reagent is available from Aldrich) was added slowly via a syringe. The coupling reaction then proceeded at reflux temperature for 14 hours before it was cooled back to ambient temperature and quenched by slow addition of saturated ammonium chloride. The solvent was evaporated and the residual dark oil was redissolved in ether. The organic layer was washed four times before it was dried over sodium sulfate and concentrated. The crude product was purified by flash chromatography (30% methylene chloride in petroleum ether). 6.1 g of alkyne coupling product (68% yield) was isolated as a lightly orange opaque liquid. ^{1}H NMR δ 1.41 (s, 18H), 2.04 (s, 3H) 3.41 (s, 3H), 3.64 (dd, J= 6 Hz, 6 Hz, 2H), 3.96 (dd, J=6 Hz, 6 Hz, 2H), 4.96 (s, 2H), 7.30 (s, 2H) ^{13}C NMR δ 4.00, 31.64, 35.38, 58.78, 68.76, 71.42, 79.86, 83.95, 99.28, 118.40, 129.58, 144.15, 153.86 EIMS, m/z, 332 (M, 2%); 258 (27%); 229 (40%); 201 (90%); 185 (30%); 128 (55%); 89 (90%); 59 (100%); HRMS 332.235 within 2 ppm calculated for $C_{21}H_{32}O_3$ 332.2351

1,1-Bis(4-bromophenyl)-2-(3,5-di-t-butyl-4-methoxyl ethoxyl methoxylphenyl) 2-buten-1-ol (17): In a 250 ml flask, 5 g of **16** and 0.37 g of bis(cyclopentadiene) titanium dichloride (0.1 equivalent) were dissolved in 40 ml of ether. The system was cooled to 0°C in an ice bath and 21 ml of isobutyl magnesium bromide solution (1 M in ether, available from Aldrich, 1.4 equivalents to **16**) was added dropwise via a syringe at such a rate that the evolution of isobutene gas was moderate. After the bubbling was no longer visible, the solution was warmed back to room temperature and the hydromagnesiation was allowed to proceed for another eight hours under vigorous stirring. (During this transformation, the solution first turned brown after the Grignard reagent was added but the deep color soon faded while a viscous dark material started to accumulate at the bottom of the flask.) In another flask, a solution of 12 g of 4,4'-dibromobenzophenone (2.4 equivalents to the alkyne **16**) in 130 ml THF was prepared. This ketone solution was transferred to the first flask via a canula under a slightly positive pressure and the resulting purple solution was refluxed for twelve hours. The solution was purple right after the addition but became orange by the end when it was quenched by saturated ammonium chloride. The solvent was removed on a rotary evaporator and the remaining mixture was redissolved in methylene chloride. The solution was washed four times with water and dried over magnesium sulfate. A complex mixture was isolated after the solvent was evaporated. Judged by NMR spectrum, it was composed of the desired product, excess benzophenone, reduced alkyne, and reduced benzophenone. The addition product could be purified with flash chromatography (60% methylene chloride in petroleum ether). However, it is far more convenient to subject the mixture to the next dehydration step without purification. ^{1}H NMR δ 1.27 (s, 18H), 1.48 (d,

J=7 Hz, 3H), 3.40 (s, 3H), 3.62 (dd, J= 7 Hz, 7 Hz, 2H), 3.92 (dd, J=7 Hz, 7 Hz, 2H), 4.93 (s, 2H), 5.25 (q, J=7 Hz, 1H), 6.74 (s, 2H), 7.29 (d, J=8 Hz, 4H), 7.44 (d, J=8 Hz, 4H) ^{13}C NMR δ 14.97, 31.62, 35.41, 58.83, 68.72, 71.40, 82.47, 99.15, 121.23, 127.11, 127.92, 128.11, 129.83, 130.58, 130.96, 131.43, 143.97; FABMS, m/z 697 (M+Na, 5%); 657 (92%); 489 (77%); 446 (56%) 403 (49%); 324 (50%); 245 (100%); 183 (65%); FABMS, m/z 674 (M, 15%); 657 (85%); 489 (72%); 446 (46%); 403 (42%); 325 (42%); 245 (100%) 183 (62%); HRMS (M+Na) 695.1325 within 3.3 ppm, calculated for $C_{34}H_{42}Br_2O_4Na$ 695.1348

1,1-Bis(4-bromophenyl)-2-(3,5-di-t-butyl-4-hydroxylphenyl) butadiene (5): In a 250 ml flask, the crude mixture from the last step and 8.4 g of pyridinium p-toluenesulfonate (2.5 equivalents to **16** used in last step) were dissolved in 120 ml of 1,1,2-trichloroethane. The mixture was refluxed under vigorous stirring. The progress of the reaction can be monitor by thin layer chromatography (TLC). The deprotected diene **5** is easily distinguishable because it has a very high RF value and is moderately fluorescent under short wave UV lamp. After no compositional change can be detected by TLC (usually about 12-15 hours), the reaction was cooled back to room temperature and diluted by methylene chloride. The solution was washed with 10% sodium bicarbonate solution, 0.5 M HCl and water (two times). The organic layer was then dried over sodium sulfate and concentrated. 1.8 g of pure deprotected diene (22% yield based on **16** used in the previous step) was isolated as a pale yellow powder after a simple flash chromatography (10% methylene chloride in petroleum ether). ^{1}H NMR δ 1.29 (s, 18H), 5.18 (bs, 1H) 5.21 (dd, J=18 Hz, 2 Hz, 1H), 5.28 (dd, J=12 Hz, 2Hz, 1H), 6.67 (d, J=8 Hz, 2H), 6.71 (dd, J=18 Hz, 12 Hz, 1H), 6.87 (s, 2H), 7.14 (d, J=8 Hz, 2H) 7.15 (d, J=8 Hz, 2H) 7.49 (d, J=8 Hz, 2H) ^{13}C NMR measured in CD_2Cl_2 δ 29.70, 33.79, 118.78, 119.55,

122.24, 127.48, 128.25, 130.07, 130.86, 132.28, 132.41, 135.00, 137.33, 138.55, 140.72, 142.08, 152.55; FABMS, 570 (M, ^{81}Br, ^{81}Br, 55%); 568 (M, ^{81}Br, ^{79}Br, 100%); 566 (M, ^{79}Br, ^{79}Br, 50%); 488 (25%); 432 (36%); 410 (70%), 233 (58%); 176 (41%); MHRMS 566.0801 within 3.3ppm, calculated for $C_{30}H_{32}Br_2O$ 566.0819

1,1-Bis(4-bromophenyl)-2-(3,5-di-t-butyl-4-hydroxylphenyl) 3,4-dibromo-1-butene (18): In a 250 ml of flask, 3 g of **5** was dissolved in 50 ml of chloroform. The solution was then cooled to -78°C in a dry ice acetone bath. A chloroform solution of Br_2 (0.46 M, 25 ml containing 0.6 ml of Br_2) was prepared. 12 ml of the Br_2 solution (1.05 equivalent) was added slowly via a syringe. To prevent over bromination, the chilled solution was well stirred and no bromine was added until the orange color from the last drop had faded. By the end of the addition, the pale orange solution was warmed back to room temperature and left overnight. Most solvent was removed on a rotary evaporator and the residual viscous liquid was further dried on a vacuum line to furnish the dibromide as a lightly brown amorphous solid. This crude product was subjected to the next elimination step without further purification. ^{1}H NMR δ 1.34 (s, 18H), 3.54 (dd, J=15 Hz, 12 Hz, 1H) 3.72 (dd, J=15 Hz, 10 Hz, 1H) 5.17 (s, 1H), 5.33 (dd, J=12 Hz, 10 Hz, 2H), 6.71 (d, J=8 Hz, 2H), 7.13 (d, J=8 Hz, 2H), 7.18 (s, 2H), 7.30 (d, J=8 Hz, 2H), 7.57 (d, J=8 Hz, 2H) ^{13}C NMR δ 30.08, 33.03, 34.00, 50.46, 121.66, 125.65, 126.26, 127.91, 130.17, 130.50, 131.13, 131.72, 132,12, 135.04, 137.37, 140.15, 153.11 FAMBS, 727.7 (M, 18%); 648 (98%); 568 (94%); 410 (55%); 233 (38%); 154 (100%)

It is worth mentioning that **18** also spontaneously lost HBr at room temperature in chloroform solution to give the partial elimination product. ^{1}H NMR δ 1.27 (s, 3H), 1.40 (s, 3H), 5.15 (bs, 1H), 6.29 (d, J=17 Hz, 1H),

6.59 (d, J=8 Hz, 2H), 6.79 (s, 2H), 7.01 (d, J=17 Hz, 1H), 7.10 (d, J=8 Hz, 2H), 7.12 (d, J=8 Hz, 2H), 7.49 (d, J=8 Hz, 2H)

1,1-Bis(4-bromophenyl)-2-(3,5-di-t-butyl-4-hydroxylphenyl) 1-butenyne (7): In a 250 ml flask with an addition funnel, 3 g of potassium t-butoxide (5 equivalent to the diene **5** used in the last step) was dissolved in 30 ml of THF. The crude dibromide **18** was dissolved in 30 ml of THF and solution was transferred into the funnel. The base solution was cooled to 0°C in an ice bath. Aluminum foil was wrapped around the flask to protect the system from light. The dibromide solution was then added in slowly in about twenty minutes. The progress of the reaction can be monitored by TLC (10% methylene chloride in petroleum ether). Compared to the staring material, the alkyne **7** is much more fluorescent and more polar. The reaction must be stopped in about another 20 minutes when it is not yet complete. [Prolonged reaction time leads to extensive decomposition.] The reaction was quenched with saturated ammonium chloride before the solvent was removed. The residual brown tar was redissolved in ether and washed with water several times. The organic layer was then dried over sodium sulfate and concentrated. Besides decomposed materials and desired product, the crude mixture also contains some intermediate elimination product. After a silica gel flash column (5%-10% methylene chloride in petroleum ether), 1.4 g of pure enyne (47% yield based on **18** used in previous step) was isolated as a yellow powder. Although this bright color quickly darkened to muddy yellow, no sign of any decomposition can be detected in NMR spectrum. The monomer was used directly in the polymerization reaction without further purification. ^{1}H NMR δ 1.27 (s, 18H), 3.11 (s, 1H), 5.20 (bs, 1H), 6.79 (d, J=8 Hz, 2H), 7.05 (s, 2H), 7.27 (d, J=8 Hz, 2H), 7.34 (d, J=8 Hz, 2H), 7.46 (d, J=8 Hz, 2H) ^{13}C NMR δ 30.66, 34.79, 82.67, 85.69, 121.87, 122.61,

127.65, 129.40, 131.64, 131.76, 132.44, 132.54, 133.08, 135.81, 141.20, 141.59, 146.40, 153.99; EIMS, m/z 568 (M, ^{81}Br, ^{81}Br, 27%); 566 (M, ^{81}Br, ^{79}Br, 42%); 564 (M, ^{79}Br, ^{79}Br, 18%); 541 (9%); 233 (75%); 176. (36%); 154 (100%); HRMS 564.0661 within 0.4 ppm, calculated for $C_{30}H_{30}Br_2O$ 564.0741

Polymerization (HDBPBOB): 1 g of monomer **7**, 20 mg of tris-(dibenzylideneacetone)dipalladium(0) (0.025 equivalent of palladium), 46 mg of triphenylphosphine (0.1 equivalent) and 7 mg of copper(I) iodide (0.02 equivalent) were placed in a Shlenk tube. The vessel was cooled in a liquid nitrogen bath before 4 ml of pyrrolidine was also added. The system was then degassed with freeze-pump-thaw cycle five times. Wrapped in aluminum foil, the tube was protected from light before it was immersed in an 85°C oil bath. The polymerization reaction was kept at this near refluxing temperature for 48 hours. After it was cooled back to room temperature, the solution was diluted with methylene chloride and was washed three times with 3 M HCl to remove the pyrrolidine. The organic phase was then washed with 10% sodium bicarbonate and finally two more times with water. The solution was dried on sodium sulfate and concentrated. Petroleum ether was added to the remaining orange solid and the suspended mixture was filtered. The resulting red orange powder was further washed twice with petroleum ether. After some residual solvent was removed on a vacuum line, the thoroughly dried product weighed 0.8 g (93% yield).

[As described in the previous chapter, the polymerization reaction only consumes one of the two bromides on the monomer. In other words, every monomer unit should carry one bromide on average. The average molecular weight for the monomer units is thus 485, calculated by

subtracting from the monomer weight the weight of a hydrogen bromide molecule which is lost in the coupling reaction.]

Polyradical generation A: 0.1 g of polymer was dissolved in a small amount of THF in a 100 ml flask and 21 ml of 0.1 M tetra-n-butyl ammonium hydroxide solution (this solution was prepared by diluting the commercially available 1 M solution, 1.02 equivalents) was added. The reaction was stirred for four hours before the solvent was removed on a vacuum line. The remaining solid was redissolved in 20 ml of THF and 20 ml of 0.5 M $K_3Fe(CN)_6$ aqueous solution (5 equivalents to monomer unit) was added. The oxidation is carried out in this heterogenous mixture with vigorous stirring for two hours. With a syringe, the organic layer was then transferred to another flask with a side arm. The solvent was evaporated on a vacuum line and, with the resulting powder sample still preserved under vacuum, the flask was taken into a glove box and the polyradical powder was loaded into the delrine SQUID sample holder.

Polyradical Generation B: The polyphenoxide was generated in identical manner as in **A** except that the reaction vessel must have two side arms. After the solvent was evaporated under vacuum, the flask is filled with argon and 68 mg of ferrocenium hexafluorophosphate (one equivalent to 0.1 g of polymer used) was added. One side arm was then connected to a lecture bottle containing chloromethane while the other arm was connected to a vacuum line. With both valves opened, the whole system was evacuated and then refilled with argon three times. The flask was then immersed into a dry ice-acetone bath. The valve of the lecture bottle was then opened to allow the condensation of the chloromethane. In order to keep the reaction at low temperature, the valve was closed once the bubbling from the bath intensifies and it was not opened until the bubbling subsides. This cycle was repeated several times until about 20 ml of solvent was collected. The

oxidation then proceeded in this suspended mixture for eight hours with vigorous stirring. The orange red color of the powder sample remains unchanged during the whole course of this transformation. With the flask still in the cold bath, the system was put under vacuum for another eight hours to remove the solvent. The rest of the operation was identical as described before. In order to move the sample into a glove box, the polyradical powder was exposed to room temperature for about 30 minutes. To prevent further decomposition, the loaded sample holder was immersed in a liqiud nitrogen bath before it was inserted into the SQUID magnetometry.

Methyl 1-bis(4-t-butylphenyl)-hydroxylmethyl cyclopropane carboxylate (21): In a 250 ml flask, 3 g of dimethyl 1,1-cyclopropane dicarboxylate was dissolved in 50 ml of THF and the solution was chilled in an ice bath. 43 ml of 4-t-butylphenyl magnesium bromide 1 M solution in ether (2.2 equivalents, available from Aldrich) was added slowly via a syringe. The solution was then refluxed for six hours. After the reaction was cooled back to room temperature, it was quenched by slow addition of saturated ammonium chloride solution. The solvent was then removed and the residual opaque liquid was redissolved in ether. The organic layer was washed with water four times and dried over sodium sulfate before it was concentrated. The crude product was further dried under vacuum to remove the t-butylbenzene. Judged by NMR, the resulting viscous oil was mainly composed of the desired hydroxyl methyl ester. No further purification is necessary before the next step. ^{1}H NMR δ 0.78 (broad multiples, 4H), 1.28 (s, 18H), 3.59 (s, 3H), 7.25 (d, J=8 Hz, 4H), 7.32 (d, J=8 Hz, 4H) ^{13}C NMR δ 12.85, 31.93, 34.95, 52.74, 81.10, 125.05, 126.22, 127.25, 127.66, 150.21 FABMS, m/z 401 (M+Li, 100%) with 3-NBA+Li matrix; 377 (100%); 295 (46%); 233 (10%); 161(17%) with 3- NBA

matrix; HRMS 401.2667 (M+Li) within 0.3 ppm,calculated for $C_{26}H_{34}O_3Li$ 401.2668

1-Bis(4-iodophenyl)hydroxylmethyl-1-bis(4-t-butylphenyl) hydroxylmethyl cyclopropane (22): In a 500 ml flask, 20 g of p-diiodobenzene (3.2 equivalents according to the dimethyl diester used in the last step) was dissolved in 250 ml of THF. In a dry ice acetone bath, the solution was cooled to -78°C. 25.5 ml of n-BuLi (2.5 M in hexane, 1.05 equivalents to diiodobenzene) was then slowly added to this chilled suspended solution. The lithium-iodo exchange was allowed to proceed for 90 minutes under vigorous stirring. The crude **21** was dissolved in 20 ml ether and this solution was transferred to the cold lithium reagent solution at once via a syringe. The reaction was warmed back to room temperature and allowed to proceed for another eight hours. (The solution slowly assumed a milky appearance and became fully suspended with white powder presumably consisting of the bisalkoxide.) The reaction was quenched with saturated ammonium chloride before the solvent was removed on a rotary evaporator. The remaining mixture was dissolved in methylene chloride and the organic phase was washed with water three times. After drying over sodium sulfate, the solution was concentrated. The side product iodobenzene can be removed on a vacuum line. 12.2 g of crude diol product (82% yield based on dimethyl diester used in the last step) was obtained. Since NMR spectrum indicates only a small amount of unknown impurity, this diol was therefore directly subjected to the next rearrangement step without further purification. ^{1}H NMR δ 0.39 (bs, 4H) 1.34 (s, 18H), 7.22 (d, J=8 Hz, 2H), 7.35 (overlapping singlets, 8H), 7.64 (d, J=8 Hz, 2H) ^{13}C NMR δ 9.22. 12.02, 31.08, 34.19, 82.02, 124.36, 127.42, 129.97, 136.29, 137.22, 139.06, 143.89, 147.03; FABMS, m/z 777 (M+Li, 15%); 443 (23%); 401 (100%); 295 (17%); 230 (14%); 161

(23%); 325 (7%); HMRS 777.1276 (M+Li) within 0.3 ppm calculated for $C_{37}H_{40}I_2O_2Li$ 777.1278

1,1-bis(4-iodophenyl)-2-ethenyl-3-(4-t-butylphenyl)-6-t-butyl indene: 12 g of the crude **22** and 0.58 g of tetra-n-butyl ammonium iodide (0.1 equivalent) were dissolved in 200 ml of methylene chloride. The solution was chilled to 0°C in an ice bath before 47 ml of chlorotrimethylsilane solution (1 M in methylene chloride, three equivalents) was added in several portions via a syringe. The color of the solution darkened after each addition but it soon faded and the next portion was added. The solution was refluxed for twelve hours. Most of the solvent was then removed on a rotary evaporator and the residual brown viscous liquid was further dried on a vacuum line. The crude rearrangement product was isolated as a light brown amorphous solid. The absence of starting material and the presence of ring opening product **23** were both confirmed by NMR spectrum. ^{1}H NMR δ 1.23 (s, 9H), 1.41 (s, 9H), 2.60-2.70 (m, 2H), 2.78-2.90 (m, 2H), 7.01 (d, J=8 Hz, 4H), 7.4-7.8 (m, 7H), 7.63 (d, J=8 Hz, 4H) ^{13}C NMR in a dilute solution δ 30.99, 31.04, 124.50, 125.46, 126.37, 127.86, 128.38, 129.85, 129.94, 137.42, 139.06

The crude **23** was dissolved in 150 ml of THF and the solution was chilled to 0°C in an ice bath. A base solution of 4.4 g of potassium t-butoxide (2.5 equivalents) and 50 ml of THF was added dropwise through an addition funnel. The elimination was then allowed to proceed at ambient temperature for six hours before it was quenched by water. The mixture was concentrated and the remaining brown solid was redissolved in ether. This solution was washed several times with water until the aqueous layer became neutral. The organic phase was dried over sodium sulfate and concentrated to furnish a dark solid. The purification was performed on a silica gel flash column (5%-10% methylene chloride in petroleum ether)

and 8.2 g of pure diene product (72% yield) was isolated as a white powder. ^{1}H NMR δ 1.23 (s, 9H), 1.39 (s, 9H), 4.93 (dd, J=17 Hz, 1 Hz, 1H), 5.01 (dd, J=12Hz, 1 Hz, 1H), 6.55 (dd, J=17 Hz, 12 Hz, 1H), 7.06 (d, J=8 Hz, 4H), 7.20-7.34 (overlapping multiples, 3H), 7.41 (d, J=8 Hz, 2H), 7.51 (d, J=8 Hz, 2H), 7.58 (d, J=8 Hz, 4H) ^{13}C NMR δ 31.15, 31.25, 34.49, 34.68, 92.06, 117.81, 120.56, 120.86, 124.07, 125.17, 128.86, 128.99, 130.66, 131.02, 136.91, 140.48, 142.19, 145.51, 150.24, 150.70, 153.52 FABMS, in 3-NBA matrix m/z 734 (M, 100%); 678 (20%); 664 (40%); 607 (20%); 473 (13%); 289 (12%); 154 (21%)

1,1-bis(4-iodophenyl)-2-(2,Z-bromo-ethenyl)-3-(4-t-butylphenyl)-7-t-butyl indene : In a 250 ml flask, 8 g of diene was dissolved in 120 ml of chloroform and the solution was cooled to 0°C in an ice bath. In another flask, 50 ml solution containing 1 ml of bromine was prepared (0.38 M). 28 ml of the bromine solution (one eqiuvalent) was added to the cold diene solution slowly via a syringe. Before each addition, time was allowed for the orange color from the last addition to fade. The reaction was then refluxed for eight hours before the solvent was removed. (The evolution of HBr was visible when the heating first started but subsided after several hours.) The residual orange oil was further dried on a vacuum line to give a colorless amorphous solid in almost quantitative yield. The stereochemistry of the newly formed bromoalkene was deduced from the NMR coupling constant of the two alkenyl protons. No purification was necessary before the next step. ^{1}H NMR δ 1.24 (s, 9H), 1.40 (s, 9H), 6.00 (d, J=17 Hz, 1H), 6.95 (d, J=17 Hz, 1H), 7.02 (d, J=8 Hz, 4H), 7.20-7.35 (overlapping multiples, 3H), 7.39 (d, J=8 Hz, 2H), 7.52 (d, J=8 Hz, 2H), 7.60 (d, J=8 Hz, 4H) ^{13}C NMR δ 31.13, 31.21, 34.54, 34.75, 65.86, 92.43, 109.31, 120.86, 120.94, 124.35, 125.37, 125.43, 126.40, 128.83, 129.57, 130.39, 137.21, 139.08, 139.91, 141.52, 143.54,150.81,

153.15 FABMS 814 (M, ^{81}BR, 100%); 812 (M, ^{79}Br, 85%); 797 (20%); 743 (36%); 733 (42%); 687 (17%); 529 (25%); 473 (37%)

1,1-bis(4-iodophenyl)-2-ethynyl-3-(4-t-butylphenyl)-7-t-butyl indene (24): In a 500 ml flask (with an addition funnel), 4.6 g of potassium t-butoxide (4 equivalents to the bromoalkene) was dissolved in 50 ml THF and the solution was cooled to 0°C in an ice bath. 8.3 g of bromoalkene was dissolved in 100 ml of THF and the solution was added to the chilled base solution through the funnel in about 30 minutes. The progress of the reaction can be monitored on a TLC plate. (The alkyne product is slightly more polar than the starting material.) The brown reaction mixture was quenched with saturated ammonium chloride solution about twenty minutes after the addition. Although the reaction was only 70% complete at this point, prolonged exposure to strong base causes the decomposition of alkyne product and dramatically reduces the yield. After the solvent was evaporated, the residual dark solid was redissolved in ether and the solution was washed with water several times. The ether layer was dried over sodium sulfate and then concentrated. The dark brown crude product was purified with flash chromatography (5%-10% methylene chloride in petroleum ether). 3.9 g of pure enyne was isolated as a pale yellow powder (52% yield based on the staring bromoalkene. When the recovered starting material was taken into account, the actual yield was about 70%.) ^{1}H NMR δ 1.27 (s, 9H), 1.38 (s, 9H), 3.35 (s, 1H), 7.04 (d, J=8 Hz, 4H), 7.31 (d, J=2 Hz, 1H), 7.38, (dd, J=8 Hz, 2 Hz, 1H), 7.47 (d, J=8 Hz, 1H), 7.53 (d, J=8 Hz, 2H), 7.61 (d, J=8 Hz, 4H), 7.69 (d, J=8 Hz, 2H) ^{13}C NMR in CH_2Cl_2 δ 30.76, 30.89, 34.41, 34.59, 67.48, 79.90, 86.66, 92.34, 121.61, 121.88, 124.60, 125.09, 128.16, 128.69, 130.07, 137.02, 138.57, 142.30, 148.89, 149.67, 151.14, 151.68 FAMBS in 3-NBA+Li

matrix, m/z 739 (M+Li, 47%); 732 (M, 38%); 675 (15%); 529 (13%); 401 (12%); 314 (36%); 294 (36%); 160 (100%)